UNIVERSITY OF TECHNOLOGY SYDNEY
Faculty of Engineering and Information Technology

Performance Analysis of Fractional Frequency Reuse in Random Cellular Networks

by

Sinh Cong Lam

A Thesis Submitted
in Partial Fulfillment of the
Requirements for the Degree

Doctor of Philosophy

Sydney, Australia

2018

Certificate of Authorship/Originality

I certify that the work in this thesis has not been previously submitted for a degree nor has it been submitted as a part of the requirements for other degree except as fully acknowledged within the text.

I also certify that this thesis has been written by me. Any help that I have received in my research and in the preparation of the thesis itself has been fully acknowledged. In addition, I certify that all information sources and literature used are quoted in the thesis.

Sydney, 30 April 2018

Production Note:
Signature removed prior to publication.

Sinh Cong Lam

ABSTRACT

Performance Analysis of Fractional Frequency Reuse in Random Cellular Networks

by

Sinh Cong Lam

In a Long Term Evolution (LTE) cellular network, Fractional Frequency Reuse (FFR) is a promising technique that improves the performance of mobile users which experience low Signal-to-Interference-plus-Noise Ratios (SINRs). Recently, the random cellular network model, in which the Base Stations (BSs) are distributed according to a Poisson Point Process (PPP), is utilised widely to analyse the network performance. Therefore, this thesis aims to model and analyse performance of two well-known FFR schemes called Strict Frequency Reuse (FR) and Soft FR, in the random cellular network. Monte Carlo simulation is used throughout the thesis to verify the analytical results.

The first part of this thesis follows 3rd Generation Partnership Project (3GPP) recommendations to model the Strict FR and Soft FR in downlink and uplink single-tier random cellular networks. The two-phase operation model is presented for both Cell-Center User (CCU) and Cell-Edge User (CEU). Furthermore, the thesis follows the resource allocation technique and properties of PPP to evaluate Intercell Interference (ICI) of the user. The closed-form expressions of the performance metrics in terms of classification probability and average coverage probability of the CCU and CEU are derived.

Thereafter, the performance of FFR is analysed in multi-tier cellular networks which are comprised of different types of cells such as macrocells, picocells and femtocells. The focus of this part is to examine the effects of the number of users and number of Resource Blocks (RBs) on the network performance. A new network

model, in which the SINR on data channels are used for user classification purpose, is proposed. The analytical results indicate that the proposed model can reduce the power consumption of the BS while improving the network data rate. This chapter introduces an approach to analyse the optimal value of SINR threshold and bias factor. The analytical results indicate that the proposed model can increase the network data rate by 16.08% and 18.63% in the case of Strict FR and Soft FR respectively while reducing power consumption of the BS on the data channel.

Finally, the thesis develops an FFR random cellular network model with an FR factor of 1 using either Joint Scheduling or Joint Transmission with Selection Combining. The performance metrics in terms of average coverage probability are derived for Rayleigh fading environment.

Generally, this thesis makes contributions to uplink and downlink of LTE networks in terms of performance analysis.

Acknowledgements

I would like to express my special gratitude to my principal supervisor, A/Prof. Dr. Kumbesan Sandrasegaran, for the patience, generous support and immense knowledge he afforded me throughout this study.

I am grateful to Prof. Dr. Ha Nguyen (University of Saskatchewan, Saskatoon, SK, Canada), A/Prof. Dr. Quoc-Tuan Nguyen (Vietnam National University - Hanoi, University of Engineering and Technology) for their time and advise in my work.

A special thanks to my mother, father, mother-in law and father-in-law. They were always supporting and encouraging me with their best wishes. I would like to express appreciation to my beloved wife and daughter who were my support in all times.

I would also like to thank to Vietnam International Education Development - Ministry of Education and Training (VIED -MoET) and University of Technology (UTS) for giving me financial support in form of a VIED-UTS scholarship.

Sinh Cong Lam

Sydney, Australia, 2018.

List of Publications

The contents of this dissertation are based on the following papers that have been published, accepted, or submitted to peer-reviewed journals and conferences.

Journal Papers

1. **Lam, S.C.** & Sandrasegaran, K, Ha. N, Tuan. N "Performance Analysis of Fractional Frequency Reuse in Multi-Tier Random Cellular Networks", submitted Springer Wireless Networks (**IF 2016 = 1.584**).

2. **Lam, S.C.**, Sandrasegaran, K. & Ghosal, P. "A Model based Poisson Point Process for Downlink Cellular Networks using Joint Scheduling", submitted Springer Wireless Personal Communication (Aug 2017) (**IF 2016 = 0.95**).

3. **Lam, S.C.** & Sandrasegaran, K "Performance Analysis of Fractional Frequency Reuse in Uplink Random Cellular Networks", Elsevier Physical Communication (Sept 2017) (**IF 2016 = 1.58**)
   doi: https://doi.org/10.1016/j.phycom.2017.09.008.

4. **Lam, S.C.**, Sandrasegaran, K. & Ghosal, P. "Performance Analysis of Frequency Reuse for PPP Networks in Composite RayleighLognormal Fading Channel", Wireless Personal Communication (2017) (**IF 2016 = 0.95**).
   doi:10.1007/s11277-017-4215-2

5. **Lam, S.C.** & Sandrasegaran, K 2016, "Analytical Coverage Probability of a Typical User In Heterogeneous Cellular Networks", Journal of Networks (**ERA 2010=A**), Vol 11, No 2 (2016), 56-61, Feb 2016, doi:10.4304/jnw.11.2.56-61.

Conference Papers

1. **S. C. Lam**, K. Sandrasegaran, "Performance Analysis of Joint Scheduling in Random Cellular Networks," 2017 17th International Symposium on Communications and Information Technologies (ISCIT), Cairns, 2017

2. **S. C. Lam**, K. Sandrasegaran, "Optimal Strict Frequency Reuse in Cellular Networks-based Stochastic Geometry Model," 2017 17th International Symposium on Communications and Information Technologies (ISCIT), Cairns, 2017

3. **S. C. Lam**, K. Sandrasegaran and T. N. Quoc, "Strict frequency reuse algorithm in random cellular networks," 2016 International Conference on Advanced Technologies for Communications (ATC), Hanoi, 2016, pp. 447-452. DOI: 10.1109/ATC.2016.7764824

4. **S. C. Lam**, K. Sandrasegaran and T. N. Quoc, "Performance of soft frequency reuse in random cellular networks in Rayleigh-Lognormal fading channels," 2016 22nd Asia-Pacific Conference on Communications (APCC), Yogyakarta, 2016, pp. 481-487. DOI: 10.1109/APCC.2016.7581454

5. **Lam, S.C.**, Heidary, R., and Sandrasegaran, K., "A closed-form expression for coverage probability of random cellular network in composite Rayleigh-Lognormal fading channels. 2015 International Telecommunication Networks and Applications Conference (ITNAC), Sydney, Australia.
   DOI: 10.1109/ATNAC.2015.7366806

6. **Lam, S.C.**, Subramanian, R., Ghosal, P., Barua, S., and Sandrasegaran, K. "Performance of well-known frequency reuse algorithms in LTE downlink 3GPP LTE systems. 9th International Conference on Signal Processing and Communication Systems (ICSPCS), Cairns, Australia 2015. DOI: 10.1109/ICSPCS.2015.7391766

Contents

List of Figures

Abbreviation

3GPP	3rd Generation Partnership Project
BS	Base Station
CC	Cell Center
CCU	Cell-Center User
CDF	Cumulative Density Function
CE	Cell Edge
CEU	Cell-Edge User
CoMP	Coordinated Multi-Point
e-UTRA	Evolved Universal Terrestrial Radio Access
FFR	Fractional Frequency Reuse
FR	Frequency Reuse
ICI	Intercell Interference
ICIC	Intercell Interference Coordination
LTE	Long Term Evolution
MRC	Maximum Ratio Combining
MIMO	Multiple-Input and Multiple-Output
PDF	Probability Density Function
PGF	Probability Generating Function
PPP	Poisson Point Process
RB	Resource Block
RV	Random Variable
SNR	Signal-to-Noise Ratio

SINR	Signal-to-Interference-plus-Noise Ratio
UE	User Equipment

List of Symbols

α	Path Loss Exponent
α_j	Path Loss Exponent of Tier-j
Δ	Frequency Reuse Factor
Δ_j	Frequency Reuse Factor of Tier-j
ϵ	Power Control Exponent
$\epsilon_k^{(c)}$	Allocation ratio in CC Area of Tier-k
$\epsilon_k^{(e)}$	Allocation ratio in CE Area of Tier-k
$\epsilon_k^{(z)}$	Allocation ratio in z Area of Tier-k
$\hat{T}$	Coverage Threshold
$\hat{T}_j$	Coverage Threshold of Tier-j
λ	Density of BSs
$\lambda^{(c)}$	Density of BSs transmitting at CC power
$\lambda_j^{(c)}$	Density of BSs transmitting at a CC power in Tier-j
$\lambda^{(e)}$	Density of BSs transmitting at a CE power
$\lambda_j^{(e)}$	Density of BSs transmitting at a CC power in Tier-j
$\lambda^{(u)}$	Density of users
λ_j	Density of BSs of Tier-j
$\mathcal{P}_c^{(c)}$	Average coverage probability of a CCU
$\mathcal{P}_{FR}^{(c)}$	Average coverage probability of a CCU under FFR
$\mathcal{P}_{Soft}^{(c)}$	Average coverage probability of a CCU under Soft FR
$\mathcal{P}_{Str}^{(c)}$	Average coverage probability of a CCU under Strict FR

$\mathcal{P}_c^{(e)}$	Average coverage probability of a CEU
$\mathcal{P}_{FR}^{(e)}$	Average coverage probability of a CEU under FFR
$\mathcal{P}_{Soft}^{(e)}$	Average coverage probability of a CEU under Soft FR
$\mathcal{P}_{Str}^{(e)}$	Average coverage probability of a CEU under Strict FR
$\mathcal{P}_c^{(z)}$	Average coverage probability of user z
$\mathcal{P}_c$	Average coverage probability of a typical user
$\mathcal{P}_{FR}$	Average coverage probability of a typical user under FFR
$\mathcal{P}_{Soft}$	Average coverage probability of a typical user under Soft FR
$\mathcal{P}_{Str}$	Average coverage probability of a typical user under Strict FR
ϕ	Ratio between Transmit Power on a CEU and CCU
ϕ_j	Ratio between Transmit Power on a CEU and CCU of Tier-j
σ	Gaussian noise
θ	Set of BSs in the networks *(Chapter 5)*
$\theta^{(c)}$	Set of interfering BSs *(Chapter 5)*
$\theta_{Sof}^{(c)}$	Set of users *(chapter 2)*, BSs *(other chapters)* transmitting at a CC power under Soft FR
$\theta_{Str}^{(c)}$	Set of users *(chapter 2)*, BSs *(other chapters)* transmitting at a CC power under Strict FR
$\theta_{Sof}^{(e)}$	Set of users *(chapter 2)*, BSs *(other chapters)* transmitting at a CE power under Soft FR
$\theta_{Str}^{(e)}$	Set of users *(chapter 2)*, BSs *(other chapters)* transmitting at a CE power under Strict FR
$A^{(c)}$	CCU classification probability
$A_{Soft}^{(c)}$	CCU classification probability under Soft FR
$A_{Str}^{(c)}$	CCU classification probability under Strict FR
$A^{(e)}$	CEU classification probability
$A_{Soft}^{(e)}$	CEU classification probability under Soft FR
$A_{Strict}^{(e)}$	CEU classification probability under Strict FR
$C_{FR,k}^{(c)}$	Average CCU data rate in Tier-k

$C_{FR,k}^{(e)}$	Average CEU data rate in Tier-k
d_{jz}	Distance between a user j and serving BS of user z
g	Channel Power Gain from user to it's serving BS
g_{jz}	Channel Power Gain from user z to BS j
$I_{Sof}^{(z)}$	InterCell Interference of user z at under Soft FR
$I_{Str}^{(z)}$	InterCell Interference of user z at under Strict FR
K	Number of Tiers *(chapter 4)*, coordinated BS *(chapter 5)*
$M_k^{(c)}$	Number of CCUs during communication phase in CE Area of Tier-k
$M_k^{(e)}$	Number of CEUs during communication phase in CE Area of Tier-k
$M_k^{(nc)}$	Number of new CCUs during communication phase in CC Area of Tier-k
$M_k^{(ne)}$	Number of new CEUs during communication phase in CE Area of Tier-k
$M_k^{(nz)}$	Number of new z users during communication phase in z Area of Tier-k
$M_k^{(oc)}$	Number of CCUs during establishment phase in CC Area of Tier-k
$M_k^{(oe)}$	Number of CEUs during establishment phase in CE Area of Tier-k
$M_k^{(oz)}$	Number of z users during establishment phase in z Area of Tier-k
$M_k^{(z)}$	Number of z users during communication phase in CE Area of Tier-ks
N_{GL}	Degree of a Laguerre polynomial
N_G	Degree of a Legendre polynomial
P	Transmit Power of a user *(chapter 2)*, a BS *(other chapters)*
$P^{(z)}$	Transmit Power of user z
P_j	Transmit Power of BS in Tier-j
r	Distance between a user and BS
R_k	Average cell data rate in Tier-k
r_{jz}	Distance between a user z and BS j
$SINR$	SINR during a communication phase
$SINR^{(o)}$	SINR during a establishment phase
T	SINR Threshold

T_j	SINR Threshold of Tier-j
t_n and w_n	n-th node and weight of Gauss - Laguerre quadrature
x_n and c_n	n-th abscissas and weight of Gauss-Legendre quadrature
z	CC or CE

Chapter 1

Introduction to FFR and Cellular Network Models

1.1 Introduction to LTE Networks

1.1.1 LTE Requirements and Architecture

In recent years, there has been a rapid rise in the number of mobile users and mobile data traffic. According to Cisco report [1], the number of mobile users has a 5-fold growth over the past 15 years. In 2015 more than a half of a million devices have joined the cellular networks. It is predicted that the number of mobile users will reach 5.5 billion by 2020 which represents 70% of the global population. This will make mobile data traffic experience eight-fold over the next five years.

The growth of mobile subscribers as well as mobile data traffic have encouraged 3rd Generation Partnership Project (3GPP), which was established in 1998 by a number of telecommunication associations, to develop a new mobile network technology. The two main projects of 3GPP mentioned in 3GPP Release 8 are Long Term Evolution (LTE) and System Architecture Evolution (SAE). The aims of these projects are to define a new Radio Access Network (RAN) and a Core Network (CN). The LTE/SAE are designed for the purpose of supporting packet-switched data transfer. The RAN and CN are also called Evolved Packet System

	Parameter	Requirement
Downlink	Peak transmission rate	>100 Mbps
	Peak spectral efficiency	>5bps/Hz
	Average cell spectral efficiency	>1.6-2.1 bps/Hz/cell
	Cell edge spectral efficiency	>0.04-0.06 bps/Hz/cell
	Broadcast spectral efficiency	>1bps/Hz
Uplink	Peak transmission rate	>50 Mbps
	Peak spectral efficiency	>2.5 bps/Hz
	Average cell spectral efficiency	>0.66-1.0 bps/Hz/cell
	Cell edge spectral efficiency	>0.02-0.03 bps/Hz/cell
System	User plane latency (two way radio delay)	<10 ms
	Connection setup latency	<100 ms
	Operating bandwidth	1.4-20 MHz

Table 1.1 : LTE requirements [3]

(EPS) or simply an LTE network. Since packet switching is deployed throughout EPS, the LTE networks can support many types of services such as Voice over IP (VoIP) and video streaming. Consequently, all the network interfaces are based on IP protocols.

The LTE networks are designed to optimise spectrum efficiency up to two to four times that of previous 3G networks and provide higher network performance, e.g. greater than 100 Mbit/s on downlink and up to 50 Mbit/s on uplink. The latencies of LTE networks, including the latency for connection setup and handover, are expected to be lower than that of the 3G networks. Furthermore, these networks can serve users who are moving at higher speeds [2]. The requirements of the LTE networks are summarised in Table 1.1

1.1.2 Physical LTE channel

In a cellular network, in order to ensure the success of data transfer, three types of channel are defined, called physical, transport and logical channels. The physical channel refers to a radio channel which is used to convey information between a terminal device such as a User Equipment (UE) and its serving BS. The typical physical channels are characterised by the transmission capacity which is measured

by data rate per second and generally divided into *Physical Data Channel* and *Physical Control Channel* [4, 5].

- *Physical Control Channel* is used to carry the control information such as signalling information and synchronization. The control channel is shared between all BSs in downlink and all users in uplink. While the BS is continuously transmitting on the downlink control channel, the user only transmits on the uplink control channel if it is active, particularly if it has data to transfer.
- *Physical Data Channel* is designed to convey the data between the user and its serving BS. In both downlink and uplink, the data channel is utilised if there are data to be transferred.

In a LTE network, the smallest unit that can be allocated to a user is called a Resource Block (RB). Each RB is defined as having a time duration of 0.5ms and a bandwidth of 180kHz which is made up of 12 subcarriers with a subcarrier spacing of 15kHz.

1.2 Introduction to Fractional Frequency Reuse

1.2.1 Intercell Interference Coordination General Classification

In a multi-cell network, one of the main factors that directly impacts the system performance is Intercell Interference (ICI), which is caused by the use of the same RBs in adjacent cells at the same time. ICI mitigation techniques have been introduced as techniques that can significantly mitigate the ICI and improve network performance, especially for users suffering low SINRs. Generally, ICI techniques can be classified into two schemes which are referred to interference mitigation and interference avoidance [2].

Interference mitigation aims to reduce or suppress the ICI at the transmitter or at the receiver. Interference mitigation techniques include interference averaging, interference cancellation and adaptive beamforming [2, 6].

Interference averaging was introduced in an effort to randomize the interfering signals among all users by scrambling the codeword at the transmitters and the decoding at the receivers. This technique is quite simple and does not require additional measurements and signalling. However, this technique does not meet Evolved Universal Terrestrial Radio Access (e-UTRA) requirements because it does not improve the received signal strength of users [2].

Interference cancellation attempts to suppress the interference by using the processing gain at the receiver. This technique estimates the interfering signal based on previously received signals and then subtracts the estimated interfering signal from the current received signal to create a more reliable signal. ICI cancellation does not improve the strength of desired signal, but it can improve the quality of the received signal. Hence, this technique can improve the network performance. However, it requires knowledge of interference statistics and creates additional complexity at the receiver [2].

Adaptive beamforming utilizes smart antennas which can automatically change their radiation patterns to improve the received signal strength for each user. This technique is quite complex and requires additional hardware elements.

Interference avoidance or Intercell Interference Coordination (ICIC) refers to FFR schemes which are used to apply some restrictions on the transmission power and resource allocation. The aims of ICI avoidance are to reduce the ICI as well as to improve the received desired signal strength. Furthermore, this scheme does not impose any additional computation or extra hardware elements at the user device. Hence, it is expected to be the most effective technique for LTE to provide high quality of services.

1.2.2 Fractional Frequency Reuse and Related Definitions

In a LTE network, every BS is allowed to use the available bandwidth to maximize the use of spectrum. Every active user thus receives the desired signal from only one BS and other BSs are treated as interfering sources. The impact of interfering BSs on a user can be analysed according to its received SINR on a particular

RB, which is given by Equation 1.1

$$SINR = \frac{P^{(s)} g_s r_s^{-\alpha}}{\sigma^2 + \sum_{u=1}^{N} P^{(u)} g_u r_u^{-\alpha}} \tag{1.1}$$

in which $P^{(s)}$ and $P^{(u)}$ are the transmission power of serving BS s and interfering BS u; g_s and r_s, g_u and r_u are the channel power gain and distance from a user to BS s, u respectively; α is the propagation path loss coefficient; σ^2 is the Gaussian noise power; and N is the number of interfering BSs.

In a practical cellular network, the distances from a user to BSs as well as Gaussian noise power are deterministic. To improve the received SINR of the user, there should be an increase in the transmission power of the serving BS or a decrease in the number and transmission power of interfering BSs. In other words, there is a need for a technique that controls the transmission power of all BSs as well as resource allocation in the LTE network. For this purpose, FFR [7] has been proposed as a simple and effective technique compared to interference averaging and interference mitigation.

The basic idea of FFR is to divide the associated users and allocated RBs of each cell into several groups such that each user group is served by a particular RB group. In this way, the transmit power on RBs and resource allocation in each group are controlled to enhance the received signal power while reducing the interfering signal power. Conventionally, the transmit power on the RBs in a particular group are the same. In order to characterise FFR and evaluate its performance in the cellular network, the following definitions and properties are introduced.

A two-phase operation 3GPP documents [4,8] state that the operation of FFR in a LTE network can be separated into two phases. During the first phase, called *establishment phase*, the BS uses the measured SINRs and compares them with the SINR threshold in order to classify associated users into groups. After that, communication between the user and the BS is established and data is transferred during the second phase, called *communication phase*. While the data transmission

between the user and the serving BS takes place continuously, the process of user classification depends on network operators and can be adjusted appropriately [9].

SNR and SINR SNR, which is defined as the ratio between the transmit power of the transmitter (BS in downlink and user in uplink) and Gaussian noise, can be used to represent the strength of the transmitted signal at the transmitter. Meanwhile, SINR represents the signal strength at the receiver (user in downlink and BS in up link) and can be found by dividing the serving signal power by the sum of interfering signal power and Gaussian noise.

SINR threshold T The SINR threshold is introduced to classify a user into either CCU or CEU. A user is served as a CCU if its measured SINR during the establishment phase is greater than the SINR threshold. In contrast, if the measured SINR of the user during the establishment phase is less than the SINR threshold, it will be classified as a CEU. In a particular network, the value of SINR threshold can be adjusted by network operators to obtain an appropriate number of CCUs and CEUs, and optimize system performance.

User classification probability User classification probability includes CCU and CEU classification probabilities which are defined as the probabilities that a user is classified as a CCU and CEU respectively. Conventionally, CCU classification probability + CEU classification probability = 1.

Resource allocation technique The resource allocation technique is designed to divide the available RBs in each cell into CC RBs and CE RBs, which are allocated to CCUs and CEUs respectively. In the literature, various methodologies have been selected as the potential resource allocation techniques such as non-cooperation and cooperation game theories, which were summarised in [6].

Transmit power ratio ϕ Conventionally, the BS transmits on the CE RB at a higher power than on the CC RB. Within the content of this thesis, the transmit

power on the CC RB and CE RB are called *CC power* and *CE power*, respectively. The ratio between the CE and CC powers is defined as a *transmit power ratio*. In a particular network, the selection of the transmit power ratio could be based on a heuristic approach [10] and depends on various network parameters, such as the network interference and user requirement.

Coverage threshold $\hat{T}$ Coverage threshold is defined as the minimum requirement for SINR during the communication phase to successfully perform specific tasks such as data transfer or modulation and coding. For example, to perform a 16 Quadrature Amplitude Modulation (16 QAM) in a LTE network, the minimum required SINR is 7.9 dB [3], then $\hat{T} = 7.9$ dB.

Frequency Reuse Factor Δ Frequency Reuse factor presents the number of BSs that use the whole allocated frequency resources, same frequency reuse patten.

Average Coverage Probability Average coverage probability is defined as the probability in which the SINR during the communication phase is greater than the coverage threshold $\hat{T}$. In other words, average coverage probability represents the probability of a successful transmission. For example, the successful transmission probability of video streaming at 2000 kbps in a LTE network with downlink $SINR > 20$ dB is 82.7% [11].

Average data rate Average data rate is the speed at which data is transferred between the user and its serving BS. Conventionally, average data rate is computed by Shannon Theory and measured in bit per second per Hz.

InterCell Interference To determine the number of interfering BSs for a user who is served on a particular RB, we denote λ (BS/km^2) as the density of BSs in the network, S (km^2) is the network coverage area. Since in a practical network the cellular network can cover an area of hundred kilometres, $\lambda S >> 1$. With an assumption that in both downlink and uplink, each RB is allocated to a user during

a given timeslot and vice versa, the number of BSs and users that transmit on the same RB in downlink and uplink respectively are the same.

In a LTE network, the BSs and users which are in adjacent cells and occupy the same RB with the user of interest are treated as the interfering sources of that user in downlink and uplink respectively. $\theta_{FR}^{(c)}$ and $\theta_{FR}^{(e)}$ are defined as the set of interfering sources transmitting on CC and CE powers, $\lambda_{FR}^{(c)}$ and $\lambda_{FR}^{(e)}$ are the density of interfering sources in the corresponding sets, $FR = (Str, Soft)$ corresponds to Strict FR and Soft FR. For interference analysis purposes, if a BS or user does not transmit on the RB of interest, we simply remove that BS or user from the network and change λ appropriately. Hence, it can be assumed that all BSs and users transmit on all allocated RBs in downlink and uplink, respectively.

In this thesis, two well-known schemes of FFR, called Strict FR as shown in Figure 1.1 and Soft FR as shown in Figure 1.2, are investigated. Under these schemes, the available RBs are divided into two groups of f_c and f_e RBs, in which the transmit powers on all RBs of a given group are the same, such as at the CC power for f_c RBs and CE power for f_e RBs.

Strict FR In a Strict FR network, f_c CC RBs are used as the common RBs for all CCUs in every BS, and consequently each CCU experiences interference originated from all $\lambda S - 1$ adjacent sources with a density of $\lambda_{Str}^{(c)} = \frac{\lambda S-1}{S} \approx \lambda$. Meanwhile f_e RBs are further partitioned by FR factor Δ into Δ CE RB groups of $\frac{f_e}{\Delta}$ RBs, in which each group is used as private RBs within a group of Δ cells so that adjacent cells within that cell group do not use the same CE RB. Therefore, each CEU is affected by interference generated from $\frac{\lambda S-1}{\Delta}$ sources with a density of $\lambda_{Str}^{(e)} = \frac{\lambda S-1}{\Delta S} \approx \frac{\lambda}{\Delta}$.

It is noticed that since there is no sharing between the CCUs and CEUs in terms of RBs, the signal on a CC RB in both downlink and uplink are not affected by the signal on a CE RB and vice versa. Hence, $\lambda_{Str}^{(e)} = 0$ in the case of CCU and $\lambda_{Str}^{(c)} = 0$ in the case of CEU.

The above discussion can be summarised by the following two properties

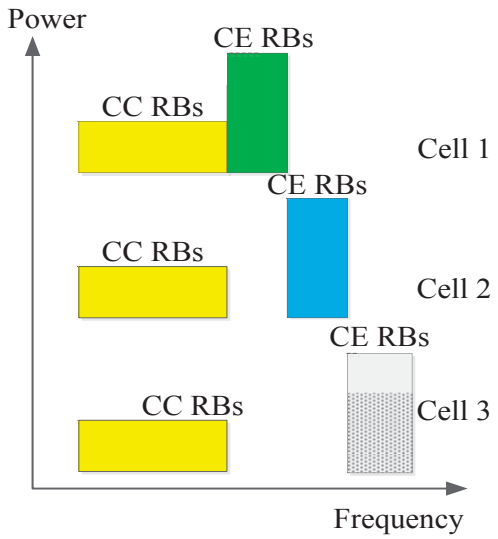

Figure 1.1 : An example of Strict FR

Property 1: The densities of interfering sources of a CCU and CEU under Strict FR are given by.

1. *In the case of CCU,* $\lambda_{Str}^{(c)} = \lambda$ *and* $\lambda_{Str}^{(e)} = 0$.
2. *In the case of CEU,* $\lambda_{Str}^{(c)} = 0$ *and* $\lambda_{Str}^{(e)} = \frac{\lambda}{\Delta}$.

Property 2: All interfering sources of a user under Strict FR have the same transmit power, which is the transmit power of the serving BS in downlink and user of interest in uplink.

Soft FR Soft FR scheme is a modification of Strict FR, in which each cell is allowed to reuse all RBs, i.e. $f_e + f_c$, in an effort to improve spectrum efficiency and system performance. Thus, an RB can be used as a CC RB at a given cell and re-used as a CE RB at an adjacent cell. As a result, both CC and CE RB experiences interference originating from sources in $\theta_{FR}^{(c)}$ and $\theta_{FR}^{(e)}$. The number of interfering sources in $\theta_{FR}^{(c)}$ and $\theta_{FR}^{(e)}$ are $\frac{\Delta-1}{\Delta}\lambda S - 1$ and $\frac{1}{\Delta}\lambda S$ in the case of CCU, and $\frac{\Delta-1}{\Delta}\lambda S$ and $\frac{1}{\Delta}\lambda S - 1$ in the case of CEU. Since $S >> 1$, $\frac{1}{S} \approx 0$. Hence, $\lambda_{Soft}^{(c)} = \frac{(\Delta-1)\lambda}{\Delta}$ and $\lambda_{Soft}^{(c)} = \frac{\lambda}{\Delta}$ This property of Soft FR can be formulated as follows

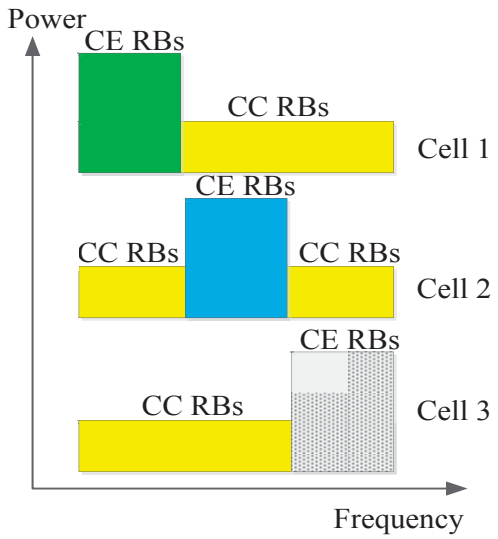

Figure 1.2 : An example of Soft FR

Property 3: The densities of interfering sources under Soft FR for both CCU and CEU are $\lambda_{Soft}^{(c)} = \frac{(\Delta-1)\lambda}{\Delta}$ *and* $\lambda_{Soft}^{(c)} = \frac{\lambda}{\Delta}$.

Consequence 4: Under both Strict FR and Soft FR, a CEU achieves a higher SINR than a CCU.

In the case of Strict FR, Property 2 on Page 9 indicates that the changes in a transmit power do not influence the impact of interference on user performance, while Property 1 on Page 9 states that the number of interfering sources of a CEU is smaller than that of a CCU. Hence, compared to a CCU, a given user will suffer lower interference and then higher SINR if it is served as a CEU. In the case of Soft FR, since both CCU and CEU experience interference with the same statistical distribution, a CEU with a higher serving power will achieve a higher SINR, which is compared to a CCU.

1.3 Cellular Network Models

1.3.1 Hexagonal and Wyner Network Models

The two-dimensional (2-D) traditional hexagonal network model with deterministic BS locations, as shown in Figure 1.3, is the most popular model that is used to analyse a cellular network. In this model, a service area is divided into several hexagonal cells with *same* radius, in which each cell is served by a BS at the center of the cell. Tractable analysis was often achieved for a fixed user with limited number of interfering BSs or by ignoring propagation path loss [12].

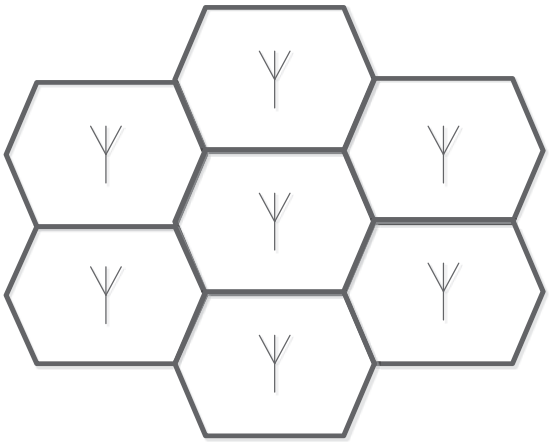

Figure 1.3 : An example of hexagonal network model

This model is not suitable for modelling a practical cellular network since cell radius and BS locations significantly vary due to user density as well as wireless transmission environment.

Another tractable and simple model is the Wyner model [13] which was developed by information theorists and has been widely used to evaluate the performance of cellular networks in both uplink and downlink [14–17]. Recently, it has been extended for Multiple-Input and Multiple-Output (MIMO) networks in [18] and CoMP networks in [19]. In Wyner and its modified models, users were assumed to have fixed locations and interference intensity was assumed to be deterministic

and homogeneous. However, for a practical wireless network, user locations may be fixed, but interference levels vary considerably depending on several factors such as receiver and transmitter locations, transmission conditions, and the number of instantaneous interfering BSs.

To validate the accuracy of the Wyner model, authors in [20] compared the performance of a 1-D Wyner model with a 1-D grid-base model of networks with a single-cell with random user locations in terms of outage probability and average throughput. The analysis indicated that for uplink, the Wyner model achieved inaccurate results for system performance for a small number of simultaneous users. For downlink, the results were better, but they were still inaccurate for outage probability and system performance in the case of equal user transmission power.

Traditional hexagonal model and Wyner model may be not suitable to evaluate the performance of multi-cell wireless networks, thus the PPP network model has been proposed and developed as the accurate and flexible tractable model for cellular networks [21, 22].

1.3.2 Poisson Point Process

A homogeneous PPP is the most common stochastic geometry object that is used to model the wireless communication. It consists of points randomly located on a plane of a d-dimensional Euclidean space $\mathbb{R}^d$ [23, 24]. Conventionally, the PPP is characterised by random points with a density of λ. Thus, the homogeneous PPP can be defined by two fundamental properties [24]:

1. The random number of points n in area A of $\mathbb{R}^d$ is given by an exponential distribution

$$P(n) = \frac{(\lambda A)^n}{n!} \exp(-\lambda A) \tag{1.2}$$

2. The numbers of points in disjoint areas are independent Random Variables (RVs), in which each point in a given area is uniformly distributed.

In the application of PPP in mobile network modelling, each point of PPP represents either a BS or a user while λ represents the corresponding density. A cellular network which is based on a PPP is called *a PPP network* or *random cellular network*. In this thesis, the following properties of PPP will be employed [25].

Distance to the nearest BS (r) In a basic PPP wireless network model, the user is assumed to be located at the origin while the BSs are randomly distributed around it. Thus, the user is allowed to associate with the nearest BS at a distance r. In this case, all neighbouring BSs must be located further than r. Since the null probability of a 2-D Poisson process with density λ in a globular area with radius R is $\exp(-2\pi\lambda R^2)$, the Cumulative Density Function (CDF) of the distance is given by [24, 26]:

$$F_R(r) = \mathbb{P}(r < R) = 1 - \mathbb{P}(r > R) = 1 - e^{-\pi\lambda R^2}$$

then the Probability Density Function (PDF) can be obtained by finding the derivative of the CDF:

$$f_R(r) = \frac{dF_r(r)}{dr} = 2\pi\lambda r e^{-\lambda\pi r^2} \tag{1.3}$$

Probability Generating Function Let $\Theta\{l_i; i = 1, 2, ...\}$ defines a PPP with a density of λ in $\mathbb{R}^2$. The Probability Generating Function (PGF) is defined by [24]

$$\mathbb{E}\left[\prod_{l_i \in \Theta} f(l_i)\right] = \exp\left(-\lambda \int_{\mathbb{R}^2} (1 - f(l)dl)\right) \tag{1.4}$$

In Equation 1.4, l represents the Cartesian coordinates in $\mathbb{R}^2$, which can be converted into polar coordinates by using a change of variable $dl = r_0 dr_0 d\theta$, in which θ is the angle of $\vec{l}$, r_0 is the distance from point l to the origin. Thus, the PGF equals

$$\mathbb{E}\left[\prod_{l_i \in \Theta} f(l_i)\right] = \exp\left(-\lambda \int\int (1 - f(r_0)dr_0 d\theta)\right) \tag{1.5}$$

Conventionally, θ is chosen as $(0 \leq \theta \leq 2\pi)$ while r_0 depends on the point's location of interest in Θ. Within the content of this thesis, the PGF is derived for points in

Θ except the nearest point whose distance to the origin is r, and then $r_0 > r$. Thus, the PGF is obtained by

$$\mathbb{E}\left[\prod_{l_i \in \Theta} f(l)\right] = \exp\left(-2\pi\lambda \int_r^{\infty} (1 - f(r_0)dr_0)\right) \tag{1.6}$$

Thinning Property Let $\Theta\{l_i; i = 1, 2, ...\}$ defines a PPP with a density of λ in $\mathbb{R}^2$. Denote Θ_1 and Θ_2 as two disjoint sub-sets of Θ and $\Theta_1 \bigcup \Theta_2 = \Theta$, thus Θ_1 and Θ_2 are PPPs with densities of λ_1 and λ_2 where $\lambda_1 + \lambda_2 = \lambda$ [26].

1.3.3 Homogeneous PPP network model

A homogeneous Poisson cellular network model is the simplest PPP model with a single hierarchical level. In this model, the service area is partitioned into non-overlapping Voronoi cells [21, 22], in which the number of cells is a Poisson RV. Each cell is served by a unique BS that is located at its nucleus (as shown by large dots in Figure 1.4). Users are distributed following a stationary point process (as shown by small dots in Figure 1.4) and allowed to connect with the strongest or the closest BSs. In the strongest model, each user measures SINR from several candidate BSs and selects the BS with the highest SINR. In the closest model, the distances between the user and BSs are estimated, and the nearest BS is selected as the serving BS.

In Figures 1.4 and 1.5, we consider a 6 km x 6 km service area where the distribution of BSs is a PPP with density $\lambda = 0.25$ and $\lambda = 0.3$ respectively. It can be observed that the boundaries of the cell as well as the locations of BSs in this model are generated randomly to correspond with a practical network. The main weakness of this model is that sometimes BSs are located very close together, but this can be overcome by taking the average from multiple simulation results of network performance.

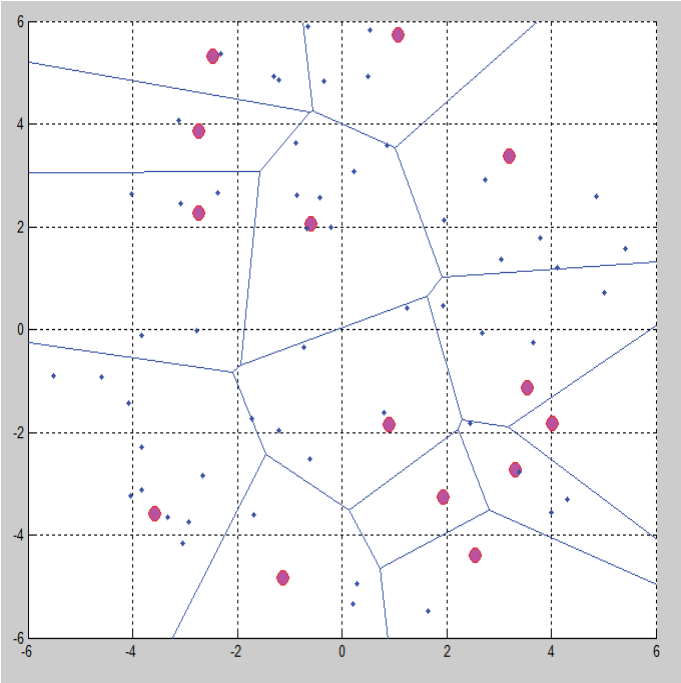

Figure 1.4 : An example of PPP network model with $\lambda = 0.25$

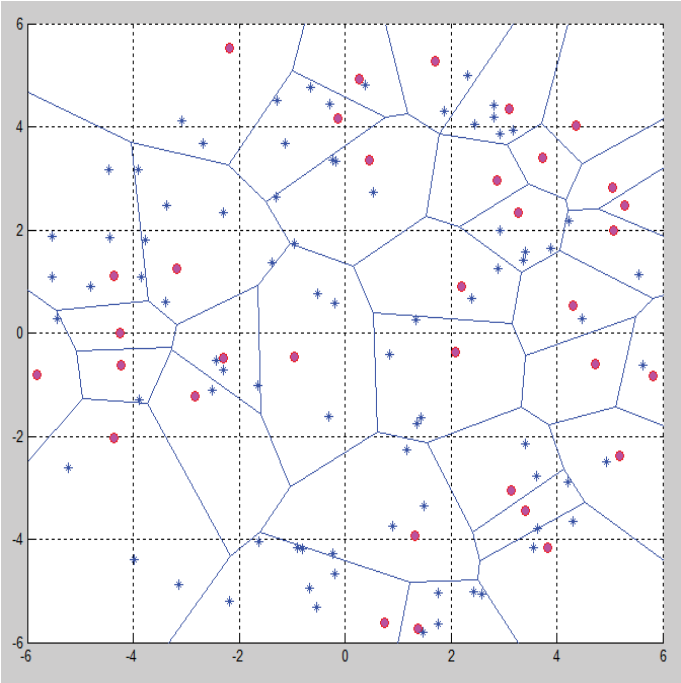

Figure 1.5 : An example of PPP network model with $\lambda = 0.3$

1.3.4 Heterogeneous network PPP model

In a heterogeneous network with K-tiers, some BSs called pico and femto cells are deployed with lower transmission powers compared to macro BSs in order to provide mobile service in small areas with a higher user density or poor coverage. The pico cells and femto cells are called small cells and are located within the coverage area of macro cells as shown in Figure 1.6. Their parameters, including location, size and shape, are usually different to macro cells due to the variation of wireless network traffic or electromagnetic transmission conditions. Hence, it is not easy to model the heterogeneous networks by using traditional hexagonal or Wyner model. This problem can be solved by considering k independent PPPs with densities of λ_1, λ_2, ..., λ_k as shown in Figure 1.6.

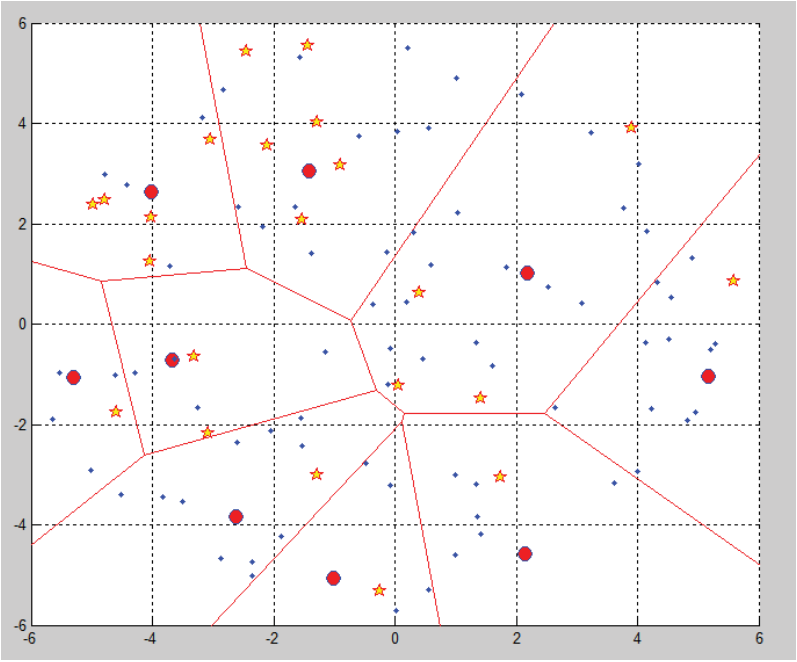

Figure 1.6 : Heterogeneous network with macro cells as large dots ($\lambda = 0.1$) and pico cells as stars ($\lambda = 0.2$).

1.3.5 Simulation of Mobile Networks based PPP

1.3.5.1 Simulation Setup

In simulation of a mobile network using the PPP model, a circular network area with radius R_A $(0 < R_A < \infty)$ is considered. The typical user is located at the origin while the location of a BS is randomly generated within the circle as shown in Figure 1.7. The coordinates of the user and BS are denoted by $UE(0,0)$ and $BS(x,y)$, respectively in which x and y are uniform RVs [26, 27] and $\sqrt{x^2+y^2} \leq R_A$.

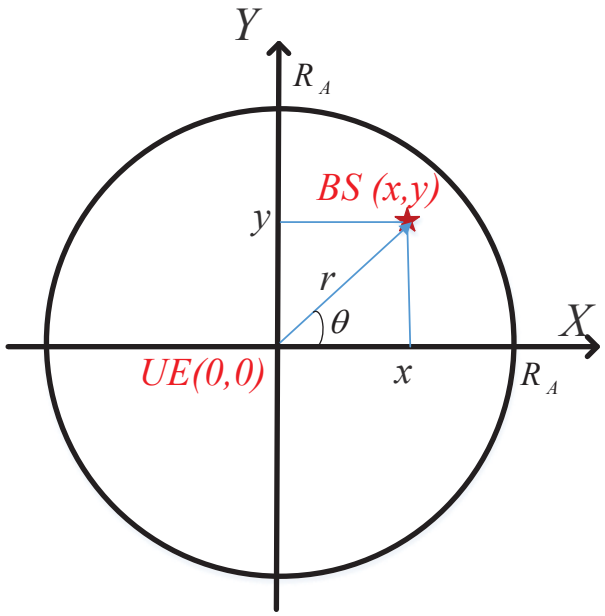

Figure 1.7 : a PPP simulation model

The joint distribution function of x and y, which in this case is the PDF of random points inside the circle, is given by

$$f_{X,Y}(x,y) = \frac{1}{\pi R_A^2} \tag{1.7}$$

Using the polar coordinate system transformation by letting $x = r\cos(\theta)$ and $y = rsin(\theta)$ in which r and θ are independent RVs $(0 \leq r \leq R_A$ and $0 \leq \theta \leq 2\pi)$, the joint distribution function in Equation 1.7 can be written as a joint distribution

function of r and θ as in Equation 1.7 [28]

$$f_{X,Y}(x,y) = \frac{1}{|J|} f_{R,\Theta}(r,\theta) \tag{1.8}$$

in which $|J|$ is the determinant of the Jacobian matrix

$$|J| = \begin{vmatrix} \frac{dx}{dr} & \frac{dy}{dr} \\ \frac{dx}{d\theta} & \frac{dy}{d\theta} \end{vmatrix} = r \tag{1.9}$$

Since r and θ are independent RVs,

$$f_R(r) f_\Theta(\theta) = f_{R,\Theta}(r,\theta) = \frac{r}{\pi R_A^2} = \frac{1}{2\pi} \frac{2\pi}{R_A^2}$$

in which $f_R(r)$ and $f_\Theta(\theta)$ are PDF of R and Θ.

For simplicity, we choose Θ as a uniform RV over the interval 0 to 2π and its PDF is $f_\Theta(\theta) = \frac{1}{2\pi}$. Then, the PDF of R is $f_R(r) = \frac{2r}{R_A^2}$ and its CDF is achieved by $F_R(r) = \int_0^r f_R(x)dx = \frac{r^2}{R_A^2}, \quad (0 \le r \le R_A)$.

Since $F_R(r)$ can be considered as a uniform RV U between 0 and 1,

$$U = \frac{R}{R_A^2} \quad \Longrightarrow \quad R = R_A\sqrt{U} \tag{1.10}$$

Consequently, the distance from the user to the BS, r, is generated by following Equation 1.10.

On Matlab, the simulation program can be based on the fundamental functions such as *poissrnd* to generate the number of BSs N and $sqrt(rand(N,1))$ to generate the corresponding distances from the user to the BSs.

1.3.5.2 Simulation Algorithm

The following general algorithm is programed in Matlab and used with appropriate changes to obtain the simulation results in Chapters 2, 3 4 and 5.

Algorithm 1 Average Coverage Probability Simulation

Input: network area S, density of BSs λ, the number of simulation runs $SimRun$

for index = 1:1:$SimRun$

Step 1: Generate the number of BSs

Step 2: Generate the distance from the user to BSs

Step 3: Generate channel power gains

Step 4: Calculate SINR

if SINR > coverage threshold

Count_Coverage_Event=Count_Coverage_Event+1 ;

end

end

Result: Coverage_Probability= Count_Coverage_Event/SimRun

In order to obtain the stable simulation results, the number of simulation runs should be greater than 10^5 and the radius of the network coverage area R should be greater than 60 km. For each run, the number of BSs, distance from the user to BSs, channel power gain are generated by the following rules:

- The number of BSs is a Poisson RVs with a mean of $\pi\lambda R^2$.
- The distance from the user to BSs are generated according to theoretical analysis in Section 1.3.5.1.
- Channel power gains are generated as exponential RVs.

In Chapters 2, 3 and 5, the user is assumed to associate with the nearest BS. Thus, the smallest RV that is generated from Step 2 is selected as the distance from the user to its serving BS while other RVs are considered as distances from the user to its interfering BSs. In Chapter 4, the user connects to the BS with the strongest received signal power or smallest path loss. Thus, the path loss are calculated as the function of the distance and the path loss exponent. The BS with the smallest path loss is selected as the serving BS while other BSs are treated as the interfering

BSs. SINR calculated by computing the ratio between the signal power from the serving BS and the sum of signal powers from the interfering BSs.

In all simulation results, the number of simulation runs and radius of the network area are selected so that the variances of simulation results are smaller than 10^{-4}.

1.4 Literature Review on FFR in Random Cellular Networks

Although, the PPP network model has been studied as early as 1997 in [29], some initial important results on the single-tier LTE network performance were presented in 2010s [22,30,31] under Rayleigh fading. The user performance in terms of average coverage probability and average data rate were derived. Following the success of these works, the network performance under various radio transmission environments were discussed such as [32] for Generalized fading, [33,34] for Rayleigh-Lognormal fading, [35] for Rician fading, and [36] for multi-slope path loss model.

Based on the results in [22, 30], the LTE networks with FFR were investigated in [37, 38] for downlink under Rayleigh and Rayleigh-Lognormal fading, and [39] for uplink. In those works, the operation of the CEU was separated into establishment phase and communication phase. The users were classified as CCUs and CEUs during the establishment phase, which was followed by data transfer during the communication phase. Thus, the user performance was defined as the conditional probability of the coverage probability during the communication phase under condition of SINR during the establishment phase. This two-phase definition was very important since it followed the recommendations of 3GPP [4, 8] and derived a new approach to analyse the performance of FFR in random cellular networks.

The multi-tier cellular networks were modelled and analysed in [40–44], in which each tier was considered as a PPP. In these networks, the density of the small cells, which have low transmit powers, is expected to be greater than the density of the macro cells, which transmit at high powers. Therefore, in the case of the nearest model, the user tends to associate with the small cells rather than macro

cells. Meanwhile, in the case of the strongest model, the macro cells usually provide higher SINRs than the small cells, and then the user prefers a connection with macro cells. These may lead to overload of small cells in the nearest model and macro cells in the strongest model. To avoid overloading, the authors in [40, 42, 43] introduced a bias factor to handover users from a given tier to other tiers. Furthermore, these works modelled the users as a PPP, and then the average numbers of users in each cell and each tier were evaluated.

The optimization problem for the PPP networks has attracted a lot of attention. In [45–47], the bias factor was optimised for both uplink and downlink. Authors in [47] stated that there exists an optimal value of the bias factor and the average coverage probability achieves its maximum. In [45, 46], the utility maximization framework was designed based on a proportionally fair measure of user coverage to optimize the bias and the reuse factor. In other works, the power consumption of the BSs was taken into the optimization problem. References [48, 48, 49] presented a method to optimise the FR factor and number of BSs to maximise the system throughput as well as minimise energy consumption. In [50], the optimal value of SINR threshold was analysed. By comparing the network performance when SINR threshold is greater and smaller than the coverage threshold, the author concluded that the optimal value of SINR threshold can be selected at the coverage threshold.

1.5 Research Problem and Thesis Organization

1.5.1 Research Problem

The performance of well-known FFR schemes, such as Strict FR and Soft FR, have been discussed in the literature. However, these research works have posed a number of questions that need to be investigated.

1. **Use of a constant coefficient to estimate the network interference**

To evaluate the network interference, authors in [37, 39] introduced a constant coefficient to consolidate the interference from $\theta_{FR}^{(c)}$ and $\theta_{FR}^{(e)}$. In the PPP model, since each BS is distributed randomly and completely independent to other BSs,

$\theta_{FR}^{(c)}$ and $\theta_{FR}^{(e)}$ are independent (*thinning property*), and thus they should not be consolidated.

2. **Simplification of the performance metrics**

The final expressions of performance metrics have been presented in the forms of the double or triple integrals. The authors in [44, 51] presented an approach to reduce the number of integral layers by assuming that the received SINR of a given user between two phases, denoted by $SINR^{(o)}$ and $SINR$, are independent RVs. Thus, the joint probability $\mathbb{P}(SINR > \hat{T}, SINR^{(o)} < T)$ was simply obtained by $\mathbb{P}(SINR > \hat{T})\mathbb{P}(SINR^{(o)} < T)$ in which T and $\hat{T}$ are SINR threshold and coverage threshold respectively. However, since both $SINR$ and $SINR^{(o)}$ are functions of the distances from the user to the interfering BSs which are RVs and do not change between two phases, $SINR^{(o)}$ and $SINR$ are correlated RVs. Therefore, this assumption is not reasonable for the downlink PPP network model.

3. **The closed-form expressions of performance metrics**

The performance metrics in terms of average coverage probability was derived in the case of Interference-Limited networks (Gaussian noise $\sigma = 0$) with an FR reuse factor of $\Delta = 1$ [45]. In the general cases such as $\sigma > 0$ and $\Delta > 1$, the closed-form expression have not been derived in the literature.

4. **Effects of the number of users and RBs on the network performance have not been well-investigated**

Effects of the number of users and RBs were discussed in [42,46,48,52]. However, it was assumed that all BSs use the same transmit power which implies that there is no difference between a CCU and CEU. Furthermore, the impact of the number of users on the network interference was not considered, and hence it was assumed that all BSs create ICI to the users, which is reasonable only if all RBs are utilised at the same time.

5. **Use of 3GPP recommendations on LTE networks to model the operation of FFR**

Although the deployment of FFR has not been standardised in a practical net-

work, the standards of LTE have been finalised by 3GPP [4, 5, 53, 54]. Hence, following 3GPP recommendations, such as downlink and uplink signal measurement for user classification purpose during the establishment phase, to model FFR is an essential step to provide a better performance examination of these schemes in the random cellular networks.

6. **Modelling of CoMP technique in random cellular networks using FFR is not well-investigated**. The literature review and problem statement of CoMP in random cellular networks will be derived in Chapter 5 as development of research work in Chapters 2-4.

1.5.2 Thesis Organization and Contributions

In this thesis, the LTE networks using FFR technique are modelled based on the recommendations of 3GPP. The PPP is utilised to model the network topology. Mathematical analysis approaches are used throughout the thesis to obtain the theoretical results while Monte Carlo simulations are used to verify the analytical results. The performance expressions and their closed-forms are derived under Rayleigh fading channel. The main contribution and organization of this thesis are briefly outlined.

Chapter 2 - Performance of FFR in Downlink Random Cellular Networks

In this chapter, Problems 1, 2, 3 and 5 are investigated for the downlink cellular networks. The single-tier downlink cellular networks using FFR are modelled by following the recommendation of 3GPP, in which SINRs on the control channels are utilised for user classification purpose. Instead of using the constant coefficient to model the network interference as in the literature, the interference originated from $\theta_{FR}^{(c)}$ and $\theta_{FR}^{(e)}$ are separately evaluated in this chapter. The closed-form expressions of user performance are derived by utilising Gauss - Laguerre and Gauss - Legendre Quadratures. The comparisons between our models and the related works are discussed in this chapter.

Chapter 3 - Performance of FFR in Uplink Random Cellular Networks

This chapter develops the problems and solutions in Chapter 2 for the uplink cellular networks. The approximation approaches are utilised to obtain the closed-form expressions of performance metrics. The effects of user transmit power on the user classification probability and network performance are discussed, and thus the optimal value of user transmit power is analysed. To examine the effects of the density of BSs on the network performance, three network scenarios corresponding to three different BS's densities are discussed and compared.

Chapter 4 - Performance of FFR in Multi-Tier Downlink Random Cellular Networks

This chapter presents a solution for Problem 4. The allocation ratio, which is defined as the ratio between the number of users and RBs, is used to represent the effects of users and RBs on the network interference. A new network model using FFR in which SINRs on the data channels are used for user classification purpose is proposed. Furthermore, optimal value of SINR threshold and bias factor are analysed.

Chapter 5 - Modelling Coordinated Multi-Point Transmission in Random Cellular Networks

This chapter provides solutions for Problem 6 by presenting models to analyse performance of two well-known CoMP techniques, called Joint Scheduling and Joint Transmission with Selection Combining, in the random cellular networks using FR with a reuse factor of 1. In the case of Joint Scheduling, a two-phase operation is proposed. In the case of Joint Transmission with Selection Combining, the downlink SINR is modelled when the user observes SINR from different RBs. In both cases, the average coverage probabilities of the user are derived under Rayleigh fading channel. For the CoMP with a cluster size of $K = 2$, the closed-form expressions are derived.

Chapter 6 - Conclusions and Future works

The main contribution of the thesis are highlighted. This chapter provides a short discussion about some potential future research directions which based on the results of this thesis.

Generally, the thesis makes contributions on network modelling and mathematical analysis. The downlink and uplink of LTE network using FFR are modelled according to 3GPP recommendations and analysed by using Stochastic Geometry. The close-form expressions of performance metrics are derived based on approximation approaches. Furthermore, the dissertation proposes a new FFR scheme to improve the network performance.

Chapter 2

Performance of FFR in Downlink Random Cellular Networks

In this chapter, a PPP model based on 3GPP recommendations [4,8] is developed to model a two-phase operation of two well-known schemes of FFR, called Strict FR and Soft FR, in the downlink single-tier cellular networks. The tractable expressions of network performance are derived in terms of CCU and CEU classification probabilities and corresponding coverage probabilities. The Gaussian Quadratures are utilised to approximate the complicated formulations of the network performance by the simple finite sum which can be considered as the closed-form expressions.

2.1 Network model

This chapter studies the model of single-tier cellular networks in which the BSs are distributed according to a PPP model with a density of λ. A typical user is randomly located according to an independent stationary point process in a Voronoi cell and has connection with the nearest BS.

Without loss of generality, a typical user is assumed to be located at the origin and served by a BS at distance r whose PDF is given by Equation 1.3:

$$f_R(r) = 2\pi\lambda r e^{-\lambda\pi r^2} \tag{2.1}$$

It is assumed that the number of users in each cell is greater than that of RBs. Thus, all RBs are fully employed to serve the active users. Consequently, each user is affected by ICI originating from all adjacent BSs.

2.1.1 Channel model

Statistical path loss model

In most statistical models of wireless networks, it is assumed that all receiver antennas have the same gain and height. The received signal power of a receiver at a distance r from the transmitter can be given by Equation 2.2 [55]:

$$P(r) = Pr^{-\alpha} \tag{2.2}$$

The propagation path loss in dB unit is obtained by

$$PL(dB) = 10\log_{10}\left(\frac{P(r)}{P}\right) = -10\alpha\log_{10} r \tag{2.3}$$

in which α is path loss exponent and P is the transmission power of the transmitter. The values of α, which were found from field measurements, are listed in Table 2.1 [56]

Environment	Path loss coefficient
Free space	2
Urban Area	2.7 - 3.5
Suburban Area	3 - 5
Indoor (line-of-sight)	1.6 - 1.8

Table 2.1 : Propagation path loss coefficient

Due to the variation of α with changes of transmission environment, a signal propagating over a wide range of areas can be affected by different attenuation mechanisms. For example, the first propagation area near the BS is free-space area where $\alpha = 2$ and the second area closer to the user may be heavily-attenuated area such as an urban area where $\alpha = 3$. In particular cellular networks, the path loss

can be estimated by measuring received signal strength at the receiver and then overcome by increasing the transmission power.

Channel fading model

In wireless systems, the signal at the receiver is a result of multipath effect which is caused by local scatters such as buildings. In the case of not dominant propagation along line of sight between the user and the BS, the multipath effect is usually modelled as Rayleigh fading whose PDF and CDF are given by [12].

$$f_H(h) = \frac{2h}{\overline{h}} e^{-\frac{h^2}{\delta^2}} \text{ and } F_H(h) = 1 - e^{-h^2/(2\delta^2)} \tag{2.4}$$

in which δ is the scale parameter. Within the content of the thesis, it is assumed that $\delta = 1$.

In the thesis, the power of the fading channel $G = H^2$ is considered. It is noted that H is the name of the RV, h is the value of the RV. The CDF of G can be obtained by following steps

$$F_G(g) = P(G < g) = P(H^2 < g) = P(H < \sqrt{g}) = F_H(\sqrt{g}) = 1 - e^{-g} \tag{2.5}$$

Then, the PDF of G is given by

$$P_G(g) = \frac{dF_G(g)}{dg} = e^{-g} \tag{2.6}$$

2.1.2 Fractional Frequency Reuse

Since a CE power is higher than a CC power, the transmit power of user z is denoted by $P^{(z)} = \phi^{(z)} P$ where $z = (c, e)$ corresponds to the CCU and CEU, $\phi^{(e)} = \phi$ ($\phi > 1$) is a transmit ratio between the CE and CC powers, and $\phi^{(c)} = 1$. Each RB can be used at adjacent cells at the same time, and consequently each user can experience interference from other BSs transmitting on the same RB. The set of BSs that create interference to user z is denoted by $\theta_{FR}^{(z)}$ and $I_{FR}^{(z)}$ is the corresponding interference power, in which $FR = (Str, Sof)$ correspond to Strict FR and Soft FR.

Denote θ as the set of all BSs in the networks, hence $\theta = \theta_{FR}^{(c)} \bigcup \theta_{FR}^{(e)}$.

Establishment phase

During the establishment phase, the users under both Strict FR and Soft FR measure and report the received SINRs on the downlink control channels [4, 8] for user classification purpose. Every BS is continuously transmitting downlink control information, and subsequently each control channel experiences the ICI from all adjacent BSs. Furthermore, since all BSs are assumed to transmit on the control channels at the CC power, the interference of the measured SINR during this phase is given by

$$I = \sum_{j \in \theta} P g_{jz} r_{jz}^{-\alpha} \tag{2.7}$$

where g_{jz} and r_{jz} are the power gain and distance from interfering BS j to user z.

Communication phase

Under Strict FR, since the CCUs do not share their own RBs with the CEUs and vice versa, $I_{Str}^{(z)}$ originates from BSs in either $\theta_{Str}^{(c)}$ or $\theta_{Str}^{(e)}$ whose densities are given by Property 1 on Page 9. The power of interference $I_{Str}^{(z)}$ of user z is

$$I_{Str}^{(z)} = \sum_{j \in \theta_{Str}^{(z)}} P_j^{(z)} g_{jz} r_{jz}^{-\alpha} \tag{2.8}$$

Under Soft FR, since each cell can reuse all RBs, each user may experience interference from both $\theta_{Sof}^{(c)}$ and $\theta_{Sof}^{(e)}$ whose densities are given by Property 3 on Page 10. In this case, $I_{Sof}^{(z)}$ is given by

$$I_{Sof}^{(z)} = \sum_{j \in \theta_{Sof}^{(c)}} P_j^{(c)} g_{jz} r_{jz}^{-\alpha} + \sum_{j \in \theta_{Sof}^{(e)}} P_j^{(e)} g_{jz} r_{jz}^{-\alpha} \tag{2.9}$$

It is noted that both CCU and CEU under Soft FR have the same statistical expression of interference (Property 1).

The received SINR at user z from the BS at distance r is given by

$$SINR(\phi^{(z)}, r) = \frac{\phi^{(z)} P g r^{-\alpha}}{\sigma^2 + I_{FR}^{(z)}} \tag{2.10}$$

in which σ^2 is the Gaussian noise power, g and r are the power gain and distance from user z to the serving BS.

2.1.3 User Classification Probability

In the downlink 3GPP cellular networks, the SINR on the control channel during the establishment phase, denoted by $SINR^{(o)}(1, r)$, is reported to the BS by the user, in which 1 in $SINR^{(o)}(1, r)$ means the transmit power on the control channel is P. If the reported SINR is greater than the SINR threshold T, the user will be classified as a CCU; otherwise it will be classified as a CEU.

The probability, that a user at a distance r from its serving BS is classified as a CCU, is denoted by $A^{(c)}(T, \lambda|r)$. Since in the PPP cellular network model, $SINR^{(o)}(1, r)$, and consequently the probability $P(SINR^{(o)}(1, r) > T)$ are functions of RVs such as the distances from the user to the BSs, to calculate $A^{(c)}(T, \lambda|r)$, the expected value of $P(SINR^{(o)}(1, r) > T)$ has to be evaluated. Hence, $\mathbb{P}$ is used to denote the probability, instead of P in this thesis. Consequently, $A^{(c)}(T, \lambda|r) = \mathbb{P}(SINR^{(o)}(1, r) > T)$.

The Strict FR and Soft FR networks use the same approach to classify the associated users. Thus, the CCU and CEU classification probabilities, which were defined in Section 1.2.2, are the same for these FR schemes. The CCU classification probability is obtained by integrating $A^{(c)}(T, \lambda|r)$ over the networks, and then it is denoted by $A^{(c)}(T, \lambda)$. It is clear that the *CEU classification probability* can be obtained by $A_{FR}^{(e)}(T, \lambda) = 1 - A_{FR}^{(c)}(T, \lambda)$.

Lemma 2.1.3.1: (CCU Classification Probability) The probability $A^{(c)}(T, \lambda|r)$ is obtained by evaluating the conditional probability $\mathbb{P}(SINR^{(o)}(1, r) > T)$ [37]

$$A^{(c)}(T, \lambda|r) = e^{-\frac{T}{SNR} r^{\alpha}} \mathscr{L}_{I_{\theta}^{(oc)}}(T, \lambda) \tag{2.11}$$

and the CCU classification probability is

$$A^{(c)}(T,\lambda) = \int_0^\infty A^{(c)}(T,\lambda|r) f_R(r) dr$$
$$= \int_0^\infty 2\pi\lambda r e^{-\pi\lambda r^2 - \frac{T}{SNR} r^\alpha} \mathscr{L}_{I_\theta^{(oc)}}(T,\lambda) dr \tag{2.12}$$

in which $f_R(r)$ is PDF of the distance between the user and its serving BS which was defined in Equation 2.1, $SNR = \frac{P}{\sigma^2}$ and

$$\mathscr{L}_{I_\theta^{(oc)}}(T,\lambda) = e^{-2\pi\lambda r^2 \int_1^\infty \left(1 - \frac{1}{1+Tx^{-\alpha}}\right) x dx}. \tag{2.13}$$

Moreover, $A^{(c)}(T,\lambda)$ can be approximated by a finite sum as given in Equation 2.14

$$A^{(c)}(T,\lambda) \approx \sum_{i=0}^{N_{GL}} w_j e^{-\frac{T}{SNR}\zeta_i^\alpha} \mathscr{L}^{(i)}_{I_\theta^{(oc)}}(T,\lambda) \tag{2.14}$$

in which $\zeta = \sqrt{\frac{t_i}{\pi\lambda}}$; $\mathscr{L}^{(i)}_{I_\theta^{(oc)}}(T,\lambda) \approx e^{-\pi\lambda\zeta_i^2 \left[\frac{2}{\alpha} \frac{\pi T^{\frac{2}{\alpha}}}{\sin\left(\frac{2\pi}{\alpha}\right)} - \sum_{n=1}^{N_G} \frac{c_n}{2} \frac{T}{T + \left(\frac{x_n+1}{2}\right)^{\alpha/2}} \right]}$ (2.15)

N_{GL} and N_G are the degree of the Laguerre and Legendre polynomials, t_i and w_i, x_i and c_i are the i-th node and weight, abscissas and weight of the corresponding quadratures.

Proof: Equations 2.11 can be proved based on the results in [22]. The brief proof and approximated form are presented in Appendix A.1. ■

2.2 Average Coverage Probability

2.2.1 Average Coverage Probability Definition

In this section, a performance expression of the CCU and CEU in the FFR networks is derived. In case of the CCU, the CCU is covered by the networks when its downlink SINR is greater than the SINR threshold T during the establishment phase and the coverage threshold $\hat{T}$ during the communication phase. Hence, the average coverage probability is defined as:

$$\mathcal{P}_{FR}^{(c)}(T,\lambda)=\mathbb{P}\left(SINR(1,r)>\hat{T}|SINR^{(o)}(1,r)>T\right) \tag{2.16}$$

Similarly, in the case of CEU, the average coverage probability is defined by the following equation:

$$\mathcal{P}_{FR}^{(e)}(T,\lambda)=\mathbb{P}\left(SINR(\phi,r)>\hat{T}|SINR^{(o)}(1,r)<T\right) \tag{2.17}$$

The definitions of SINR threshold, coverage threshold and average coverage probability as well as their meanings were discussed in Section 1.2.2.

2.2.2 Average Coverage Probability of CCU and CEU

Theorem 2.2.2.1: (Strict FR, CCU) The average coverage probability of the CCU in the Strict FR networks is given by

$$\mathcal{P}_{Str}^{(c)}(T,\lambda)=\frac{\int_0^\infty re^{-\pi\lambda r^2-\frac{T+\hat{T}}{SNR}r^\alpha}\mathscr{L}(T,\hat{T},\lambda)dr}{\int_0^\infty re^{-\pi\lambda r^2-\frac{T}{SNR}r^\alpha}\mathscr{L}_{I_\theta^{(oc)}}(T,\lambda)dr} \tag{2.18}$$

where $\mathscr{L}_{I_\theta^{(oc)}}(T,\lambda)$ was defined in Equation 2.13, and

$$\mathscr{L}(T,\hat{T},\lambda)=e^{-2\pi\lambda r^2\int_1^\infty\left[1-\frac{1}{(1+Tx^{-\alpha})(1+\hat{T}x^{-\alpha})}\right]xdx} \tag{2.19}$$

The average coverage probability in Equation (2.18) is approximated by

$$\mathcal{P}_{Str}^{(c)}(T,\lambda)\approx\frac{\sum_{j=1}^{N_{GL}}w_je^{-\frac{(T+\hat{T})}{SNR}\zeta_j^\alpha}\mathscr{L}^{(j)}\left(T,\hat{T},\lambda\right)}{\sum_{j=1}^{N_{GL}}w_je^{-\frac{T}{SNR}\zeta_j^\alpha}\mathscr{L}_{I_\theta^{(oc)}}^{(j)}(T,\lambda)} \tag{2.20}$$

in which $\mathscr{L}_{I_\theta^{(oc)}}^{(j)}(T,\lambda)$ was defined in Equation 2.13

$$\mathscr{L}^{(j)}(T,\hat{T},\lambda)\approx e^{-\pi\lambda\zeta_j^2\left[\frac{2}{\alpha}\frac{T^{1+\frac{2}{\alpha}}-\hat{T}^{1+\frac{2}{\alpha}}}{T-\hat{T}}\frac{\pi}{\sin\left(\frac{2\pi}{\alpha}\right)}-\sum_{i=1}^{N_G}\frac{ci}{2}\frac{(T+\hat{T})\left(\frac{x_n+1}{2}\right)^{\frac{\alpha}{2}}+T\hat{T}}{\left[\left(\frac{x_n+1}{2}\right)^{\frac{\alpha}{2}}+T\right]\left[\left(\frac{x_n+1}{2}\right)^{\frac{\alpha}{2}}+\hat{T}t^\alpha\right]}\right]} \tag{2.21}$$

Proof: See Appendix A.2. ■

Theorem 2.2.2.2: (Strict FR, CEU) The average coverage probability of the

CEU in the Strict FR networks is given by

$$\mathcal{P}^{(e)}_{Str}(T,\lambda) = \frac{2\pi\lambda\int_0^\infty re^{-\pi\lambda r^2}\left[\begin{array}{r} e^{-\frac{Tr^\alpha}{\phi SNR}}\mathscr{L}_{I^{(oc)}_\theta}(\hat{T},\frac{\lambda}{\Delta}) \\ -e^{-\left(\frac{\hat{T}}{\phi}+T\right)\frac{r^\alpha}{SNR}}\mathscr{L}(T,\hat{T},\lambda) \\ \times\mathscr{L}_{I^{(oc)}_\theta}\left(T,\frac{(\Delta-1)\lambda}{\Delta}\right)\end{array}\right]dr}{1-2\pi\lambda\int_0^\infty re^{-\pi\lambda r^2-\frac{Tr^\alpha}{SNR}}\mathscr{L}_{I^{(oc)}_\theta}(T,\lambda)dr} \tag{2.22}$$

In the case of $\hat{T}\neq T$, the approximation can be expressed as

$$\mathcal{P}^{(e)}_{Str}(T,\lambda) \approx \frac{\sum_{j=1}^{N_{GL}} w_j\left[\begin{array}{r} e^{-\frac{T}{\phi SNR}\zeta_j^\alpha}\mathscr{L}^{(j)}_{I^{(oc)}_\theta}(\hat{T},\frac{\lambda}{\Delta}) \\ -e^{-\left(\frac{\hat{T}}{\phi}+T\right)\frac{\zeta_j^\alpha}{SNR}}\mathscr{L}^{(j)}_{I^{(oc)}_\theta}\left(\hat{T},\frac{\hat{T}}{\Delta(\hat{T}-T)}\right) \\ \times\mathscr{L}^{(j)}_{I^{(oc)}_\theta}\left(T,\lambda-\frac{\hat{T}\lambda}{\Delta(\hat{T}-T)}\right)\end{array}\right]}{1-\sum_{j=1}^{N_{GL}} w_j e^{-\frac{T}{SNR}\zeta_j^\alpha}\mathscr{L}^{(j)}_{I^{(oc)}_\theta}(T,\lambda)} \tag{2.23}$$

Proof: See Appendix A.3 ■

Theorem 2.2.2.3: (Soft FR, CCU) The average coverage probability of the CCU in the Soft FR networks is given by

$$\mathcal{P}^{(c)}_{Sof}(T,\lambda) = \frac{\int_0^\infty re^{-\pi\lambda r^2-\frac{T+\hat{T}}{SNR}r^\alpha}\mathscr{L}(T,\hat{T},\frac{\Delta-1}{\Delta}\lambda)\mathscr{L}(T,\phi\hat{T},\frac{\lambda}{\Delta})dr}{\int_0^\infty re^{-\pi\lambda r^2-\frac{Tr^\alpha}{SNR}}\mathscr{L}_{I^{(oc)}_\theta}(T,\lambda)dr} \tag{2.24}$$

The approximated value of $\mathcal{P}^{(c)}_{Sof}(T,\lambda)$ is given by

$$\mathcal{P}^{(c)}_{Sof}(T,\lambda) \approx \frac{\sum_{j=1}^{N_{GL}} w_j e^{-\frac{T+\hat{T}}{SNR}\zeta_j^\alpha}\mathscr{L}^{(j)}(T,\hat{T},\frac{\Delta-1}{\Delta}\lambda)\mathscr{L}^{(j)}(T,\phi\hat{T},\frac{\lambda}{\Delta})}{\sum_{j=1}^{N_{GL}} w_j e^{-\frac{T}{SNR}\zeta_j^\alpha}\mathscr{L}^{(j)}_{I^{(oc)}_\theta}(T,\lambda)} \tag{2.25}$$

in which $\mathscr{L}^{(j)}_{I^{(oc)}_\theta}(T,\lambda)$ was given in Equation 2.15; $\mathscr{L}^{(j)}(T,\hat{T},\frac{\Delta-1}{\Delta}\lambda)$ and $\mathscr{L}^{(j)}(T,\phi\hat{T},\frac{\lambda}{\Delta})$ were defined in Equation 2.21.

Proof: See Appendix A.4. ■

Theorem 2.2.2.4: (Soft FR, CEU) The average coverage probability of the CEU in the Soft FR networks is given by

$$\mathcal{P}_{Sof}^{(e)}(T,\lambda) = \frac{2\pi\lambda \int_0^\infty r e^{-\pi\lambda r^2} \left[\begin{array}{l} e^{-\frac{\hat{T} r^\alpha}{\phi SNR}} \mathscr{L}_{I_\theta^{(oc)}}(\frac{\hat{T}}{\phi}, \frac{\Delta-1}{\Delta}\lambda) \mathscr{L}_{I_\theta^{(oc)}}(\hat{T}, \frac{1}{\Delta}\lambda) dr \\ \quad - e^{-\left(\frac{\hat{T}}{\phi}+T\right)\frac{r^\alpha}{SNR}} \mathscr{L}(T, \frac{\hat{T}}{\phi}, \frac{\Delta-1}{\Delta}\lambda) \mathscr{L}(T, \hat{T}, \frac{\lambda}{\Delta}) \end{array} \right] dr}{1 - 2\pi\lambda \int_0^\infty r e^{-\pi\lambda r^2 - \frac{T r^\alpha}{SNR}} \mathscr{L}_{I_\theta^{(oc)}}(T,\lambda) dr} \tag{2.26}$$

and its approximation is

$$\mathcal{P}_{Sof}^{(e)}(T,\lambda) \approx \frac{\sum_{j=1}^{N_{GL}} w_j \left[\begin{array}{l} e^{-\frac{\hat{T}}{\phi SNR}\zeta_j^\alpha} \mathscr{L}_{I_\theta^{(oc)}}^{(j)}(\frac{\hat{T}}{\phi}, \frac{\Delta-1}{\Delta}\lambda) \mathscr{L}_{I_\theta^{(oc)}}^{(j)}(\hat{T}, \frac{1}{\Delta}\lambda) \\ \quad - e^{-\frac{T+\frac{\hat{T}}{\phi}}{SNR}\zeta_j^\alpha} \mathscr{L}^{(j)}(T, \frac{\hat{T}}{\phi}, \frac{\Delta-1}{\Delta}\lambda) \mathscr{L}^{(j)}(T, \hat{T}, \frac{\lambda}{\Delta}) \end{array} \right]}{1 - \sum_{j=1}^{N_{GL}} w_j e^{-\frac{T}{SNR}\zeta_j^\alpha} \mathscr{L}_{I_\theta^{(oc)}}^{(j)}(T,\lambda)} \tag{2.27}$$

Proof: The average coverage probability of the CEU in Soft FR is given by

$$\begin{aligned} \mathcal{P}_{Sof}^{(e)}(T,\lambda) &= \frac{\mathbb{P}\left(\frac{P^{(e)} g r^{-\alpha}}{\sigma^2 + I_{Sof}^{(e)}} > \hat{T}, \frac{P^{(c)} g^{(o)} r^{-\alpha}}{\sigma^2 + I_{Sof}^{(oc)}} < T\right)}{\mathbb{P}\left(\frac{P g r^{-\alpha}}{\sigma^2 + I_{Sof}^{(oc)}} < T\right)} \\ &= \frac{\mathbb{P}\left(\frac{P^{(c)} g r^{-\alpha}}{\sigma^2 + I_{Sof}^{(e)}} > \frac{\hat{T}}{\phi}\right)}{1 - \mathbb{P}\left(\frac{P g r^{-\alpha}}{\sigma^2 + I_{Sof}^{(oc)}} > T\right)} - \frac{\mathbb{P}\left(\frac{P^{(c)} g r^{-\alpha}}{\sigma^2 + I_{Sof}^{(e)}} > \frac{\hat{T}}{\phi}, \frac{P^{(c)} g^{(o)} r^{-\alpha}}{\sigma^2 + I_{Sof}^{(oc)}} > T\right)}{1 - \mathbb{P}\left(\frac{P g r^{-\alpha}}{\sigma^2 + I_{Sof}^{(oc)}} > T\right)} \end{aligned} \tag{2.28}$$

In Equation 2.28, the first part can be obtained from Appendix A.1 while the second part is given by Appendix A.4. Hence, the average coverage probability of the CEU is obtained as in Theorem 2.2.2.4. ■

2.2.3 Average Coverage Probability of the typical user

A user at a distance r from its serving BS in the FFR cellular networks can be served as a CCU with a probability of $\mathbb{P}(SINR^{(o)}(1,r) > T|r)$ and a coverage prob-

ability of $\mathbb{P}(SINR(1,r) > \hat{T}|r)$ or a CEU with a probability of $\mathbb{P}(SINR^{(o)}(1,r) < T|r)$ and a coverage probability of $\mathbb{P}(SINR(\phi,r) > \hat{T}|r)$. The coverage probability of the typical user at a distance r from its serving BS is given by:

$$\begin{aligned}\mathcal{P}_{FR}(T,\lambda|r) =& \mathbb{P}(SINR^{(o)}(1,r) > T|r)\mathbb{P}(SINR(1,r) > \hat{T}|r) \\ &+ \mathbb{P}(SINR^{(o)}(1,r) < T|r)\mathbb{P}(SINR(\phi,r) > \hat{T}|r) \end{aligned} \tag{2.29}$$

The average coverage probability of the typical user can be obtained by integrating the conditional coverage probability $\mathcal{P}_{FR}(T,\lambda|r)$ over the network

$$\mathcal{P}_{FR}(T,\lambda) = 2\pi\lambda \int_0^\infty r^2 e^{-\pi\lambda r^2} \mathcal{P}_{FR}(T,\lambda|r) dr \tag{2.30}$$

Strict FR In the case of interference-limited networks ($\sigma \approx 0$ or SNR $\to \infty$), by using the results in Section 2.2.2, the average coverage probability of the typical user in the Strict FR networks is given by

$$\begin{aligned}\mathcal{P}_{Str}(T,\lambda) =& \int_0^\infty r e^{-\pi\lambda r^2} e^{-2\pi\lambda r^2 \int_1^\infty \left[1-\tau(T)\tau(\hat{T})\right]dt} dr \\ &+ 2\pi\lambda \int_0^\infty r e^{-\pi\lambda r^2} \left[\begin{array}{l} e^{-\frac{\pi\lambda r^2}{\Delta}\int_1^\infty \left[1-\tau(\hat{T})\right]dt} \\ \quad -e^{-\frac{2\pi\lambda r^2}{\Delta}\int_1^\infty \left[1-\tau(T)\tau(\hat{T})\right]dt} \\ \qquad \times e^{-\frac{2\pi\lambda(\Delta-1)r^2}{\Delta}\int_1^\infty [1-\tau(T)]dt} \end{array}\right] dr \\ =& \frac{1}{1+\frac{1}{\Delta}\int_1^\infty \left[1-\tau(\hat{T})\right]dt} \\ &- \frac{\frac{\Delta-1}{\Delta}\int_1^\infty \tau(T)\left[1-\tau(\hat{T})\right]dt}{\left[\begin{array}{r}\left(1+\frac{1}{\Delta}\int_1^\infty \left[1-\tau(T)\tau(\hat{T})\right]dt + \frac{\Delta-1}{\Delta}\int_1^\infty [1-\tau(T)]\right) \\ \times \left(1+\int_1^\infty \left[1-\tau(T)\tau(\hat{T})\right]dt\right)\end{array}\right]} \end{aligned} \tag{2.31}$$

in which $\tau(T) = \frac{1}{1+Tt^{-\alpha/2}}$.

Soft FR In the case of interference-limited networks ($\sigma \approx 0$ or SNR $\to \infty$), the average coverage probability of the typical user in the Soft FR networks is obtained

by $\mathcal{P}_{Sof}(T,\lambda)$

$$
\begin{aligned}
=&2\pi\lambda\int_0^\infty re^{-\pi\lambda r^2}e^{-\frac{2\pi\lambda(\Delta-1)r^2}{\Delta}\int_1^\infty\left[1-\tau(T)\tau(\hat{T})\right]dt}e^{-\frac{2\pi\lambda r^2}{\Delta}\int_1^\infty\left[1-\tau(T)\tau(\phi\hat{T})\right]dt}dr\\
&+2\pi\lambda\int_0^\infty re^{-\pi\lambda r^2}\left[\begin{array}{l}e^{-\frac{2\pi\lambda(\Delta-1)r^2}{\Delta}\int_1^\infty\left[1-\tau\left(\frac{\hat{T}}{\phi}\right)\right]dt}e^{-\frac{2\pi\lambda r^2}{\Delta}\int_1^\infty\left[1-\tau\left(\hat{T}\right)\right]dt}\\ \quad-e^{-\frac{2\pi\lambda(\Delta-1)r^2}{\Delta}\int_1^\infty\left[1-\tau(T)\tau\left(\frac{\hat{T}}{\phi}\right)\right]dt}e^{-\frac{2\pi\lambda r^2}{\Delta}\int_1^\infty\left[1-\tau(T)\tau(\hat{T})\right]dt}\end{array}\right]dr\\
=&\frac{1}{1+\frac{\Delta-1}{\Delta}\int_1^\infty\left[1-\tau\left(\frac{\hat{T}}{\phi}\right)\right]dt+\frac{1}{\Delta}\int_1^\infty\left[1-\tau(\hat{T})\right]dt}\\
&-\frac{\frac{\Delta-1}{\Delta}\int_1^\infty\tau(T)\left[\tau\left(\frac{\hat{T}}{\phi}\right)-\tau(\hat{T})\right]dt+\frac{1}{\Delta}\int_1^\infty\tau(T)\left[\tau\left(\hat{T}\right)-\tau(\phi\hat{T})\right]dt}{\left[\begin{array}{l}\left(1+\frac{\Delta-1}{\Delta}\int_1^\infty\left[1-\tau(T)\tau(\hat{T})\right]dt+\frac{1}{\Delta}\int_1^\infty\left[1-\tau(T)\tau(\phi\hat{T})\right]dt\right)\\ \quad\times\left(1+\frac{\Delta-1}{\Delta}\int_1^\infty\left[1-\tau(T)\tau\left(\frac{\hat{T}}{\phi}\right)\right]dt+\frac{1}{\Delta}\int_1^\infty\left[1-\tau(T)\tau(\hat{T})\right]dt\right)\end{array}\right]}
\end{aligned}
\tag{2.32}
$$

in which $\tau(T)=\frac{1}{1+Tt^{-\alpha/2}}$.

Since the coverage threshold $\hat{T}$, the FR factor and path loss exponent α in a practical network are usually known, the first fractions in Equations 2.31 and 2.32 are constant numbers.

Since $\tau(T)=\frac{1}{1+Tt^{-\alpha/2}}$ is a monotonically decreasing function with respect to T and $0<\tau(T),\tau(\hat{T})<1$, $\tau\left(\frac{\hat{T}}{\phi}\right)-\tau(\hat{T})>0$, $\tau\left(\hat{T}\right)-\tau(\phi\hat{T})>0, \forall\phi>1, T>0, \hat{T}>0$. Moreover, $\int_1^\infty\left[1-\tau(T)\tau(\hat{T})\right]dt$ and $\int_1^\infty\left[1-\tau(T)\right]dt$ are monotonically increasing functions. Therefore, the second fractions in Equations 2.31 and 2.32 reduce with increments of T. Consequently, the average coverage probability of the typical user under both Strict FR and Soft FR networks, $\mathcal{P}_{Str}(T,\lambda)$ and $\mathcal{P}_{Sof}(T,\lambda)$, increase with SINR threshold T.

When $T\to\infty$ which is equivalent to all users being classified as CEUs , $\tau(T)$ and consequently the second fractions in Equations 2.31 and 2.32 approximate to 0. In this case, the average coverage probabilities of the typical user, $\mathcal{P}_{Str}(T,\lambda)$ and $\mathcal{P}_{Sof}(T,\lambda)$, reach the maximum values as given below

$$
\mathcal{P}_{Str}(T,\lambda)=\frac{1}{1+\frac{1}{\Delta}\int_1^\infty\left[1-\tau(\hat{T})\right]dt} \tag{2.33a}
$$

$$\mathcal{P}_{Sof}(T,\lambda) = \frac{1}{1 + \frac{\Delta-1}{\Delta}\int_1^\infty \left[1 - \tau\left(\frac{\hat{T}}{\phi}\right)\right] dt + \frac{1}{\Delta}\int_1^\infty \left[1 - \tau(\hat{T})\right] dt} \tag{2.33b}$$

The effects of SINR threshold on the network performance can be explained based on Consequence 4 on Page 10 which stated that the CEU achieves a higher SINR and consequently a higher average coverage probability than a CCU. Thus, the optimal value of SINR threshold is selected so that all users are classified as CEUs, at which the average coverage probability of the typical user is at the maximum value. However, the selection of SINR threshold in practical networks should depend on the required user performance as well as overall power consumption of the BSs.

2.3 Simulation and Discussion

In this section, the numerical and simulation results are presented to validate the accuracy of the analytical approach. The analytical results are compared to the well-known results from [37] and [44] in terms of average coverage probability, then effects of SINR threshold and SNR on the network performance are analysed. The limitations of analytical approaches in [37] and [44] were discussed in Section 1.5.1.

2.3.1 Validate of the proposed analytical approach

The analytical results, which are conducted for $SNR = 10$ dB, $\alpha = 3.5$, are compared to the Monte Carlo simulation and the results in [37] and [44]. In Figure 2.1(a), the performance of CCU under the proposed two-phase operation is compared to the corresponding result in [37], while in Figure 2.1(b), the proposed analytical approach by separately evaluating interference generated from BSs transmitting on CC and CE RBs is compared to the use of the constant coefficient to evaluate network interference in [37] and the accuracy of approach in [44].

As shown in Figure 2.1, the solid lines representing the analytical results of CCU and CEU perfectly match with the points representing the corresponding simulation results but have gaps with the lines which are plotted from the corresponding results in [37] and [44].

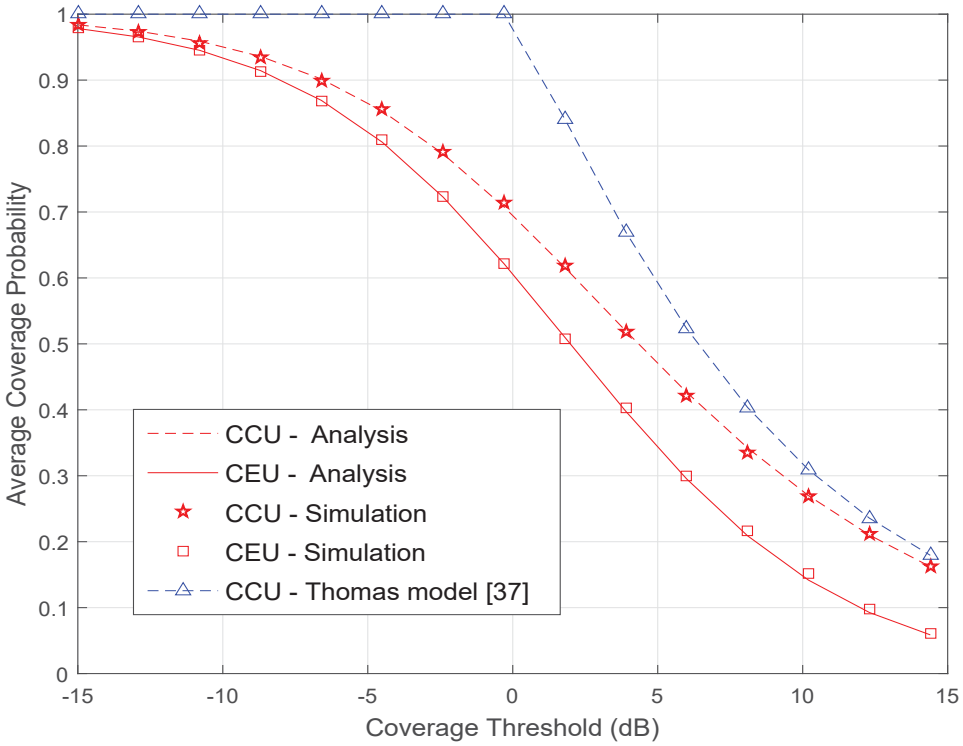

(a) Strict FR

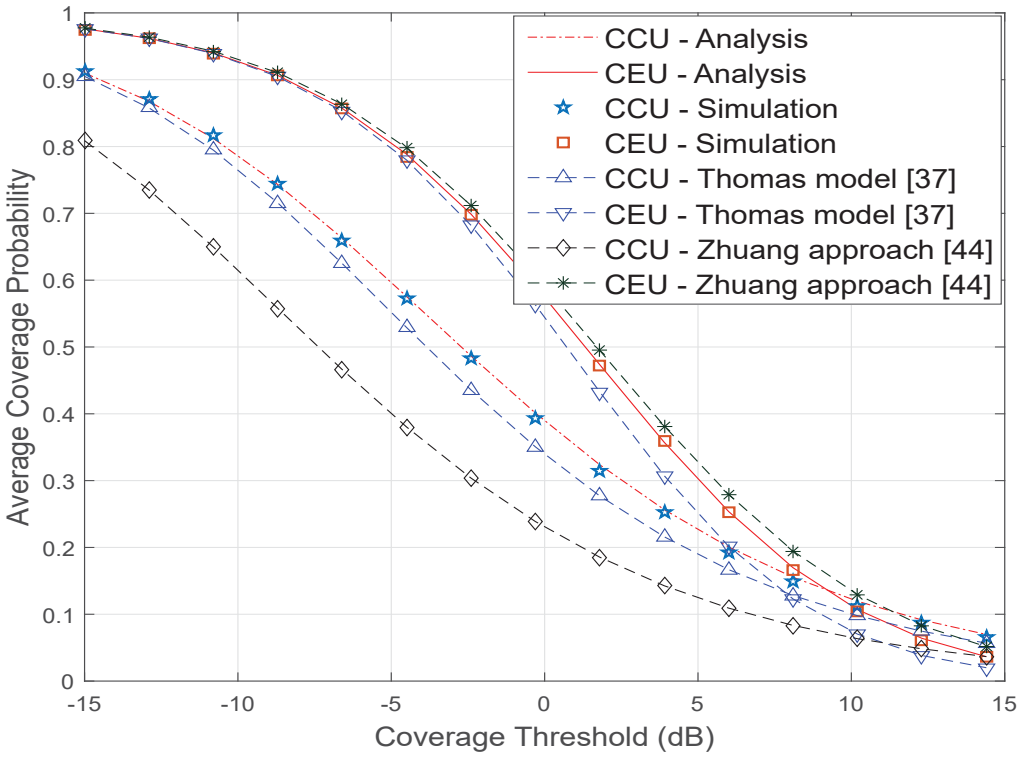

(b) Soft FR

Figure 2.1 : Comparison of the analytical results and Monte Carlo simulation ($SNR = 10$ dB, $T = 0$ dB)

Discussion on the Results in [37]

In the case of Strict FR : Since [37] assumed that the user transmits the signal for user classification purpose and data at the same time, the user was under the network coverage if the received SINR is greater than both SINR threshold T and coverage threshold $\hat{T}$. Thus, the average coverage probability of the CCU, $\mathcal{P}_c$, was defined as $\mathbb{P}(SINR > T|SINR > \hat{T})$. Therefore, $\mathcal{P}_c = 1$ if $\hat{T} > T$.

In the case of Soft FR : In [37], the set of interfering BSs transmitting on CC and CE RBs, $\theta_{Sof}^{(c)}$ and $\theta_{Sof}^{(e)}$, were consolidated by a constant coefficient $\zeta = (\Delta - 1 + \phi)/\Delta$. Thus, the network interference in Equation 2.9 is given by $I = \sum_{j \in \theta_{Sof}} \zeta P_j^{(c)} g_{jz} r_{jz}^{-\alpha}$ in which $\theta_{Sof}^{(c)} \bigcup \theta_{Sof}^{(e)} = \theta_{Sof}$. In other words, $\theta_{Sof}^{(c)}$ of BSs with transmit power P and density $\frac{\Delta-1}{\Delta}\lambda$ was replaced by θ_{Sof} of BSs with transmit power $\frac{\Delta-1}{\Delta}P$ and density λ; $\theta_{Sof}^{(e)}$ of BSs with transmit power ϕP and density $\frac{1}{\Delta}\lambda$ was considered as equivalent to θ_{Sof} of BSs with transmit power $\frac{\phi}{\Delta}P$ and density λ. However, since two independent sets $\theta_{Sof}^{(c)}$ and $\theta_{Sof}^{(e)}$ are subsets of θ_{Sof}, use of equivalent sets to represent $\theta_{Sof}^{(c)}$ and $\theta_{Sof}^{(e)}$ are not feasible.

In our approach, instead of using the coefficient ζ, $\theta_{Sof}^{(c)}$ and $\theta_{Sof}^{(e)}$ are evaluated separately, hence the analytical results perfectly match with the simulation results.

Discussion on the Results in [44]

In [44], it was assumed that the interference between the establishment phase and communication phase are independent, thus the joint probability in the numerator of Equation A.17 was evaluated as $\mathbb{P}(SINR^{(o)} < T, SINR^{(e)} > \hat{T}|r) = \mathbb{P}(SINR^{(o)} < T|r)\mathbb{P}(SINR^{(e)} > \hat{T}|r)$. However, in downlink cellular networks, the user during both establishment phase and communication phase experiences interference from the same BSs, thus the interference during both phases are functions of the distances from the user to adjacent BSs. Consequently, $SINR^{(o)}$ and $SINR^{(e)}$ are correlated random variables. As a results, there are also gaps between the results in [44] and simulation results.

2.3.2 Effects of SNR on the network performance

In this section, the effects of SNR on the network performance is analysed for two values of SINR threshold $T = -5$ dB and $T = 5$ dB. It can be observed

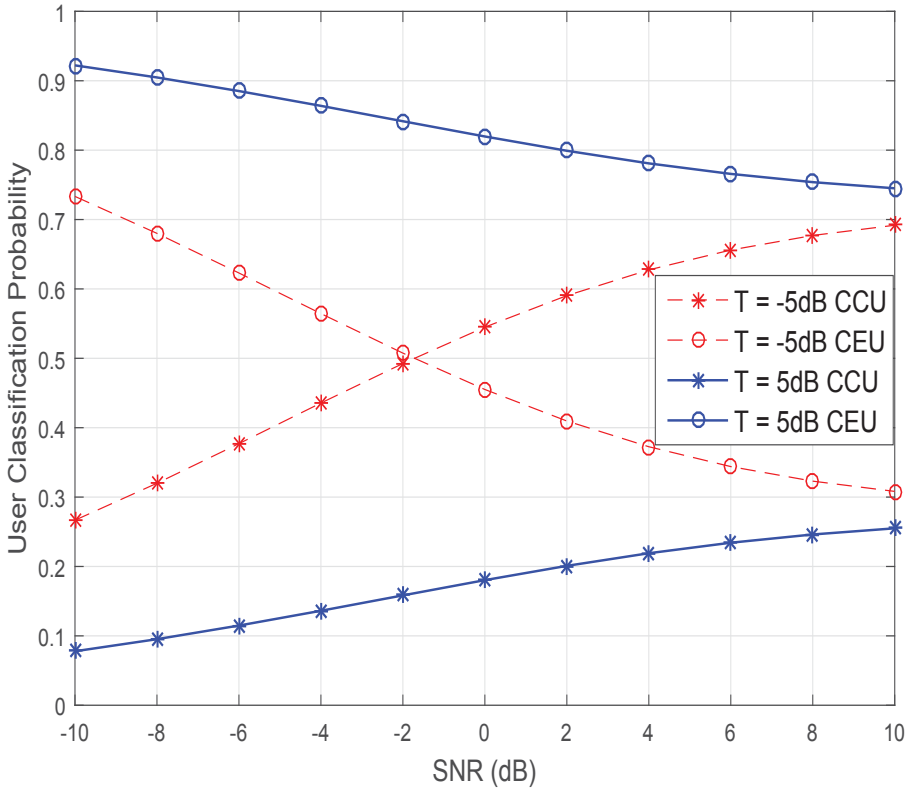

Figure 2.2 : User Classification Probability with two values of SINR Threshold T

from Figure 2.2 that with an increase in SNR, the measured SINR on the downlink control channel during the establishment phase increases, which leads to an increase in CCU classification probability and a decline in CEU classification probability. In addition, since more users are served as CCUs when SINR threshold increases, CCU classification probability in the case of $T = 5$ dB is always greater than that in the case of $T = -5$ dB.

Now, the performance of users in the cases of $T = -5$ dB and $T = 5$ dB are considered. In the case of Strict FR where the user is only affected by interference originating from the BSs transmitting at the same power as the serving BS, an increase in SNR leads to an increase in average coverage probability as shown Figures

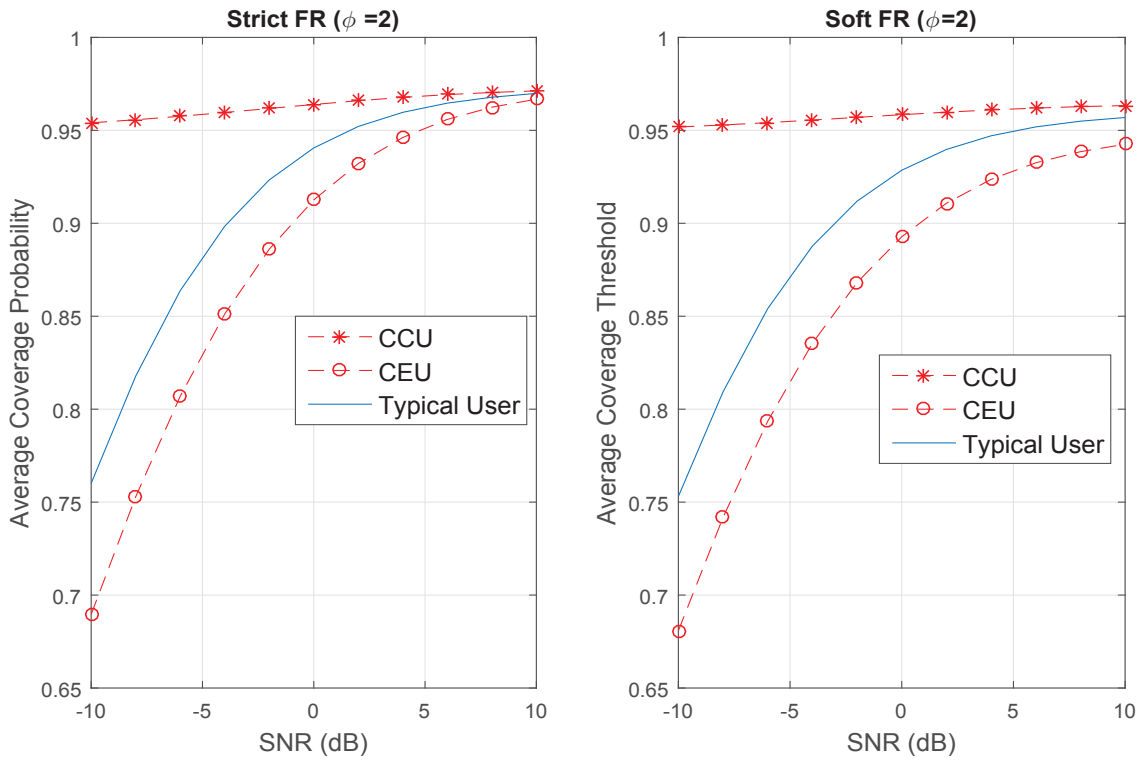

Figure 2.3 : User Average Coverage Probability with $T = -5$ dB and $\hat{T} = -15$ dB, $\phi = 2$

2.3 and 2.4, which is similar to that found in the literature such as [22, 34].

In the case of Soft FR where the user experiences interference originating from BSs in both $\theta_{Sof}^{(c)}$ and $\theta_{Sof}^{(e)}$, when SNR on the CC RB increases by an mount of δ, the transmit power on CE RBs rises by $\phi\delta$.

From the CCU viewpoint whose serving power is the CC power, when the transmit power ratio is small such as $\phi = 2$, the increase of interference from BSs in $\theta_{Sof}^{(e)}$ can be overcome by the benefits due to an increase in the serving signal power when SNR increases. Thus, the average coverage probability slightly increases as shown in Figure 2.3. By contrast, when the transmit power ratio is large such as $\phi = 20$, the growth of the serving signal power cannot counterbalance the interference from BSs in $\theta_{Sof}^{(e)}$, which leads to a significant decline in average coverage probability as shown in Figure 2.4.

From the CEU viewpoint, the serving power is the CE power and when the CEU

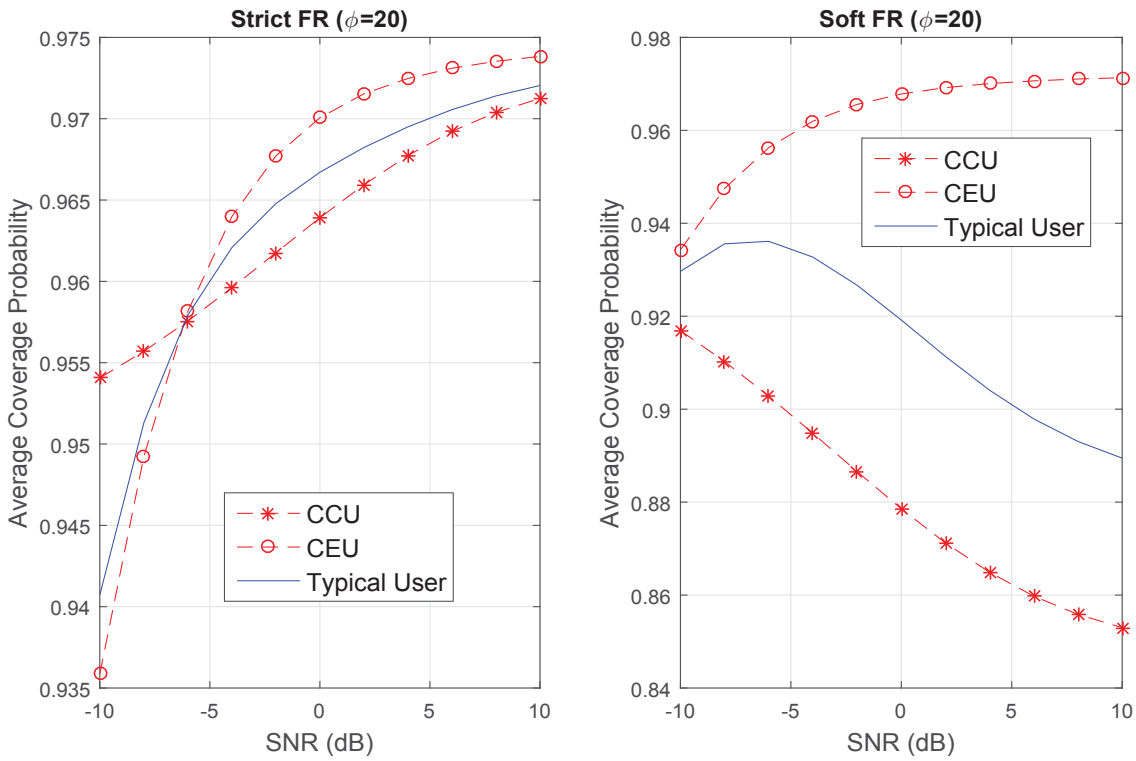

Figure 2.4 : User Average Coverage Probability with $T = 5$ dB and $\hat{T} = -15$ dB, $\phi = 20$

serving signal rises by $\delta\phi$, the interfering sources in $\theta_{Sof}^{(c)}$ only increases by δ. Hence, the CEU average coverage probabilities increases with SNR in both cases of $\phi = 2$ and $\phi = 20$.

The average coverage probability in Equation 2.30 is a function of the number of CCU and CEU and the corresponding average coverage probabilities. Thus, the average coverage probability of the typical user increases with SNR in the case of Strict FR and Soft FR with $\phi = 2$. In the case of Soft FR with $\phi = 20$, since there are opposite trends between CCU and CEU performance, the average coverage probability of the typical reaches a peak of 0.9361 at $SNR = -6$ dB. Therefore, increasing SNR is not an optimal solution in this case since the user coverage probability can reduce with high SNR.

2.3.3 Effects of Transmit Power Ratio on the network performance

An increase in the transmit power ratio ϕ leads to an increase in interference to both CCU and CEU which were evident in Equation 2.9. Therefore, the received SINR of the CCU, and consequently average coverage probability reduce when ϕ increases as shown in Figure 2.5. In contrast, increasing ϕ enhances the desired signal of the CEU while maintaining the transmit power of the CCUs, which can improve the received SINR and average coverage probability of the CEU.

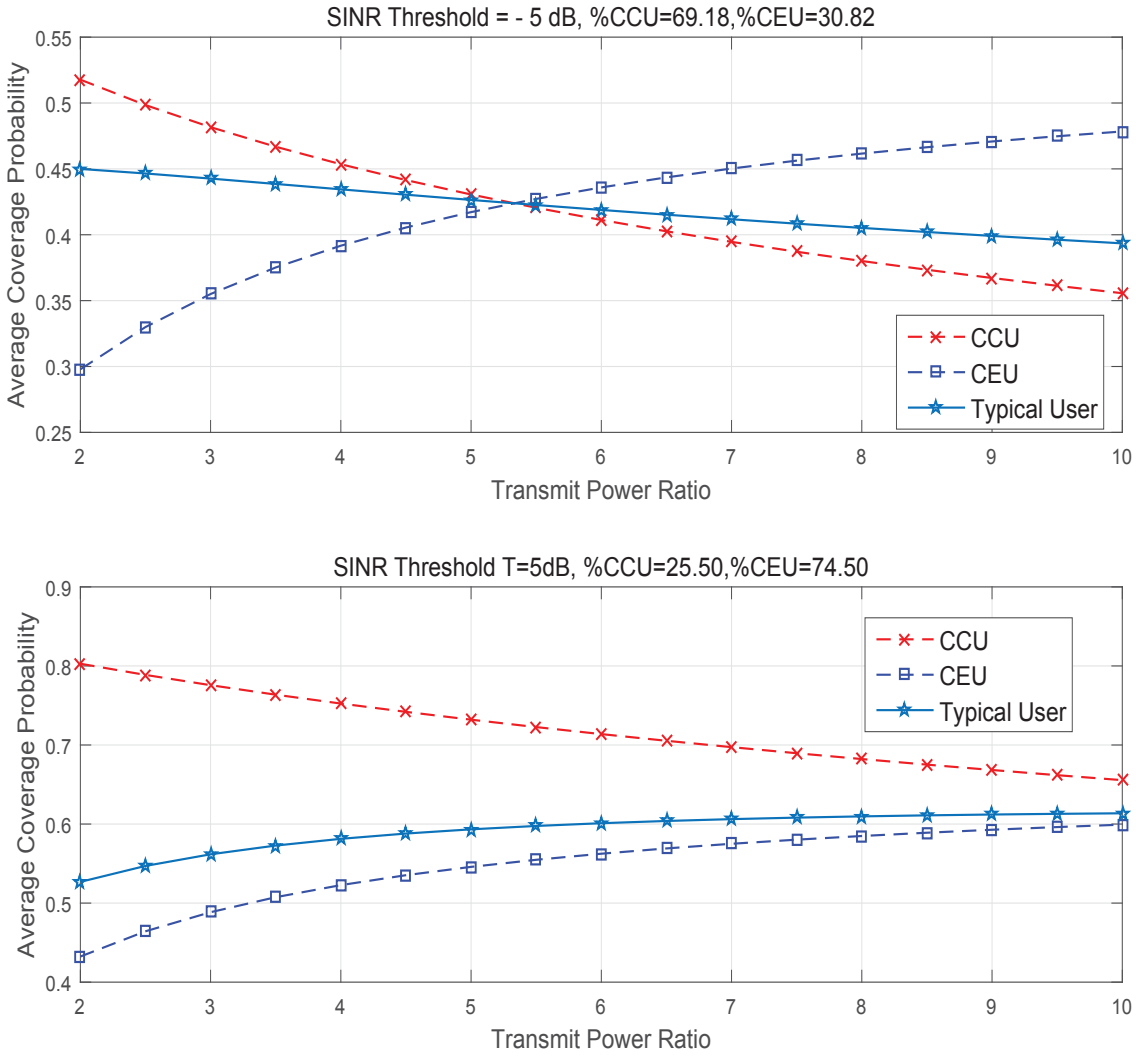

Figure 2.5 : Effects of Transmit Power Ratio on the Network Performance ($\hat{T} = 0$ dB, $SNR = 10$ dB)

Since there is an opposite trend between average coverage probability of the CCU and CEU, upward and downward trends of the average coverage probability of the typical user in Equation 2.30 strongly depends on percentage of CCU and CEU in the networks. Take SINR threshold $T = -5$ dB for example, the percentage of the CCU is up to 69.18% while that of the CEU is only 30.82%. Hence, although the average coverage probability of the CEU increases with ϕ, the average coverage probability of the typical user decreases when ϕ increases.

2.4 Conclusion

In this chapter, the downlink random cellular networks using FFR were modelled in which the two-phase operation was proposed for both CCU and CEU based on 3GPP recommendations. An proposed analytical approach, that is more accurate than other approaches in the literature, was presented and verified by Monte Carlo simulation. The performance metrics in terms of CCU and CEU classification probabilities, average coverage probabilities are derived for Rayleigh fading channels. The Gauss - Laguerre and Gauss - Legendre were utilised to derive the closed-form expressions of the performance metrics. In contrast to the previous work which stated that the system achieves the highest performance when SINR threshold T equals coverage threshold $\hat{T}$, the work in this chapter concluded that when more users are served as CEUs, a higher performance is achieved. Furthermore, this chapter also concluded that increasing SNR is not an optimal solution to improve the system performance when the transmit power ratio is at a high value since this leads to a decline in CCU average coverage probability.

Chapter 3

Performance of FFR in Uplink Random Cellular Networks

In this chapter, the uplink cellular network model is developed based on the results in Chapter 2. The main differences between the two-phase operation of uplink and downlink are highlighted as follows

- During the establishment phase: although each uplink RB under Strict FR experiences interference from the CCUs which is similar to the case of downlink, each uplink RB under Soft FR is affected by interference originating from the CCUs in $\theta_{Soft}^{(c)}$ and CEUs in $\theta_{Soft}^{(e)}$.
- During the communication phase: since the CEUs during the communication phase are served on the different RB (CE RB), they experience interference originating from different users.

Furthermore, the users in uplink adjust their transmission powers in an effort to reduce power consumption and improve network performance. Hence, the modelling and analytical approach for downlink and uplink are significantly different.

3.1 Network model

This chapter studies the uplink model of a PPP cellular network in which both users and BSs are distributed according to a spatial PPP model with densities of λ (BS/km^2) and $\lambda^{(u)}$ $(user/km^2)$ respectively. Conventionally, in the cellular network system, the number of users is expected to be much greater the number of the BSs, thus it can be assumed that $\lambda^{(u)} \gg \lambda$, so that all the BSs and RBs are activated to serve the associated users. It is also assumed that in a given time slot, an RB is only allocated to a single user per cell.

In the uplink networks, each mobile user's transmit power is controlled to achieve a desired received signal power P at the serving BS. Conventionally, the user transmit power is adjusted based on pathloss-inversion of a form $Pr^{\alpha\epsilon}$ [30, 39], in which α and ϵ are pathloss and power control exponents, $(0 < \epsilon < 1)$. In particular networks, the selection of ϵ is based upon interference, channel fading and battery consumption.

3.1.1 Fractional Frequency Reuse

The transmit power of user z is denoted by $P^{(z)} = \phi^{(z)} Pr^{\alpha\epsilon}$ where $z = (c, e)$ corresponds to the CCU and CEU, $\phi^{(e)} = \phi$ $(\phi > 1)$ is a transmit power ratio between the CE and CC powers, and $\phi^{(c)} = 1$.

The average transmit powers of the CCU and CEU are given by

$$E[P^{(c)}] = \int_0^\infty 2\pi\lambda r^{\epsilon\alpha+1} e^{-\pi\lambda r^2} dr \quad \text{and} \quad E[P^{(e)}] = \phi \int_0^\infty 2\pi\lambda r^{\epsilon\alpha+1} e^{-\pi\lambda r^2} dr \quad (3.1)$$

The set of users that create interference to the uplink of the user is denoted by $\theta_{FR}^{(z)}$, thus $I_{FR}^{(z)}$ is denoted as the corresponding interference, in which $FR = (Str, Sof)$ corresponds to Strict FR and Soft FR. With an assumption that each RB is allocated to a user, each user in $\theta_{FR}^{(e)}$ is located independently to others in $\theta_{FR}^{(c)}$.

The CCU during the communication phase is served on the same RB, and consequently experiences interference originating from the same users as the establishment

phase. Meanwhile, since the CEU during the communication phase is served on a different RB compared to the establishment phase and in combination with the assumption that each RB is only allocated to a user during a given timeslot, the interference sources between the two phases are different.

- Under Strict FR: Since the CCUs do not share their RBs with the CEUs and vice versa, the $I_{Str}^{(z)}$ originates from either $\theta_{Str}^{(c)}$ or $\theta_{Str}^{(e)}$. The interference power $I_{Str}^{(z)}$ at the serving BS of user z is

$$I_{Str}^{(z)} = \sum_{j \in \theta_{Str}^{(z)}} P_j^{(z)} g_{jz} d_{jz}^{-\alpha} \tag{3.2}$$

  in which g_{jz} and d_{jz} are the power gain and distance from interfering user j to the serving BS of user z.

  During the establishment phase, since the BS measures the uplink SINR on the CC RBs which are common RBs and shared by all BSs, the density of interfering users of the measured SINR during the establishment phase is λ. During the communication phase, the density of interfering users is determined in Property 1 on Page 9.

- Under Soft FR: Since each cell can reuse all RBs, each CC RB as well as CE RB may experience interference from both $\theta_{Sof}^{(c)}$ and $\theta_{Sof}^{(e)}$ whose densities are given by Property 3 on Page 10. In this case, $I_{Sof}^{(z)}$ is given by

$$I_{Sof}^{(z)} = \sum_{j \in \theta_{Sof}^{(c)}} P_j^{(c)} g_{jz} d_{jz}^{-\alpha} + \sum_{j \in \theta_{Sof}^{(e)}} P_j^{(e)} g_{jz} d_{jz}^{-\alpha} \tag{3.3}$$

  Equation 3.3 represents interference of the measured SINR during the establishment phase, and both CCU and CEU during the communication phase.

The received SINR at the BS from user z is given by

$$SINR(\phi^{(z)}, \epsilon) = \frac{\phi^{(z)} P g r^{\alpha(\epsilon-1)}}{\sigma^2 + I_{FR}^{(z)}(\phi^{(z)})} \tag{3.4}$$

in which σ^2 is the Gaussian noise power, g and r are the power gain and distance from user z to the serving BS. The channel fading has a Rayleigh distribution with an average power of 1. Hence, g has an exponential distribution and $E[g_{jz}] = 1$.

3.1.2 User Classification Probability

A user is defined as a CCU if its uplink SINR during establishment phase, denoted by $SINR^{(o)}(1, \epsilon)$, is greater than the SINR threshold T. The CCU classification probabilities under Strict FR and Soft FR are given by Lemma 3.1.2.1 and Lemma 3.1.2.2.

Lemma 3.1.2.1: (*Strict FR, CCU Classification Probability*): The probability $A^{(c)}_{Str}(T, \epsilon|r)$ that a user at a distance r from its serving BS is defined as a CCU is

$$A^{(c)}_{Str}(T, \epsilon|r) = e^{-\frac{T}{SNR} r^{\alpha(1-\epsilon)}} \mathscr{L}_{I^{(oc)}_{\theta}}(s_1, \lambda) \tag{3.5}$$

and thus CCU classification probability is given by

$$\begin{aligned} A^{(c)}_{Str}(T, \epsilon) &= \int_0^{\infty} A^{(c)}_{Str}(T, \epsilon|r) f_R(r) dr \\ &= \int_0^{\infty} \upsilon(T) \mathscr{L}_{I^{(oc)}_{\theta}}(s_1, \lambda) dr \end{aligned} \tag{3.6}$$

in which the related symbols were defined before; $f_R(r)$ is defined in Equation 2.1, $\upsilon(T) = 2\pi\lambda r e^{-\pi\lambda r^2 - \frac{T}{SNR} r^{\alpha(1-\epsilon)}}$, $SNR = \frac{P}{\sigma^2}$, $s_1 = Tr^{-\alpha\epsilon}$ and
$\mathscr{L}_{I^{(oc)}_{\theta}}(s_1, \lambda) = e^{-2\pi\lambda r^2 \int_1^{\infty} \left(1 - \int_0^{\infty} \frac{\pi\lambda t e^{-\lambda\pi t^2}}{1 + s_1 t^{\alpha\epsilon} x^{-\alpha}} dt\right) x dx}$. (3.7)

Proof: This lemma can be proved based on Theorem 1 in [39] or using the results of Appendix B.1 with $\phi = 1$. ■

Lemma 3.1.2.2: (*Soft FR, CCU Classification Probability*): The probability $A^{(c)}_{Sof}(T, \epsilon|r)$ that a user at a distance r from its serving BS is defined as a CCU is given by

$$A^{(c)}_{Sof}(T, \epsilon|r) = e^{-\frac{Tr^{\alpha(1-\epsilon)}}{SNR}} \mathscr{L}_{I^{(oc)}_{\theta}}\left(s_1, \frac{\Delta - 1}{\Delta}\lambda\right) \mathscr{L}_{I^{(oc)}_{\theta}}\left(\phi s_1, \frac{1}{\Delta}\lambda\right) \tag{3.8}$$

and thus CCU classification probability is given by

$$A_{Sof}^{(c)}(T,\epsilon) = \int_0^\infty \upsilon(T)\mathscr{L}_{I_\theta^{(oc)}}\left(s_1, \frac{\Delta-1}{\Delta}\lambda\right)\mathscr{L}_{I_\theta^{(oc)}}\left(\phi s_1, \frac{1}{\Delta}\lambda\right)dr \tag{3.9}$$

Proof: This lemma is proved in Appendix B.1. ■

Proposition 3.1.2.3: The CCU classification probabilities in Lemma 3.1.2.1 and 3.1.2.2 can be approximated by using the Gauss Quadratures as follows

$$A_{Str}^{(c)}(T,\epsilon) \approx \sum_{j=1}^{N_{GL}} w_j e^{-\frac{T}{SNR}\zeta_j^{\alpha(1-\epsilon)}}\mathscr{L}_{I_\theta^{(oc)}}^{(j)}\left(T\zeta_j^{-\alpha\epsilon}, \lambda\right) \tag{3.10}$$

$$A_{Sof}^{(c)}(T,\epsilon) \approx \sum_{j=1}^{N_{GL}} w_j e^{-\frac{T}{SNR}\zeta_j^{\alpha(1-\epsilon)}}\mathscr{L}_{I_\theta^{(oc)}}^{(j)}\left(T\zeta_j^{-\alpha\epsilon}, \frac{\Delta-1}{\Delta}\lambda\right)\mathscr{L}_{I_\theta^{(oc)}}^{(j)}\left(\phi T\zeta_j^{-\alpha\epsilon}, \frac{1}{\Delta}\lambda\right) \tag{3.11}$$

in which $\mathscr{L}_{I_\theta^{(oc)}}^{(j)}(s,\lambda) \approx e^{-\pi\lambda\zeta_j^2\left[\frac{\pi s^{\frac{2}{\alpha}}}{\alpha\sin\left(\frac{2\pi}{\alpha}\right)}\sum_{m=1}^{N_{GL}} w_j\zeta_m^{\epsilon} - \frac{s}{4}\sum_{m=1}^{N_{GL}} w_m\zeta_j^{\alpha\epsilon}\sum_{i=1}^{N_G}\frac{c_i}{\eta_i^{\frac{\alpha}{2}}+s\zeta_m^{\frac{\alpha\epsilon}{2}}}\right]}$ (3.12)

where N_{GL} and N_G are the degree of the Laguerre and Legendre polynomial, t_i and w_i, x_i and c_i are the i-th node and weight, abscissas and weight of the corresponding quadratures; $\zeta_j = \sqrt{\frac{t_j}{\pi\lambda}}$; $\eta_i = \frac{x_i+1}{2}$

For both Gauss-Laguerre and Gauss-Legendre Quadrature, the higher the degree of the polynomials the better accuracy of the approximation. The values of t_i, w_1, x_i and c_i can be found from [57].

Proof: See Appendix B.1.

3.2 Average Coverage Probability

3.2.1 Average Coverage Probability of CCU and CEU

In this section, the average coverage probabilities of the CCU and CEU which were defined in Section 2.2.1 are evaluated for uplink with the power control exponent.

Theorem 3.2.1.1: (*Strict FR, CCU*) The average coverage probability of the CCU is given by

$$\mathcal{P}_{Str}^{(c)}(T,\epsilon) = \frac{\int_0^\infty \upsilon(T+\hat{T})\mathscr{L}(s_1,s_2,\lambda)dr}{\int_0^\infty \upsilon(T)\mathscr{L}_{I_\theta^{(oc)}}(s_1)dr} \tag{3.13}$$

where $\mathscr{L}_{I_\theta^{(oc)}}(s_1)$ and $\upsilon(T)$ are defined in Equation (3.6); $s_1 = Tr^{-\alpha\epsilon}$; $s_2 = \hat{T}r^{-\alpha\epsilon}$ and $\mathscr{L}(s_1,s_2,\lambda) = e^{-2\pi\lambda r^2 \int_1^\infty \left[1-\int_0^\infty \frac{\pi\lambda t e^{-\pi\lambda t^2}}{(1+s_1 t^{\alpha\epsilon}x^{-\alpha})(1+s_2 t^{\alpha\epsilon}x^{-\alpha})}dt\right]xdx}$.

The average coverage probability in Equation 3.13 can be approximated by

$$\mathcal{P}_{Str}^{(c)}(T,\epsilon) \approx \frac{\sum_{j=1}^{N_{GL}} w_j e^{-\frac{(T+\hat{T})}{SNR}\zeta_j^{\alpha(1-\epsilon)}} \mathscr{L}^{(j)}\left(\hat{T}\zeta_j^{-\alpha\epsilon}, T\zeta_j^{-\alpha\epsilon}, \lambda\right)}{\sum_{j=1}^{N_{GL}} w_j e^{-\frac{T}{SNR}\zeta_j^{\alpha(1-\epsilon)}} \mathscr{L}_{I_\theta^{(oc)}}^{(j)}(T\zeta_j^{-\alpha\epsilon})} \tag{3.14}$$

in which $\mathscr{L}^{(j)}(s_1,s_2,\lambda) \approx e^{-\pi\lambda\zeta_j^2\sum_{m=1}^{N_{GL}} w_m(I_0(\zeta_m)-I_1(\zeta_m))}$, $I_0(t) = \frac{2t^\epsilon}{\alpha}\frac{s_1^{1+\frac{2}{\alpha}}-s_2^{1+\frac{2}{\alpha}}}{s_1-s_2}\frac{\pi}{\sin\left(\frac{2\pi}{\alpha}\right)}$ and $I_1(t) = \sum_{i=1}^{N_G}\frac{ci}{2}\frac{(s_1+s_2)t^{\alpha\epsilon}\eta_i^{\frac{\alpha}{2}}+s_1s_2t^{\alpha\epsilon}}{\left(\eta_i^{\frac{\alpha}{2}}+s_1t^{\alpha\epsilon}\right)\left(\eta_i^{\frac{\alpha}{2}}+s_2t^{\alpha\epsilon}\right)}$; $\eta_i = \frac{x_i+1}{2}$.

Proof: See Appendix B.2

Theorem 3.2.1.2: (*Strict FR, CEU*) The average coverage probability of the CEU is given by

$$\mathcal{P}_{Str}^{(e)}(T,\epsilon) = \frac{\int_0^\infty \upsilon(\frac{\hat{T}}{\phi})\mathscr{L}_{I_\theta^{(oc)}}(s_2,\frac{\lambda}{\Delta})\left(1-e^{-\frac{T}{SNR}r^{\alpha(1-\epsilon)}}\mathscr{L}_{I_\theta^{(oc)}}(s_1,\lambda)\right)dr}{1-\int_0^\infty \upsilon(T)\mathscr{L}_{I_\theta^{(oc)}}(s_1)dr} \tag{3.15}$$

Using the same approach in Appendix B.1, the approximated value of $\mathcal{P}_{Str}^{(e)}(T,\epsilon)$ is

$$\mathcal{P}_{Str}^{(e)}(T,\epsilon) \approx \frac{\sum_{j=1}^{N_{GL}} w_j e^{-\frac{\hat{T}}{\phi SNR}\zeta_j^{\alpha(1-\epsilon)}} \mathscr{L}_{I_\theta^{(oc)}}^{(j)}(\hat{T}\zeta_j^{-\alpha\epsilon},\frac{\lambda}{\Delta})\left(1-e^{-\frac{T}{SNR}\zeta_j^{\alpha(1-\epsilon)}}\mathscr{L}_{I_\theta^{(oc)}}^{(j)}(T\zeta_j^{-\alpha\epsilon},\lambda)\right)}{1-\sum_{j=1}^{N_{GL}} w_j e^{-\frac{T}{SNR}\zeta_j^{\alpha(1-\epsilon)}} \mathscr{L}_{I_\theta^{(oc)}}^{(j)}(T\zeta_j^{-\alpha\epsilon},\lambda)} \tag{3.16}$$

Proof: See Appendix B.3

Theorem 3.2.1.3: (*Soft FR, CCU*) The average coverage probability of the CCU is given by

$$\mathcal{P}_{Sof}^{(c)}(T,\epsilon) = \frac{\int_0^\infty \upsilon(T+\hat{T})\mathscr{L}(s_1, s_2, \frac{\Delta-1}{\Delta}\lambda)\mathscr{L}(\phi s_1, \phi s_2, \frac{\lambda}{\Delta})dr}{\int_0^\infty \upsilon(T)\mathscr{L}_{I_\theta^{(oc)}}(s_1, \frac{\Delta-1}{\Delta}\lambda)\mathscr{L}_{I_\theta^{(oc)}}(\phi s_1, \frac{1}{\Delta}\lambda)dr} \tag{3.17}$$

The approximated value of $\mathcal{P}_{Sof}^{(c)}(T,\epsilon)$ is given by

$$\frac{\sum_{j=1}^{N_{GL}} w_j e^{-\frac{T+\hat{T}}{SNR}\zeta_j^{\alpha(1-\epsilon)}} \mathscr{L}^{(j)}(T\zeta_j^{-\alpha\epsilon}, \hat{T}\zeta_j^{-\alpha\epsilon}, \frac{\Delta-1}{\Delta}\lambda)\mathscr{L}^{(j)}(\phi T\zeta_j^{-\alpha\epsilon}, \phi\hat{T}\zeta_j^{-\alpha\epsilon}, \frac{\lambda}{\Delta})}{\sum_{j=1}^{N_{GL}} w_j e^{-\frac{T}{SNR}\zeta_j^{\alpha(1-\epsilon)}} \mathscr{L}^{(j)}_{I_\theta^{(oc)}}(T\zeta_j^{-\alpha\epsilon}, \frac{\Delta-1}{\Delta}\lambda)\mathscr{L}^{(j)}_{I_\theta^{(oc)}}(\phi T\zeta_j^{-\alpha\epsilon}, \frac{1}{\Delta}\lambda)} \tag{3.18}$$

Proof: See Appendix B.4

Theorem 3.2.1.4: (*Soft FR, CEU*) The average coverage probability of the CEU is given by

$$\mathcal{P}_{Sof}^{(e)}(T,\epsilon) = \frac{\left[\begin{array}{l}\int_0^\infty \upsilon\left(\frac{\hat{T}}{\phi}\right)\mathscr{L}_{I_\theta^{(oc)}}(\frac{s_2}{\phi}, \frac{\Delta-1}{\Delta}\lambda)\mathscr{L}_{I_\theta^{(oc)}}(s_2, \frac{1}{\Delta}\lambda) \\ \quad \times \left(1 - e^{-\frac{Tr^{\alpha(1-\epsilon)}}{SNR}}\mathscr{L}_{I_\theta^{(oc)}}(s_1, \frac{\Delta-1}{\Delta}\lambda)\mathscr{L}_{I_\theta^{(oc)}}(\phi s_1, \frac{1}{\Delta}\lambda)\right)\end{array}\right]}{1 - \int_0^\infty \upsilon(T)\mathscr{L}_{I_\theta^{(oc)}}(s_1, \frac{\Delta-1}{\Delta}\lambda)\mathscr{L}_{I_\theta^{(oc)}}(\phi s_1, \frac{1}{\Delta}\lambda)dr} \tag{3.19}$$

and its approximation is derived by $\mathcal{P}_{Sof}^{(e)}(T,\epsilon) \approx$

$$\frac{\sum_{j=1}^{N_{GL}} w_j \left[\begin{array}{l} e^{-\frac{\hat{T}}{\phi SNR}\zeta_j^{\alpha(1-\epsilon)}} \mathscr{L}^{(j)}_{I_\theta^{(oc)}}\left(\frac{\hat{T}\zeta_j^{-\alpha\epsilon}}{\phi}, \frac{\Delta-1}{\Delta}\lambda\right)\mathscr{L}^{(j)}_{I_\theta^{(oc)}}(\hat{T}\zeta_j^{-\alpha\epsilon}, \frac{1}{\Delta}\lambda) \\ \quad \times \left(1 - e^{-\frac{T}{SNR}\zeta_j^{\alpha(1-\epsilon)}}\mathscr{L}^{(j)}_{I_\theta^{(oc)}}\left(T\zeta_j^{-\alpha\epsilon}, \frac{\Delta-1}{\Delta}\lambda\right)\mathscr{L}^{(j)}_{I_\theta^{(oc)}}(\phi T\zeta_j^{-\alpha\epsilon}, \frac{1}{\Delta}\lambda)\right)\end{array}\right]}{1 - \sum_{j=1}^{N_{GL}} w_j e^{-\frac{T}{SNR}\zeta_j^{\alpha(1-\epsilon)}} \mathscr{L}^{(j)}_{I_\theta^{(oc)}}(T\zeta_j^{-\alpha\epsilon}, \frac{\Delta-1}{\Delta}\lambda)\mathscr{L}^{(j)}_{I_\theta^{(oc)}}(\phi T\zeta_j^{-\alpha\epsilon}, \frac{1}{\Delta}\lambda)}$$

Proof: See Appendix B.5

3.2.2 Average Coverage Probability of a Typical User

In the cellular networks, a typical user can be classified as a CCU with the transmit power $Pr^{\alpha\epsilon}$ or CEU with the transmit power $\phi Pr^{\alpha\epsilon}$. Therefore, evaluating the performance of the typical user can give an overall view on trends of the network performance as well as user's power consumption. The transmit power of the typical

user at a distance r from its serving BS is obtained by

$$\begin{aligned} P_u(r) &= \mathbb{P}(SINR^{(o)}(1,\epsilon) > T|r)P^{(c)} + \mathbb{P}(SINR^{(o)}(1,\epsilon) < T|r)P^{(e)} \\ &= Pr^{\alpha\epsilon}A_{FR}^{(c)}(T,\epsilon|r) + \phi Pr^{\alpha\epsilon}\left(1 - A_{FR}^{(c)}(T,\epsilon|r)\right) \end{aligned} \tag{3.20}$$

in which $\mathbb{P}(SINR^{(o)}(1,\epsilon) > T|r)$ and $\mathbb{P}(SINR^{(o)}(1,\epsilon) < T|r)$ are the probabilities where the user at a distance r from its serving BS is classified as a CCU and CEU, $P^{(c)}$ and $P^{(e)}$ are corresponding transmit powers; $A_{FR}^{(c)}(T,\epsilon|r)$ is defined in Lemma 3.1.2.1 and Lemma 3.1.2.2.

Thus, the average transmit power of the typical user is obtained by

$$\overline{P_u} = \int_0^\infty 2\pi\lambda r e^{-\pi\lambda r^2} Pr^{\alpha\epsilon}A_{FR}^{(c)}(T,\epsilon|r) + \phi Pr^{\alpha\epsilon}A_{FR}^{(e)}(T,\epsilon|r)dr \tag{3.21}$$

Employing a change of variable $t = \pi\lambda r^2$ and using Gauss-Laguerre Quadrature, the average transmit power is approximated by

$$\overline{P_u} \approx \sum_{j=1}^{N_{GL}} \omega_j P\zeta_j^{\frac{\alpha\epsilon}{2}} A_{FR}^{(c)}\left(T,\epsilon|r=\zeta_j\right) + \phi P\zeta_j^{\alpha\epsilon}A_{FR}^{(e)}\left(T,\epsilon|r=\zeta_j\right) \tag{3.22}$$

where $\zeta_j = \sqrt{\frac{t_j}{\pi\lambda}}$; N_{GL} is the degree of the Laguerre polynomial, t_i and w_i are the i-th node and weight of the quadrature.

The average coverage probability of the typical user is given by:

$$\begin{aligned} \mathcal{P}_{FR}(T,\epsilon|r) =& \mathbb{P}(SINR^{(o)}(1,\epsilon) > T|r)\mathcal{P}_{FR}^{(c)}(T,\epsilon|r) \\ &+ \mathbb{P}(SINR^{(o)}(1,\epsilon) < T|r)\mathcal{P}_{FR}^{(c)}(T,\epsilon|r) \end{aligned} \tag{3.23}$$

in which $\mathbb{P}(SINR(1,\epsilon) > T|r)$ and $\mathbb{P}(SINR(\phi,\epsilon) < T|r)$ are the coverage probabilities of the CCU and CEU whose distance to the serving BSs is r.

Therefore, the average coverage probability of the typical users is

$$\begin{aligned}\mathcal{P}_{FR}(T,\epsilon) &= \int_0^\infty 2\pi\lambda r e^{-\pi\lambda r^2}\Big[A_{FR}^{(c)}(T,\epsilon|r)\mathcal{P}_{FR}^{(c)}(T,\epsilon|r) \\ &\qquad + \Big(1-A_{FR}^{(c)}(T,\epsilon|r)\Big)\mathcal{P}_{FR}^{(e)}(T,\epsilon|r)\Big]\,dr \\ &\approx \sum_{j=1}^{N_{GL}}\omega_i\Big[A_{FR}^{(c)}\left(T,\epsilon|r=\zeta_j\right)\mathcal{P}_{FR}^{(c)}\left(T,\epsilon|r=\zeta_j\right) \\ &\qquad + \Big(1-A_{FR}^{(c)}\left(T,\epsilon|r=\zeta_j\right)\Big)\mathcal{P}_{FR}^{(e)}\left(T,\epsilon|r=\zeta_j\right)\Big]\end{aligned} \tag{3.24}$$

Using the results in Section 3.2.1, the average coverage probability of the typical user under Strict FR and Soft FR are given by:

In the case of Strict FR

$$\begin{aligned}\mathcal{P}_{Str}^{(c)}(T,\epsilon) &= \int_0^\infty \upsilon(T+\hat{T})\mathscr{L}(s_1,s_2,\lambda)dr \\ &\quad + \int_0^\infty \upsilon\left(\frac{\hat{T}}{\phi}\right)\mathscr{L}_{I_\theta^{(oc)}}\left(s_2,\frac{\lambda}{\Delta}\right)\left(1-e^{-\frac{T}{SNR}r^{\alpha(1-\epsilon)}}\mathscr{L}_{I_\theta^{(oc)}}(s_1,\lambda)\right)dr\end{aligned} \tag{3.25}$$

In the case of Soft FR

$$\begin{aligned}\mathcal{P}_{Sof}^{(e)}(T,\epsilon) &= \int_0^\infty \upsilon(T+\hat{T})\mathscr{L}\left(s_1,s_2,\frac{\Delta-1}{\Delta}\lambda\right)\mathscr{L}\left(\phi s_1,\phi s_2,\frac{\lambda}{\Delta}\right)dr \\ &\quad + \int_0^\infty \upsilon\left(\frac{\hat{T}}{\phi}\right)\mathscr{L}_{I_\theta^{(oc)}}(\frac{s_2}{\phi},\frac{\Delta-1}{\Delta}\lambda)\mathscr{L}_{I_\theta^{(oc)}}(s_2,\frac{1}{\Delta}\lambda) \\ &\quad \times\left(1-e^{-\frac{Tr^{\alpha(1-\epsilon)}}{SNR}}\mathscr{L}_{I_\theta^{(oc)}}(s_1,\frac{\Delta-1}{\Delta}\lambda)\mathscr{L}_{I_\theta^{(oc)}}(\phi s_1,\frac{1}{\Delta}\lambda)\right)\end{aligned} \tag{3.26}$$

3.2.3 Average Data Rate

3.2.3.1 Average User Data Rate

The average capacity of the user with a received uplink signal of $SINR$ is given by the Shannon Theorem, i.e, $C = \mathbb{E}\left[\, ln(1+SINR)\right]$ where the expectation is taken over the SINR distribution. In the FFR networks, the CCU experiences a received

SINR at $SINR(1,\epsilon)$ during the communication phase if the measured uplink SINR during the establishment phase is $SINR^{(o)}(1,\epsilon) > T$. Hence, the average capacity of the CCU is obtained by [37]:

$$\begin{aligned} C_{FR}^{(c)}(T,\epsilon) &= \mathbb{E}\left(\ln\left(SINR(1,\epsilon)+1\right)|SINR^{(o)}(1,\epsilon) > T\right) \\ &= \int_0^\infty \mathbb{P}\left(\ln\left(SINR(1,\epsilon)+1\right) > \gamma | SINR^{(o)}(1,\epsilon) > T\right) d\gamma \\ &= \int_0^\infty \frac{\mathbb{P}\left(SINR(1,\epsilon) > e^\gamma - 1, SINR^{(o)}(1,\epsilon) > T\right)}{\mathbb{P}\left(SINR^{(o)}(1,\epsilon) > T\right)} d\gamma \end{aligned} \tag{3.27}$$

Employing a change of variable $t = e^\gamma - 1$, Equation (3.27) becomes

$$C_{FR}^{(c)}(T,\epsilon) = \int_0^\infty \frac{1}{t+1} \frac{\mathbb{P}\left(SINR(1,\epsilon) > t, SINR^{(o)}(1,\epsilon) > T\right)}{\mathbb{P}\left(SINR^{(o)}(1,\epsilon) > T\right)} dt \tag{3.28}$$

The second part of the integrand in Equation (3.28) is the average coverage probability of the CCU with the coverage threshold $\hat{T} = t$. Therefore, the average data rate of the CCU is given by

$$C_{FR}^{(c)}(T,\epsilon) = \int_0^\infty \frac{1}{t+1} \mathcal{P}_{FR}^{(c)}(T,\epsilon|\hat{T}=t) dt \tag{3.29}$$

Similarly, the average data rate of the CEU in this case is obtained by [37]:

$$C_{FR}^{(e)}(T,\epsilon) = \int_0^\infty \frac{1}{t+1} \mathcal{P}_{FR}^{(e)}(T,\epsilon|\hat{T}=t) dt \tag{3.30}$$

in which $FR = (Str, Sof)$ corresponds to Strict FR and Soft FR.

Using the results in Section 3.2.1 for Equations 3.29 and 3.30, the average capacity of the CCU and CEU under Strict FR and Soft FR can be obtained.

3.2.3.2 Average Network Data Rate

In order to examine the network performance, it is assumed that the cellular network is allocated N RBs. Under Strict FR, the RBs are separated into $N_{Str}^{(c)}$ common RBs and Δ CE RB groups of $\frac{N_{Str}^{(e)}}{\Delta}$ RBs, in which $N_{Str}^{(c)} + N_{Str}^{(e)} = N$. Since each CE RB group is a private RBs with a group of Δ cells, each BS is allowed to

utilise $N_{Str}^{(c)}$ CC RBs and $\frac{N_{Str}^{(e)}}{\Delta}$ CE RBs. Under Soft FR, since each BS can transmit on all allocated RBs, each BS is allocated $N_{Sof}^{(c)}$ CC RBs and $N_{Sof}^{(e)}$ CE RBs, in which $N_{Sof}^{(c)} + N_{Sof}^{(e)} = N$.

Due to the assumption that each user is allocated a RB during a given timeslot, the BS can serve a maximum of $N_{Str}^{(c)}$ CCUs and $\frac{N_{Str}^{(e)}}{\Delta}$ CEUs in the case of Strict FR and $N_{Sof}^{(c)}$ CCUs and $N_{Sof}^{(e)}$ CEUs in the case of Soft FR. Therefore, the average network data rates under Strict FR and Soft FR are given by

- Under Strict FR

$$C_{Str}(T) = N_{Str}^{(c)} C_{Str}^{(c)}(T, \epsilon) + \frac{N_{Str}^{(e)}}{\Delta} C_{Str}^{(e)}(T, \epsilon) \tag{3.31}$$

- Under Soft FR

$$C_{Sof}(T) = N_{Sof}^{(c)} C_{Sof}^{(c)}(T, \epsilon) + N_{Sof}^{(e)} C_{Sof}^{(e)}(T, \epsilon) \tag{3.32}$$

in which $C_{FR}^{(c)}$ and $C_{FR}^{(e)}$ are average data rates of the CUU and CEU and defined in Equations 3.28 and 3.30.

3.3 Simulation and Discussion

In this section, the numerical and simulation results are presented to verify analytical results and the relationship between the SINR threshold and power control exponent with the network performance. The analytical parameters are based on 3GPP recommendations [58] such as path loss exponent $\alpha = 3.5$ and $P = -76\ dBm$ and $\sigma^2 = -99\ dBm$.

Since the numerical results of the exact expressions in forms of integrals are equal to those of the corresponding approximated expressions, a term *analytical results* is used to represent the numerical results of these approximated expressions.

3.3.1 Validation of the Analytical Results

The analytical results in Section 3.2.1 are compared with the Monte Carlo simulation. There are 8 curves in each Figures 3.1(a) and 3.1(b), in which 4 curves representing the analytical results perfectly match with the 4 star curves representing the simulation results.

The path loss increases with the distance from the receiver to the transmitter. Furthermore, when the user connects to the nearest BS, the distances from the typical user to interference sources are expected to be greater than that to the serving BS. Hence, when the path loss exponent increases, the interfering signals experience higher path loss than the serving signal, which results in an increase in SINR and user performance. Consequently, it can be observed from Figure 3.1 that the CCU and CEU achieve higher average coverage probabilities when the path loss exponent increases.

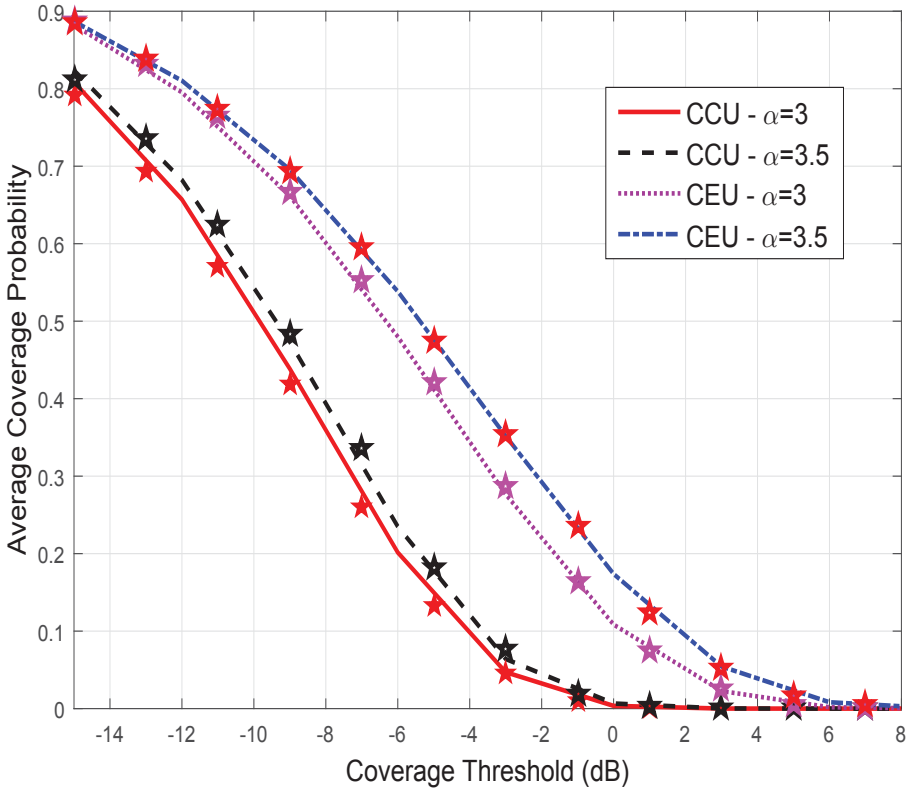

(a) Strict FR

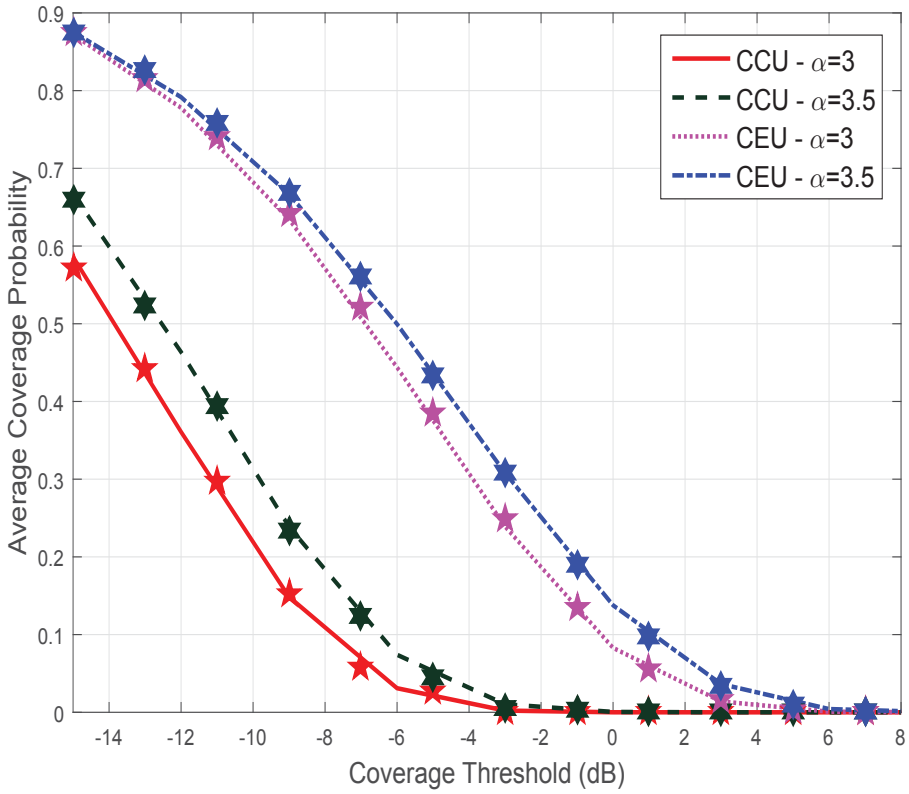

(b) Soft FR

Figure 3.1 : Comparison of the analytical results and Monte Carlo simulation

As shown in Figure 3.1, the Strict FR outperforms Soft FR in terms of average probability for both CCU and CEU. In the case of CCU, the CCU under Strict FR experiences interference, which is generated by the CCUs while under Soft FR, each CCU is affected by interference from both CCUs and CEUs. Hence, the CCU under Soft FR experiences higher interference and achieves a lower performance than that under Strict FR. For example, when coverage threshold $\hat{T} = -9$ dB and $\alpha = 3.5$, the average coverage probability of the CCU under Strict FR is 0.4839, which is 18% greater than that under Soft FR.

Properties 1 on Page 9 and 3 on Page 10 indicate that the CEU under Strict FR experiences a lower interference and consequently outperforms the CEU under Soft FR. However, the differences between performance of the CEU under Strict FR as shown in Figure 3.1(a) and Soft FR as shown in Figure 3.1(b) are not significant. For example, when coverage threshold is -9 dB, CEU average coverage probabilities are

0.7 in the case of Strict FR and around 0.68 in the case of Soft FR. The difference in this case approximates 2.9%.

Since the analytical results were verified by Monte Carlo in Section 3.3.1, in next sections only the analytical results are presented and discussed.

3.3.2 Effects of the Density of BSs

When the density of BSs increases which means more BSs are deployed in the networks, the distances between the user and BSs reduce, which leads to a decline in pathloss of both serving and interfering signals. However, the improvement of the serving signal overcomes an increase in interference [22], then the uplink SINR increases with the density of BSs. Therefore, it can be observed in Figure 3.2 that for both Strict FR and Soft FR, the CEU classification probability reduces when the density of BSs increases. For example, when the density of BSs increases from 1 BS/km^2 to 2 BS/km^2, the CEU classification probability reduces by 27.95% from 0.1850 to 0.1333 in the case of Strict FR and 7.10% from 0.3944 to 0.3664 in the case of Soft FR. Since CCU classification probability = 1 - CEU classification probability, CCU classification probability increases with the density of BSs.

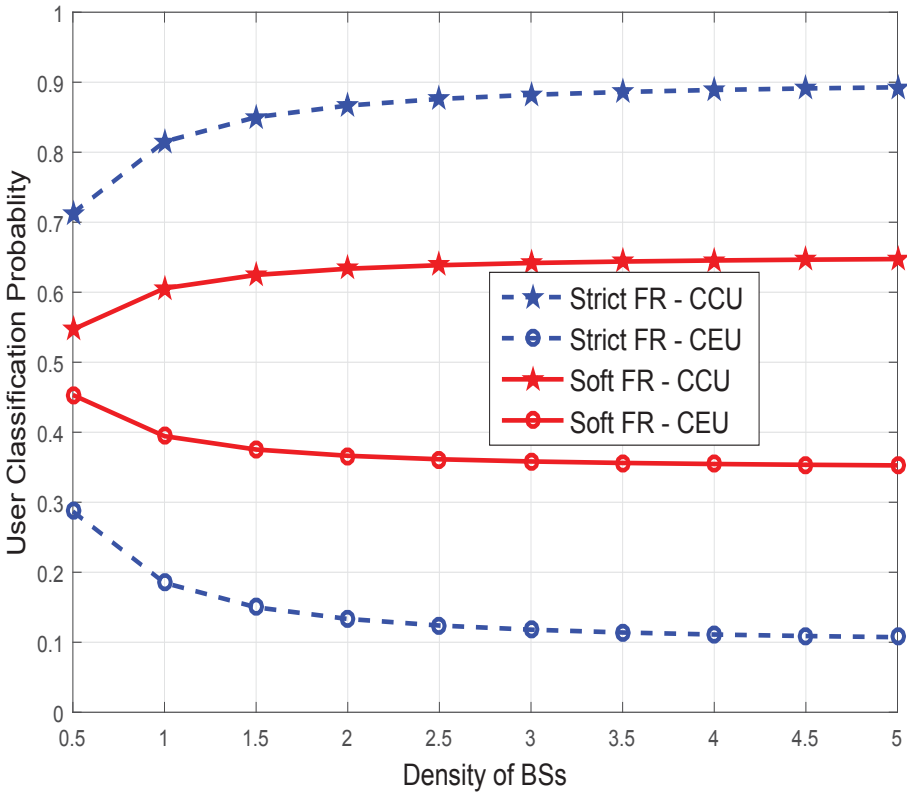

Figure 3.2 : Effects of BS Density on the User Classification Probability

It can be seen that when the density of BSs increases, *(i)* the distance from the user to the serving BS and consequently the transmit power of both CCU and CEU reduce, *(ii)* the CEU classification probability and consquently the number of CEU reduces as discussed above. Furthermore, since the CEUs always transmit at higher powers than the CCUs, the average transmit power of the typical user in Equation 3.21 reduces as shown in Figure 3.3.

The user under Soft FR experiences a higher interference level as dicussed in 3.3.1, and consequently more users are classifed as CEUs compared to Strict FR. Hence, the typical user under Soft FR consumes more energy than that under Strict FR as shown in Figure 3.3. For example, the typical user under Soft FR transmits at $-71.66\ dBm$ on average, which is 2.3 dBm (approximately 1.706 times) greater than that under Strict FR.

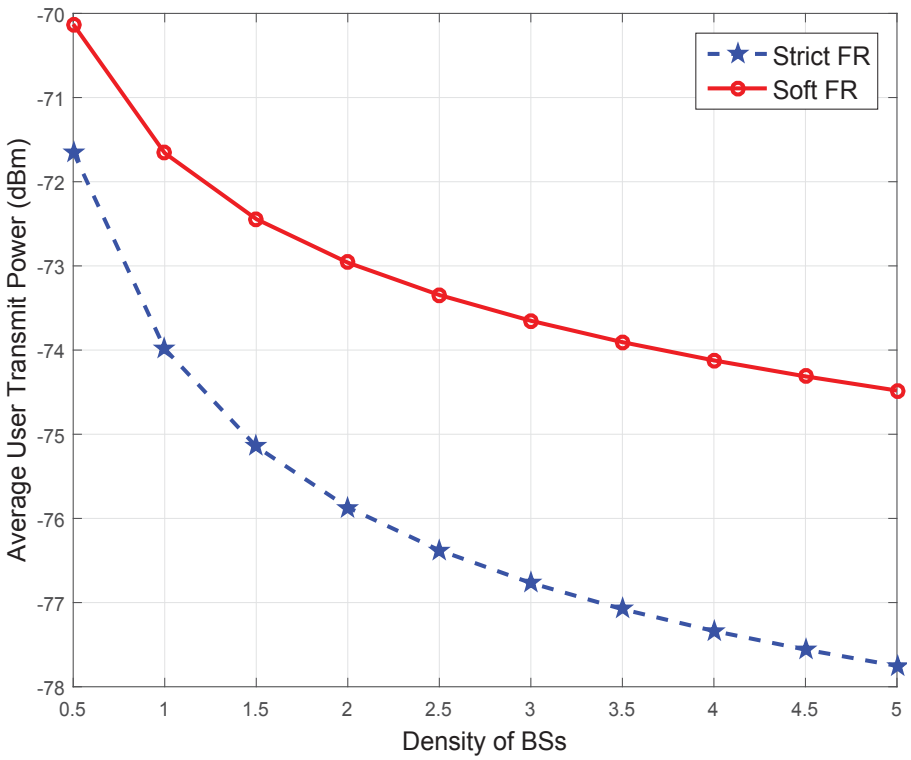

Figure 3.3 : Effects of BS Density on the Average User Transmit Power

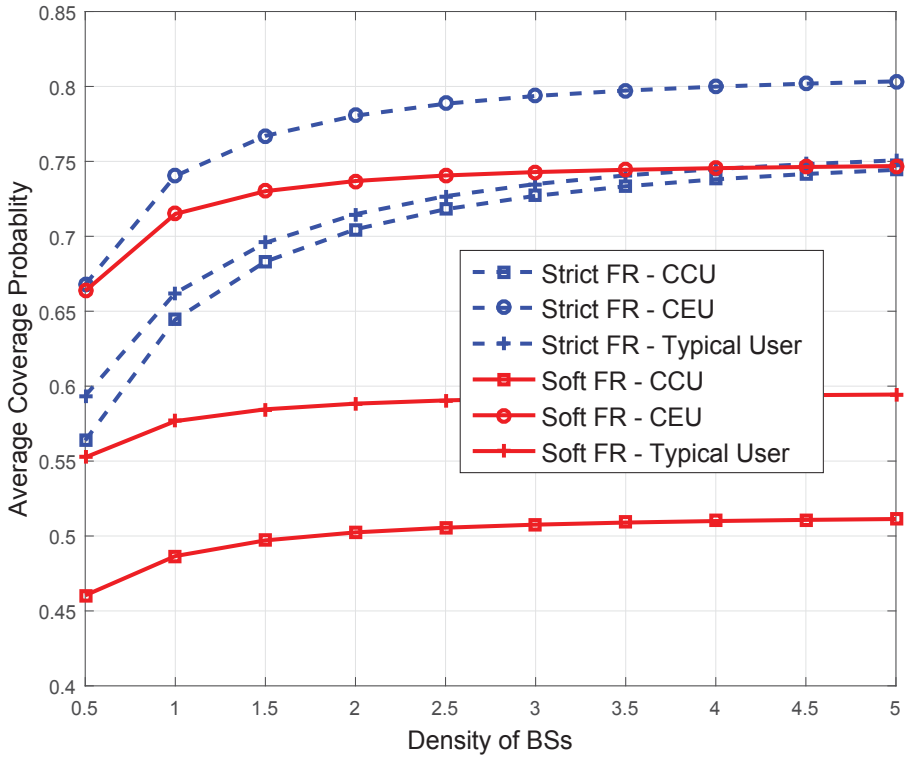

Figure 3.4 : Effects of BS Density on the Average Coverage Probability

Although the average transmit power reduces as shown in Figure 3.3, the uplink SINR can increases with the density of BSs as discussion for Figure 3.2. Thus, the average coverage probability of both CCU and CEU increase as shown in Figure 3.4. Take Strict FR for example, when λ increases from 1 BS/km^2 to 3 BS/km^2, the user transmit power reduces by 2.79 dBm from -73.98 dBm to -76.77 dBm but the average coverage probabilities increase by 14.03% from 0.6445 to 0.7349 in the case of CCU and by 4.0% from 0.7149 to 0.7429 in the case of CEU. Therefore, increasing the number of BSs in the networks can be considered as one approach to save user power consumption and improve network performance.

3.3.3 Effects of the Power Control Exponent

To evaluate the effect of the power control exponent ϵ on the user's performance, different network scenarios from sparse to dense networks [54] are considered. Figures 3.6 and 3.7 show that the user transmit power increases in the case of $\lambda = 0.1$ BS/km^2, reduces in the case of $\lambda = 1$ BS/km^2 but a decline followed by an increase in the case of $\lambda = 0.5$ BS/km^2. This finding contradicts the conclusion for $\lambda = 0.24$ BS/km^2 in [30], which stated that the average transmit power of the users greatly reduces with an increase in ϵ.

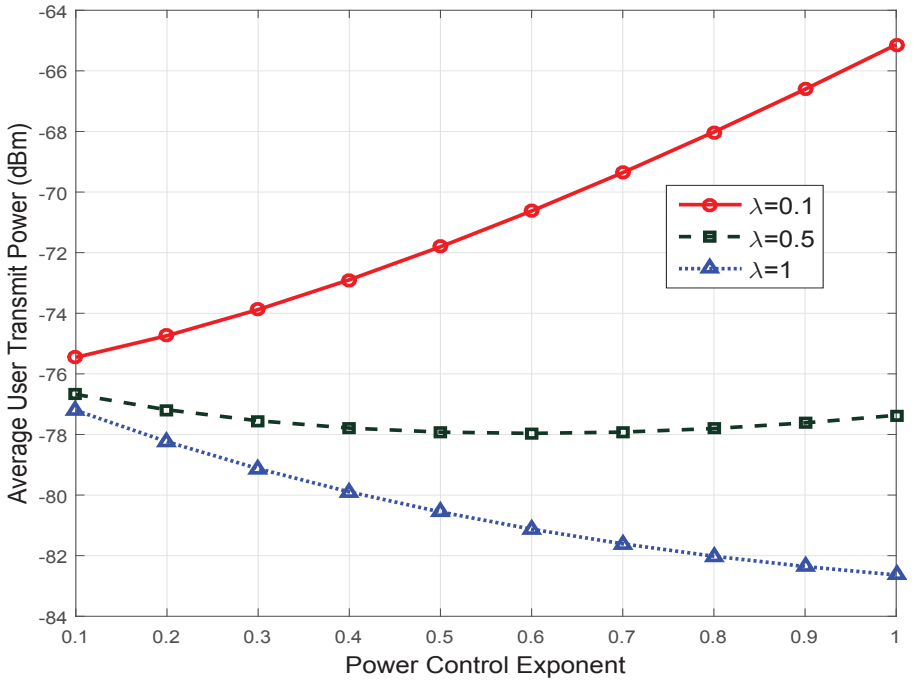

Figure 3.5 : Average User Transmit Power

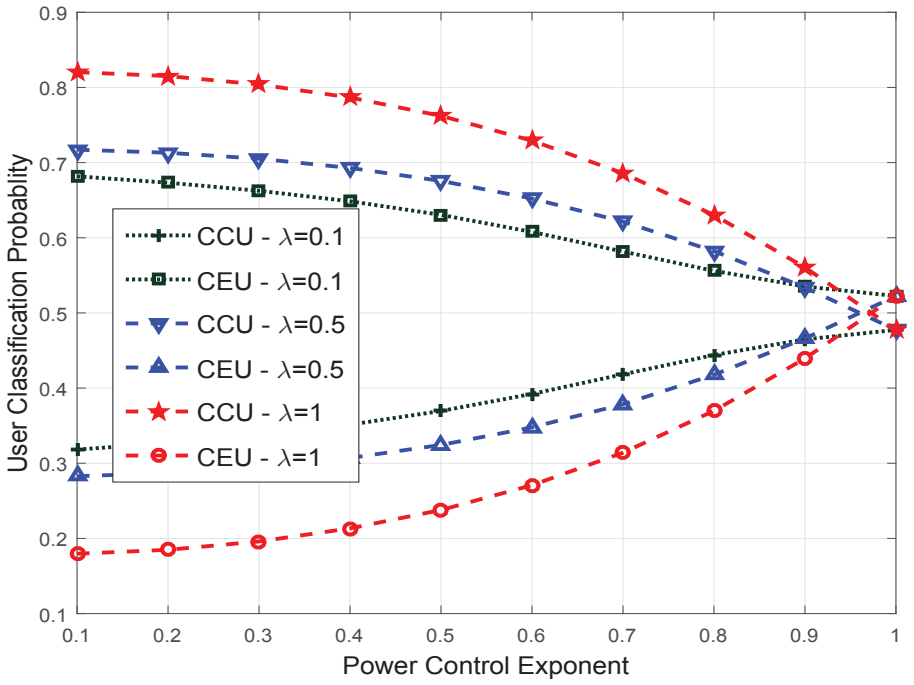

(a) (*Strict FR*) User Classification Probability and Average Transmit Power

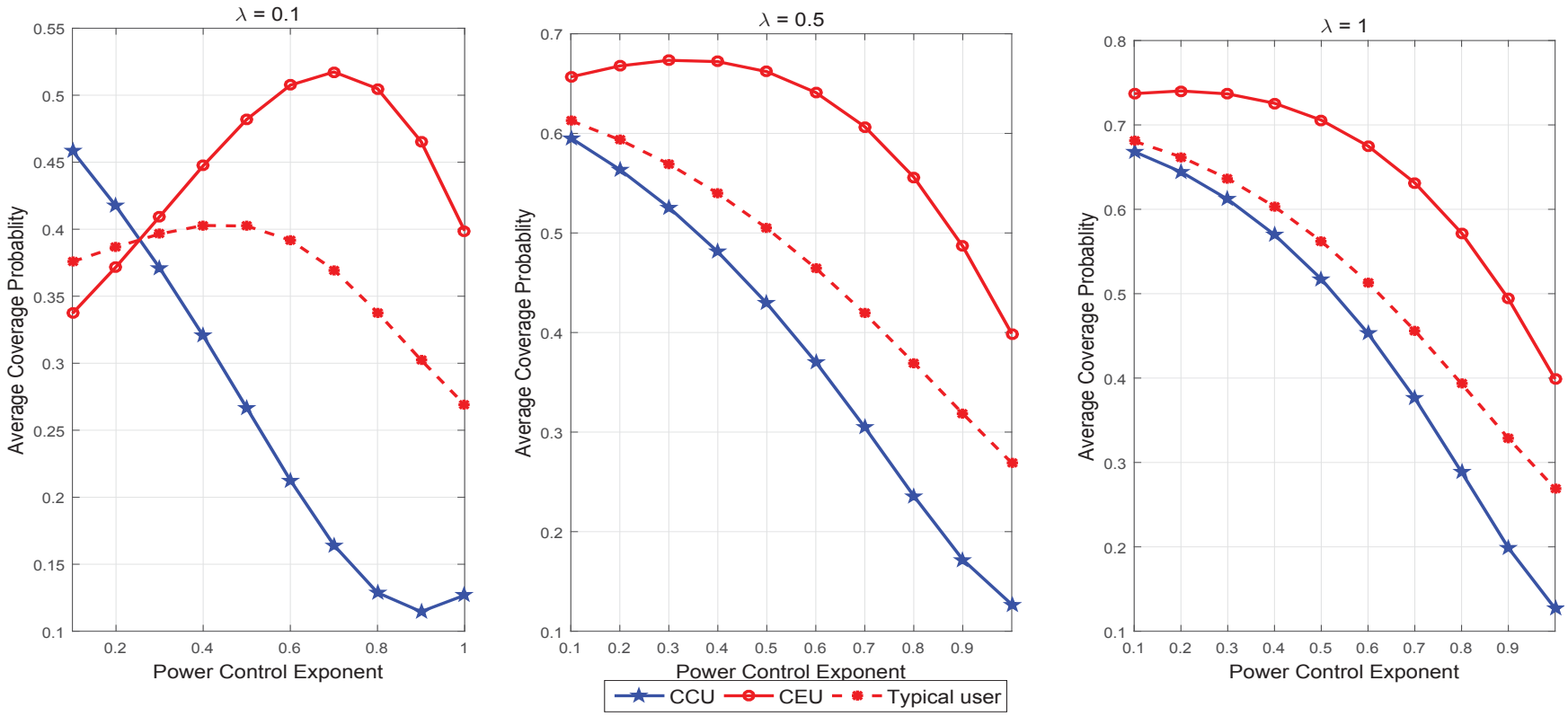

(b) (*Strict FR*) User Average Coverage Probability

Figure 3.6 : (*Strict FR*): Effects of the Power Control Exponent on the Network Performance

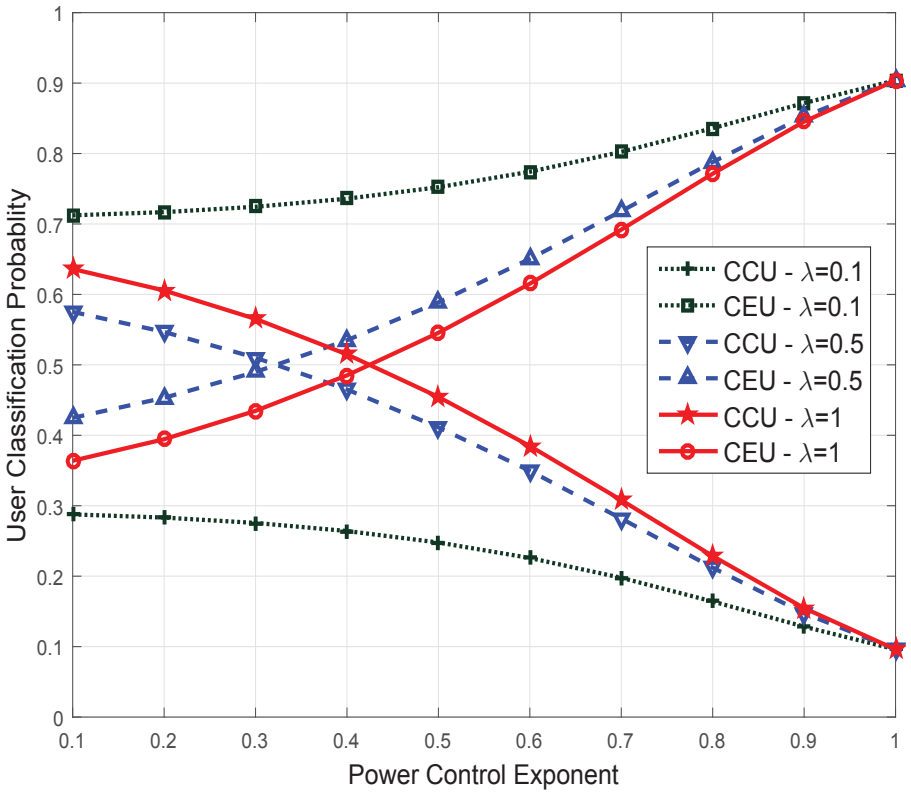

(a) (*Soft FR*) User Classification Probability

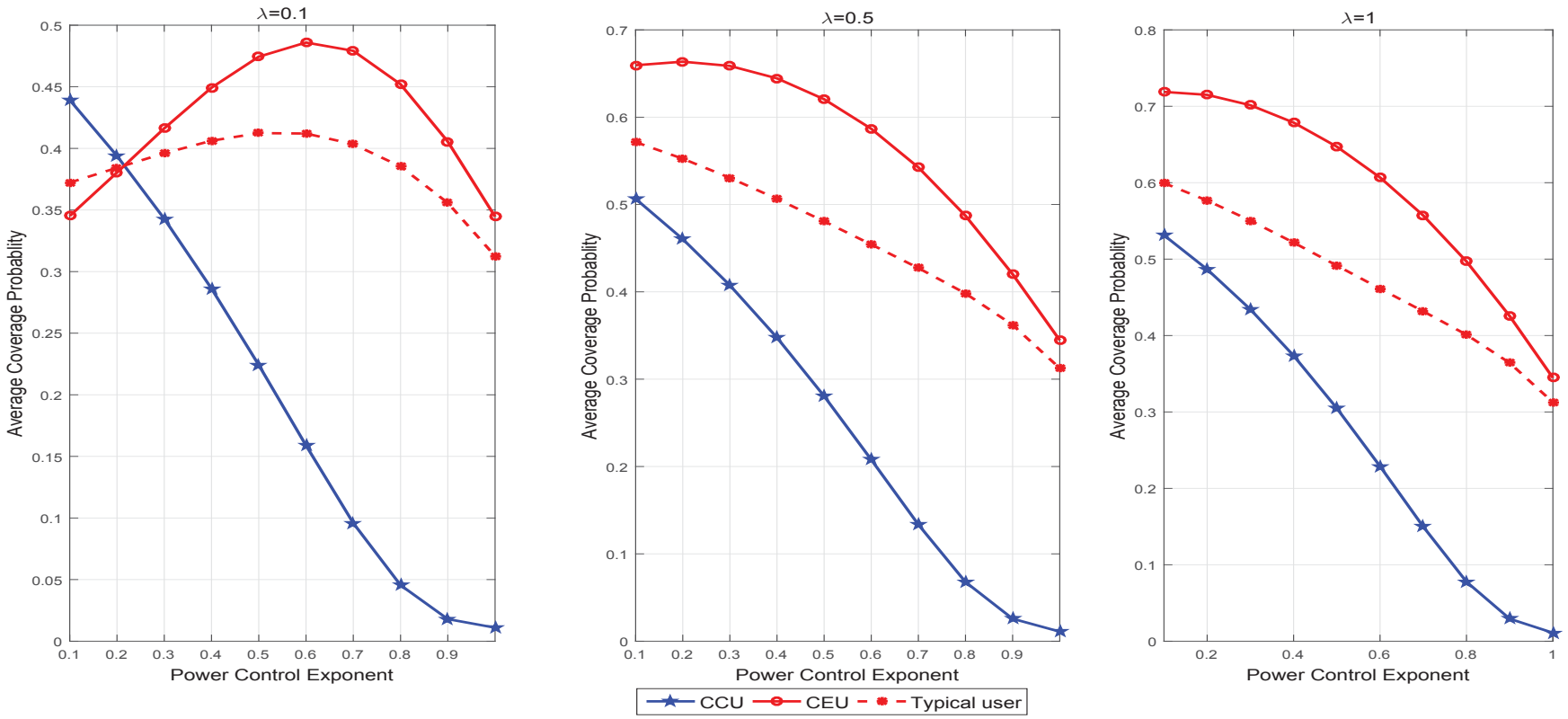

(b) (*Soft FR*) User Average Coverage Probability

Figure 3.7 : (*Soft FR*): Effects of the Power Control Exponent on the Network Performance

For sparse network such as in rural area

The BSs are distributed approximately every 10 km^2 and the density of BSs is approximately $\lambda \approx 0.1\ BS/km^2$. The average distance from the user to the serving BS is $E[r] = \int_0^\infty 2\pi\lambda r^2 e^{-\pi\lambda r^2} = 1.581\ km$. Thus, there exist users with the distances to the serving BSs $r < 1\ km$ and others with $r > 1$. When ϵ increases, the transmit power drops rapidly for the users having distances $r < 1\ km$ and exponentially increases for the users having distances $r > 1$. Since the average distance is 1.581 km, the number of users with $r > 1\ km$ is much greater than those with $r < 1\ km$. Therefore, the average transmit power of the typical user increases with ϵ.

It is very interesting that in the case of Strict FR, although the average uplink SINR on the CC RB during the establishment phase improves with the power control exponent ϵ, which is represented through an increase in the number of CCUs, the average coverage probability of the CCU undergoes a rapid decline as shown in Figure 3.6. The phenomenon can be explained by the following hypothesis: when ϵ increases, the interference from the users with $r > 1\ km$ increases while that from the users with $r < 1\ km$ reduces. Since in this scenario, the number of users with $r > 1\ km$ is much greater than those with $r < 1\ km$, the total uplink interference can increase with ϵ though all interfering users transmit at the same power. Thus, the users with $r < 1\ km$ experience lower uplink SINRs but most of these users are still defined as the CCUs due to a very small value of SINR threshold, e.g $T = -10dB$, while the users with $r > 1\ km$ may achieve higher uplink SINR and may be classified as the CCUs. Hence, it is obviously that more users are classified as the CCU in this case. In other words, the CCU classification probability during the establishment phase increases with ϵ.

During the communication phase, in the case of the CCU that is usually close to the serving BS $r < 1\ km$, when ϵ increases, the CCU transmit power decreases while its interference increases. Thus, the uplink SINR of the CCUs decreases rapidly, which is represented by a reducing trend of average coverage probability as shown in Figure 3.6. In the case of the CEU which is usually far from the serving BS, the CEU transmit power significantly increases with ϵ, which can overcome the rise of

interference. Hence, the CEU may achieve a higher performance when ϵ increases. However, at a high value of ϵ such as $\epsilon = 0.7$, the increase in the CEU transmit power can not trade off with the growth of interference, which results in a reduction of the average coverage probability.

In the case of Soft FR, since the CC RB experiences interference from both CCUs and CEUs in which CEUs are usually farther from the serving BSs (conventionally $r > 1\ km$) than CCUs and transmit at a high power. When ϵ increases, the interference from the CEUs increases with a higher rate than the reduction in interference from the CCUs. Therefore, the interference on the CC RB increases with ϵ, which causes of a drop in uplink SINR of the users, especially for the users with $r < 1\ km$. Therefore, in this case, more users are served as the CEUs when ϵ increases, which is presented through the upward trend of the CEU classification probability in Figure 3.7.

When the user is classified as the CEU on the uplink, it will transmit at a high transmit power while the interference is unlikely to change. Therefore, classifying more users to be CEUs can improve the average uplink SINR and average coverage probability of the CEU. However, when ϵ increases to a high value such as $\epsilon = 0.7$ in the case of Soft FR, the interference from the CEUs may be much greater than that from the CCUs and the Gaussian noise. Thus, the uplink SINR is approximated by $SINR \approx \frac{g r^{\alpha(\epsilon-1)}}{\sum_{j \in \theta_{Sof}^{(e)}} r_j^{\alpha\epsilon} g_{jz} d_{jz}^{-\alpha}}$. Consequently, the use of the high transmit power to serve user in this case may not bring any benefit to the user performance. As a result, the average coverage probability in this case is smaller than that in the case of a low value of ϵ. Furthermore, the optimal values of the power control exponent can be selected at $\epsilon = 0.7$ in the case of Strict FR and $\epsilon = 0.6$ in the case of Soft FR where the average coverage probabilities of the typical user are at the peaks of 0.52 and 0.48 respectively.

For network medium dense such as in urban

The BSs is distributed around every 2 km^2 and the density of BSs is around 0.5 BS/km^2. The average distance in this case is $E[r] = 0.7071\ km$. Hence the transmit

power of both a CCU $Pr^{\epsilon\alpha}$ and a CEU $\phi Pr^{\epsilon\alpha}$ reduces when ϵ increases. However, since the CCU classification probability increases with ϵ, the average transmit power of the typical user slowly reduces to the bottom at -77.92 dBm when $\epsilon = 0.7$ and before marginally increasing. As shown in the figure, the average coverage probability of the user reduces very quickly since high values of ϵ lead to an increase in the transmit power from interfering users having great path loss, and growth of interference at the BS .

For dense network such as in the city center

The BSs may be distributed every square kilometre, and thus the density of BSs is $\lambda = 1\ BS/km^2$. In this case, the user is usually very close its serving BS with an average distance of $E[r] = 0.5\ km$. Hence, both the average transmit power of the CCU and CEU reduces when ϵ increase. However, the trend of the coverage probability on average is similar in the case of the urban networks. Therefore, the optimal values of ϵ in this case can be chosen at $\epsilon = 0$ as seen in Figures 3.6(b) and 3.7(b) , at which the user's performance is at the maximum value.

3.3.4 Average Network Data Rate Comparison

In this section, the average data rates of the networks using Strict FR and Soft FR are compared as shown in Figure 3.8(c). It is assumed that the network is allocated 75 RBs, which corresponds to 15 MHz. As discussed in Section 3.2.3.2, the number of CC and CE RBs under Strict FR are $N_{Str}^{(c)} = 30$ and $N_{Str}^{(e)}$ in the case of Strict FR, and $N_{Sof}^{(c)} = 50$ and $N_{Sof}^{(e)} = 25$ in the case of Soft FR.

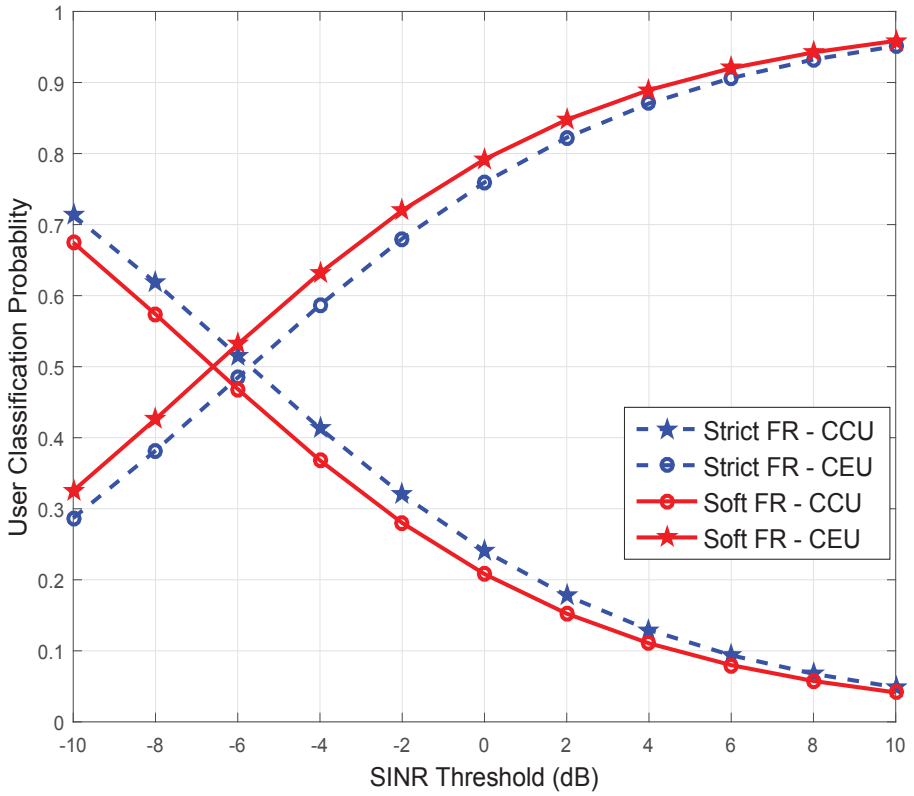

(a) User Classification Probability

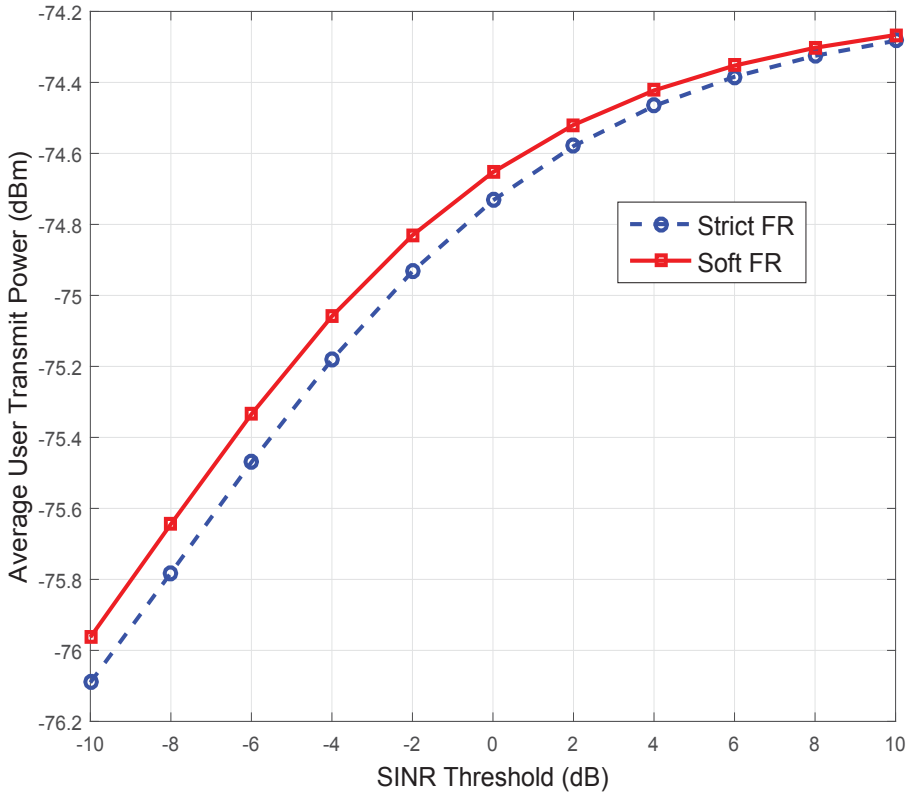

(b) User Average Coverage Probability

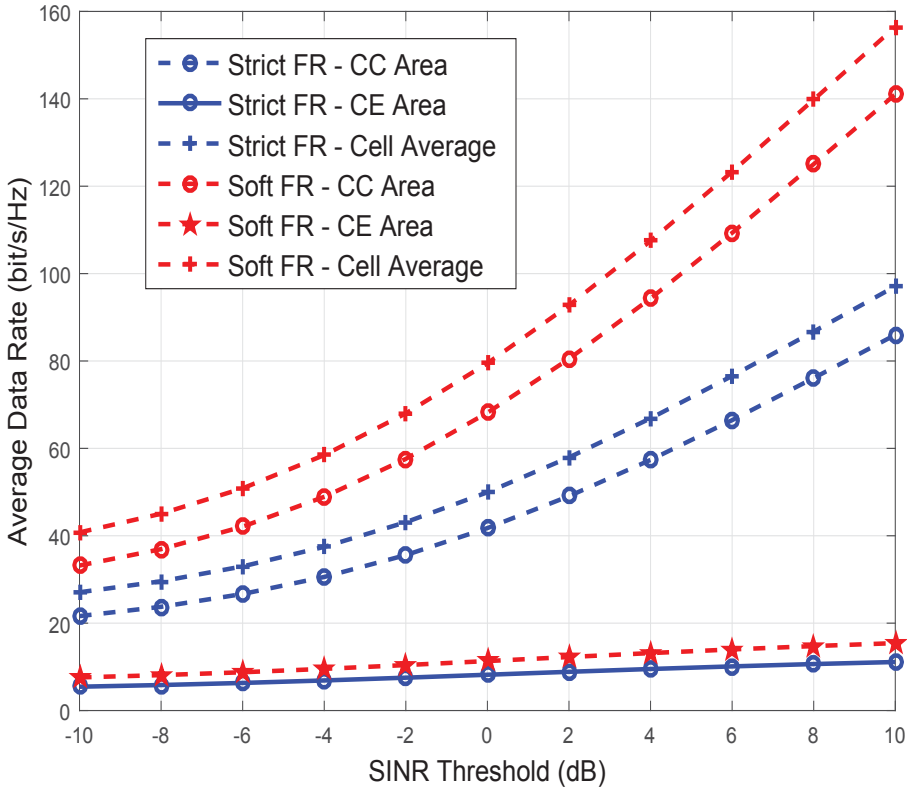

(c) User Average Coverage Probability

Figure 3.8 : Effects of the SINR Threshold on the Network Performance

As expected, the CEU classification probability increases significantly with the SINR threshold. As discussed in previous sections, the uplink in the case of Strict FR achieves a higher SINR than that in the case of Soft FR. In other words, more users under Strict FR achieve higher uplink SINRs than under Soft FR. Hence, most users under Soft FR are classified as CEUs even when SINR threhold is at a low value. Consequently, when SINR threshold increases to a high value, more users in the Strict FR are being classified as new CEUs. Therefore, although the user under Soft FR can be classified as the CEU with a higher probability than that under Strict FR, the probability of CEU classification under Strict FR increases at a higher rate than that under Strict FR. For example, when the SINR threshold increases from -4 dB to 0 dB, the rate under Strict FR is 0.294 while that under Soft FR is 0.253.

In contradiction to the conclusion in Section 3.3.1 that stated that the Strict

FR outperforms Soft FR in terms of average coverage probability of both CCU and CEU, Figure 3.8(c) indicates that Soft FR achieves a significantly higher average cell data rate than Strict FR. Take SINR threshold $T = 0$ for example, the average data rate of the networks using Soft FR is approximately 79.48 (bit/s/Hz), which is 58.96% greater than that using Strict FR. This is due to the fact that although Soft FR can create more interference than Strict FR, each cell in the network using Soft FR allows to reuse all RBs, i.e. $N_c + N_e$, while under Strict FR, each cell is only allowed to resue $N_c + \frac{N_e}{\Delta}$ RBs and thus more users can be served at the same time than Strict FR.

3.4 Conclusion

In this chapter, the uplink of the PPP cellular networks using Strict FR and Soft FR are modelled, in which 3GPP recommendations are followed. The analytical results which are verified by the Monte Carlo simulation focus on the network performance matrices such as the CCU and CEU classification probabilities, the average transmit power, and average coverage probability. The close-form expressions of the performance metrics were derived by using Gaussian Quadratures. While the Strict FR outperforms Soft FR in terms of average coverage probability and power consumption of both CCU and CEU, Soft FR can achieve a higher cell data rate. For both Strict FR and Soft FR, the user can achieve higher performance and consumes lower power when the density of BSs increases. For medium dense networks with $\lambda = 0.5\ BS/km^2$ and dense networks with $\lambda = 1\ BS/km^2$, the user performance is at the maximum value when all users transmit at their constant powers, e.g. P for CCUs and ϕP for CEUs. Meanwhile, for sparse networks with $\lambda = 0.1\ BS/km^2$, the average coverage probability of the CEU during the communication phase increases significantly to the peak before undergoing a rapid decline when the power control exponent increases.

Chapter 4

Performance of FFR in Downlink Multi-Tier Random Cellular Networks

Chapters 2 and 3 presented performance of FFR in downlink and uplink single-tier networks respectively. In this chapter, the performance of multi-tier PPP networks using Strict FR and Soft FR are investigated for a number of users and a number of RBs.

4.1 Multi-Tier Network and Biased User Association

We consider a PPP cellular network with K tiers in which Tier-k ($1 \leq k \leq K$) is characterised by a density of BSs λ_k, a transmit power P_k on CC RBs and a bias factor B_k. The bias factor is used for load-balancing between tiers in the heterogeneous networks by handover users from a given tier to other tiers. The downlink signals in each tier experience different path loss exponents, and for Tier-k, it is denoted by α_k. The list of symbols associated with Tier-k is presented in Table 4.1.

Table 4.1 : Symbol Descriptions for Tier-k

Symbol	**Meaning of Symbol**
K	Number of Tiers in a heterogeneous network.
λ_k	Density of BSs
α_k	Pathloss exponent
g_k	Channel power gain
r_k	Distance from the user to the nearest BS
P_k	Transmit power on CC RBs
ϕ_k	Transmit power ratio between transmit power on the CE RB and CC RB
B_k	Bias factor of Tier k is an operator set parameter that is used for load-balancing in heterogeneous networks by handing over users from a heavily loaded to less loaded tier.
A_k	Average Probability with which a user connects to a BS in Tier-k (Equation 4.2) [42]
T_k	SINR threshold
$\hat{T}_k$	Coverage threshold is dependent on the UE sensitivity. For both CCU and CEU , the received $SINR > \hat{T}_k$ for communication to be possible.
$M_k^{(n)}$	Average number of new users associated with a cell as defined in Equation 4.3

During the establishment phase, $M_k^{(o)}$ is denoted as the average number of existing users in a typical cell in Tier-k. The average number of new users who request communications with the networks is modelled as a Poisson RV with mean $\lambda^{(u)}$.

The user prefers a connection with a tier which has the greatest long-term average Biased-Received-Power (BRP) [42]. The BRP of the user in Tier-k is $B_k P_k r_k^{-\alpha_k} E[g_k]$ in which r_k and g_k are the distance and channel power gain between the user and the serving BS in Tier-k. The fading channel is i.i.d Rayleigh RV with a mean of 1, i.e. $E[g_k] = 1$. Hence, the typical user is associated with a BS in Tier-k if $\forall 1 \leq j \leq K, j \neq k$ [42]

$$B_k P_k r_k^{-\alpha_k} = \max\left(B_j P_j r_j^{-\alpha_j}\right) \quad \text{or} \quad r_j > \left(\frac{B_j P_j}{B_k P_k}\right)^{1/\alpha_j} r_k^{\alpha_k/\alpha_j}, \tag{4.1}$$

Therefore, the average probability that a user connects to a BS in Tier-k is obtained by [42]:

$$A_k = \mathbb{E}_{R_k}\left[\prod_{j=1,j\neq k}^{K} \mathbb{P}\left(R_j > \left(\frac{B_j P_j}{B_k P_k}\right)^{1/\alpha_j} R_k^{\alpha_k/\alpha_j} | R_k\right)\right]$$
$$= \pi\lambda_k \int_0^{\infty} \exp\left\{-\pi \sum_{j=1}^{K} \lambda_j C_j t^{\alpha_k/\alpha_j}\right\} dt \tag{4.2}$$

in which $C_j = \left(\frac{B_j P_j}{B_k P_k}\right)^{2/\alpha_j}$.

We denote S as the area of the PPP network. Thus, $A_k\lambda^{(u)}S$ and $\lambda_k S$ represent the number of new users and number of BSs in Tier-k respectively. The average number of new users that are associated with a typical cell of Tier-k is given by:

$$M_k^{(n)} = \frac{A_k\lambda^{(u)}S}{\lambda_k S} = \pi\lambda^{(u)} \int_0^{\infty} \exp\left\{-\pi \sum_{j=1}^{K} \lambda_j C_j t^{\alpha_k/\alpha_j}\right\} dt \tag{4.3}$$

Furthermore, the PDF of the distance from the user to its associated BS, r_k, is shown in [42]:

$$f_{R_k}(r_k) = \frac{2\pi\lambda_k}{A_k} r_k \exp\left\{-\pi \sum_{j=1}^{K} \lambda_j C_j r_k^{2\alpha_k/\alpha_j}\right\} \tag{4.4}$$

4.2 Fractional Frequency Reuse

We assume that all cells in a given tier use the same FR pattern including a resource allocation technique and an FR factor. During the establishment phase, the SINR threshold is used to classify $M_k^{(o)}$ existing users in each cell into $M_k^{(oc)}$ CCUs and $M_k^{(oe)}$ CEUs . Similarly, the $M_k^{(n)}$ new users are also classified into $M_k^{(ne)}$ CEUs and $M_k^{(nc)}$ CCUs . Correspondingly, N_k allocated RBs in Tier-k are divided into $N_k^{(c)}$ CC RBs and $N_k^{(e)}$ CE RBs. In the case of the Soft FR, each BS is allowed to use the entire $N_k^{(c)}$ RBs for CCUs and $N_k^{(e)}$ RBs for CEUs while each BS under the Strict FR is only allowed to use $N_k^{(c)}$ RBs for CCUs and $\frac{N_k^{(e)}}{\Delta_k}$ RBs for CEUs . We denote the transmission ratio of Tier-k, which is a ratio between a transmit

power on a CEU and CCU as ϕ_k.

We denote $\theta_k^{(c)}$, $\theta_k^{(e)}$ as the set of interfering BSs transmitting at the CC and CE powers in Tier-k; $\lambda_k^{(c)}$ and $\lambda_k^{(e)}$ are the densities of BSs in $\theta_k^{(c)}$ and $\theta_k^{(e)}$ in which $\lambda_k^{(c)} = \lambda_k$ and $\lambda_k^{(e)} = \frac{\lambda_k}{\Delta_k}$ under the Strict FR (Property 1), and $\lambda_k^{(c)} = \frac{\Delta_k - 1}{\Delta_k}\lambda_k$ and $\lambda_k^{(e)} = \frac{1}{\Delta_k}\lambda_k$ under the Soft FR (Property 3). The set of BS in Tier-k is denoted by θ_k, then $\theta_k = \theta_k^{(c)} \bigcap \theta_k^{(e)}$.

4.2.1 A proposed network model using FFR

In LTE networks, every BS is continuously transmitting downlink control information, and subsequently each control channel experiences the ICI from all adjacent BSs. Thus, the measured SINR on the control channel does not depend on the network status such as the average number of RBs and number of users. In contrast, the BS transmits on the data channel only if the user requires data from the BS. Thus, the measured SINR on the data channel strongly depends on the network status and consequently, this can provide more accuracy on the ICI. Hence, we propose a network model using FFR that the BS uses SINR on the data channel to classify CCUs and CEUs.

The reporting interval can be adjusted based on the uplink traffic load [9]. Hence, it is assumed that when new users arrive, the existing users do not report the channel state to the BSs. Thus, the existing CCUs (CEUs) are continuously served as CCUs (CEUs) while each new user is defined as either CCU or CEU .

We denote $z = (c, e)$ in which $z = c$ and $z = e$ correspond to the CC and CE, respectively. The numbers of CCUs and CEUs per cell in Tier-k are related by the following equation:

$$M_k^{(oz)} + M_k^{(nz)} = M_k^{(z)} \tag{4.5}$$

4.2.2 Scheduling Algorithm

Each typical user z in Tier-k can be randomly allocated an available RB out of $N_k^{(z)}$ RBs. We define $\tau_k^{(z)}$ as an indicator function that takes value of 1 if the RB b is used at z cell area of Tier-k and zero otherwise. The expected values of $\tau_k^{(z)}$, can be called as the *interfering probability* or the *allocation ratio* of the number of users and the number of RBs, and it is given by:

$$\epsilon_k^{(z)} = \mathbb{E}[\tau_k^{(z)}] = \begin{cases} \frac{M_k^{(z)}}{N_k^{(z)}} & \text{, when} \quad M_k^{(z)} < N_k^{(z)} \\ 1 & \text{, otherwise} \end{cases} \tag{4.6}$$

During the establishment phase when $M_k^{(nz)} = 0$ for both $z = c$ and $z = e$, the indicator function and allocation ratio for z cell area in Tier-k is denoted by $\epsilon_k^{(oz)}$ and $\tau_k^{(oz)}$ respectively.

Strict FR

The ICI of user z in a multi-tier network can be obtained by expanding Equation 2.8 for a single-tier downlink network:

$$I_{Str}^{(z)} = \sum_{j=1}^{K} \left\{ \sum_{y \in \theta_j^{(z)}} \tau_k^{(z)} \tau_j^{(y)} \phi_j^{(z)} P_j g_{jy} r_{jy}^{-\alpha_j} \right\} \tag{4.7}$$

in which $z = (c, e)$, $\phi_j^{(c)} = 1, \phi_j^{(e)} = \phi_j$; g_{jy} and r_{jy} are the channel power gain and distance from the user to the interfering BS y in Tier-j, respectively.

Soft FR

Similarly, the ICI at user z in Tier-k can be obtained from Equation 2.9:

$$I_{Sof}^{(z)} = \sum_{j=1}^{K} \left\{ \sum_{z_c \in \theta_j^{(z)}} \tau_k^{(z)} \tau_j^{(z_c)} P_j g_{jz_c} r_{jz_c}^{-\alpha_j} + \sum_{z_e \in \theta_j^{(e)}} \tau_k^{(z)} \tau_j^{(z_e)} \phi_j P_j g_{jz_e} r_{jz_e}^{-\alpha_j} \right\} \tag{4.8}$$

4.2.3 Signal-to-Interference-plus-Noise Ratio

The instantaneous received SINR of user z from the serving BS in Tier-k is obtained by:

$$SINR_k(\phi_k^{(z)}, r_k) = \frac{\phi_k^{(z)} P_k g_k r_k^{-\alpha_k}}{\sigma^2 + I_{FR}^{(z)}} \tag{4.9}$$

in which $I_{FR}^{(z)}$ is the ICI of the user z, $FR = (Sof, Str)$ corresponds to Soft FR and Strict FR.

4.2.4 Number of new CCUs and CEUs

The probability that the user in Tier-k is served as the CCU is given by $\mathbb{P}(SINR^{(o)}(1, r_k) > T_k)$. The average number of new CCUs and CEUs in a typical cell in Tier-k are $M_k^{(n)}\mathbb{P}(SINR^{(o)}(1, r_k) > T_k)$ and $M_k^{(n)} - M_k^{(n)}\mathbb{P}(SINR^{(o)}(1, r_k) > T_k)$ respectively.

Theorem 4.2.4.1: (Strict FR) The average number of new CCUs per cell in Tier-k is given by

$$M_{Str,k}^{(nc)}(T_k) = \pi\lambda^{(u)} \int_0^{\infty} e^{-\frac{T_k t^{\alpha/2}}{SNR_k} - \pi \sum_{j=1}^{K} \lambda_j C_j t^{\alpha_k/\alpha_j} \left(1+\epsilon_k^{(oc)} \upsilon_j^{(oc)}(T_k)\right)} dt \tag{4.10}$$

and the average number of CEUs is

$$\begin{aligned} M_{Str,k}^{(ne)}(T) =& \frac{\pi\lambda^{(u)}}{\lambda_k} \int_0^{\infty} e^{-\pi \sum_{j=1}^{K} \lambda_j C_j t^{\frac{\alpha_k}{\alpha_j}}} dt \\ & - \pi\lambda^{(u)} \int_0^{\infty} e^{-\frac{T_k t^{\alpha/2}}{SNR_k} - \pi \sum_{j=1}^{K} \lambda_j C_j t^{\alpha_k/\alpha_j} \left(1+\epsilon_k^{(oc)} \upsilon_j^{(oc)}(T_k)\right)} dt \end{aligned} \tag{4.11}$$

where the symbols are defined in Table 4.1 and $\upsilon_j^{(oc)}(T_k) = \int_0^1 \frac{\epsilon_j^{(oc)}}{\frac{1}{T_k}\frac{B_j}{B_k} x^{2-\alpha_j/2} + x^2} dx$.

Proof: Since in Strict FR, the CC RB is only affected by the ICI from the BSs transmitting at the CC power, the probability that the user in Tier-k is defined as the CCU is obtained by using Appendix C.1 with $\lambda_k^{(c)} = \lambda_k$ and $\lambda_k^{(e)} = 0$.

Theorem 4.2.4.2: (Soft FR) The average number of new CCUs and CEUs per cell in Tier-k are given by $M^{(nc)}_{Sof,k}(T_k)$ and $M^{(ne)}_{Sof,k}(T_k)$ where

$$M^{(nc)}_{Sof,k}(T_k) = \pi\lambda^{(u)} \int_0^{\infty} e^{-\frac{T_k r_k^{\alpha_k/2}}{SNR_k} - \pi \sum_{j=1}^{K} \lambda_j C_j \epsilon_k^{(oc)} \rho_j^{(o)}(T_k) t^{\frac{\alpha_k}{\alpha_j}}} dt \tag{4.12a}$$

$$\begin{aligned} M^{(ne)}_{Sof,k}(T_k) =& \frac{\pi\lambda^{(u)}}{\lambda_k} \int_0^{\infty} e^{-\pi \sum_{j=1}^{K} \lambda_j C_j t^{\frac{\alpha_k}{\alpha_j}}} dt \\ & - \pi\lambda^{(u)} \int_0^{\infty} e^{-\frac{T_k r_k^{\alpha_k/2}}{SNR_k} - \pi \sum_{j=1}^{K} \lambda_j C_j \epsilon_k^{(oc)} \rho_j^{(o)}(T_k) t^{\frac{\alpha_k}{\alpha_j}}} dt \end{aligned} \tag{4.12b}$$

in which

$$\rho_j^{(o)}(T_k) = \frac{1}{\Delta_j} \int_0^1 \frac{\epsilon_j^{(oe)}}{\frac{1}{T_k}\frac{B_j}{\phi_j B_k} x^{2-\alpha_j/2} + x^2} dx + \frac{\Delta_j - 1}{\Delta_j} \int_0^1 \frac{\epsilon_j^{(oc)}}{\frac{1}{T_k}\frac{B_j}{B_k} x^{2-\alpha_j/2} + x^2} dx \tag{4.13}$$

Proof: See Appendix C.1. ■

4.3 Coverage Probability

4.3.1 Coverage Probability Definition

The coverage probability of a CCU and CEU in a single-tier network for a given coverage threshold were defined in Section 2.2.1. When the user connects to Tier-k, the average coverage probability in Equations 2.16 and 2.17 can be re-written as follows

$$\text{For CCU}: \mathcal{P}_k^{(c)}(T_k, \hat{T}_k) = \mathbb{P}\left(SINR(1, r_k) > \hat{T}_k | SINR^{(o)}(1, r_k) > T_k\right) \tag{4.14a}$$

$$\text{For CEU}: \mathcal{P}_k^{(e)}(T_k, \hat{T}_k) = \mathbb{P}\left(SINR(\phi_k, r_k) > \hat{T}_k | SINR^{(o)}(1, r_k) < T_k\right) \tag{4.14b}$$

in which T_k and $\hat{T}_k$ are the SINR threshold and coverage threshold for Tier-k (defined in Table 4.1); $SINR_k^{(o)}(1, r_k)$ and $SINR_k(\phi_k, r_k)$ are defined as in Equation 4.9.

The user is under the coverage of the multi-tier network if it is under the coverage area of any tier. Hence, the average coverage probability of user z in the networks

is

$$\mathcal{P}_c^{(z)} = \sum_{k=1}^{K} A_k P_k^{(z)}(T_k, \hat{T}_k) \tag{4.15}$$

in which $z = (c, e)$ and A_k is defined in Equation 4.2.

4.3.2 Coverage Probabilities of CCU and CEU

Theorem 4.3.2.1: (Strict FR, CCU) The average coverage probability of a CCU in Tier-k of a Strict FR network is given by

$$\mathcal{P}_{Str,k}^{(c)}(T_k, \hat{T}_k) = \frac{\int_0^\infty e^{-\frac{(\hat{T}_k+T_k)t^{\frac{\alpha_k}{2}}}{SNR_k} - \pi\sum_{j=1}^{K}\lambda_j C_j t^{\frac{\alpha_k}{\alpha_j}} \times \left[\begin{matrix}\epsilon_k^{(oc)}\upsilon_j^{(c)}(T_k) + \epsilon_k^{(c)}\upsilon_j^{(c)}(\hat{T}_k) \\ + 1 - \epsilon_k^{(oc)}\epsilon_k^{(c)}\kappa^{(c)}(T_k, \hat{T}_k)\end{matrix}\right]} dt}{\int_0^\infty e^{-\frac{T_k t^{\alpha_k/2}}{SNR_k} - \pi\sum_{j=1}^{K}\lambda_j t^{\alpha_k/\alpha_j}\left(1+\epsilon_k^{(oc)}\upsilon_j^{(oc)}(\hat{T}_k)\right)} dt} \tag{4.16}$$

in which $\kappa^{(c)}(T_k, \hat{T}_k) = \int_0^1 \frac{\epsilon_j^{(oc)}\epsilon_j^{(c)}}{x^2\left(\frac{1}{T_k}\frac{B_j}{B_k}x^{-\alpha_j/2}+1\right)\left(\frac{1}{\hat{T}_k}\frac{B_j}{B_k}x^{-\alpha_j/2}+1\right)} dx$ and
$\upsilon_j^{(c)}(\hat{T}_k) = \int_0^1 \frac{\epsilon_j^{(c)}}{\frac{1}{\hat{T}_k}\frac{B_j}{B_k}x^{2-\alpha_j/2}+x^2} dx.$

Proof: See Appendix C.2 ■

Theorem 4.3.2.2: (Strict FR, CEU) The average coverage probability of a CEU in Tier-k of a Strict FR network is given by

$$\begin{aligned}
&\mathcal{P}_{Str,k}^{(e)}(T_k, \hat{T}_k) \\
&= \frac{\pi\lambda_k \int_0^\infty \left[\begin{matrix} e^{-\frac{\hat{T}_k t^{\alpha_k/2}}{\phi_k SNR_k} - \pi\sum_{j=1}^{K}\lambda_j t^{\alpha_k/\alpha_j}\left(1+\epsilon_k^{(e)}\upsilon_j^{(e)}(\hat{T}_k)\right)} - e^{-\frac{t^{\alpha_k/2}}{SNR_k}\left(\frac{\hat{T}_k}{\phi_k}+T_k\right)} \\ \times e^{-\pi\sum_{j=1}^{K}\lambda_j C_j t^{\alpha_k/\alpha_j} \times \left[\begin{matrix}\epsilon_k^{(oc)}\upsilon_j^{(oc)}(T_k) + \frac{1}{\Delta_j}\epsilon_k^{(e)}\upsilon_j^{(e)}(\hat{T}_k) \\ + 1 - \frac{1}{\Delta_j}\epsilon_k^{(oc)}\epsilon_k^{(e)}\kappa^{(e)}(T_k, \hat{T}_k)\end{matrix}\right]}\end{matrix}\right] dt}{1 - \int_0^\infty e^{-\frac{T_k t^{\alpha_k/2}}{SNR_k} - \pi\sum_{j=1}^{K}\lambda_j t^{\alpha_k/\alpha_j}\left(1+\epsilon_k^{(oc)}\upsilon_j^{(oc)}(\hat{T}_k)\right)} dt}
\end{aligned} \tag{4.17}$$

in which $\kappa^{(e)}(T_k, \hat{T}_k) = \int_0^1 \frac{\epsilon_j^{(oc)}\epsilon_j^{(e)}}{x^2\left(\frac{1}{T_k}\frac{B_j}{B_k}x^{-\alpha_j/2}+1\right)\left(\frac{1}{\hat{T}_k}\frac{B_j}{B_k}x^{-\alpha_j/2}+1\right)}$ and

$$v_j^{(e)}(\hat{T}_k) = \int_0^1 \frac{\epsilon_j^{(e)}}{\frac{1}{\hat{T}_k}\frac{\phi_k}{\phi_j}\frac{B_j}{B_k}x^{2-\alpha_j/2}+x^2}dx$$

Proof: See Appendix C.3 ■

Theorem 4.3.2.3: (Soft FR, CCU) The average coverage probability of a CCU associated with Tier-k of a Soft FR network is given by

$$\mathcal{P}_{Sof,k}^{(c)}(1,\hat{T}_k) = \frac{\int_0^\infty e^{-\frac{t^{\alpha_k/2}}{SNR_k}\left(\hat{T}_k+T_k\right)-\pi\lambda_j C_j t^{\alpha_k/\alpha_j}\times\left[\begin{array}{c}\epsilon_k^{(oc)}\rho_j^{(o)}(T_k)+\epsilon_k^{(c)}\rho_j(\hat{T}_k)\\ +1-\epsilon_k^{(oc)}\epsilon_k^{(c)}\Gamma^{(c)}(T_k,\hat{T}_k)\end{array}\right]}dt}{\int_0^\infty e^{-\frac{T_k t^{\alpha_k/2}}{SNR_k}-\pi\sum\limits_{j=1}^{K}\lambda_j C_j t^{\alpha_k/\alpha_j}\left(1+\epsilon_k^{(oc)}\rho_j^{(o)}(T_k)\right)}dt} \tag{4.18}$$

where $\rho_j(T_k) = \frac{1}{\Delta_j}\int_0^\infty \frac{\epsilon_j^{(e)}}{\frac{1}{T_k}\frac{B_j}{\phi_j B_k}x^{2-\alpha_j/2}+x^2}dx + \frac{\Delta_j-1}{\Delta_j}\int_0^\infty \frac{\epsilon_j^{(c)}}{\frac{1}{T_k}\frac{B_j}{B_k}x^{2-\alpha_j/2}+x^2}dx$; and

$\Gamma_j(T_k,\hat{T}_k) = \frac{\Delta_j-1}{\Delta_j}\int_0^1 \frac{\epsilon_j^{(oc)}\epsilon_j^{(c)}}{x^2\left(1+\frac{1}{T_k}\frac{B_j}{B_k}x^{-\alpha_j/2}\right)\left(1+\frac{1}{\hat{T}_k}\frac{B_j}{B_k}x^{-\alpha_j/2}\right)}dx + \frac{1}{\Delta_j}\int_0^1 \frac{\epsilon_j^{(oe)}\epsilon_j^{(e)}}{x^2\left(1+\frac{1}{T_k}\frac{B_j}{\phi_j B_k}x^{-\alpha_j/2}\right)\left(1+\frac{1}{\hat{T}_k}\frac{B_j}{\phi_j B_k}x^{-\alpha_j/2}\right)}$.

Proof: See Appendix C.4. ■

Theorem 4.3.2.4: (Soft FR, CEU) The average coverage probability of a CEU in Tier-k of a Soft FR network is

$$\begin{aligned}&\mathcal{P}_{Str,k}^{(e)}(T_k,\hat{T}_k)\\ &= \frac{\pi\lambda_k\int_0^\infty\left[\begin{array}{l}e^{-\frac{\hat{T}_k t^{\alpha_k/2}}{\phi_k SNR_k}-\pi\sum\limits_{j=1}^{K}\lambda_j C_j t^{\alpha_k/\alpha_j}\left(1+\epsilon_k^{(e)}\rho_j\left(\frac{\hat{T}_k}{\phi_k}\right)\right)}-e^{-\frac{t^{\alpha_k/2}}{SNR_k}\left(\frac{\hat{T}_k}{\phi_k}+T_k\right)}\\ \qquad\times e^{-\pi\sum_{j=1}^{K}\lambda_j C_j t^{\alpha_k/\alpha_j}\times\left[\begin{array}{c}\epsilon^{(oc)}\rho_j^{(o)}(T_k)+\epsilon^{(e)}\rho_j\left(\frac{\hat{T}_k}{\phi_k}\right)\\ +1-\epsilon_k^{(oc)}\epsilon_k^{(e)}\Gamma_j\left(\frac{\hat{T}_k}{\phi_k}\right)\end{array}\right]}\end{array}\right]dt}{1-\pi\lambda_k\int_0^\infty e^{-\frac{T_k t^{\alpha_k/2}}{SNR_k}-\pi\sum\limits_{j=1}^{K}\lambda_j C_j t^{\alpha_k/\alpha_j}\left(1+\epsilon_k^{(oc)}\rho_j^{(o)}(T_k)\right)}dt}\end{aligned} \tag{4.19}$$

in which $\rho_j^{(o)}(T_k)$, $\rho_j(T_k)$ and $\Gamma_j(T_k,\hat{T}_k)$ were defined in Theorem 4.3.2.3.

Proof: The coverage probability expression of the CEU under the Soft FR is

$$\mathcal{P}_c^{(c)}(T_k,\hat{T}_k) = \frac{\mathbb{P}\left(\frac{\phi_k P_k g'_k r_k^{-\alpha_k}}{\sigma^2+I_{Soft}^{(e)}} > \hat{T}_k, \frac{P_k g_k r_k^{-\alpha_k}}{\sigma^2+I_{Soft}^{(oc)}} < T_k\right)}{\mathbb{P}\left(\frac{P_k g_k r_k^{-\alpha_k}}{\sigma^2+I_{Soft}^{(oc)}} < T_k\right)}$$
$$= \frac{\int_0^\infty 2\pi\lambda_k r_k e^{-\pi\lambda_k r_k^2}\mathbb{E}\left[e^{-\frac{\hat{T}_k r_k^{\alpha_k}}{\phi_k P_k}\left(\sigma^2+I_{Soft}^{(e)}\right)}\left(1-e^{-\frac{T_k r_k^{\alpha_k}}{P_k}\left(\sigma^2+I_{Soft}^{(oc)}\right)}\right)\right]dr_k}{1-\int_0^\infty 2\pi\lambda_k r_k e^{-\pi\lambda_k r_k^2}\mathbb{E}\left[e^{-\frac{T_k}{P_k}\left(\sigma^2+I_{Soft}^{(oc)}\right)}\right]dr_k}$$

The numerator is evaluated using the results of Appendices C.1 and C.2 with coverage threshold $\frac{\hat{T}_k}{\phi_k}$ and allocation ratio for the second phase of $\epsilon_k^{(e)}$. The denominator is obtained by Appendix C.1. Therefore, the CEU average coverage probability is given by Equation 4.19.

4.4 Average Cell data rate

4.4.1 Average data rate of CCU and CEU

The average data rate of a CCU and CEU were presented in Equations 3.29 and 3.30 for a single-tier uplink cellular network. Thus, when the CCU connects to a BS in Tier-k, the average data rate is given by

$$C_{FR,k}^{(c)}(T_k,1) = \int_0^\infty \frac{1}{t+1}\mathcal{P}_{FR,k}^{(c)}(T_k,t)dt \tag{4.20}$$

in which average coverage probability $\mathcal{P}_{FR,k}^{(c)}(T_k,t)$ is defined by Equation 4.16 in the case of Strict FR and Equation 4.18 in the case of Soft FR.

Similarly, the average data rate of the CEU associated with a BS in Tier-k is obtained by [37]:

$$C_{FR,k}^{(e)}(T_k,\phi_k) = \int_0^\infty \frac{1}{t+1}\mathcal{P}_{FR,k}^{(e)}(T_k,\hat{T}_k)dt \tag{4.21}$$

in which $\mathcal{P}_{FR,k}^{(e)}(T_k,t)$ is defined by Equation 4.17 in the case of Strict FR and Equation 4.19 in the case of Soft FR.

4.4.2 Average Cell data rate

The average cell data rate can be obtained by calculating a sum of the data rate of all users within that cell. For Tier-k, the average cell data rate is defined as:

$$R_k(T_k) = M_k^{(e)} C_k^{(e)}(T_k, \phi_k) + M_k^{(c)} C_k^{(c)}(T_k, 1) \tag{4.22}$$

in which $M_k^{(e)}$ and $M_k^{(c)}$ are the average numbers of CEUs and CCUs per cell, which were given in Section 4.2.4.1 and 4.2.4.2; $C_{FR,k}^{(e)}(T_k, \phi_k)$ and $C_{FR,k}^{(c)}(1, \phi_k)$ are CEU and CCU average data rates in Tier-k which were given by Equations 4.20 and 4.21.

The total network data rate is obtained by finding the sum of cell data rate of all cells in the networks.

4.5 Simulation Results and Discussion

In this section, the numerical results for a 2-tier networks are analysed. Conventionally, the macro BSs with a higher transmit power are distributed with a lower density than pico BSs with a lower transmit power. The macro BSs are distributed with a density of $\lambda_1 = 0.05\ BS/km^2$ which is 10 times less than that of the pico BSs $\lambda_2 = 0.5\ BS/km^2$. Since the average number of existing users during the initial network state is used to estimate the ICI of the networks when new users arrive and do not affect the trends of the network performance, the average number of existing users can be assumed to be constant. In our simulation study, 3 CCUs and 6 CEUs are randomly chosen for each cell in Tier-1, while 3 CCUs and 5 CEUs are selected for each cell in Tier-2. In a practical network, the BSs can select some of users with high SINRs to establish the establishment phase. The average number of new users requesting communication with the networks is assumed to be a Poisson RV with a mean of $\lambda^{(u)} = 5\ user/km^2$.

Each cell in each tier of the network is allowed to share 75 RBs corresponding to 15 MHz and utilises the FR scheme with a reuse factor of 3. Under Soft FR, the 75 RBs are divided in 3 groups of 25 RBs, two of the groups are assigned to CC Area and the last group is assigned to CE Area. Under Strict FR, the 75 RBs are

partitioned into a common group of 30 RBs that is assigned to CC Area of each cell and 3 private groups of 15 RBs. Each private group is assigned to CE Area of each cell in a group of 3 cells. The simulation parameters are summarised in Table 4.3.

Table 4.3 : Analytical and simulation parameters

Parameters	**Value**
Number of tiers	$K = 2$
Density of BSs	$\lambda_1 = 0.05$, $\lambda_2 = 0.5$ BS/km^2
Frequency Reuse factor	$\Delta_1 = 3$, $\Delta_2 = 3$
Density of new users	$\lambda^{(u)} = 5$ $user/km^2$
Transmit power on a CC RB	$P_1 = 53$ dBm, $P_2 = 33$ dBm
Thermal noise	-99 dBm (corresponding to 15 MHz bandwidth)
Transmit power ratio	$\phi_1 = 20$, $\phi_2 = 10$
Number of RBs per cell - Soft FR - Strict FR	75 50 CC RBs; 25 CE RBs 30 CC RBs; 15 CE RBs
Network area	$S = 100$ km^2

In Figure 4.1, the average coverage probability of the CCU and CEU in a 2-tier PPP network are simulated for 2 cases ($(\phi_1 = 1, \phi_2 = 1)$ and $(\phi_1 = 20, \phi_2 = 10)$) with an assumption that the coverage thresholds are the same in every tier. The solid lines represent the analytical results which visually match with the stars representing the simulation results. The dashed lines represent CEU average coverage probability if the CEU is served with the CC power, i.e, $\phi_1 = \phi_2 = 1$. It is noted that there are 4 theoretical curves and 2 simulation curves in both Figures 4.1(a) and 4.1(b)

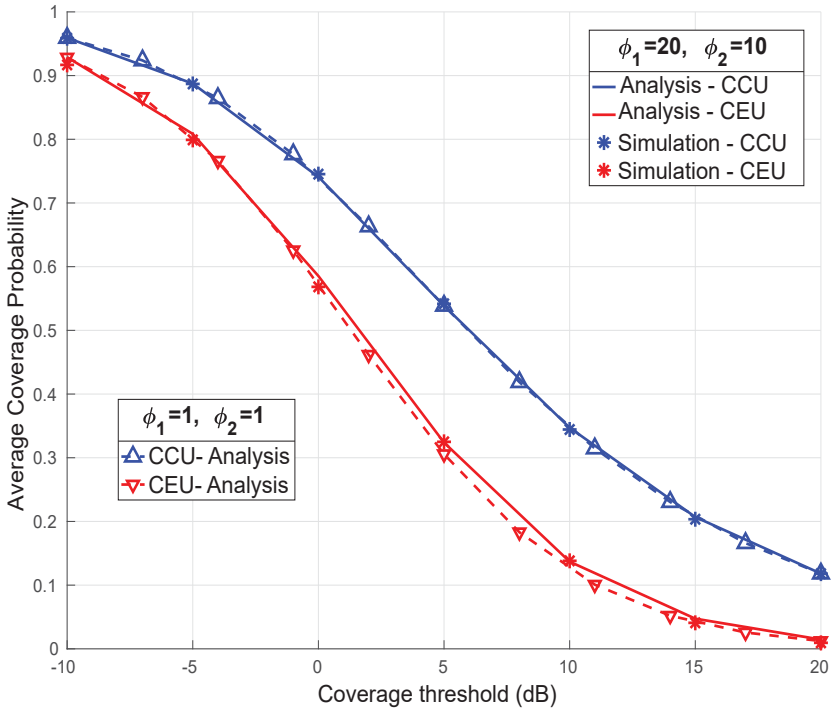

(a) Strict FR

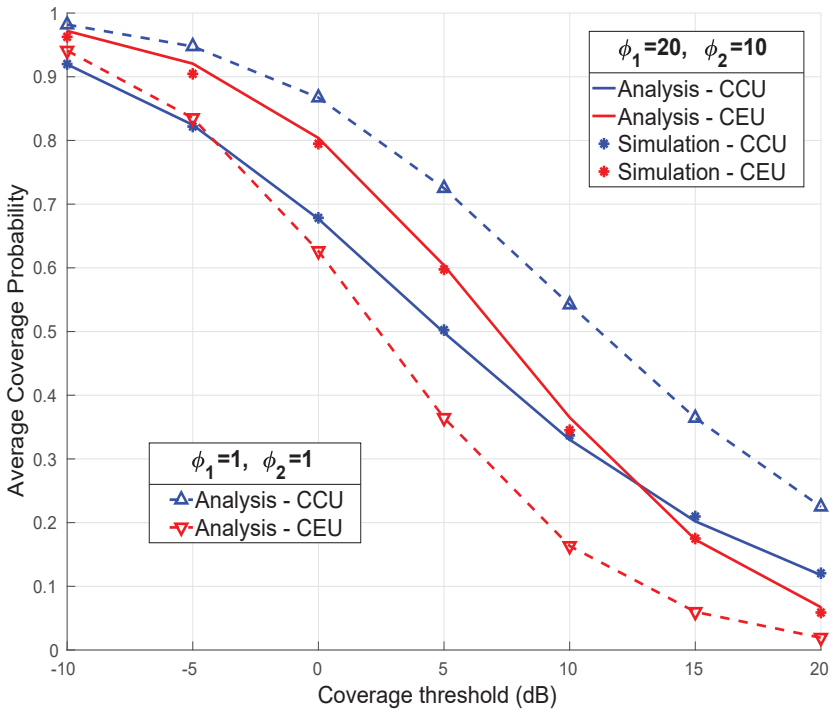

(b) Soft FR

Figure 4.1 : Comparison between theoretical and simulation results of the average coverage probabilities of the CCU and CEU

An increase in the serving power of the CEU also increases the power of the interfering BSs under Strict FR (Property 1 on Page 9) while this only influences some interfering BSs under Soft FR (Property 3 on Page 10). Hence, using higher transmit power for the CEU under the Soft FR leads to better efficiency than that under the Strict FR. From the analytical results in Figure 4.1, it is observed that a high transmit power increases the CEU average coverage probability significantly under the Soft FR, but only marginally under the Strict FR. For example, when the coverage threshold is set to $5dB$, the CEU average coverage probability under the Soft FR is 0.3 when $(\phi_1, \phi_2) = (1, 1)$ and increases to approximately 0.5778 when $(\phi_1, \phi_2) = (20, 10)$, which is a 92.6 % improvement. On the other hand, under the Strict FR, the CEU average coverage probability has a 6.31% improvement, from 0.3057 to 0.325.

It is noted that the use of a high transmit power to serve CEUs leads to an increase in the ICI of the CEU under Strict FR and of both the CCU and CEU under the Soft FR. Therefore, an increase in the transmit power on the CE RB does not affect the CCU in the case of Strict FR but can reduce the performance of the CCU under the Soft FR. For example, when the coverage threshold is 5 dB and the transmit ratios (ϕ_1, ϕ_2) increase from $(1, 1)$ to $(20, 10)$, the average coverage probability of the CCU reduces by 30.73% from 0.7251 to 0.5023. Hence, it can be said that with Soft FR, the performance of the CCU is sacrificed to improve the performance of the CEU .

4.5.1 SINR Threshold

In this section, the average number of CCUs and CEUs as well as their average data rates are analysed for different values of SINR thresholds for Tier-1 and Tier-2. Since the changes in the SINR threshold for a given tier has a small impact on the performance of other tiers, either the performance of Tier-1 or Tier-2 is plotted in each figure from Figure 4.2 to Figure 4.5.

By examining Figures 4.2 - 4.5, the optimal values of SINR threshold T_1, T_2 under Strict FR and Soft FR are selected so that the corresponding average cell

data rates are at peaks.

Average user data rate analysis

It is observed from Figures 4.2, 4.3, 4.4 and 4.5 that there are opposite trends between the average numbers of CCUs and CEUs in a given cell. When the SINR threshold increases, more users are forced to be served as CEUs and there is a decline in the average number of CCUs . Since, at a given timeslot, each BS in Tier-k can only serve a maximum of $N_k^{(e)}$ CEUs in which $N_k^{(e)}$ is the average number of CE RBs in the corresponding cell, the average number of served users keeps constant at 9 in Figure 4.2(a) and 19 in Figure 4.4(a) when the SINR threshold is greater than 35 dB and 40 dB, respectively.

CCU average data rate From the CCU view, having more CEUs means that less users are defined as CCUs in the networks. An increase in SINR threshold can provide more opportunities for each CCU to be allocated a RB in order to avoid reusing frequency and thus the ICI can reduce, especially under the Strict FR where the CCU is only affected by the ICI from the BSs transmitting at the CC power. As indicated in Figures 4.2(b) and 4.3(b), the average data rate of the CCU in both Tier-1 and Tier-2 dramatically goes up from 2.972 (bit/s/Hz) to 12.29 (bit/s/Hz) and from 2.314 (bit/s/Hz) to 10.89 (bit/s/Hz) when the average number of CCUs falls from 24.54 to 1.22 and from 4.965 to 0.0268 at $T_2 = 10$ dB and $T_2 = 50$ dB, respectively. For the case of Soft FR, since the CCUs suffers the ICI from BSs transmitting at the CC and CE powers, pushing more users to be CEUs can increase the ICI from BSs transmitting at the CE power. However, this negative impact is not significant and can counterbalance with a decrease in the ICI from BSs transmitting at the CC power (refers to Property 3). Therefore, it can be observed from Figure 4.5(b) that the average data rate of the CCU under the Soft FR also dramatically goes up but a little bit slower than that under the Strict FR.

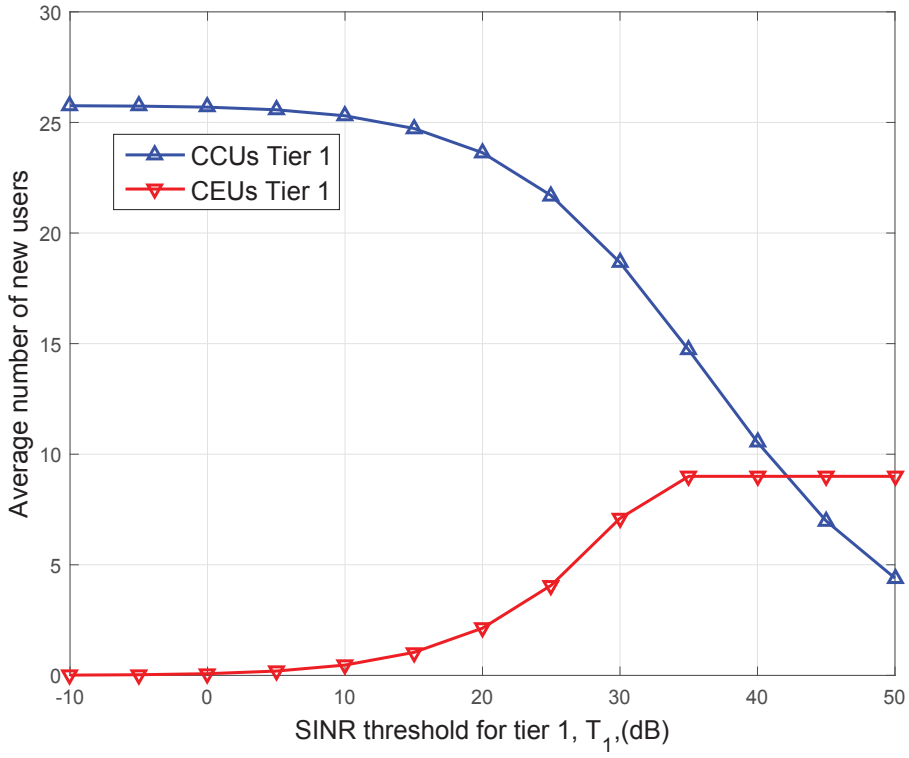

(a) (*Strict FR, Tier-1*) Average Number of Users vs. SINR Threshold T_1

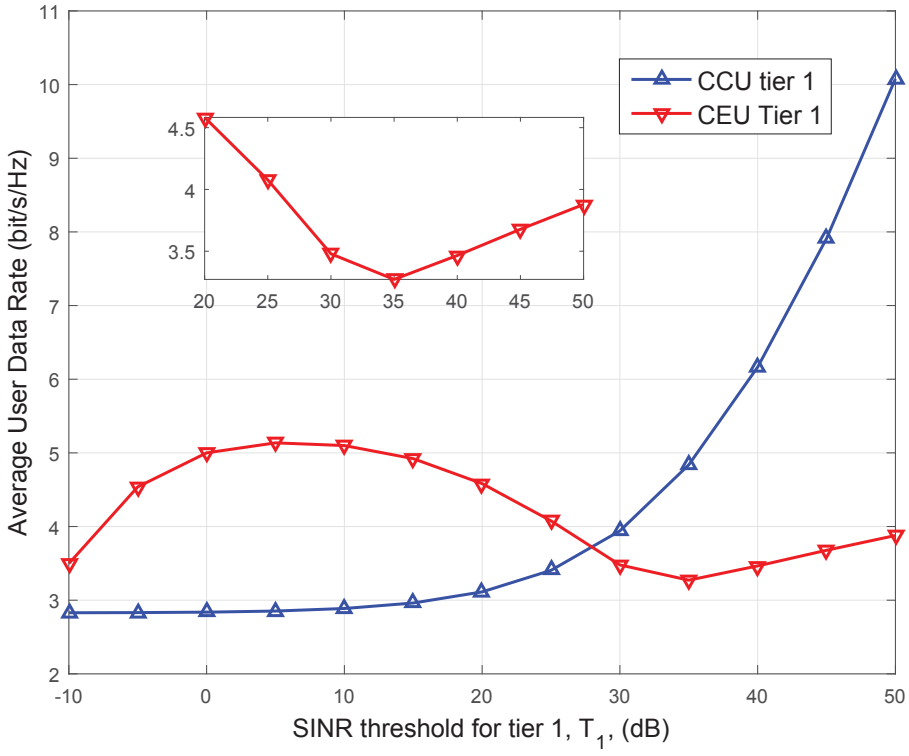

(b) (*Strict FR, Tier-1*), Average Number of Users vs. SINR Threshold T_1

Figure 4.2 : (*Strict FR*): Performance of Tier-1 vs. SINR threshold T_1

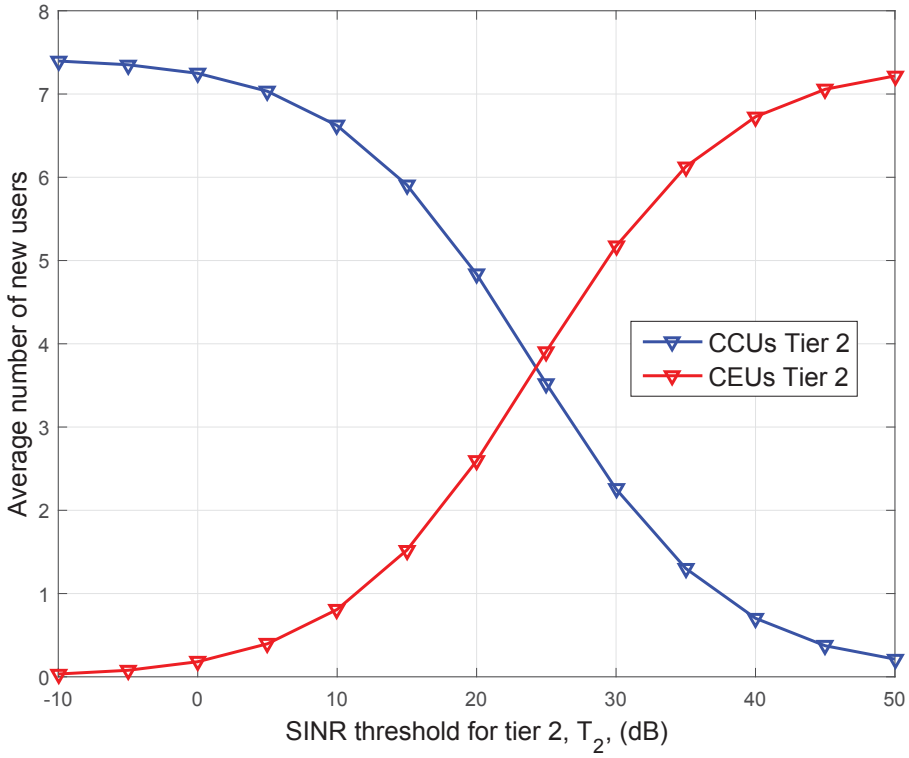

(a) (*Strict FR, Tier-2*), Average Number of Users vs. SINR threshold T_2

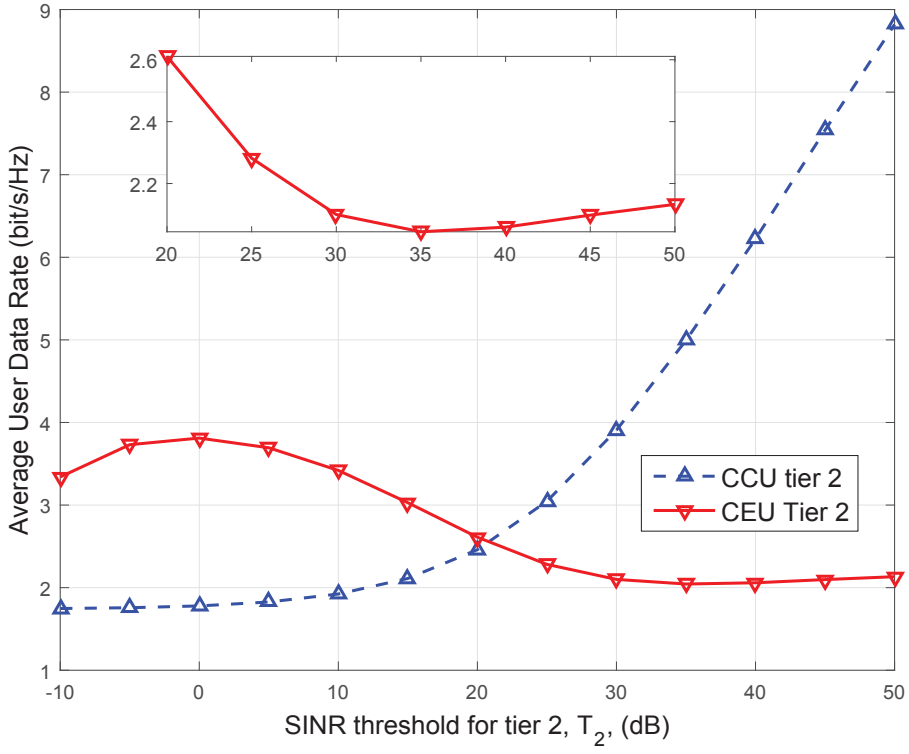

(b) (*Strict FR, Tier-2*), Average User Data Rates vs. SINR threshold T_2

Figure 4.3 : (*Strict FR*) Performance of Tier-2 vs. SINR threshold T_2

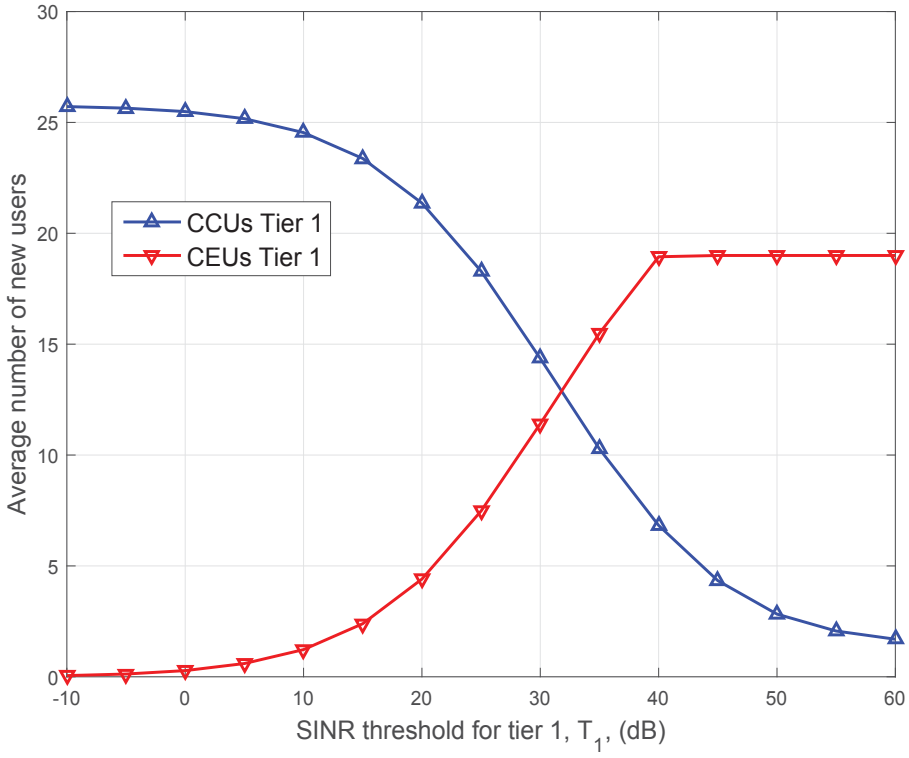

(a) (*Soft FR, Tier-1*), Average Number of Users vs. SINR Threshold T_1

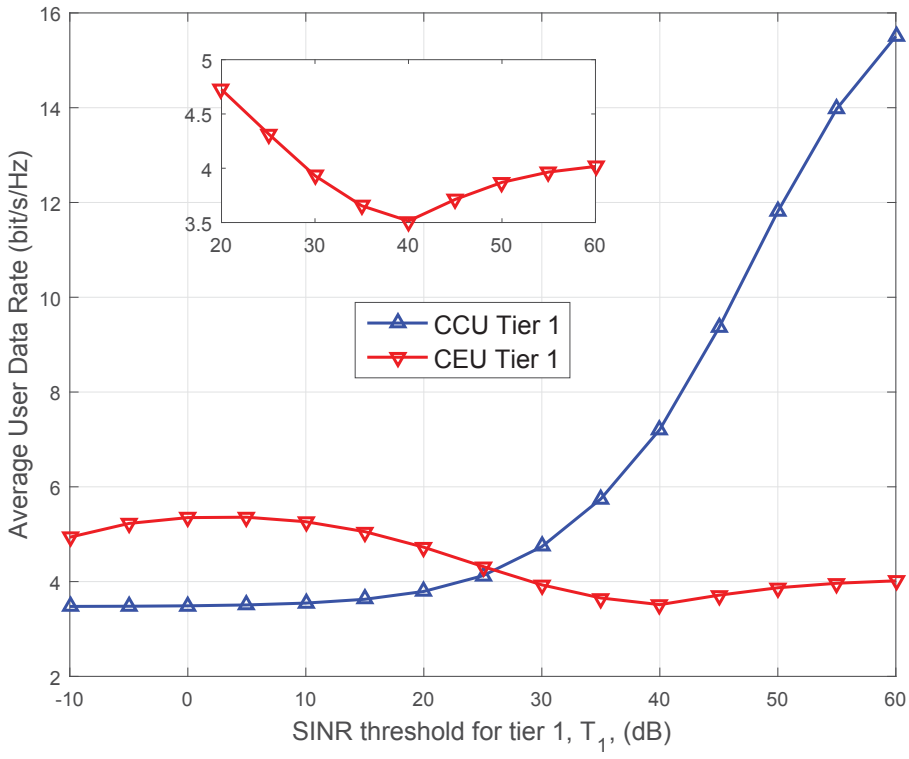

(b) (*Soft FR, Tier-1*), Average User Data Rates vs. SINR Threshold T_1

Figure 4.4 : (*Soft FR*): Performance of Tier-1 vs. SINR threshold T_1

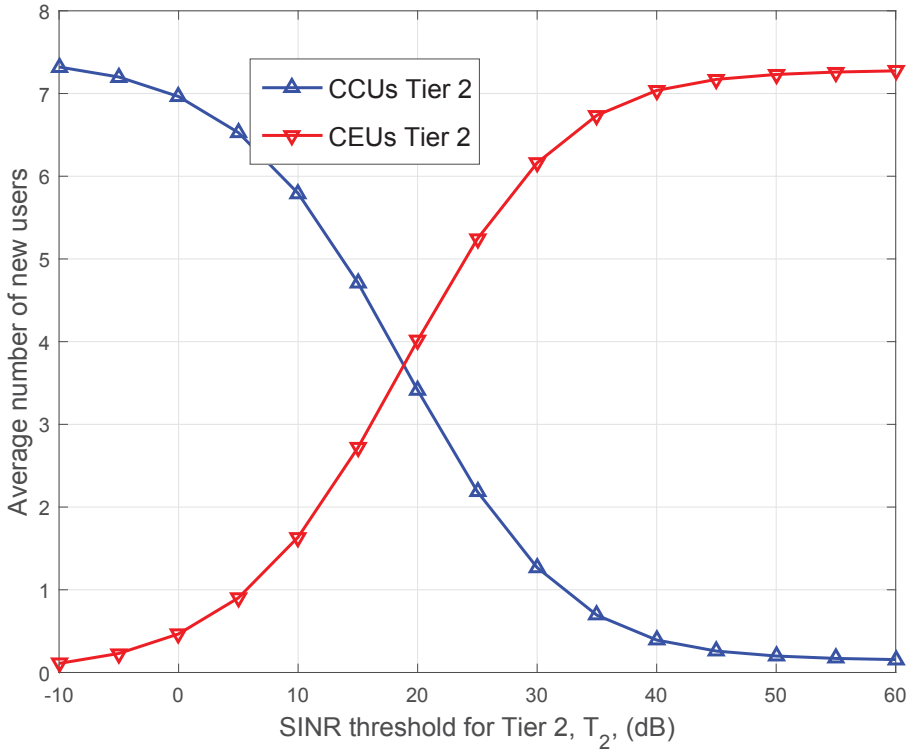

(a) (*Soft FR, Tier-2*), Average Number of Users vs. SINR Threshold T_2

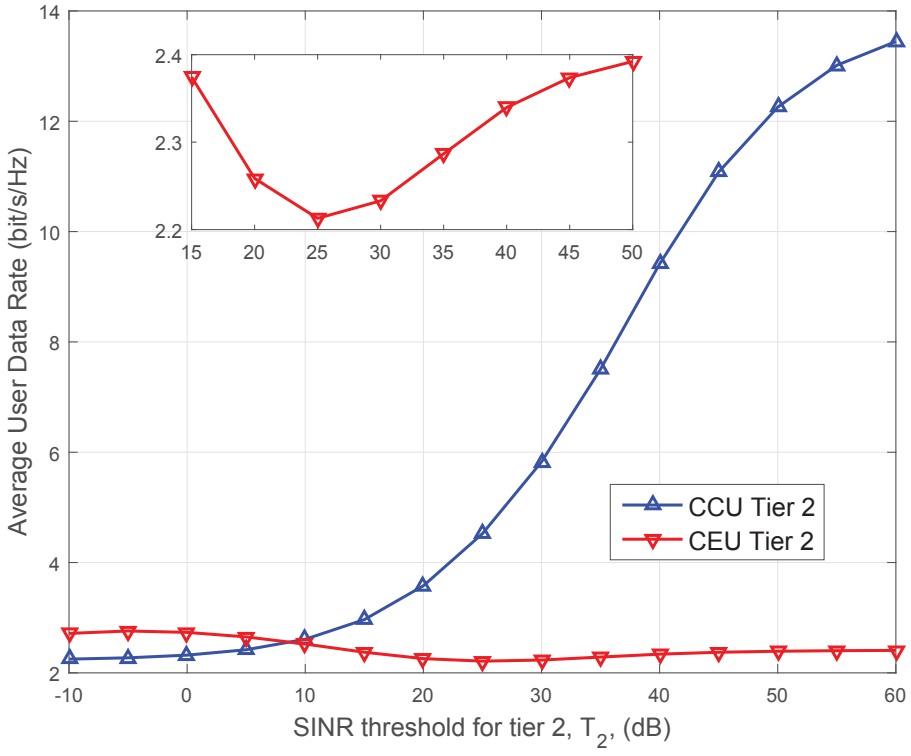

(b) (*Soft FR, Tier-2*), Average User Data Rates vs. SINR Threshold T_2

Figure 4.5 : (*Soft FR*): Performance of Tier-2 vs. SINR threshold T_2

CEU average data rate From the CEU view, although each CEU experiences a higher level of ICI when more users are served as the CEUs , the average data rate of the CEU fluctuates and can be divided into three regimes. In *the first regime*, which corresponds to low values of the SINR threshold ($T_1 < 5$ dB and $T_2 < 0$ dB), the average data rate moderately increases to a peak value, e.g. of 4.534 (bit/s/Hz) at $T_1 = 5$ dB under the Strict FR. As can be seen from these two figures, a very small number of users are served as CEUs . Thus, the probability that two BSs use the same RB at the same time (called interfering probability), and consequently the ICI are infinitesimal. In the case of Strict FR with $T_2 = 0$ dB, the average number of CEUs is 0.1811 and thus the interfering probability is $\epsilon_2^{(e)}\epsilon_2^{(e)} = 1.46.10^{-4}$. Therefore, the effect of ICI in this case can be neglected and the average data rate of the CEU mainly depends on the SNR. Therefore, when more users with high SINRs (high data rate) are forced to be CEUs , the average data rate of the CEU increases.

In *the second regime*, which corresponds to medium values of the SINR threshold ($5\ dB < T_1, T_2 < 35\ dB$ in the case of Strict FR; $0\ dB < T_1 < 40\ dB$ and $0\ dB < T_2 < 25\ dB$ in the case of Soft FR), the average number of CEUs increases rapidly as shown in Figure 4.2 and Figure 4.4 which leads to a significant increase in the interfering probability. As shown in Figure 4.2, when T_2 changes from 0 dB to 10 dB, the interfering probability increases by a factor of 19.5 from $1.46.10^{-4}$ to 0.0028. Hence, the ICI has a considerably negative impact on the user performance which results in a decline in the CEU's data rate.

In *the third regime* which corresponds to high values of the SINR threshold as highlighted on boxes of figures. For Tier-1 of both Strict FR and Soft FR, the average number of CEUs exceeds the average number of RBs, thus each BS has to transmit on all allocated CE RBs to serve the associated CEUs and this creates ICI to all CEUs in adjacent cells. This can be considered as the worst case of the CEU as it suffers from the ICI coming from all BSs transmitting at the CE power. For Tier-2, the interfering probability remains at high values when the SINR threshold changes. For example, under the Strict FR, when T_2 increases from 35 dB to 45 dB, the interfering probability increases by 1.33 times from 0.1669 to 0.2225 which

is much smaller compared to 19.5 times when T_2 increases from 0 dB to 10 dB. Therefore, there is a small change in the ICI. Consequently, when more users with high SINR are pushed to be CEUs, the effect of the ICI on the CEU is unlikely to change but the average SINR of CEUs increases. Hence, the average data rate of the CEU is pushed up. It is pointed out that the average data rate of the CEU in Tier-2 in the third regime is always smaller than that in the first regime since more users are served as CEUs, hence more severe ICI effect on the CEU. Meanwhile in Tier-1, due to the constant ICI in the third regime, the average data rate of the CEU may be higher than that in the first regime.

Average cell data rate analysis

Although the average data rate of the CCU increases when the SINR threshold increases, the rapid decline in the average number of CCUs leads to a decrease of the average data rate of the CC Area in each cell of each Tier for both Strict FR and Soft FR. Meanwhile, the average data rate of CE Area steadily increases. Therefore, the average data rate per cell reaches to a peak value before passing a significant decline. Thus, the optimal value of the SINR threshold for Tier-1 and Tier-2 can be found when the average data rate is at the peak. For example, under the Soft FR $T_1 = 40$ dB and $T_2 = 25$ dB are chosen in order to achieve the maximum average data rate per cell of 115.8 (bit/s/Hz) for Tier-1 and 21.5 (bit/s/Hz) for Tier-2.

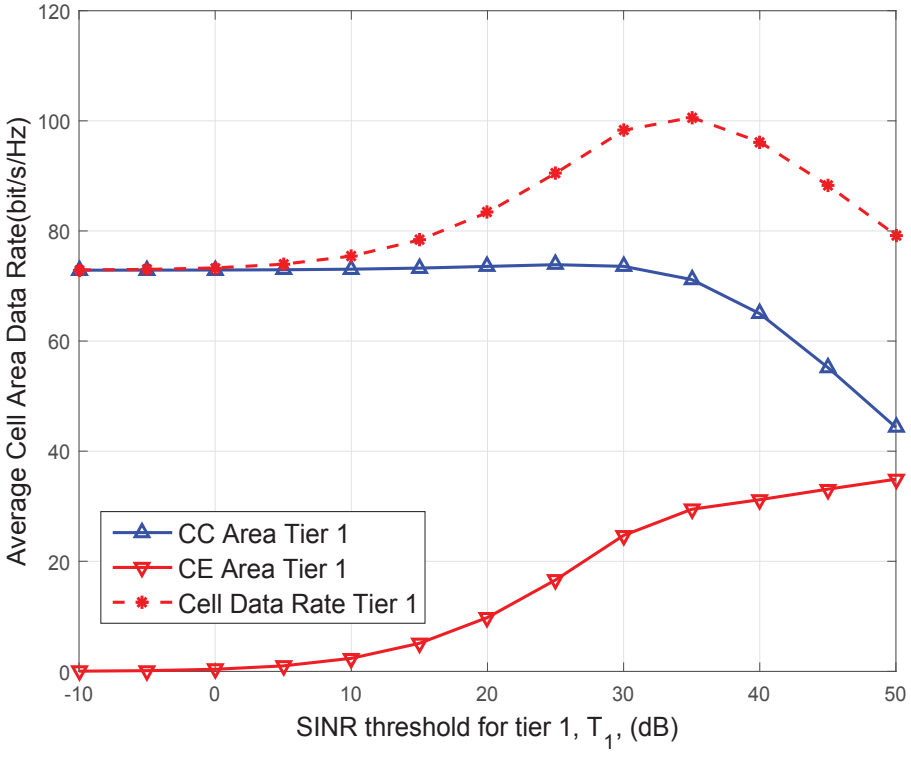

Figure 4.6 : (*Strict FR, Tier-1*), Average Cell Area Data Rate vs. SINR Threshold T_1

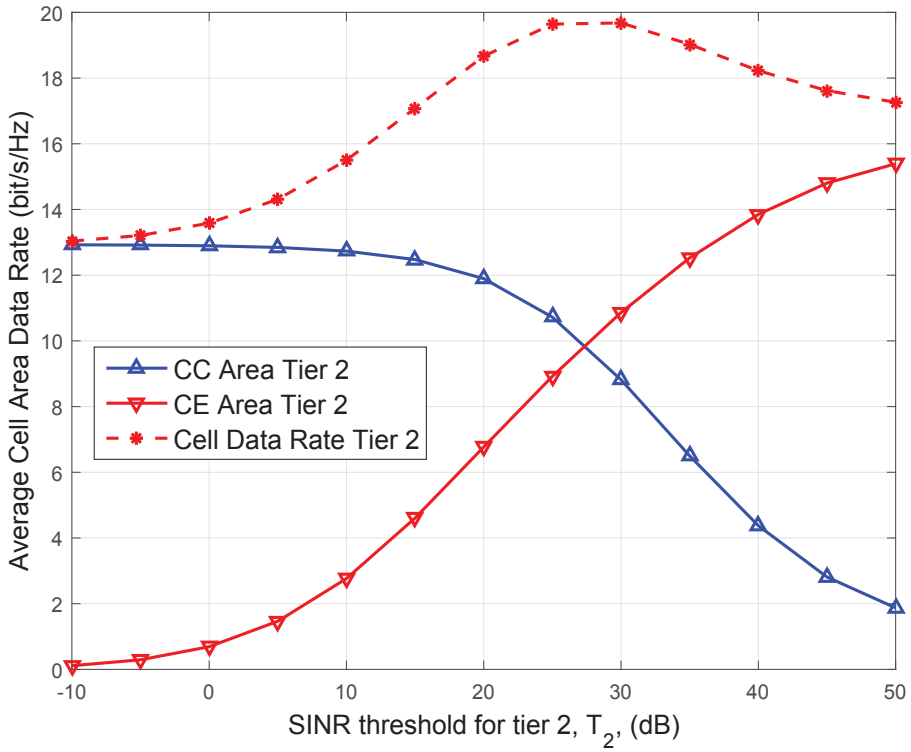

Figure 4.7 : (*Strict FR, Tier-2*), Average Cell Area Data Rate vs. SINR threshold T_2

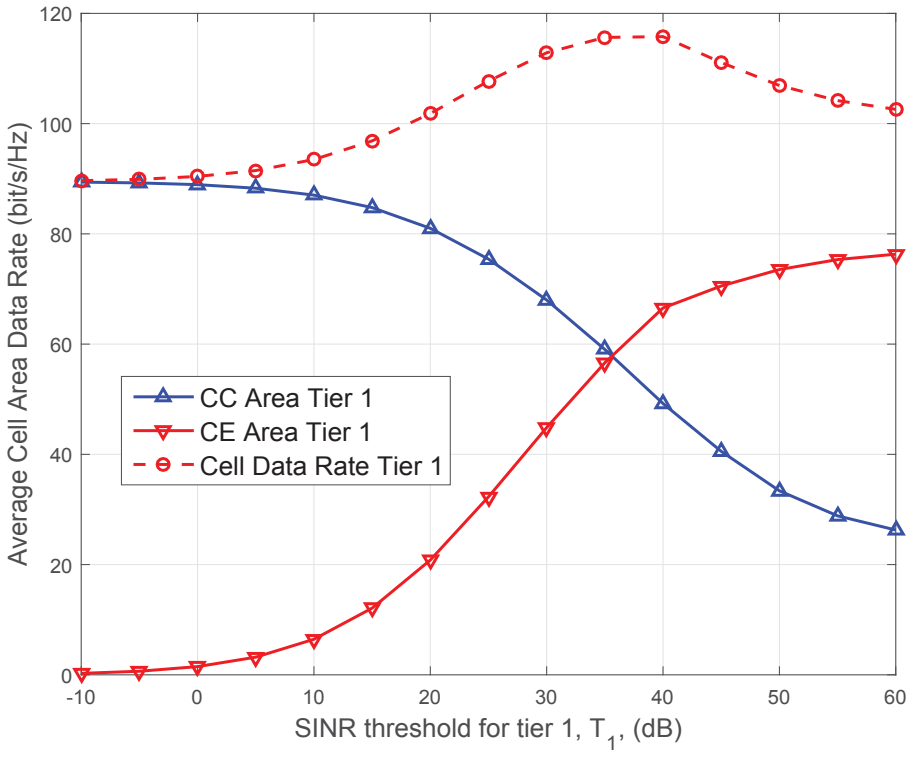

Figure 4.8 : (*Soft FR, Tier-1*), Average Cell Area Data Rate vs. SINR Threshold T_1

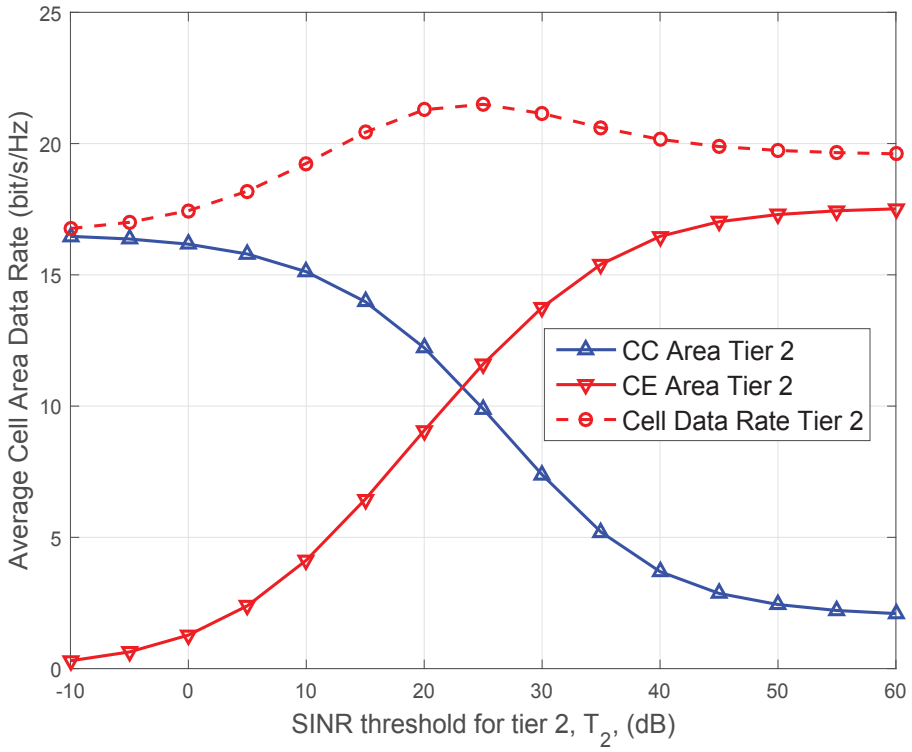

Figure 4.9 : (*Soft FR, Tier-2*), Average Cell Area Data Rate vs. SINR Threshold T_2

4.5.2 Bias Association

The bias factor is used for handover users from Tier-1 to Tier-2 to maintain load balancing between tiers in the networks. It can be observed from Figures 4.10(a) and 4.12(a) that when the bias factor B_2 for Tier-2 increases, more users from Tier-1 are pushed to Tier-2. However, since the density of BSs in Tier-2 is 10 times that of Tier-1, the changes in the average number of users in Tier-1 only result in a small change in the average number of users in Tier-1. Take the case of Soft FR in Figure 4.12(a) as an example, the average number of users including CCUs and CEUs in Tier-1 goes down by around 50% from 25.77 at $B_2 = 10$ to 13.045 at $B_2 = 50$, while the average number of users in Tier-2 goes up by 14.6% from 7.43 to 8.70. As discussed in Section 4.5.1, these changes reflect a rapid downward trend in the ICI from BSs in Tier-1 and a slow upward trend in the ICI from BSs in Tier-2. In other words, the ICI in this case is mitigated. Therefore, as illustrated in Figure 4.10(b) and Figure 4.12(b), the average data rate of both CCU and CEU in Tier-1 moderately increase while the changes in Tier-2 are marginal.

It is observed from Figures 4.11(b) and 4.13(b) that the total network data rate for both Strict FR and Soft FR reach the peak value at 1437 (bit/s/Hz) and 1457 (bit/s/Hz) respectively before passing a steady decline. Hence, the optimal values of bias factor can be selected at 70 for Strict FR and 40 for Soft FR.

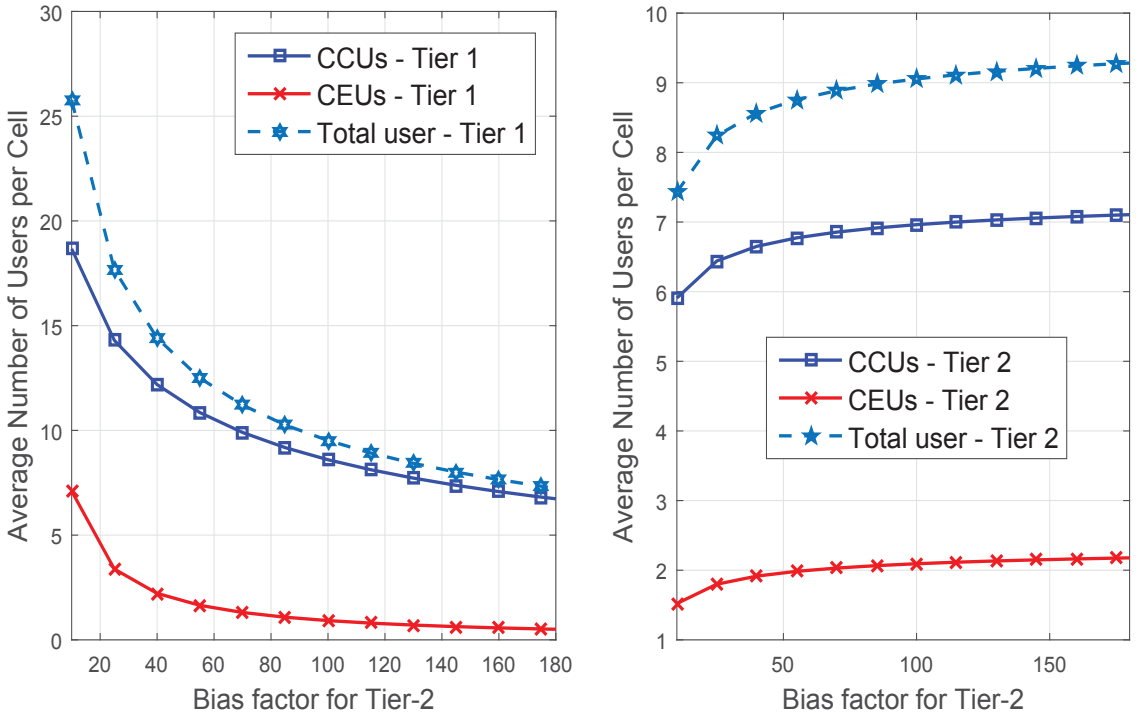

(a) (*Strict FR*): Average number of users

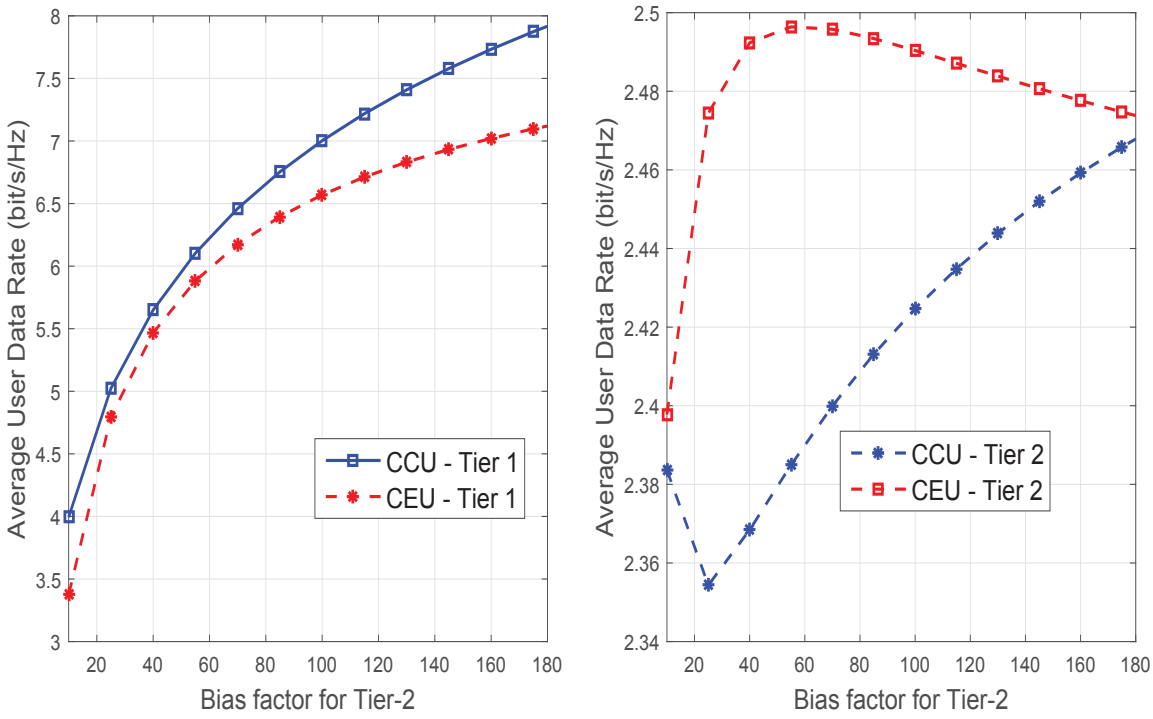

(b) (*Strict FR*): Average User Data Rates

Figure 4.10 : (*Strict FR*): Average number of users and Data Rate vs. the bias factor for Tier-2, B_2

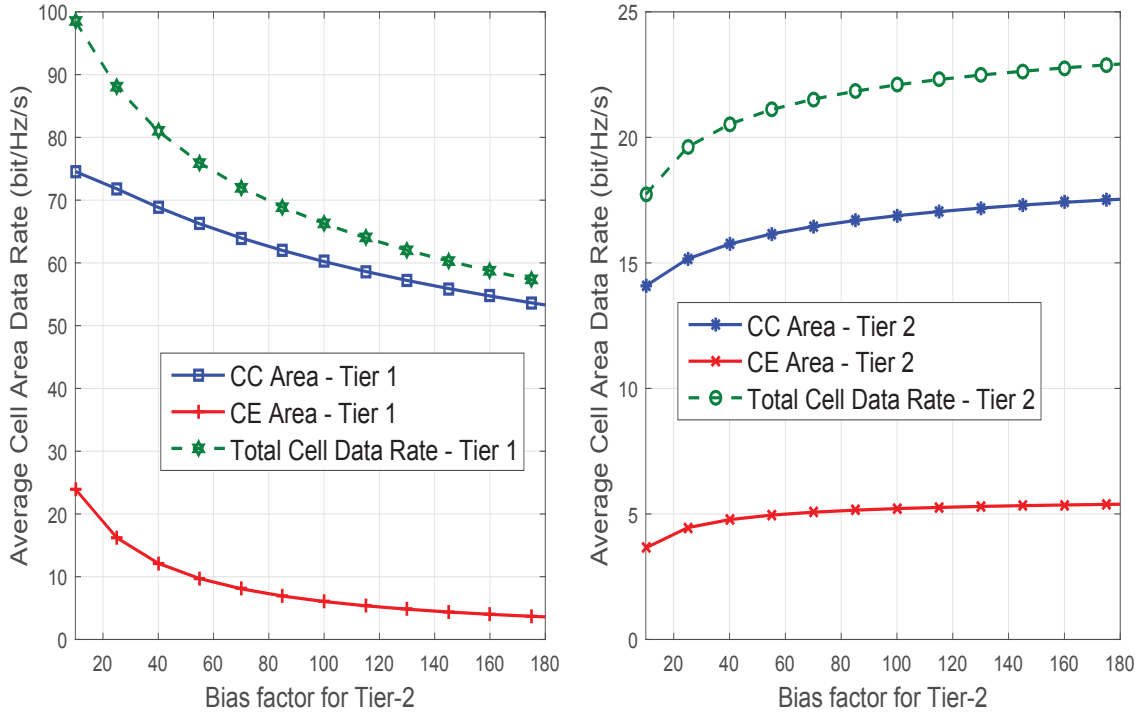

(a) (*Strict FR*): Average Cell Area Data Rate

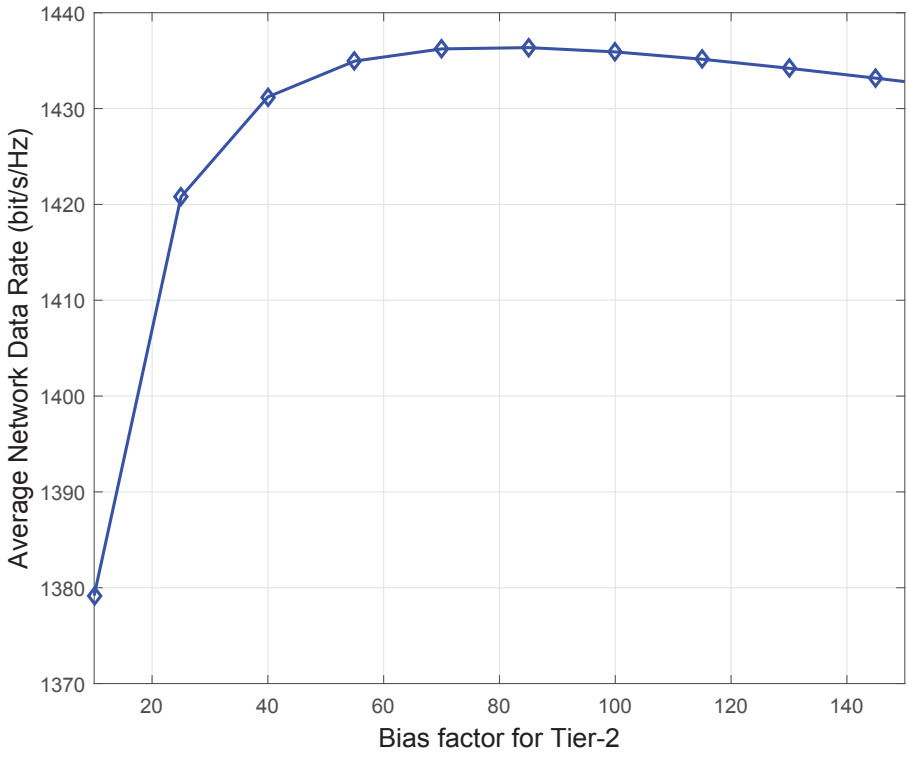

(b) (*Strict FR*): Average Network Data Rate

Figure 4.11 : (*Strict FR*): Cell Area and Network Data Rate vs. the bias factor for Tier-2, B_2

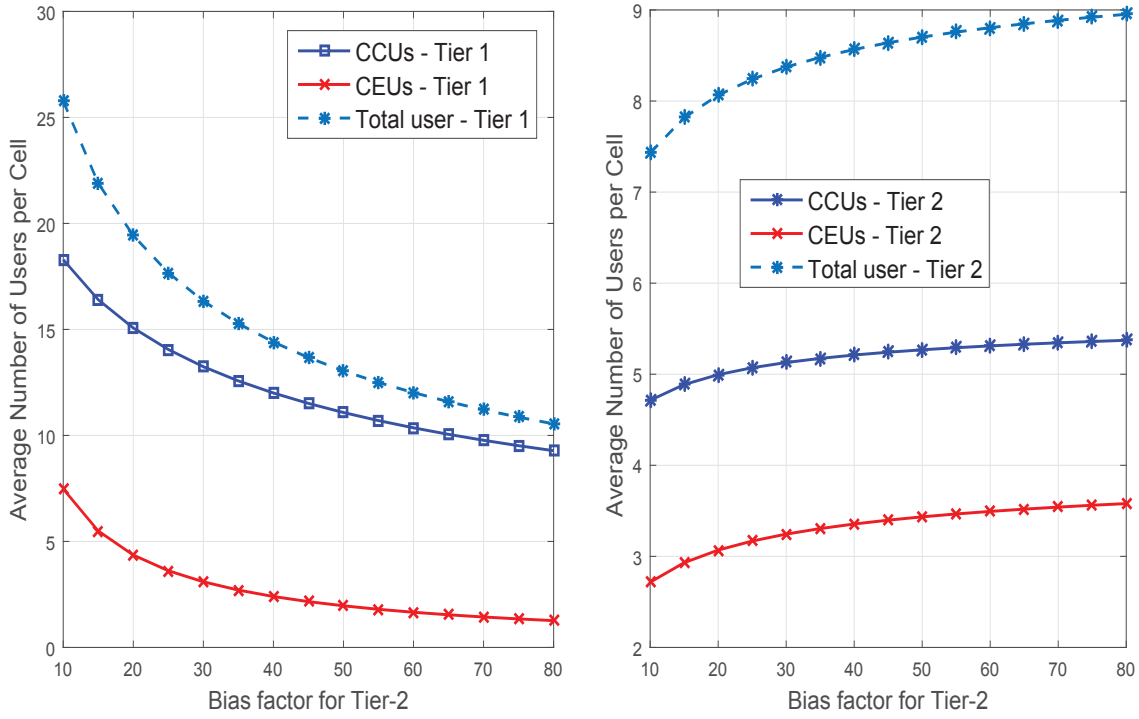

(a) *(Soft FR)*: Average Number of Users

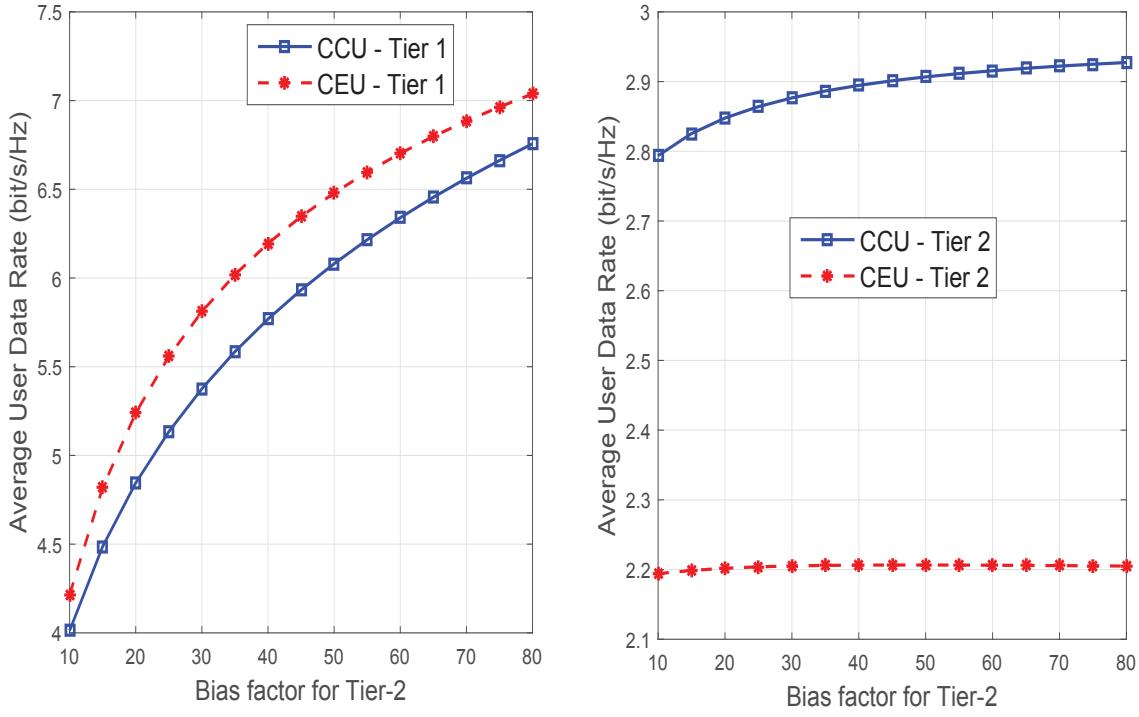

(b) (*Soft FR*): User Average Data Rate

Figure 4.12 : (*Soft FR*): Average Number of Users and Data Rate vs. the bias factor for Tier-2, B_2

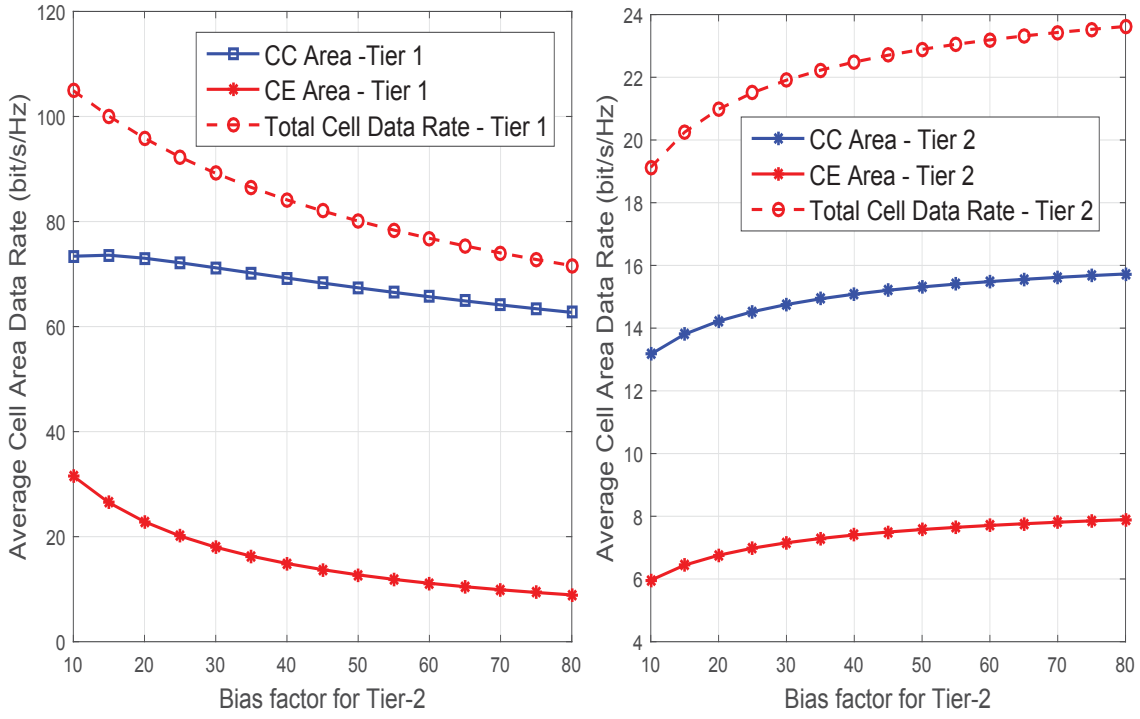

(a) (*Soft FR*): Average Cell Area Data Rate

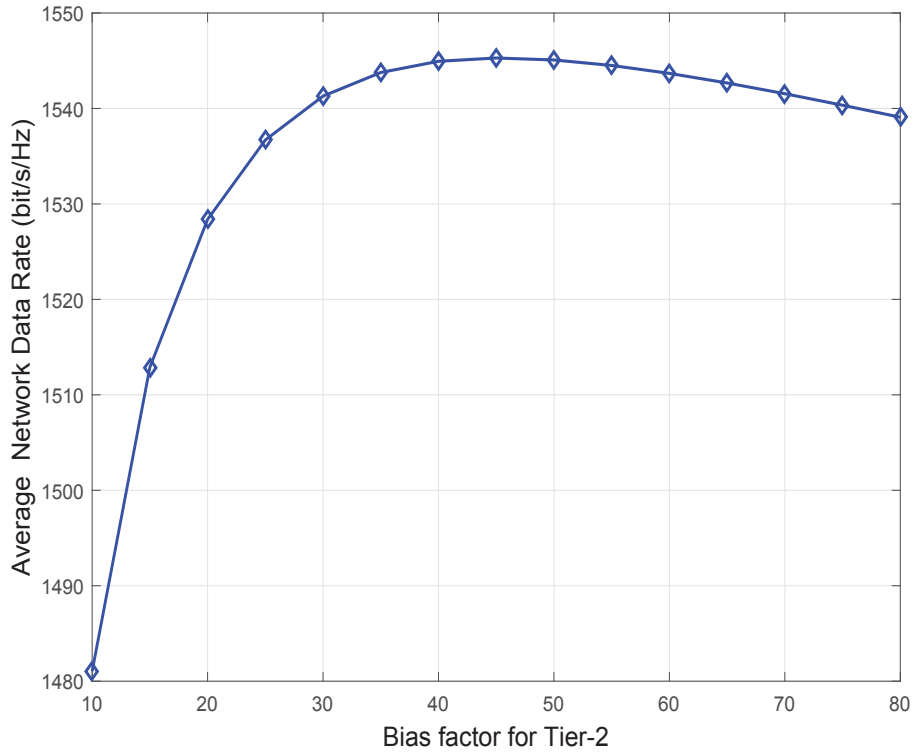

(b) (*Soft FR*): Average Network Data Rate

Figure 4.13 : (*Soft FR*): Cell Area and Network Data Rate vs. the Bias Factor for Tier-2, B_2

4.5.3 Comparison between the 3GPP model and the proposed model

In this section, the 3GPP and proposed models are compared in terms of performance metrics, in which SINR threshold and bias factor for each model are selected so that the corresponding model achieves the maximum performance. The values of SINR threshold and bias factor are obtained from analytical approaches in Sections 4.5.1 and 4.5.2 and listed in Table 4.4

Table 4.4 : SINR threshold and bias factor for comparisons

Parameters	**SINR Threshold**	**Bias factor**
3GPP model		
- Strict FR	$T_1 = 10$ dB, $T_2 = 5$ dB	40
- Soft FR	$T_1 = 10$ dB, $T_2 = 5$ dB	50
Proposed model		
- Strict FR	$T_1 = 35$ dB, $T_2 = 30$ dB	50
- Soft FR	$T_1 = 40$ dB, $T_2 = 25$ dB	40

Comparison between the numbers of CCUs

The 3GPP model using FR schemes was discussed in Chapter 2 in which the measured SINR on the control channel during the establishment phase was utilised for user classification purpose. The downlink SINR on the control channel of the user associated with Tier-k in the 3GPP model is given by

$$SINR_{3GPP,k} = \frac{g_k r_k^{-\alpha_k}}{\sum_{j=1}^{K} \sum_{y \in \theta_j \setminus \{k\}} \frac{P_j}{P_k} g_{jy} r_{jy}^{-\alpha_j} + 1/SNR_k} \tag{4.23}$$

When the average number of interfering BSs is large enough, $\sum_{j=1}^{K} \sum_{y \in \theta_j \setminus \{k\}} \frac{P_j}{P_k} g_{jy} r_{jy}^{-\alpha_j} >> 1/SNR_k$, hence the measured SINR in Equation 4.23 and consequently the average number of CCUs depend on $\sum_{j=1}^{K} \sum_{y \in \theta_j \setminus \{k\}} \frac{P_j}{P_k} g_{jy} r_{jy}^{-\alpha_j}$ rather than SNR_k. Therefore, an

increase in SNR makes a very small change in the average number of CCUs and CEUs for both Tier-1 and Tier-2 under both Strict FR and Soft FR as shown in Figures 4.14 and 4.15.

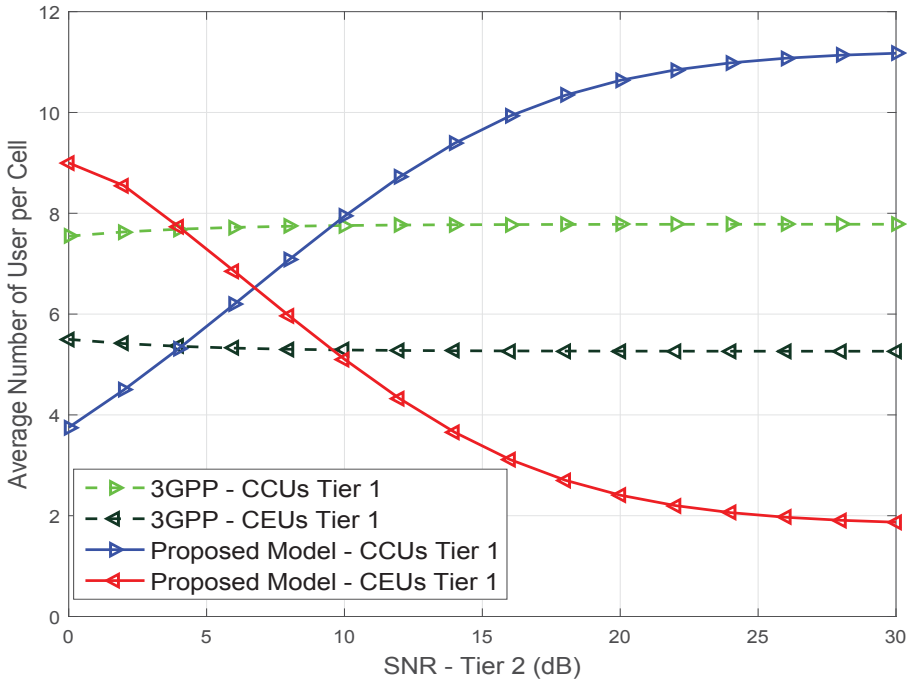

(a) (*Strict FR, Tier-1*), Comparison between number of CCUs and CEUs

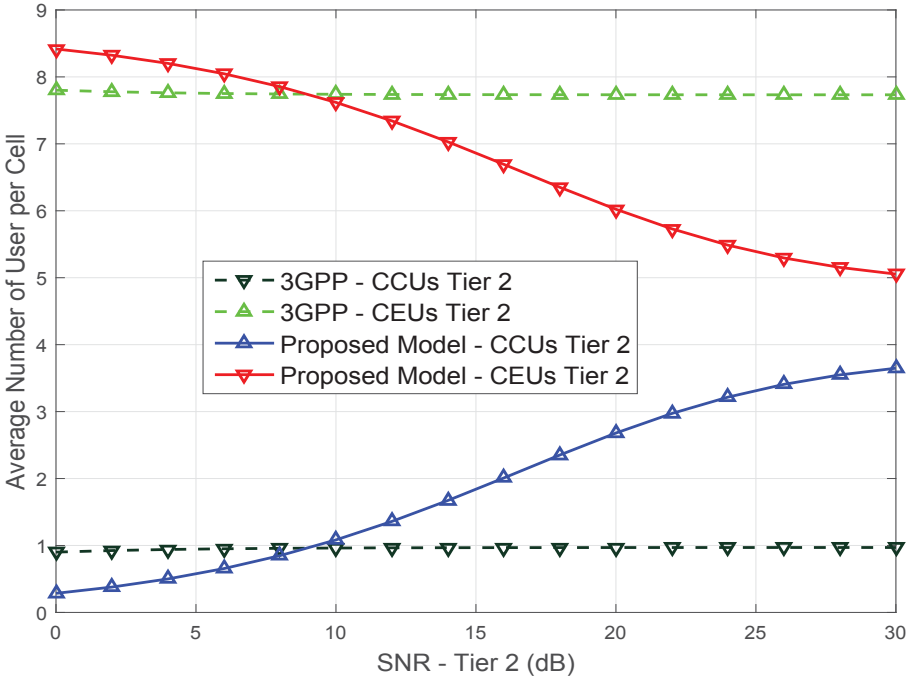

(b) (*Strict FR, Tier-2*), Comparison between number of CCUs and CEUs

Figure 4.14 : (*Strict FR*): Comparison between number of CCUs and CEUs

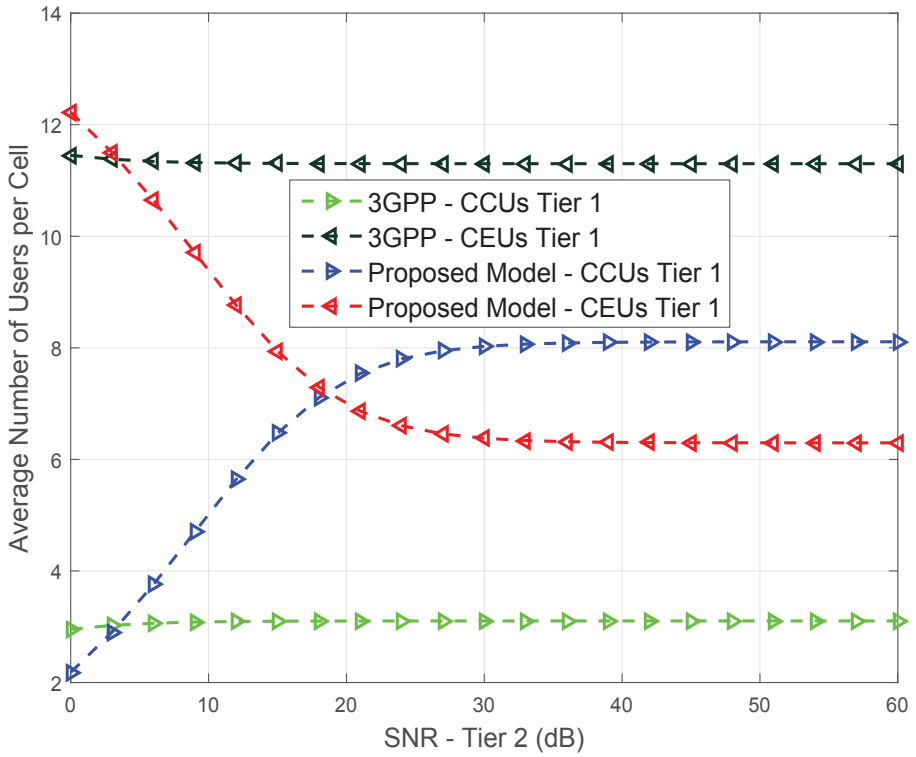

(a) (*Soft FR, Tier-1*), Comparison between number of CCUs and CEUs

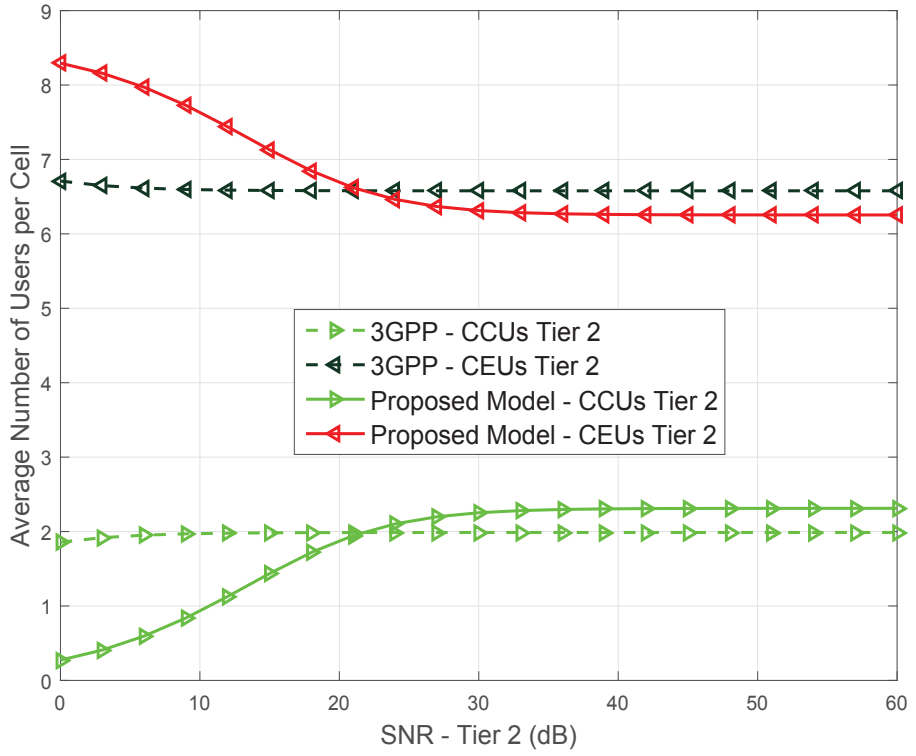

(b) (*Soft FR, Tier-2*), Comparison between number of CCUs and CEUs

Figure 4.15 : (*Soft FR*): Comparison between number of CCUs and CEUs

In our proposed model, the measured SINR for user classification purpose experiences interference as evident in Equations 4.7 and 4.8 in which the interfering probabilities $E[\tau_1^{(oc)}] = \epsilon_1^{(oc)} = 0.1$, $E[\tau_1^{(oe)}] = \epsilon_1^{(oe)} = 0.4$, $E[\tau_2^{(oc)}] = \epsilon_2^{(oc)} = 0.1$, and $E[\tau_2^{(oe)}] = \epsilon_2^{(oe)} = 0.133$. Hence, the interference in this case is much smaller than SNR, and consequently effect of interference on the measured SINR is not significant compared to SNR. Hence, an increase in SNR can result in a significant rise of SINR, and consequently number of CCUs as shown in Figures 4.14 and 4.15. Take Tier-1 under Strict FR for example, when SNR increases by 8 dB from 0 dB to 8 dB, the average number of CCUs rises by 88.83% from 3.751 to 7.083.

Comparison between BS transmit power

In the cellular networks, every BS transmits on both data channel and control channel. In this section, the transmit power of the BS in Tier-k on the data channel is discussed and given by the following equation

$$\overline{P} = P_k M_k^{(c)} + \phi_k P_k M_k^{(e)} \tag{4.24}$$

in which $M_k^{(c)}$ and $M_k^{(e)}$ are the average number of CCUs and CEUs, P_k and $\phi_k P_k$ are the serving power of CCU and CEU.

As seen from Equation 4.24 and the previous discussion, compared to 3GPP model, our proposed model can reduce a significant amount of transmits power on data channel by reducing the average number of CEUs. In the case of Soft FR and $SNR = 30$ dB, the transmit power on data channel of a BS in Tier-1 and Tier-2 of the proposed model are $135.607P_1$ and $128.51P_2$ respectively while those are $229.01P_1$ and $133.57P_2$ in the case of the 3GPP model. Hence, it can be said that the BS in Tier-1 and Tier-2 of our proposed model can reduce upto 40.79% and 3.8% power consumption on the data channel compared to 3GPP model.

Comparison between the user data rates

In 3GPP model, since the changes of SNR has a small effect on the user classification probability, an increase of SNR can improve the SINR which results in

growth of both CCU and CEU average data rates as shown in Figures 4.16 and 4.17. However, the average data rate of the CCU increase at a significantly lower rate than that of the CEU, since the CEU is always served at a higher transmit power than the CCU. It is observed from Figure 4.15(a), when SNR increases from 0 dB to 8 dB, the CCU average data rate increases by 10.21% from 7.979 to 8.794 while that of the CEU rises by 2.84% from 5.17 to 5.317.

In the proposed model, when SNR increases under Strict FR, the average number of CCUs and consequently interference of the CCU increase while the average number of CEUs and interference power originating from BSs transmitting on the same RB at the CE power reduce. As a result, the average data rate of the CCU decreases while that of the CEU increases as shown in Figure 4.17.

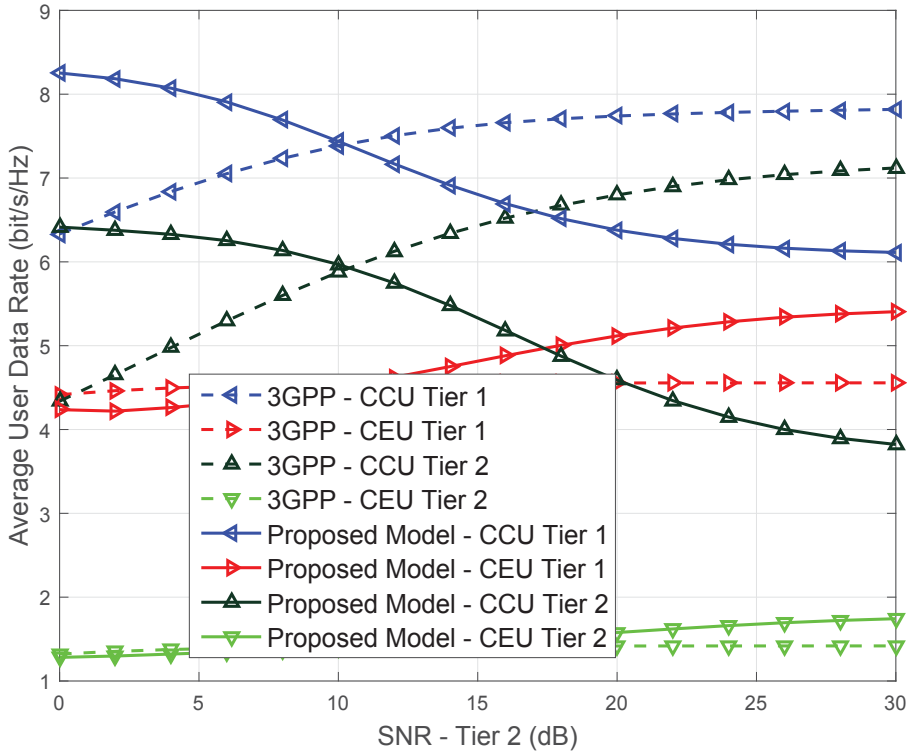

Figure 4.16 : (*Strict FR, Tier-1*), Comparison between Average User Data Rates

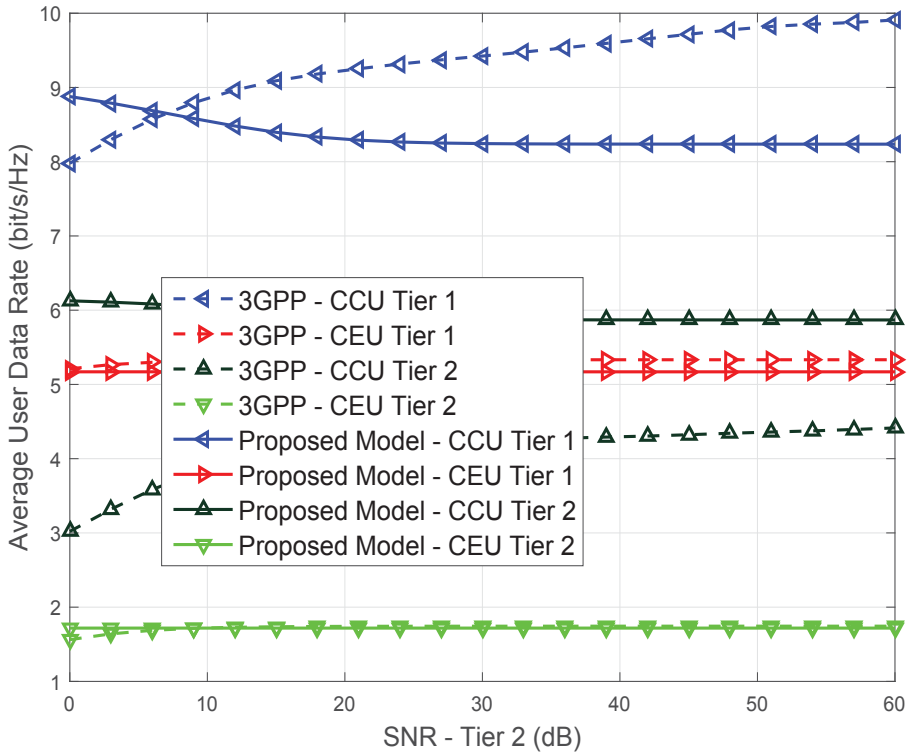

Figure 4.17 : (*Soft FR, Tier-1*), Comparison between Average User Data Rates

Under Soft FR, an increase in the average number of CCUs is equivalent to a decline in the average number of CEUs. Since, the density of BSs in $\theta^{(c)}_{Soft}$ is $\Delta_j - 1$ times than that $\theta^{(e)}_{Soft}$, a rise in interference originating from $\theta^{(e)}_{Soft}$ can counterbalance a decline in interference originating from $\theta^{(c)}_{Soft}$ though BSs in $\theta^{(e)}_{Soft}$ transmit at higher powers than those in $\theta^{(c)}_{Soft}$. It is noticed that the CEU is served at high transmit power, thus a change of SNR does not significantly affect the downlink SINR. Therefore, as shown in Figure 4.17, the average data rate of the CCU rises moderately while that of the CEU is unlikely to change.

Comparison between Cell Area and Network Data Rates In the 3GPP model, since the average number of CCUs and CEUs are unlikely to change while the average data rate of both CCU and CEU increase with SNR, the average data rate of every cell area, which is defined as the product of the average data of a typical user and number of users in the corresponding cell area, increases with SNR.

In our proposed model, variance of the average number of CCUs and CEUs

results in differences between trends of cell area performance as shown in Figures 4.19 and 4.21. Although, CCU average data rate reduces when SNR rise, the increase in the average number of CCUs leads to a rise in average cell data rate of CC Area under both Strict FR and Soft FR. By contrast, the average number of CEUs reduces while the average data rate of CEUs lightly changes, the average data rate of the CE Area under both Strict FR and Soft FR decline when SNR increases.

It is observed from Figures 4.20 and 4.22 that when SNR is large enough, such as $SNR > 8$ dB in the case of Strict FR and $SNR > 10$ dB in the case of Soft FR, the average network data rates of the proposed model are significantly greater than those of the 3GPP model. For example, in the case of $SNR = 30$ dB, the proposed model achieves 1700 (bit/s/Hz) in terms of average network data rate, which is 18.63% greater than the 3GPP model does.

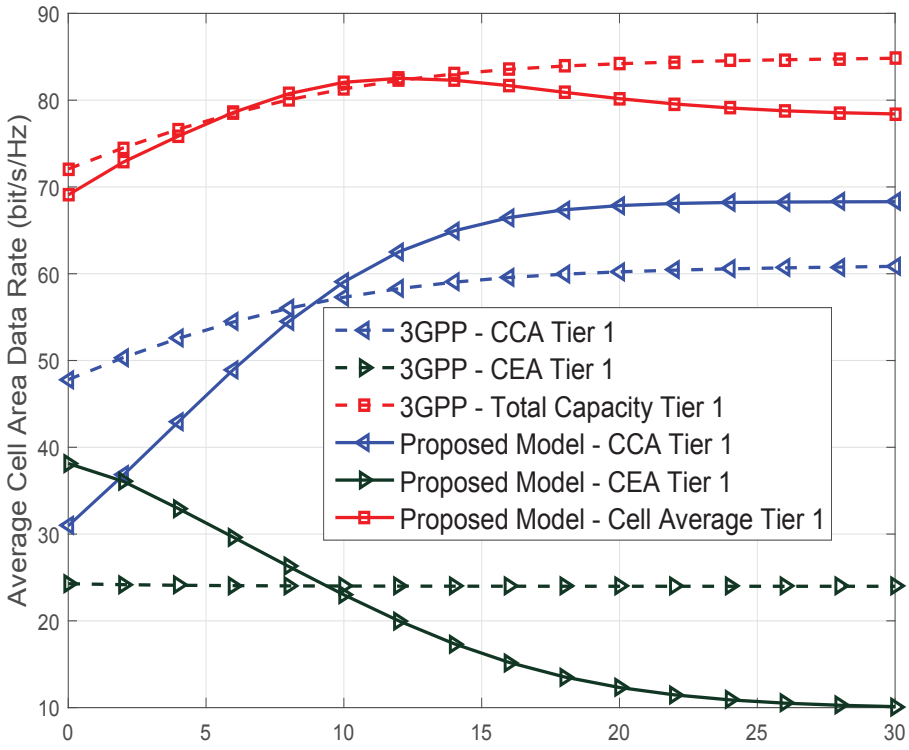

(a) (*Strict FR, Tier-1*), Comparison between Performance of Cell Areas

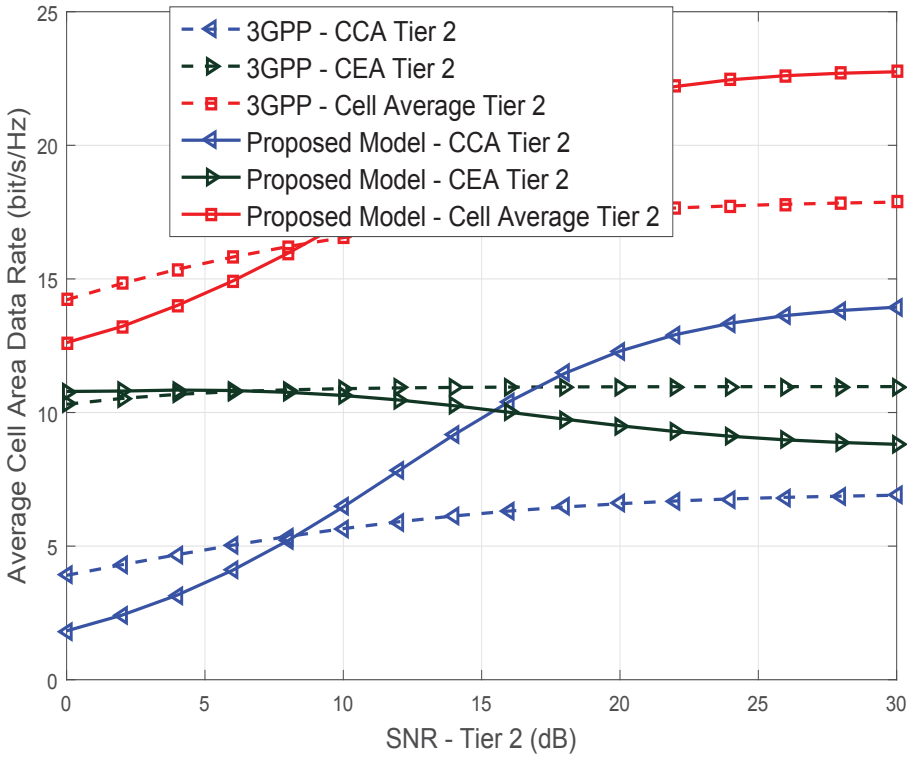

(a) (*Strict FR, Tier-2*), Comparison between Performance of Cell Areas

Figure 4.19 : (*Strict FR*), Comparison between Performance of Cell Areas

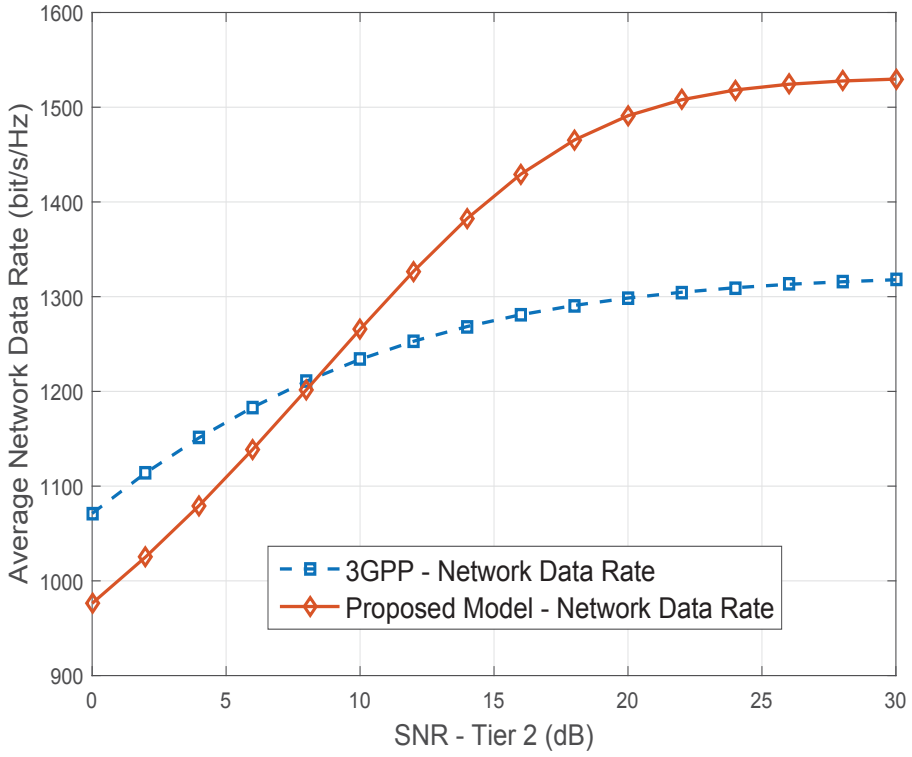

Figure 4.20 : (*Strict FR*), Average Network Data Rate Comparison

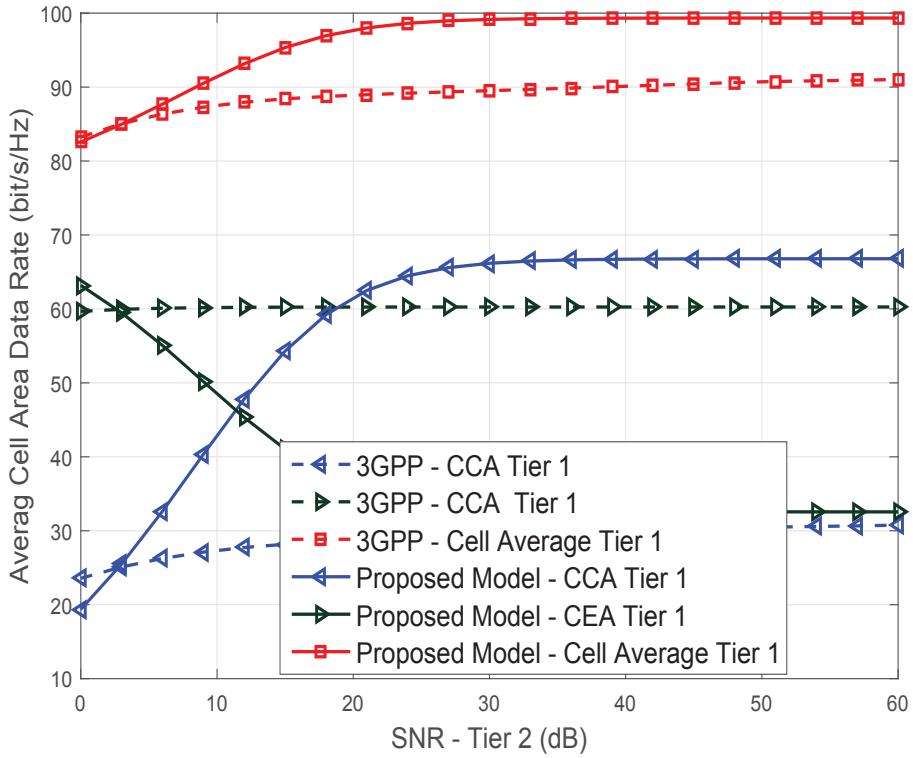

(a) (*Soft FR, Tier-1*), Comparison between Performance of Cell Areas

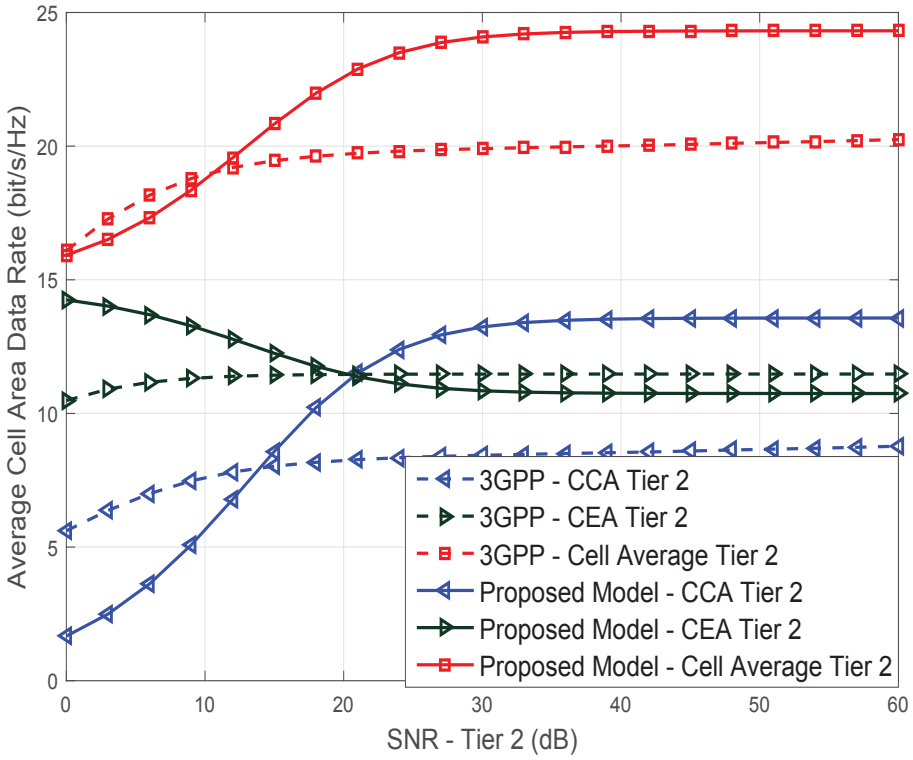

(b) (*Soft FR, Tier-2*), Comparison between Performance of Cell Areas

Figure 4.21 : (*Soft FR*), Comparison between Performance of Cell Areas

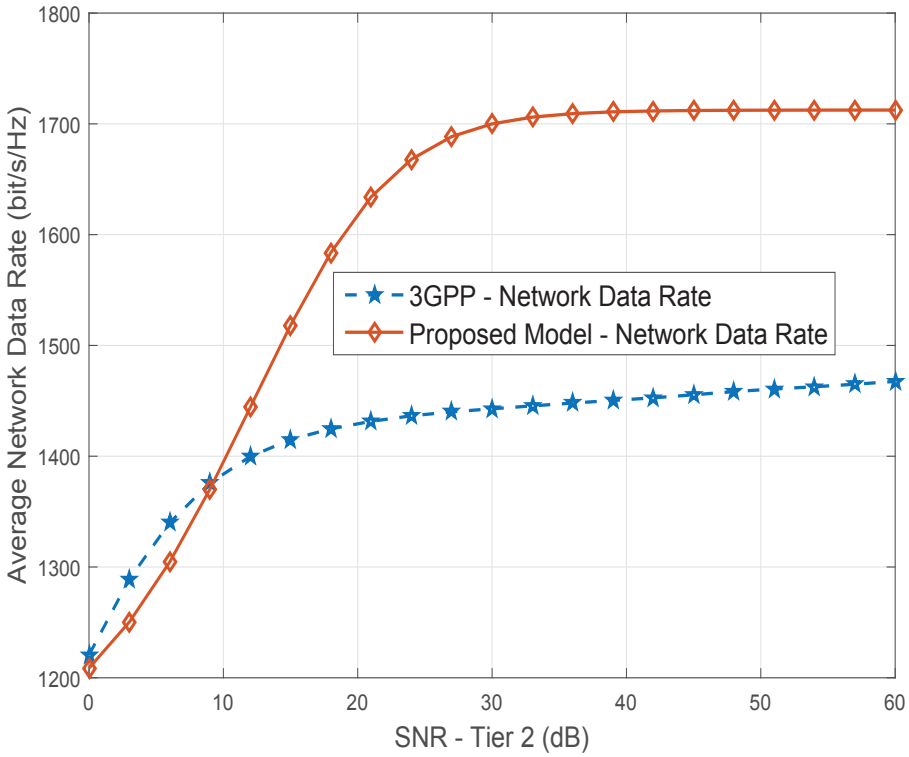

Figure 4.22 : (*Soft FR*), Average Network Data Rate Comparison

4.6 Conclusion

In this chapter, the average coverage probabilities and average data rates of CCU and CEU as well as CC and CE Areas in the heterogeneous networks using Strict FR and Soft FR were derived. Through the analytical results, the effects of the SINR threshold and the bias factor on the network performance were clearly presented. While the average data rate of the CCU rapidly increases when the SINR threshold increases, the average data rate of the CEU fluctuates and can be partitioned into 3 regimes corresponding to 3 ranges of the SINR threshold values. Moreover, an increase in the bias factor can improve the average data rates of both CEU and CCU in all tiers for both Strict FR and Soft FR. Hence, an optimal value of the SINR threshold and the bias factor can be selected to obtain the maximum network data rate. Furthermore, the analytical results indicate that compared to the 3GPP model, our proposed model not only reduce upto 40.79% and 3.8% power consumption of a BS on the data channel but also achieves 16.08% and 18.63% higher network data rates in the case of Strict FR and Soft FR respectively.

Chapter 5

Modelling CoMP in Random Cellular Networks

In this chapter, models based on random cellular networks and 3GPP recommendations are proposed to analyse the performance of networks using either Joint Scheduling or Joint Transmission with Selection Combining. The FFR with a reuse factor of $\Delta = 1$, in which all BSs use the same RBs and transmit at the same power, is considered. The performance metrics in terms of average coverage probability of the typical user, which is randomly located in the network, are derived.

5.1 Introduction to Coordinated Multi-Point

Coordinated Multi-Point (CoMP) transmission and reception [59, 60] has been studied by 3GPP for LTE-Advanced as a new technique to enhance the quality of the received signals and improve spectral efficiency. The main idea of CoMP is to enable dynamic association or transmission and reception for a user with a set of BSs. In a CoMP network with K coordinated BSs, every K adjacent BSs are grouped into a group, called a cluster. Conventionally, each cluster uses a centralized scheduling mechanism to control and mitigate the ICI within the cluster.

The CoMP technique generally can be classified into Joint Transmission or Joint Scheduling. In Joint Transmission, a typical user receives data packets from all

coordinated BSs at the same time, and these packets are always available for transmission at these BSs. This significantly leads to an increase in the volume of data traffic on the backhaul link. Meanwhile, the centralized scheduling mechanism in Joint Scheduling technique select one BS to transmit data to the typical user in every timeslot. Thus, the data packets need to be available at only one BS during a given timeslot, which may reduce the traffic on the backhaul link.

5.1.1 Joint Scheduling

According to 3GPP document [59], the operation of Joint Scheduling can be divided into *establishment phase* followed by *communication phase*, in which the selection of the serving BS takes place during the first phase and data is transferred during the second phase. Figure 5.1 illustrates an example of Joint Scheduling with two coordinated BSs, $K = 2$.

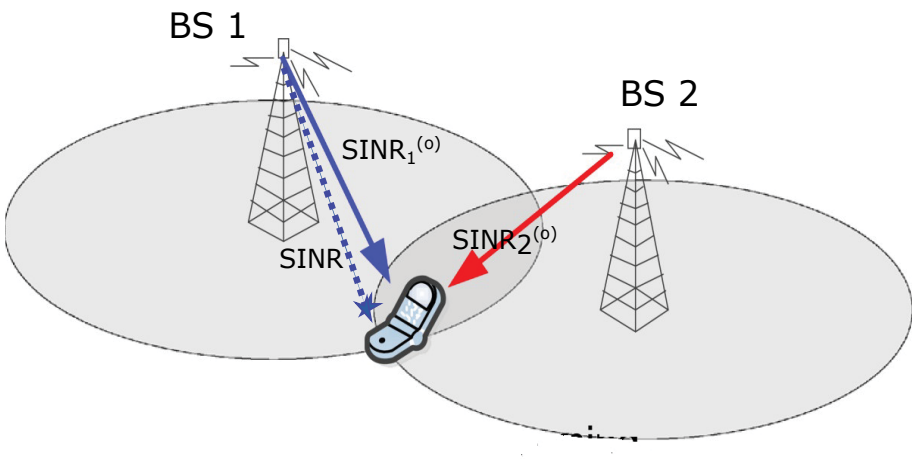

Figure 5.1 : An example of Joint Scheduling with 2 coordinated BSs

The operation of Joint Scheduling is described as below:

- During the *establishment phase*, the user measures the downlink SINRs on every RB from every BS in the cluster to select the RB with the highest SINR of each cell. After that, the user compares the SINRs of the selected RBs to find the serving BS which provides the highest SINR of K coordinated BSs.

In the case of $K = 2$, the greatest SINRs from the BS 1 and BS 2 are denoted by $SINR_1^{(o)}$ and $SINR_2^{(o)}$, which are represented as the solid lines in the figure. The BS with higher SINR, e.g. BS 1 in this case, is selected as the serving BS of the user for this timeslot, and this is reported to the centralized scheduling mechanism.

- During the *communication phase*, the data packets are conveyed to the typical user by BS 1, which is represented as the dashed line.

5.1.2 Joint Transmission with Selection Combining

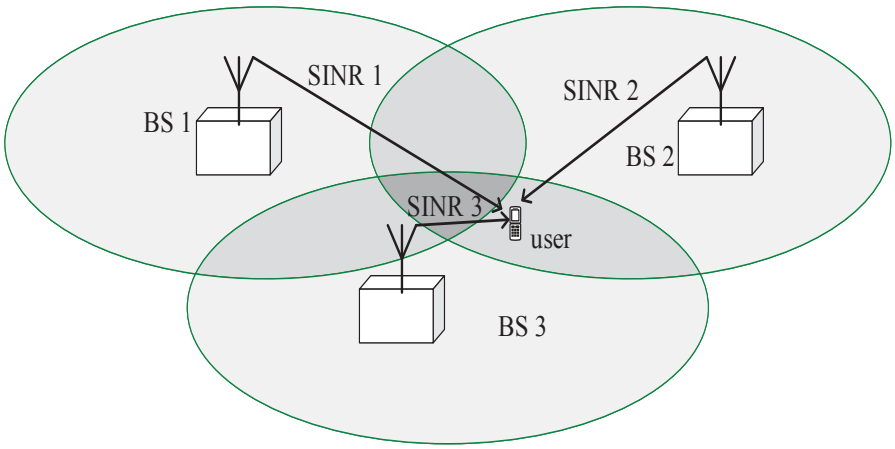

Figure 5.2 : An example of Joint Transmission with Selection Scheduling

In Joint Transmission cellular networks with a cluster size of K, the user data is conveyed by K coordinated BSs. Conventionally, the Maximum Ratio Combining (MRC) is used to combined these K signals, thus the total received signal is the sum of K serving signals [61]. However, MRC requires more complicated processing such as synchronisation and data processing for K signals. Furthermore, MRC may not be optimal in LTE networks since it does not consider interference of the combined signals [62].

Selection Combining [62] is the simplest combining technique, in which only the data from the BS with the highest SINR is received and processed by the user. Thus, Selection Combining only needs to perform synchronisation and data processing for a signal. Hence, Selection Combining is investigated in this chapter.

5.1.3 Coordinate Multi-Point Literature Review

5.1.3.1 Joint Scheduling

To the best of our knowledge, the study on performance evaluation of Joint Scheduling in random cellular networks has not been well-investigated [63]. The most substantial work was presented in [64]. In that work, the author investigated the optimization solution for CoMP by finding the optimal extraction approach of a cluster from a large cellular network. Therefore, there should be more research works on Joint Scheduling in the cellular networks - based on PPP.

5.1.3.2 Joint Transmission with Selection Combining

In contrast to Joint Scheduling, a lot of research works have been conducted to evaluate the performance and optimize Joint Transmission for both hexagonal and random cellular networks, which were summarized in [63, 65]. In most works, the MRC was utilized to combine the signals from K coordinated BSs. In [61], a model of multi-tier cellular networks using Joint Transmission was proposed, and thence the performance was evaluated for both regular and the worst case user under Rayleigh fading channel. Following [61], the non-coherent Joint Transmission BSs was modelled for general fading environment. Author in [66] proposed a model that combined Joint Transmission and ICIC to enhance the network spectral efficiency.

Based on my knowledge, the most substantial work on Joint Transmission with Selection Combining was presented in [67] in which the worst case user with equal distances to three nearest BSs was studied. In addition, the paper assumed that the worst case user measures SINR on the same RB, which causes all measured signals at the typical user to have the same interference. Thus, the serving BS was selected according to fading channels between the user and BSs only.

As discussed above, the shortage of research works has driven requirements for modelling and analysing CoMP in the random cellular networks. It is highly recommended that the 3GPP recommendations should be strictly followed in these works.

5.2 Network model

We consider the cellular networks using CoMP with a cluster size of K. We denote r_k as the distance from the typical user to the BS k which is a RV whose PDF is given by [68]

$$f_{R_k}(r_k) = \frac{2(\pi\lambda)^k}{(k-1)!} r_k^{2k-1} e^{-\pi\lambda r_k^2} \tag{5.1}$$

The joint probability density of R_1, R_2,.., and R_N is defined by $f(r_1, r_2, ..., r_N)$ and given by [68]

$$f(r_1, r_2, ..., r_N) = (2\pi\lambda)^N e^{-\pi\lambda r_N^2} \prod_{m=1}^{N} r_m \tag{5.2}$$

Therefore, the joint PDF of any N RVs in S which is a subset of $\{1, 2, .., K\}$ is denoted by $f_S(S)$ and obtained by integrating $K-N$ integrals of $f_{R_1,...,R_K}(r_1, ..., r_K)$ with respect to r_j ($r_j \in S^c$) as the following equation

$$f_S(S) = (2\pi\lambda)^K \int ... \int e^{-\pi\lambda r_K^2} \prod_{m=1}^{K} r_m \prod_{j \in S^c} dr_j \tag{5.3}$$

in which S^c is the complementary set of S, $S^c = \{1, 2, ..., K\} \backslash \{S\}$, the bounds of integrations satisfy the following rule: $0 < r_1 < ... < r_K < \infty$.

The downlink SINR

The downlink interference at the typical user associated with BS k is stated as

$$I_k = \underbrace{\sum_{j=1, j\neq k}^{K} P_j g_j r_j^{-\alpha}}_{\text{Intra-Cluster Interference}} + \underbrace{\sum_{j \in \theta^c} P_j g_j r_j^{-\alpha}}_{\text{Inter-Cluster Interference}} \tag{5.4}$$

in which g_j and r_j are the power channel gain and distance from the typical user to interfering BS j whose transmit power is P_j; α is the path-loss exponent; θ^c is the set of interfering BSs which belong to adjacent clusters. We denote θ as the set of

BSs in the network, then $\theta = \theta^c \bigcup \{1, 2, ..., K\}$.

Since the BSs in a given cluster fully exchange the channel state information, the Intra-Cell Interference which originates from the BSs within the same cluster can be controlled by the scheduling mechanism. Meanwhile, the Inter-Cluster Interference which originates from the BSs at adjacent clusters cannot be controlled [69]. For simplicity, it is assumed that the typical user only experiences Inter-Cluster Interference. Furthermore, since the transmit power of the BS in the cellular networks is usually much greater than Gaussian noise, then Gaussian noise can be neglected. Thus, the downlink SINR from BS k at the typical user is given by

$$SIR = \frac{P_k g_k r_k^{-\alpha}}{\sum_{j \in \theta^c} P_j g_j r_j^{-\alpha}} \tag{5.5}$$

We assume that all BSs transmit at the same power, thus the serving signal of the typical user is given by

$$SIR = \frac{g_k r_k^{-\alpha}}{\sum_{j \in \theta^c} g_j r_j^{-\alpha}} \tag{5.6}$$

5.3 Joint Scheduling

5.3.1 User Association Probability

The typical user connects to the BS k $(1 \leq j \leq K)$ if the BS k provides the highest SINR to the typical user during the establishment phase, i.e $SINR_k^{(o)} > SINR_j^{(o)}$ $(\forall 1 \leq j \leq K, j \neq k)$.

With an assumption that the typical user measure on the same data channel, all measured SINRs have the same instantaneous interference. Thus, the typical user association problem becomes

$$g_k^{(o)} r_k^{-\alpha} > g_j^{(o)} r_j^{-\alpha} \qquad \forall (1 \leq j \leq K, j \neq k) \tag{5.7}$$

Lemma 5.3.1.1: The average probability in which the user associates with BS k is given by

$$A_k = 2(2\pi\lambda)^K \int_0^\infty \int_{r_1}^\infty ... \int_{r_{K-1}}^\infty e^{-\pi\lambda r_K^2} \prod_{j=1}^{K} \frac{r_j}{1 + r_j^{-\alpha} r_k^{\alpha}} dr_{K-j+1} \tag{5.8}$$

Proof: The user association probability can be evaluate by the following steps

$$\begin{aligned} A_k &= \mathbb{P}\left(\bigcap_{j=1, j\neq k}^{K} g_k^{(o)} r_k^{-\alpha} > g_j^{(o)} r_j^{-\alpha} \right) \\ &= \mathbb{E}_{G_j, R_j, R_k}\left[\mathbb{P}\left(\bigcap_{j=1, j\neq k}^{K} g_k^{(o)} > g_j^{(o)} r_j^{-\alpha} r_k^{\alpha} \right) \right] \end{aligned}$$

Since all fading channels are independent Rayleigh RVs,

$$\begin{aligned} A_k &= \mathbb{E}_{R_j, R_k, G_j}\left[\prod_{j=1, j\neq k}^{K} \mathbb{P}\left(g_k^{(o)} > g_j^{(o)} r_j^{-\alpha} r_k^{\alpha} \right) \right] \\ &= \mathbb{E}_{R_j, R_k}\left[\prod_{j=1, j\neq k}^{K} \mathbb{E}_{G_j}\left(e^{-g_j^{(o)} r_j^{-\alpha} r_k^{\alpha}} \right) \right] \end{aligned}$$

With assumption that the fading channel has a unit power, e.g. its probability density function is $PDF(\gamma) = \exp(-\gamma)$, then its Moment Generate Function is given by $E[e^{-s\gamma}] = \frac{1}{1+s\gamma}$. Therefore, the association probability is given by

$$\begin{aligned} A_k &= \mathbb{E}_{R_j, R_k}\left[\prod_{j=1, j\neq k}^{K} \frac{1}{1 + r_j^{-\alpha} r_k^{\alpha}} \right] \\ &= (2\pi\lambda)^K \int_0^\infty \int_{r_1}^\infty ... \int_{r_{K-1}}^\infty e^{-\pi\lambda r_K^2} \prod_{m=1}^{K} r_m \prod_{j=1, j\neq k}^{K} \frac{1}{1 + r_j^{-\alpha} r_k^{\alpha}} dr_K ... dr_2 dr_1 \end{aligned} \tag{5.9}$$

Since $\frac{1}{1+r_j^{-\alpha} r_k^{\alpha}} = \frac{1}{2}$ when $j = k$, Equation 5.9 can be re-written as follows

$$A_k = 2(2\pi\lambda)^K \int_0^\infty \int_{r_1}^\infty ... \int_{r_{K-1}}^\infty e^{-\pi\lambda r_K^2} \prod_{j=1}^{K} \frac{r_j}{1 + r_j^{-\alpha} r_k^{\alpha}} dr_{K-j+1} \tag{5.10}$$

The Lemma is proved. ■

5.3.2 Average Coverage Probability Definition

The typical user achieves SINR from the BS k during the communication phase as in Equation (5.6) if its received signal during the establishment phase satisfies Equation (5.7). Hence, the coverage probability of the typical user associated with BS k at distance r_k is defined as the following condition probability

$$\begin{aligned}\mathbb{P}_k^{(c)}(T|r_k) &= \mathbb{P}(SINR_k > \hat{T}| \bigcap_{\substack{j=1,\\ j\neq k}}^{K} g_k^{(o)} r_k^{-\alpha} > g_j^{(o)} r_j^{-\alpha}) \\ &= \frac{\mathbb{P}\left(SINR_k > \hat{T}, \bigcap_{\substack{j=1,\\ j\neq k}}^{K} g_k^{(o)} r_k^{-\alpha} > g_j^{(o)} r_j^{-\alpha} | r_k\right)}{\mathbb{P}\left(\bigcap_{\substack{j=1,\\ j\neq k}}^{K} g_k^{(o)} r_k^{-\alpha} > g_j^{(o)} r_j^{-\alpha} | r_k\right)} \end{aligned} \tag{5.11}$$

Since the typical user can associate with any BS, the coverage probability of the typical user at a distance r_k from its serving BS k is defined as

$$\sum_{k=1}^{K} \mathbb{P}\left(\bigcap_{\substack{j=1,\\ j\neq k}}^{K} g_k^{(o)} r_k^{-\alpha} > g_j^{(o)} r_j^{-\alpha} | r_k\right) \mathbb{P}_k^{(c)}(T|r_k)$$

Thus, the average coverage probability of the typical user in the network is

$$\mathcal{P}_c(\hat{T}) = \sum_{k=1}^{K} \mathbb{E}_{R_k}\left[\mathbb{P}\left(SINR_k > \hat{T}, \bigcap_{\substack{j=1,\\ j\neq k}}^{K} g_k^{(o)} r_k^{-\alpha} > g_j^{(o)} r_j^{-\alpha}\right)\right] \tag{5.12}$$

The definition of average coverage probability is different from previous work for the hexagonal network layout such as in [69–72] since in those work the establishment phase and communication phase were not distinguished.

5.3.3 Average Coverage Probability Evaluation

Theorem 5.3.3.1: The average coverage probability of the typical user in the network is given by

$$\mathcal{P}_c(\hat{T}) = \sum_{k=1}^{K} \underbrace{\mathbb{E}_{R_j}}_{1\leq j\leq K} \left[e^{-2\pi\lambda \int_{r_K}^{\infty} \frac{\hat{T}t^{1-\alpha} r_k^{\alpha}}{1+\hat{T}t^{-\alpha} r_k^{\alpha}} dt} \prod_{\substack{j=1,\\ j\neq k}}^{K} \frac{1}{1+r_j^{-\alpha} r_k^{\alpha}} \right] \tag{5.13}$$

Employing the joint expectation definition of K RVs whose joint probability density function is defined in Equation 5.2, the average coverage probability can be re-written as the following equation

$$\begin{aligned} \mathcal{P}_c(\hat{T}) =& (2\pi\lambda)^K \sum_{k=1}^{K} \int_0^{\infty} \int_{r_1}^{\infty} \ldots \int_{r_{K-1}}^{\infty} e^{-\pi\lambda r_K^2} \\ & \left[\prod_{\substack{j=1,\\ j\neq k}}^{K} \frac{e^{-2\pi\lambda \int_{r_K}^{\infty} \frac{\hat{T}t^{1-\alpha} r_k^{\alpha}}{1+\hat{T}t^{-\alpha} r_k^{\alpha}} dt}}{1+r_j^{-\alpha} r_k^{\alpha}} \right] \prod_{m=1}^{K} r_m dr_{K-m+1} \end{aligned} \tag{5.14}$$

Proof: The conditional probability in Equation (5.12) can be evaluated by using the following steps

$$\mathbb{P}\left(g_k > \hat{T} \frac{\sum_{j\in\theta^c} P_j g_j r_j^{-\alpha}}{P_k r_k^{-\alpha}}, \bigcap_{\substack{j=1,\\ j\neq k}}^{K} g_k^{(o)} > g_j^{(o)} r_j^{-\alpha} r_k^{\alpha} \right)$$

Since the channel power gains are independent exponential RVs,

$$\begin{aligned}
\mathcal{P}_c(\hat{T}) &= \mathbb{E}\left[e^{-\hat{T}\sum_{j\in\theta^c} g_j r_j^{-\alpha} r_k^{\alpha} - \sum_{\substack{j=1,\\ j\neq k}}^{K} g_j^{(o)} r_j^{-\alpha} r_k^{\alpha}}\right] \\
&\overset{(a)}{=} \mathbb{E}_{R_j}\left[\prod_{j\in\theta^c} \mathbb{E}_{G_j}\left[e^{-\hat{T} r_j^{-\alpha} r_k^{\alpha} g_j}\right] \prod_{\substack{j=1,\\ j\neq k}}^{K} \mathbb{E}_{G_j^{(o)}}\left[e^{-g_j^{(o)} r_j^{-\alpha} r_k^{\alpha}}\right]\right] \\
&\overset{(b)}{=} \underbrace{\mathbb{E}_{R_j}}_{\substack{1\leq j\leq K,\\ j\neq k}} \left[\underbrace{\mathbb{E}_{R_j}}_{j>K}\left[\prod_{j\in\theta^c} \frac{1}{1+\hat{T} r_j^{-\alpha} r_k^{\alpha}}\right] \prod_{\substack{j=1,\\ j\neq k}}^{K} \frac{1}{1+r_j^{-\alpha} r_k^{\alpha}}\right] \\
&\overset{(c)}{=} \underbrace{\mathbb{E}_{R_j}}_{\substack{1\leq j\leq K,\\ j\neq k}} \left[e^{-2\pi\lambda \int_{r_K}^{\infty} \frac{\hat{T} t^{1-\alpha} r_k^{\alpha}}{1+\hat{T} t^{-\alpha} r_k^{\alpha}} dt} \prod_{\substack{j=1,\\ j\neq k}}^{K} \frac{1}{1+r_j^{-\alpha} r_k^{\alpha}}\right]
\end{aligned} \tag{5.15}$$

in which (a) follows the assumption that all fading channels are RVs; (b) due to the assumption that g_j is an exponential RV; (c) obtained by using the properties of Probability Generating Function.

Substituting Equation 5.15 into Equation 5.12 , the Theorem is proved. ■

5.3.4 Special Cases

In the case of Joint Scheduling with $K = 2$ in the interference-limited networks ($\sigma = 0$) with $\alpha = 4$ The average coveage probability of the typical user is obtained by

$$\mathcal{P}_c(\hat{T}) = (2\pi\lambda)^2 \int_0^{\infty} \int_{r_1}^{\infty} r_1 r_2 e^{-\pi\lambda r_2^2} \left[\frac{e^{-2\pi\lambda\kappa_{r_2}(r_1)}}{1+r_2^{-\alpha} r_1^{\alpha}} + \frac{e^{-2\pi\lambda\kappa_{r_2}(r_2)}}{1+r_1^{-\alpha} r_2^{\alpha}}\right] dr_2 dr_1 \tag{5.16}$$

in which $\kappa_{r_2}(r_1) = \int_{r_2}^{\infty} \frac{\hat{T} t^{1-\alpha} r_1^{\alpha}}{1+\hat{T} t^{-\alpha} r_1^{\alpha}} dt$, $\alpha = 4$.

By using a change of variable $t = (r_2/y)^2$ and given that $\alpha = 4$, $\kappa_{r_2}(r_1)$ equals

$$\begin{aligned}\kappa_{r_2}(r_1) &= r_2^2 \int_0^1 \frac{\hat{T}y}{r_1^{-4} r_2^4 + \hat{T}y^4} dy \\ &= \frac{\sqrt{\hat{T}} r_1^2}{2} \arctan\left(\frac{\sqrt{\hat{T}} r_1^2}{r_2^2}\right)\end{aligned} \tag{5.17}$$

Similarly, $\kappa_{r_2}(r_2)$ is obtained by $\kappa_{r_2}(r_2) = \frac{r_2^2}{2}\sqrt{\hat{T}} \arctan\left(\sqrt{\hat{T}}\right)$.

Considering the first part of the Equation 5.16 which contains $\kappa_{r_2}(r_1)$, the integral can be re-written in the following form

$$(2\pi\lambda)^2 \int_0^\infty r_2 e^{-\pi\lambda r_2^2} \int_0^{r_2} r_1 \frac{e^{-\pi\lambda\sqrt{\hat{T}} r_1^2 \arctan\left(\frac{\sqrt{\hat{T}} r_1^2}{r_2^2}\right)}}{1 + r_2^{-4} r_1^4} dr_1 dr_2$$

This is due to the fact that $\int_0^\infty \int_y^\infty f_{X,Y}(x,y)dxdy = \int_0^\infty \int_0^x f_{X,Y}(x,y)dydx$, $\forall X > Y > 0$. Employing a change of variable $y = r_1^2/r_2^2$, the equation above equals

$$\begin{aligned}&2(\pi\lambda)^2 \int_0^\infty r_2 e^{-\pi\lambda r_2^2} \int_0^1 \frac{e^{-\pi\lambda r_2^2 y\sqrt{\hat{T}} \arctan\left(y\sqrt{\hat{T}}\right)}}{1+y^2} dy dr_2 \\ =&2(\pi\lambda)^2 \int_0^1 \frac{1}{1+y^2} \int_0^\infty r_2^3 e^{-\pi\lambda r_2^2\left(1+y\sqrt{\hat{T}} \arctan\left(y\sqrt{\hat{T}}\right)\right)} dr_2 dy \\ =&\int_0^1 \frac{1}{(1+y^2)\left(1+y\sqrt{\hat{T}} \arctan\left(y\sqrt{\hat{T}}\right)\right)} dy\end{aligned}$$

The second part of Equation 5.16 which contains $\kappa_{r_2}(r_2)$ is obtained by

$$\int_0^1 \frac{1}{(1+y^2)\left(1+y\sqrt{\hat{T}} \arctan\left(\sqrt{\hat{T}}\right)\right)} dy$$

Consequently, the average coverage probability of the typical user is given by

$$\mathcal{P}_c(\hat{T}) = \int_0^1 \frac{1}{(1+y^2)} \left[\frac{1}{1+y\sqrt{\hat{T}} \arctan\left(\sqrt{\hat{T}}\right)} + \frac{1}{1+y\sqrt{\hat{T}} \arctan\left(\sqrt{\hat{T}}\right)}\right] dy$$

Interestingly, the average coverage probability of the typical user in this case does

not depend on the density of BSs in the network. This is consistent with the previous results which was found in the case of no-coordinated scheduling [22].

In the case of worst case user In the cellular networks, the typical user which has the same distance to three nearest BSs is called the worst case user. The PDF of the distance from the worst case user to its serving BS is given by [67]

$$f_w(r) = 2(\pi\lambda)^2 r^3 e^{-\pi\lambda r^2} \tag{5.18}$$

Using the results from Equation 5.13 with $K = 3$ and $r_1 = r_2 = r_3 = r$, the average coverage probability of the worst case user is obtained by the following equation

$$\begin{aligned}\mathcal{P}_c(\hat{T}) =& \frac{3}{4}\mathbb{E}_R\left[e^{-2\pi\lambda\int_r^\infty \frac{\hat{T}t^{1-\alpha}r^\alpha}{1+\hat{T}t^{-\alpha}r^\alpha}dt}\right] \\ =& \frac{3(\pi\lambda)^2}{2} r^3 e^{-\pi\lambda r^2} e^{-2\pi\lambda\int_r^\infty \frac{\hat{T}t^{1-\alpha}r^\alpha}{1+\hat{T}t^{-\alpha}r^\alpha}dt}\end{aligned} \tag{5.19}$$

This result on the worst case user performance is different from the results given in [67] since authors in [67] merged the establishment phase and communication phase of Joint Scheduling.

5.4 Joint Transmission with Selection Combining

5.4.1 Coverage Probability Definition

In the networks using Joint Transmission with Selection Combining, the user data is conveyed by all K coordinated on different RBs. However, only the data from the BS with the highest SINR is received and processed by the user. Thus, since interferences on different RBs are different, the downlink SIR of the typical user is given by

$$SIR = \max_{1\le k\le K}\left(\frac{g_k r_k^{-\alpha}}{\sum_{j\in\theta^c} g_j r_j^{-\alpha}}\right) \tag{5.20}$$

Thus, the average coverage probability can be defined as the following equation

$$P(\hat{T}) = \mathbb{P}\left(\max_{1\leq k\leq K}\left(\frac{g_k r_k^{-\alpha}}{\sum_{j\in\theta^c} g_j r_j^{-\alpha}}\right) > \hat{\hat{T}}\right) \tag{5.21}$$

5.4.2 Average Coverage Probability Evaluation

The average coverage probability can be evaluated by the following steps

$$\begin{aligned} P(\hat{T}) &= \mathbb{P}\left(\max_{1\leq k\leq K}\left(\frac{g_k r_k^{-\alpha}}{\sum_{j\in\theta^c} g_j r_j^{-\alpha}}\right) > \hat{\hat{T}}\right) \\ &= 1 - \mathbb{P}\left(\max_{1\leq k\leq K}\left(\frac{g_k r_k^{-\alpha}}{\sum_{j\in\theta^c} g_j r_j^{-\alpha}}\right) < \hat{T}\right) \\ &= 1 - \mathbb{E}\left[\prod_{1\leq k\leq K} P\left(\frac{g_k r_k^{-\alpha}}{\sum_{j\in\theta^c} g_j r_j^{-\alpha}} < \hat{T}\right)\right] \end{aligned}$$

With the assumption that all fading channels are independent Rayleigh RVs, the average coverage probability is given by

$$\begin{aligned} P(\hat{T}) &= 1 - \mathbb{E}\left[\prod_{1\leq k\leq K}\left(1 - \prod_{j\in\theta^c} e^{-\hat{T} r_k^{\alpha} r_j^{-\alpha} g_j}\right)\right] \\ &= \mathbb{E}\left[\sum_{S}(-1)^{N+1}\prod_{k\in S}\prod_{j\in\theta^c} e^{-\hat{T} r_k^{\alpha} r_j^{-\alpha} g_j}\right] \end{aligned}$$

in which S is the subset of $\{1, 2, ..., K\}$ and $S \neq \emptyset$, N is the number of elements of S. Thus, the average coverage probability can be re-written as the following equations

$$\begin{aligned} P(\hat{T}) &= \mathbb{E}\left[\sum_{S}(-1)^{N+1}\prod_{j\in\theta^c}\prod_{k\in S}\mathbb{E}_{G_j}\left[e^{-\hat{T} r_k^{\alpha} r_j^{-\alpha} g_j}\right]\right] \\ &= \mathbb{E}\left[\sum_{S}(-1)^{N+1}\mathbb{E}_{\theta^c}\left[\prod_{j\in\theta^c}\prod_{k\in S}\frac{1}{1+\hat{T} r_k^{\alpha} r_j^{-\alpha}}\right]\right] \end{aligned}$$

By employing the properties of PGF and given that the distance from any interfering BS to the typical user must be greater than r_K, $P(\hat{T})$ is obtained by

$$\begin{aligned} P(\hat{T}) =& \mathbb{E}\left[\sum_{S}(-1)^{N+1} e^{-2\pi\lambda\int_{r_K}^{\infty} t\left[1-\prod_{k\in S}\frac{1}{1+\hat{T}r_k^{\alpha}t^{-\alpha}}\right]dt}\right] \\ =& (2\pi\lambda)^K \sum_{S}(-1)^{N+1}\int_0^{\infty}\int_{r_1}^{\infty}...\int_{r_{K-1}}^{\infty} e^{-\pi\lambda r_K^2} \\ & e^{-2\pi\lambda\int_{r_K}^{\infty} t\left[1-\prod_{k\in S}\frac{1}{1+\hat{T}r_k^{\alpha}t^{-\alpha}}\right]dt}\prod_{j=1}^{K} r_j dr_{K-j+1} \end{aligned} \tag{5.22}$$

in which Equation 5.22 above is the result of taking the expected values of N random variables, $(R_1, R_2, ..., R_K)$, whose joint PDF was defined in Equation (5.3).

By employing changes of variable $t^2 = r_K y$ and $x_j = \pi\lambda r_j^2$, $(1 \le j \le K)$, $P(\hat{T})$ is obtained by

$$\begin{aligned} P(\hat{T}) =& \sum_{S}(-1)^{N+1}\int_0^{\infty}\int_{x_1}^{\infty}...\int_{x_{K-1}}^{\infty} e^{-x_K} \\ & e^{-x_K\int_1^{\infty}\left[1-\prod_{k\in S}\frac{1}{1+\hat{T}x_k^{\alpha/2}(x_K y)^{-\alpha/2}}\right]dy}\prod_{j=1}^{K} dx_{K-j+1} \end{aligned} \tag{5.23}$$

Equation (5.23) provides the most important result of this section which derives the average coverage probability of the typical user. It is interesting that the average coverage probability does not depend on the density of BS, which is consistent with the conclusion for the cellular networks without Joint Scheduling [22].

5.4.3 Special case

A special case of Joint Scheduling with $K = 2, S \subset \{1, 2\}$ and $S \neq \emptyset$ By employing a change of variable $t = \frac{r_1}{r_2}$, the average coverage probability is obtained

by the following equations

$$
\begin{aligned}
P(\hat{T}) &= (2\pi\lambda)^2 \int\int e^{-\pi\lambda r_2^2} e^{-2\pi\lambda r_2^2 \int_1^\infty \left[1-\frac{1}{1+\hat{T} r_1^{\alpha} r_2^{-\alpha} y^{-\alpha/2}}\right] dy} r_1 r_2 dr_1 dr_2 \\
&\quad + (2\pi\lambda)^2 \int\int e^{-\pi\lambda r_2^2} e^{-2\pi\lambda r_2^2 \int_1^\infty \left[1-\frac{1}{1+\hat{T} y^{-\alpha/2}}\right] dy} r_1 r_2 dr_1 dr_2 \\
&\quad - (2\pi\lambda)^2 \int\int e^{-\pi\lambda r_2^2} e^{-2\pi\lambda r_2^2 \int_1^\infty \left[1-\frac{1}{1+\hat{T} r_1^{\alpha} r_2^{-\alpha} y^{-\alpha/2}} \frac{1}{1+\hat{T} y^{-\alpha/2}}\right] dy} r_1 r_2 dr_1 dr_2 \\
&= 2(\pi\lambda)^2 \int_0^\infty r_2^3 e^{-\pi\lambda r_2^2} \int_0^1 e^{-2\pi\lambda r_2^2 \int_1^\infty \left[1-\frac{1}{1+\hat{T} t^{\alpha/2} y^{-\alpha/2}}\right] dy} dt dr_2 \\
&\quad + 2(\pi\lambda)^2 \int_0^\infty r_2^3 e^{-\pi\lambda r_2^2} e^{-2\pi\lambda r_2^2 \int_1^\infty \left[1-\frac{1}{1+\hat{T} y^{-\alpha/2}}\right] dy} dr_2 \\
&\quad - 2(\pi\lambda)^2 \int_0^\infty r_2^3 e^{-\pi\lambda r_2^2} \int_0^1 e^{-2\pi\lambda r_2^2 \int_1^\infty \left[1-\frac{1}{1+\hat{T} t^{\alpha/2} y^{-\alpha/2}} \frac{1}{1+\hat{T} y^{-\alpha/2}}\right] dy} dr_2 \\
&= \int_0^\infty r_2 e^{-r_2} \left[\int_0^1 e^{-r_2 \upsilon(\hat{T},t)} dt + e^{-r_2 \upsilon(\hat{T},1)} - \int_0^1 e^{-r_2 \frac{t^{\alpha/2} \upsilon(\hat{T},t) - \upsilon(\hat{T},1)}{t^{\alpha/2}-1}} dt \right] dr_2
\end{aligned}
\tag{5.24}
$$

in which $\upsilon(\hat{T},t) = \int_1^\infty \frac{\hat{T} t^{\alpha/2} y^{-\alpha/2}}{1+\hat{T} t^{\alpha/2} y^{-\alpha/2}} dy$.

In Equation 5.24, the infinite integral has a suitable form of Gauss - Legendre Quadrature while the integral defined from $[0,1]$ can be approximated by using Gauss-Laguerre Quadrature. Hence, the average coverage probability can be approximated by

$$
P(\hat{T}) \approx \sum_{j=1}^{N_{GL}} w_j t_i \left[\sum_{i=1}^{N_G} \frac{c_i}{2} e^{-t_j \upsilon\left(\hat{T},\eta_i\right)} + e^{-t_j \upsilon(\hat{T},1)} \right] \quad - \sum_{j=1}^{N_{GL}} w_j t_j \sum_{i=1}^{N_G} \frac{c_i}{2} e^{-\zeta_j \left[\frac{\eta_i^{\alpha/2} \upsilon(\hat{T},\eta_i) - \upsilon(\hat{T},1)}{\eta_i^{\alpha/2}-1} \right]}
$$

where N_{GL} and N_G are the degrees of the Laguerre and Legendre polynomial, t_i and w_i, c_i and x_i are the i-th node and weight, abscissas and weight of the corresponding quadratures; $\eta_j = \frac{x_i+1}{2}$.

Furthermore, the integral $\upsilon(\hat{T},t)$ can be presented as the difference of two integrals I_0 and I_1 which are defined on intervals $[0,\infty]$ and $[0,1]$, respectively. While I_0 is evaluated by employing changes of variables $\gamma = \hat{T} t^{\alpha/2} y^{-\alpha/2}$ and using the properties of Gamma function, I_1 is approximated by Gauss-Legendre rule. Hence,

$v(\hat{T}, t)$ can be approximated by [38]

$$v(\hat{T}, t) \approx \frac{2t\hat{T}^{2/\alpha}}{\alpha} \frac{\pi}{\sin\left(\frac{2\pi}{\alpha}\right)} - \sum_{i=1}^{N_G} \frac{c_i}{2} \frac{\hat{T}t^{\alpha/2}}{\left(\frac{x_i+1}{2}\right)^{\alpha/2} + \hat{T}t^{\alpha/2}} \tag{5.25}$$

5.5 Simulation and Discussion

In this section, the numerical and simulation results are presented to verify analytical results and the relationship between the coverage threshold on the network performance. As shown in Figures 5.3 and 5.4, the solid lines representing the analytical results match with the points representing the simulation results, which confirms the accuracy of the analytical results.

Joint Scheduling It is noted that in the case of $K = 1$, since the establishment phase is not necessary and only communication phase is considered, the comparison between Joint Scheduling with $K = 1$ and $K = 2$ is not reasonable.

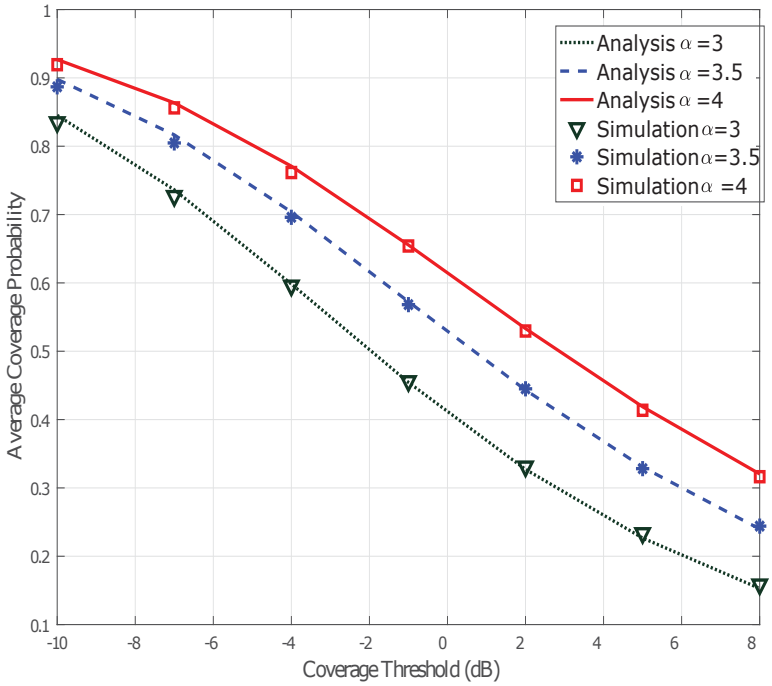

Figure 5.3 : *(Joint Scheduling)* Average Coverage Probability with different values of α and coverage threshold ($\lambda = 0.5$ and $K = 2$)

In the Joint Scheduling cellular network systems in which the typical user prefers a connection with the BS in the nearest cluster, the distance from the typical user to the serving BS must be greater than that to the interfering BSs. Hence, the interference signal experiences a higher path loss, which is proportional to the distance, than the serving signal. In other words, the received SINR increases with α. Consequently, the average coverage probability of the typical user with path loss exponent α. For example, when α increases from 3 to 4 for coverage threshold $T = 2$ dB, the average coverage probability increases by approximately 59.9% from 0.3312 to 0.5296

Joint Transmission with Selection Combining As shown in Fig. 5.4, Joint Scheduling technique can significantly improve the average coverage probability of the typical user. Take $\alpha = 3$ for example, when coverage threshold $T = 2dB$, the average coverage probability increases by 34.88% from 0.3908 to 0.5271.

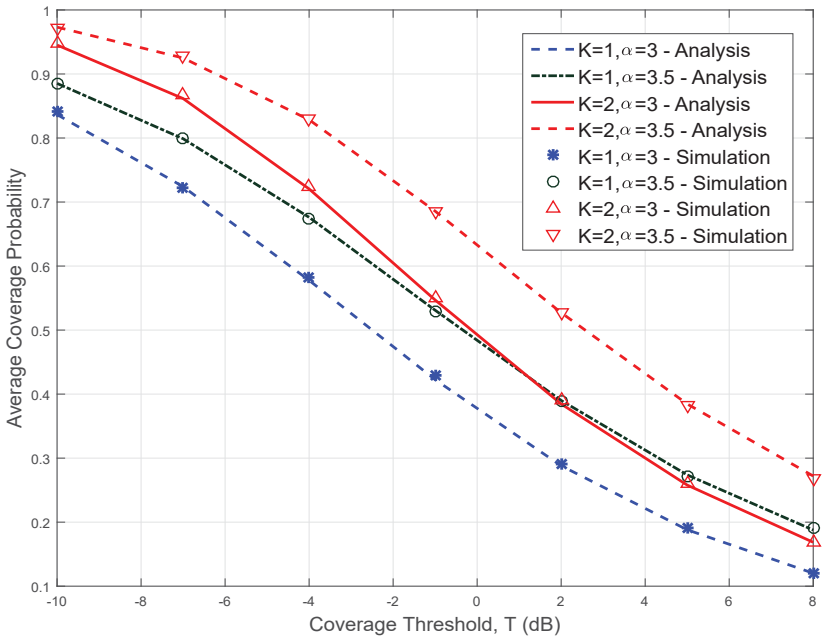

Figure 5.4 : *(Joint Transmission with Selection Combining)* A comparison between analytical and Monte Carlo simulation results

5.6 Conclusion

In this chapter, the models based on PPP are proposed to analyse the performance of Joint Scheduling and Joint Transmission with Selection Combining. In the case of Joint Scheduling, the proposed model follows the recommendation of 3GPP to separate the operation of Join Scheduling into establishment phase and communication phase. The analytical approach is not only used for the Joint Scheduling but also for non-Joint Scheduling and the worst case user. In the case of Joint Transmission with Selection Combining, the cellular network, in which the user observes SINR on different RBs and select the strongest BS as the serving BS, was presented. The analytical results indicated that the Joint Transmission with Selection Combining can significantly improve the user average coverage probability.

Chapter 6

Conclusions and Future works

6.1 Summary of Thesis Contributions

This dissertation has discussed a study on two well-known Frequency Reuse algorithms, called Strict FR and Soft FR, in Random Cellular Networks in which the BSs are distributed according to a PPP. The background, objectives and related works as well as the contribution of the research work are presented in Chapter 1.

In Chapter 2, we used the recommendations of 3GPP to model the FFR, in which two phases of FFR operation, called establishment phase and communication phase, were defined for both CCU and CEU. During the establishment phase, each BS measures SINR on the downlink control channel to classify each user into either CCU or CEU. This is followed by the data transfer process between the user and its serving BS during the communication phase. Highly tractable expressions of network performance were derived in terms of CCU and CEU classification probabilities and corresponding average coverage probabilities. The Gaussian Quadratures were utilised to approximate the complex expressions of the network performance by a simple finite sums which can be considered as the closed-form expressions. The analytical results of the proposed model are more accurate than well-known results in [44] and [37] since we consider the dependence of SINRs during two phases and the independence of the interfering BSs serving CCUs and CEUs. While authors in [50] stated that the optimal SINR threshold can be selected at the coverage threshold,

this chapter concluded that when more users are served as CEUs, a higher network performance is achieved. This conclusion is more reasonable because while the ICI in downlink is unlikely to change when SINR increases, the user achieves higher performance if it is served with a high transmit power. Furthermore, in the case of high transmit power ratios, an increase in SNR can reduce the performance of the CCU as well as the typical user.

Chapter 3 extended the results of Chapter 2 to model the uplink Random Cellular Networks using FFR. In the uplink, the power control exponent coefficient was used to control the user transmit power. Besides deriving the close-form expressions of the network performance, the following interesting conclusions, which contradicted with the related works, were found in this chapter: *(i)* For both Strict FR and Soft FR, the user can achieve a higher performance and consume lower power when the density of BSs increases. For medium dense networks with $\lambda = 0.5\ BS/km^2$ and dense networks with $\lambda = 1\ BS/km^2$, the user performance is at a maximum value when all users transmit at constant powers, e.g. P for CCUs and ϕP for CEUs. *(ii)* For sparse networks with $\lambda = 0.1\ BS/km^2$, the average uplink SINR of the user during establishment phase increases with the power control exponent while the corresponding average data rate of the CCU during the communication phase reduces. *(iii)* For sparse networks with $\lambda = 0.1\ BS/km^2$, the average coverage probability of the CEU during the communication phase increases significantly to a peak value before undergoing a rapid decline when the power control exponent increases.

In Chapter 4, the Multi-tier Random Cellular Networks with multi-RBS and multi-users were modelled in which the BS observes SINR on the data channel for user classification purpose during the establishment phase. The effects of the number of RBs and the number of users were investigated. Our analytical results indicate that with an increase in SINR threshold, the average CEU data rate increases to a peak value before undergoing a rapid decline to a minimum value which is followed by a slight growth. Furthermore, our results stated that the coverage network data rate increases rapidly before undergoing a decline. These findings contradicted the

well-known results in previous works since the number of users and the number of RBs were not carefully discussed in those works. In addition, the analytical results in this chapter indicated that by using SINR on the data channel for user classification purpose, the BS power consumption can be reduced and a higher network data rate is achieved.

In Chapter 5, we proposed a two-phase model based PPP to analyse the performance of CoMP techniques, particularly Joint Scheduling and Joint Transmission using Selection Combining. In the case of Joint Scheduling, the proposed model followed the recommendation of 3GPP to separate the operation of Join Scheduling into establishment phase and communication phase. Thus, the performance of the typical user was defined as conditional probability of the performance during the communication phase under condition of the establishment phase. The analytical method was not only used for the Joint Scheduling but also for non-Joint Scheduling and the worst case user. In the case of Joint Transmission with Selection Combining, the networks were modelled in which the serving BS was selected based on the downlink SINR on different RBs from different BS.

In conclusion, this dissertation provided useful mathematical technique to model and analyse LTE networks using FFR. The numerical solution of the equations provides the close-form of equations. Since the original equation contains infinity integral that is very difficult to compute exactly, the numerical solution makes the computation simpler and more accurate. For practical use, the network models in this work can be utilised to examine effects of fading environment, density of BSs, number of RBs, number of users and CoMP technique on the network performance. The thesis also provided an approach based on graph analysis to find the optimal values of network parameters such as SINR threshold, bias factor. Furthermore, the dissertation proposed a new FFR schemes that can improve the network performance and can be implemented in real networks.

6.2 Future Work Directions

The works carried out in this dissertation have derived essential results on network performance of FFR schemes in random cellular networks. However, the study posed some research directions such as the combination of FFR and CoMP with a reuse factor $\Delta > 1$, and performance evaluation with multi-path loss scopes.

Combination of FFR and CoMP with a reuse factor $\Delta > 1$ In the case of a reuse factor $\Delta > 1$, the analytical approach turns into more complicated expression since the typical user experiences interference originating from BSs transmitting at different transmit powers. It can be seen that CoMP requires more bandwidth than FFR. Thus, when FFR coexists with CoMP technique, the networks should decide which user is supported by either FFR scheme with a high transmit power or CoMP with coordinated BSs, or both FFR and CoMP schemes. The benefits of FFR and CoMP should be compared together for specific cases of the user to find optimal solution for network performance.

Performance evaluation with multi-path loss In practical networks, the signal between a transmitter and receiver usually experiences different radio transmission environments, particularly different fading models as well as path loss slopes as discussed in Section 2.1.1. Variances of transmission environments significantly effect on the SINR at the receiver. Thus, the network performance metrics, such as user classification probabilities and average coverage probabilities, are subject to change. Furthermore, modelling FFR for Ultra Dense Networks [73], which can be considered as a new paradigm shift in future wireless networks, have not been investigated.

Appendix A

Appendices of Chapter 2

A.1 Lemma 2.1.3.1 - CCU classification probability

The probability in which the user at distance r from it's serving BS is served as a CCU is given by

$$A^{(c)}(T,\epsilon|r) = \mathbb{P}\left(\frac{Pgr^{-\alpha}}{\sigma^2 + I} > T\right) \tag{A.1}$$

in which I is defined in Equation (2.7). Since g has an exponential distribution,

$$\begin{aligned} A^{(c)}(T,\epsilon|r) &= e^{-\frac{Tr^{\alpha}}{SNR}}\mathbb{E}\left[e^{-T\sum_{j\in\theta} g_{jz} r_{jz}^{-\alpha} r^{\alpha}}\right] \\ &\overset{(a)}{=} e^{-\frac{Tr^{\alpha}}{SNR}}\prod_{j\in\theta}\mathbb{E}\left[e^{-Tr^{\alpha} r_{jz}^{-\alpha} g_{jz}}\right] \\ &\overset{(b)}{=} e^{-\frac{Tr^{\alpha}}{SNR}}\prod_{j\in\theta}\mathbb{E}\left[\frac{1}{1+Tr^{\alpha} r_{jz}^{-\alpha}}\right] \\ &\overset{(c)}{=} e^{-\frac{Tr^{\alpha}}{SNR}} e^{-2\pi\lambda\int_r^{\infty}\left[1-\frac{1}{1+Tr^{\alpha} r_{jz}^{-\alpha}}\right] r_{jz} d(r_{jz})} \end{aligned}$$

in which (a) due to the independence of the power channel gains; (b) follows the assumption that the channel gain has a Rayleigh distribution; (c) follows the properties of PGF.

Employing a change of variable $t = (r_{jz}/r)^2$, we obtain

$$\begin{aligned} A^{(c)}(T,\epsilon|r) =& e^{-\frac{Tr^{\alpha}}{SNR}} e^{-\pi\lambda r^2 \int_1^{\infty}\left[1-\frac{1}{1+Tt^{-\alpha/2}}\right]dt} \\ =& e^{-\frac{Tr^{\alpha}}{SNR}} \mathscr{L}_{I_{\theta}^{(oc)}}(T,\lambda) \end{aligned} \tag{A.2}$$

in which $\mathscr{L}_{I_{\theta}^{(oc)}}(T,\lambda) = e^{-\pi\lambda r^2 \int_1^{\infty}\left[1-\frac{1}{1+Tt^{-\alpha/2}}\right]dt}$.

The CCU classification probability is defined as the following equation

$$\begin{aligned} A^{(c)}(T,\epsilon) &= \int_0^{\infty} A_{Str}^{(c)}(T,\epsilon|r) f_R(r) dr \\ &= \int_0^{\infty} 2\pi\lambda r e^{-\pi\lambda r^2 - \frac{T}{SNR} r^{\alpha}} \mathscr{L}_{I_{\theta}^{(oc)}}(T,\lambda) dr \end{aligned} \tag{A.3}$$

Approximate the analytical results The integral $I = \int_1^{\infty} \frac{Tt^{-\alpha}}{1+Tt^{-\alpha}} dt$ can be separated into two integrals

$$I = \int_0^{\infty} \frac{Tt^{-\alpha}}{1+Tt^{-\alpha}} dt - \int_0^{1} \frac{Tt^{-\alpha}}{1+Tt^{-\alpha}} dt \tag{A.4}$$

The first integral is evaluated using the properties of Gamma function [74] and the second one is approximated by employing Gauss-Legendre Quadrature [75]. Hence,

$$I \approx \frac{2}{\alpha} \frac{\pi T^{\frac{2}{\alpha}}}{\sin\left(\frac{2\pi}{\alpha}\right)} - \sum_{n=1}^{N_G} \frac{c_n}{2} \frac{T}{T + \left(\frac{x_n+1}{2}\right)^{\alpha/2}} \tag{A.5}$$

where N_G is the degree of the Legendre polynomial; c_n and x_n are the n-th weight and abscissas and of the quadrature. Consequently, we obtain

$$\mathscr{L}_{I_{\theta}^{(oc)}}(T,\lambda) \approx e^{-\pi\lambda r^2 \left[\frac{2}{\alpha} \frac{\pi T^{\frac{2}{\alpha}}}{\sin\left(\frac{2\pi}{\alpha}\right)} - \sum_{n_G=1}^{N_{GL}} \frac{c_{n_G}}{2} \frac{T}{T+\left(\frac{x_{n_{GL}}+1}{2}\right)^{\alpha/2}}\right]} \tag{A.6}$$

Employing a change of variable $\zeta = \pi\lambda r^2$, the average probability can be re-written in the following equation

$$A^{(c)}(T,\epsilon) = \int_0^\infty e^{-\zeta - \frac{T}{SNR}\left(\frac{\zeta}{2\pi\lambda}\right)^{\alpha/2}} \mathscr{L}_{I_\theta^{(oc)}}(T,\lambda | r = \sqrt{\frac{\zeta}{\pi\lambda}}) dr \tag{A.7}$$

This equation has a suitable form of Gauss-Laguerre, and can be approximated by

$$A^{(c)}(T,\epsilon) \approx \sum_{j=1}^{N_{GL}} \omega_j e^{-\frac{T}{SNR}\zeta_j^\alpha} \mathscr{L}^{(j)}_{I_\theta^{(oc)}}(T,\lambda) \tag{A.8}$$

where N_{GL} is the degree of the Laguerre polynomial, t_j and w_j node and weight of the quadrature; $\zeta_j = \sqrt{\frac{t_j}{\pi\lambda}}$; $\mathscr{L}^{(j)}_{I_\theta^{(oc)}}(T,\lambda)$ is approximated value at point j of $\mathscr{L}_{I_\theta^{(oc)}}(T,\lambda)$.

$$\mathscr{L}^{(j)}_{I_\theta^{(oc)}}(T,\lambda) \approx e^{-\pi\lambda\zeta_j^2\left[\frac{2}{\alpha}\frac{\pi T^{\frac{2}{\alpha}}}{\sin\left(\frac{2\pi}{\alpha}\right)} - \sum\limits_{n=1}^{N_G}\frac{c_n}{2}\frac{T}{T+\left(\frac{x_n+1}{2}\right)^{\alpha/2}}\right]} \tag{A.9}$$

Hence, the Lemma 2.1.3.1 is proved by using the results in Equation A.3 and Equation A.8.

A.2 Theorem 2.2.2.2 - CCU under Strict FR

The coverage probability of a CCU under the Strict FR networks is obtained by

$$\begin{aligned}\mathcal{P}^{(c)}_{Str}(T,\epsilon) &= \frac{\mathbb{P}\left(\frac{P^{(c)}gr^{-\alpha}}{\sigma^2+I^{(c)}_{Str}} > \hat{T}, \frac{P^{(c)}g^{(o)}r^{-\alpha}}{\sigma^2+I^{(oc)}_{Str}} > T\right)}{\mathbb{P}\left(\frac{Pgr^{-\alpha}}{\sigma^2+I^{(oc)}_{Str}} > T\right)} \\ &= \frac{\int_0^\infty re^{-\pi\lambda r^2} e^{-\frac{(T+\hat{T})\sigma^2}{P^{(c)}r^{-\alpha}}} \mathbb{E}\left[e^{-\frac{\hat{T}I^{(c)}_{Str}}{P^{(c)}r^{-\alpha}} - \frac{TI^{(oc)}_{Str}}{P^{(c)}r^{-\alpha}}}\right] dr}{\int_0^\infty re^{-\pi\lambda r^2}\left(e^{-\frac{T\sigma^2}{P^{(c)}r^{-\alpha}}}\mathbb{E}\left[-\frac{TI^{(oc)}_{Str}}{P^{(c)}r^{-\alpha}}dr\right]\right)dr}\end{aligned} \tag{A.10}$$

The expectation in the numerator of (A.10) is the joint Laplace transform of interference during the establishment $I^{(oc)}_{Str}$ and communication phase $I^{(c)}_{Str}$, denoted by

$\mathscr{L}(T, \hat{T}, \lambda)$ and jointly evaluated at T and $\hat{T}$.

$$\begin{aligned}\mathscr{L}(T, \hat{T}, \lambda) &= \mathbb{E}\left[e^{-T\sum_{j\in\theta} r^{\alpha} g_{jz} r_{jz}^{-\alpha} - \hat{T}\sum_{j\in\theta_{Str}^{(c)}} r^{\alpha} g_{jz}^{(o)} r_{jz}^{-\alpha}}\right] \\ &= \prod_{j\in\theta} \mathbb{E}\left[\frac{1}{1+Tr^{\alpha}r_{jz}^{-\alpha}} \frac{1}{1+\hat{T}r^{\alpha}r_{jz}^{-\alpha}}\right] \qquad \text{(A.11)}\end{aligned}$$

in which (A.11) due to the assumption that all channel gains are independent Rayleigh fading.

Employing the properties of PGF and the change of variable $x = (r_{jz}/r)^2$, Equation (A.11) becomes

$$\mathscr{L}(T, \hat{T}, \lambda) = e^{-\pi\lambda r^2 \int_1^{\infty}\left[1 - \frac{1}{\left(1+Tx^{-\alpha/2}\right)\left(1+\hat{T}x^{-\alpha/2}\right)} dt\right] dx} \qquad \text{(A.12)}$$

Approximate $\mathscr{L}(T, \hat{T}, \lambda)$ Denote $\upsilon(T, \hat{T}, \lambda)$ as the integral of the exponent in the joint Laplace transform, hence

$$\upsilon(T, \hat{T}, \lambda) = \int_1^{\infty} \frac{\left(T + \hat{T} + T\hat{T}x^{-\frac{\alpha}{2}}\right) x^{-\frac{\alpha}{2}}}{\left(1 + Tx^{-\frac{\alpha}{2}}\right)\left(1 + \hat{T}x^{-\frac{\alpha}{2}}\right)} dx$$

The integral can be presented as the result of the abstraction between into integrals $I_0(t)$ and $I_1(t)$ which are defined on intervals $[0, \infty]$ and $[0, 1]$, respectively.

In order to evaluate $I_0(t)$, a change of variable $\gamma = x^{-\frac{\alpha}{2}}$ is employed, and in case of $\hat{T} \neq T$, we obtained

$$I_0(t) = \frac{2}{\alpha} \frac{1}{T - \hat{T}} \int_0^{\infty} \left[\frac{T^2 \gamma^{-\frac{2}{\gamma}}}{1 + T\gamma} - \frac{\hat{T}^2 \gamma^{-\frac{2}{\gamma}}}{1 + \hat{T}\gamma}\right] d\gamma$$

The integral can be separated into two integrals which are evaluated by employing changes of variables $\gamma_1 = T\gamma$ and $\gamma_2 = \hat{T}\gamma$, and following the properties of Gamma

function. Consequently, $I_0(t)$ is given by

$$I_0(t) = \frac{2}{\alpha}\frac{T^{1+\frac{2}{\alpha}} - \hat{T}^{1+\frac{2}{\alpha}}}{T-\hat{T}}\frac{\pi}{\sin\left(\frac{2\pi}{\alpha}\right)} \tag{A.13}$$

The integral $I_1(t)$ is approximated by using Gauss - Legendre approximation

$$I_1(t) = \sum_{i=1}^{N_G}\frac{ci}{2}\frac{\left(T+\hat{T}\right)\left(\frac{x_n+1}{2}\right)^{\frac{\alpha}{2}} + T\hat{T}t^{\alpha}}{\left(\left(\frac{x_n+1}{2}\right)^{\frac{\alpha}{2}}+T\right)\left(\left(\frac{x_n+1}{2}\right)^{\frac{\alpha}{2}}+\hat{T}\right)} \tag{A.14}$$

Consequently, using the properties of Gauss - Laguerre Quadrature, $\upsilon(T,\hat{T},\lambda)$ is approximated by

$$\upsilon(T,\hat{T},\lambda) = \sum_{j=1}^{N_{GL}}\frac{w_j}{2}\left(I_0(\zeta_j) - I_1(\zeta_j)\right) \tag{A.15}$$

Approximate Average Coverage Probability of the CCU The average coverage probability expression in Equation 2.18 has a suitable form of Gauss - Laguerre. Thus, it can be approximated by

$$\mathcal{P}^{(c)}_{Str}(T,\epsilon) \approx \frac{\sum_{j=1}^{N_{GL}} w_j e^{-\frac{(T+\hat{T})}{SNR}\zeta_j^{\alpha}}\mathscr{L}^{(i)}\left(\hat{T},T,\lambda\right)}{\sum_{j=1}^{N_{GL}} w_j e^{-\frac{T}{SNR}\zeta_j^{\alpha}}\mathscr{L}^{(i)}_{I^{(oc)}_{Str}}(T,\lambda)} \tag{A.16}$$

The Theorem 2.2.2.1 is proved.

A.3 Theorem 2.2.2.1 - CEU under Strict FR

The coverage probability of a CCU under the Strict FR networks is obtained based on approach in [39] given that the density of interfering BSs is λ during

establishment phase and λ/Δ during communication phase. Hence,

$$\begin{aligned}\mathcal{P}^{(e)}_{Sof}(T,\epsilon) =& \frac{\mathbb{P}\left(\frac{P^{(e)}gr^{-\alpha}}{\sigma^2+I^{(e)}_{Str}} > \hat{T}, \frac{P^{(c)}g^{(o)}r^{-\alpha}}{\sigma^2+I^{(oc)}_{Str}} < T\right)}{\mathbb{P}\left(\frac{Pgr^{-\alpha}}{\sigma^2+I^{(oc)}_{Str}} < T\right)} \\ =& \frac{\int_0^\infty 2\pi\lambda r e^{-\pi\lambda r^2}\mathbb{E}\left[e^{-\frac{\hat{T}\left(\sigma^2+I^{(e)}_{Str}\right)}{P^{(e)}r^{-\alpha}}}\left(1-e^{-\frac{T\left(\sigma^2+I^{(oc)}_{Str}\right)}{P^{(c)}r^{-\alpha}}}\right)\right]dr}{1-\int_0^\infty 2\pi\lambda r e^{-\pi\lambda r^2}e^{-\frac{T\sigma^2}{P^{(c)}r^{-\alpha}}}\mathbb{E}\left[-\frac{TI^{(oc)}_{Str}}{P^{(c)}r^{-\alpha}}dr\right]dr}\end{aligned} \tag{A.17}$$

The expected value of the numerator can be separated into two expectations in which the first one is evaluated using the same approach as in Appendix A.1, i.e, $\mathbb{E}\left[e^{-\frac{\hat{T}}{\phi P}\left(I^{(e)}_{Str}+\sigma^2\right)r^\alpha}\right] = e^{-\frac{\hat{T}r^\alpha}{\phi SNR}}\mathscr{L}_{I^{(oc)}_{Str}}(\hat{T},\frac{\lambda}{\Delta})$, and the second one,
i.e. $E_2 = \mathbb{E}\left[e^{-\frac{\hat{T}I^{(e)}_{Str}}{P^{(e)}r^{-\alpha}}}e^{-\frac{TI^{(oc)}_{Str}}{P^{(c)}r^{-\alpha}}}\right]$ can be computed based on the following steps

$$\begin{aligned}E_2 &= \mathbb{E}\left[e^{-\hat{T}\sum_{j\in\theta^{(e)}_{Str}} r^{-\alpha}_{je}r^\alpha g_{je}}e^{-T\sum_{j\in\theta_{Str}} r^{-\alpha}_{jc}r^\alpha g^{(o)}_{jc}}\right] \\ &= \mathbb{E}\left[\prod_{j\in\theta^{(e)}_{Str}} e^{-\hat{T}r^{-\alpha}_{je}r^\alpha g_{je}}\prod_{j\in\theta_{Str}} e^{-Tr^{-\alpha}_{jc}r^\alpha g^{(o)}_{jc}}\right] \\ &= \mathbb{E}\left[\prod_{j\in\theta^{(e)}_{Str}}\frac{1}{1+Tr^{-\alpha}_{je}r^\alpha}\frac{1}{1+\hat{T}r^{-\alpha}_{je}r^\alpha}\prod_{j\in\theta_{Str}\setminus\theta^{(e)}_{Str}}\frac{1}{1+Tr^{-\alpha}_{jc}r^\alpha}\right]\end{aligned}$$

Since $\theta^{(e)}_{Str}$ and $\theta^{(c)}_{Str}$ are independent Poisson Process, and employing the properties of PGF and Property 3 of Soft FR, the expectation equals

$$\begin{aligned}&= e^{-\frac{2\pi\lambda}{\Delta}\int_r^\infty\left[1-\frac{1}{1+Tr^{-\alpha}_{je}r^\alpha}\frac{1}{1+\hat{T}r^{-\alpha}_{je}r^\alpha}\right]r_{je}dr_{je}}e^{-\frac{2\pi\lambda(\Delta-1)}{\Delta}\int_r^\infty\left[1-\frac{1}{1+Tr^{-\alpha}_{jc}r^\alpha}\right]r_{jc}dr_{jc}} \\ &= e^{-\frac{2\pi\lambda r^2}{\Delta}\int_1^\infty\left[1-\frac{1}{1+Tt^{-\alpha/2}}\frac{1}{1+\hat{T}t^{-\alpha/2}}\right]dt}e^{-\frac{2\pi\lambda(\Delta-1)r^2}{\Delta}\int_1^\infty\left[1-\frac{1}{1+Tt^{-\alpha/2}}\right]dt}\end{aligned} \tag{A.18}$$

in which Equation A.18 follows changes of variable $t = (r_{je}/r)^2$ for the first integral and $t = (r_{jc}/r)^2$ for the second integral.

Substituting Equation A.17 into Equation A.18, Equation 2.22 is proved.

In the case of $\hat{T} \neq T$, we obtain

$$\begin{aligned}
&= e^{-\frac{\pi\lambda}{\Delta} r^2 \frac{\hat{T}}{\hat{T}-T} \int_1^\infty \left[\frac{\hat{T}t^{-\alpha/2}}{1+\hat{T}t^{-\alpha/2}} - \frac{Tt^{-\alpha/2}}{1+Tt^{-\alpha/2}} \right] dt} e^{-\pi\lambda r^2 \int_1^\infty \frac{Tt^{-\alpha/2}}{1+Tt^{-\alpha/2}} dt} \\
&= e^{-\left(\lambda - \frac{\hat{T}\lambda}{\Delta(\hat{T}-T)}\right)\pi r^2 \int_1^\infty \frac{Tt^{-\alpha/2}}{1+Tt^{-\alpha/2}} dt} e^{-\frac{\hat{T}\lambda}{\Delta(\hat{T}-T)}\pi r^2 \int_1^\infty \frac{t^{-\alpha/2}}{1+\hat{T}t^{-\alpha/2}} dt} \\
&= \mathscr{L}_{I_\theta^{(oc)}}\left(T, \lambda - \frac{\hat{T}\lambda}{\Delta(\hat{T}-T)}\right) \mathscr{L}_{I_\theta^{(oc)}}\left(\hat{T}, \frac{\hat{T}\lambda}{\Delta(\hat{T}-T)}\right) \qquad \text{(A.19)}
\end{aligned}$$

in which $\mathscr{L}_{I_\theta^{(oc)}}(T,\lambda) = e^{-\pi\lambda r^2 \int_1^\infty \left[1 - \frac{1}{1+Tt^{-\alpha/2}}\right] dt}$

By substituting Equation A.19 into Equation A.18 and employing the approximation approach in Appendix A.1, the Theorem 2.2.2.2 is proved.

A.4 Theorem 2.2.2.3 - CCU under Soft FR

The average coverage probability of the CCU under Soft FR is given by

$$\begin{aligned}
\mathcal{P}_c^{(c)}(T,\epsilon) &= \frac{\mathbb{P}\left(\frac{P^{(c)} g r^{-\alpha}}{\sigma^2 + I_{Sof}^{(c)}} > \hat{T}, \frac{P^{(c)} g^{(o)} r^{-\alpha}}{\sigma^2 + I_{Sof}^{(oc)}} > T\right)}{\mathbb{P}\left(\frac{P g r^{-\alpha}}{\sigma^2 + I_{Sof}^{(oc)}} > T\right)} \\
&= \frac{\int_0^\infty r e^{-\pi\lambda r^2} e^{-\frac{(T+\hat{T})\sigma^2}{P^{(c)} r^{-\alpha}}} \mathbb{E}\left[e^{-\frac{\hat{T} I_{Sof}^{(c)}}{P^{(c)} r^{-\alpha}} - \frac{T I_{Sof}^{(oc)}}{P^{(c)} r^{-\alpha}}} \right] dr}{\int_0^\infty r e^{-\pi\lambda r^2} \left(e^{-\frac{T\sigma^2}{P^{(c)} r^{-\alpha}}} \mathbb{E}\left[-\frac{T I_{Sof}^{(oc)}}{P^{(c)} r^{-\alpha}} dr \right] \right) dr} \qquad \text{(A.20)}
\end{aligned}$$

The expectation of the numerator in (A.20) is the joint Laplace transform $\mathscr{L}_{Sof}(T,\hat{T})$ of interferences during the establishment phase communication phase. By separating the set of interfering BSs during the establishment phase, θ_{Sof}, into $\theta_{Sof}^{(e)}$ and $\theta_{Sof}^{(c)}$ and using the definition of $I_{Sof}^{(z)}$ in Equation (2.9),

$$\mathscr{L}_{Sof}(T,\hat{T}) = = \mathbb{E}\left[e^{-\sum_{j\in\theta_{Sof}^{(c)}} \left(\hat{T} r^\alpha r_{jz}^{-\alpha} g_{jz} + T r^\alpha r_{jz}^{-\alpha} g_{jz}^{(o)} \right) - \sum_{j\in\theta_{Sof}^{(e)}} \left(\phi\hat{T} r^\alpha r_{jz}^{-\alpha} g_{jz} + T r^\alpha g_{jz} r_{jz}^{-\alpha} g_{jz}^{(o)} \right)} \right]$$

Since each BS in $\theta_{Sof}^{(c)}$ is distributed independently to any BS in $\theta_{Sof}^{(e)}$ and all channels are independent Rayleigh fading channels, $\mathscr{L}_{Sof}(\hat{T}, T) =$

$$\prod_{j\in\theta_{Sof}^{(c)}} \mathbb{E}\left[e^{-\left(\hat{T}r^{\alpha}r_{jz}^{-\alpha}g_{jz}+Tr^{\alpha}r_{jz}^{-\alpha}g_{jz}^{(o)}\right)}\right] \prod_{j\in\theta_{Sof}^{(e)}} \mathbb{E}\left[e^{-\left(\phi\hat{T}r^{\alpha}r_{jz}^{-\alpha}g_{jz}+Tr^{\alpha}r_{jz}^{-\alpha}g_{jz}^{(o)}\right)}\right]$$

$$= \prod_{j\in\theta_{Sof}^{(c)}} \mathbb{E}\left[\frac{1}{1+\hat{T}r^{\alpha}r_{jz}^{-\alpha}}\frac{1}{1+Tr^{\alpha}r_{jz}^{-\alpha}}\right] \prod_{j\in\theta_{Sof}^{(e)}} \mathbb{E}\left[\frac{1}{1+\phi\hat{T}r^{\alpha}r_{jz}^{-\alpha}}\frac{1}{1+Tr^{\alpha}r_{jz}^{-\alpha}}\right]$$

Given that r is the distance from user z to interfering BS j, whose PDF follows Equation (2.1), and using the properties of PGF with respect to variable r_{jz} over $\theta_{Sof}^{(c)}$ and $\theta_{Sof}^{(e)}$, the joint Laplace transform $\mathscr{L}_{Sof}(\hat{T}, T)$ is given by

$$\begin{aligned}
&= e^{-\frac{2\pi(\Delta-1)}{\Delta}\lambda\int_r^{\infty}\left[1-\frac{1}{\left(1+\hat{T}r^{\alpha}r_{jz}^{-\alpha}\right)\left(1+Tr^{\alpha}r_{jz}^{-\alpha}\right)}\right]r_{jz}d(r_{jz})} \\
&\qquad\qquad e^{-\frac{2\pi}{\Delta}\lambda\int_r^{\infty}\left[1-\frac{1}{\left(1+\phi\hat{T}r^{\alpha}r_{jz}^{-\alpha}\right)\left(1+Tr^{\alpha}r_{jz}^{-\alpha}\right)}\right]r_{jz}d(r_{jz})} \\
&= \mathscr{L}(T, \hat{T}, \frac{\Delta-1}{\Delta}\lambda)\mathscr{L}(T, \phi\hat{T}, \frac{\lambda}{\Delta}) \qquad \text{(A.21)}
\end{aligned}$$

By substituting Equation (A.21) into Equation (A.20) and remind that the denominator is given by Appendix A.1, the Theorem 2.2.2.4 is proved.

The approximated value of the average coverage probability is obtained by using a change of variable $\zeta = \pi\lambda r^2$ and Gauss-Laguerre Quadrature.

Appendix B

Appendices of Chapter 3

B.1 Lemma 3.1.2.2 - CCU classification probability

The probability in which the user is served as a CCU is given by

$$A_{Str}^{(c)}(T,\epsilon|r) = \mathbb{P}\left(\frac{Pgr^{\alpha(\epsilon-1)}}{\sigma^2 + I_{Sof}^{(c)}(\phi)} > T\right) \tag{B.1}$$

in which $I_{Sof}^{(c)}(\phi)$ is defined in Equation (3.3).

Since g has a exponential distribution, we have

$$\begin{aligned}
A_{Str}^{(c)}(T,\epsilon|r) &= e^{-\frac{Tr^{\alpha(1-\epsilon)}}{SNR}}\mathbb{E}\left[e^{-\frac{T}{Pr^{\alpha(\epsilon-1)}}\left[\sum_{j\in\theta_{Sof}^{(c)}} P_j^{(c)} g_{jz} d_{jz}^{-\alpha} + \sum_{j\in\theta_{Sof}^{(e)}} P_j^{(e)} g_{jz} d_{jz}^{-\alpha}\right]}\right] \\
&\overset{(a)}{=} e^{-\frac{Tr^{\alpha(1-\epsilon)}}{SNR}} \prod_{j\in\theta_{Sof}^{(c)}} \mathbb{E}\left[e^{-s' r_j^{\alpha\epsilon} d_{jz}^{-\alpha} g_{jz}}\right] \prod_{j\in\theta_{Sof}^{(e)}} \mathbb{E}\left[e^{-\phi s' r_j^{\alpha\epsilon} d_{jz}^{-\alpha} g_{jz}}\right] \\
&\overset{(b)}{=} e^{-\frac{Tr^{\alpha(1-\epsilon)}}{SNR}} \prod_{j\in\theta_{Sof}^{(c)}} \mathbb{E}\left[\frac{1}{1+s' r_j^{\alpha\epsilon} d_{jz}^{-\alpha}}\right] \prod_{j\in\theta_{Sof}^{(e)}} \mathbb{E}\left[\frac{1}{1+\phi s' r_j^{\alpha\epsilon} d_{jz}^{-\alpha}}\right]
\end{aligned}$$

in which (a) due to the independence of $\theta_{Sof}^{(c)}$ and $\theta_{Sof}^{(e)}$, and $s' = Tr^{\alpha(1-\epsilon)}$; (b) follows the assumption that the channel gain has a Rayleigh distribution.

Since r_j is the distance from user j to it's serving BS, the PDF of r_j follows (2.1). Taking the expectation on r_j, we obtain

$$A_{Str}^{(c)}(T,\epsilon|r) = e^{-\frac{Tr^{\alpha(1-\epsilon)}}{SNR}} \prod_{j\in\theta_{Sof}^{(c)}} \mathbb{E}\left[\int_0^\infty \frac{\frac{2\pi(\Delta-1)\lambda}{\Delta} t e^{-\frac{\pi(\Delta-1)\lambda}{\Delta}t^2}}{1+s' r_j^{\alpha\epsilon} d_{jz}^{-\alpha}} dt\right] \prod_{j\in\theta_{Sof}^{(e)}} \mathbb{E}\left[\int_0^\infty \frac{\frac{2\pi\lambda t}{\Delta} e^{-\frac{\pi\lambda}{\Delta}t^2}}{1+\phi s' r_j^{\alpha\epsilon} d_{jz}^{-\alpha}} dt\right]$$

By using the properties of PGF and property 3 of Soft FR, then

$$A_{Str}^{(c)}(T,\epsilon|r) = e^{-\frac{Tr^{\alpha(1-\epsilon)}}{SNR}} e^{-\frac{2\pi(\Delta-1)\lambda}{\Delta}\left[1-\int_0^\infty \frac{\frac{2\pi(\Delta-1)\lambda}{\Delta} t e^{-\frac{\pi(\Delta-1)\lambda}{\Delta}t^2}}{1+s' r_j^{\alpha\epsilon} d_{jz}^{-\alpha}} dt\right] d_{jz} d(d_{jz})} e^{-\frac{2\pi\lambda}{\Delta}\left[1-\int_0^\infty \frac{\frac{2\pi\lambda t}{\Delta} e^{-\frac{\pi\lambda}{\Delta}t^2}}{1+\phi s' r_j^{\alpha\epsilon} d_{jz}^{-\alpha}} dt\right] d_{jz} d(d_{jz})}$$

By letting $s_1 = Tr^{\alpha\epsilon}$, and using the change of variable $x = \frac{d_{jz}}{r}$,

$$A_{Str}^{(c)}(T,\epsilon|r) = e^{-\frac{Tr^{\alpha(1-\epsilon)}}{SNR}} \mathscr{L}_{I_\theta^{(oc)}}(s_1, \frac{\Delta-1}{\Delta}\lambda) \mathscr{L}_{I_\theta^{(oc)}}(\phi s_1, \frac{1}{\Delta}\lambda) \tag{B.2}$$

The Lemma 3.1.2.2 is proved.

Approximate Results in Lemma 3.1.2.1 and Lemma 3.1.2.2

Approximate $\mathscr{L}_{I_\theta^{(oc)}}(s,\lambda)$ Due to the fact that $\int_0^\infty \pi\lambda t e^{-\pi\lambda t^2} dt = 1$, the integral in $\mathscr{L}_{I_\theta^{(oc)}}(s)$, denoted by $f(s,\lambda)$, can be obtained by

$$f(s,\lambda) = \int_0^\infty \pi\lambda t^{\alpha\epsilon} t e^{-\pi\lambda t^2} \int_1^\infty \frac{s x^{1-\alpha}}{1+s t^{\alpha\epsilon} x^{-\alpha}} dx dt$$

Employing the change of variable $\gamma = s x^{-\alpha} t^{\alpha\epsilon}$, then $f(s,\lambda) =$

$$\int_0^\infty \frac{\pi\lambda s^{\frac{2}{\alpha}}}{\alpha} t^\epsilon t e^{-\pi\lambda t^2} \int_0^\infty \frac{\gamma^{-2/\alpha}}{1+\gamma} d\gamma dt - \int_0^\infty \frac{\pi\lambda s}{2} t^{\alpha\epsilon} t e^{-\pi\lambda t^2} \int_0^1 \frac{1}{x^{\frac{\alpha}{2}} + s t^{\alpha\epsilon}} dx dt$$

In case of $\alpha > 2$, according to the properties of Gamma function [74], $\int_0^\infty \frac{\gamma^{-2/\alpha}}{1+\gamma} d\gamma = \frac{\pi}{\sin\left(\frac{2\pi}{\alpha}\right)}$. Employing Gauss - Legendre approximation for $\int_0^1 \frac{1}{x^{\frac{\alpha}{2}} + st^{\alpha\epsilon}} dx$, thus

$$f(s,\lambda) \approx \frac{\pi s^{\frac{2}{\alpha}}}{\alpha \sin\left(\frac{2\pi}{\alpha}\right)} \int_0^\infty t^\epsilon \pi\lambda t e^{-\pi\lambda t^2} dt - \frac{s}{4} \int_0^\infty \sum_{i=0}^{N_G} \frac{c_i t^{\alpha\epsilon} \pi\lambda t e^{-\pi\lambda t^2}}{\eta_i^{\frac{\alpha}{2}} + st^{\alpha\epsilon}} dt$$

in which $\eta_i = \frac{x_i+1}{2}$.

Using a change of variable $\zeta = \pi\lambda t^2$, the integral has a suitable form of Gauss - Laguerre Quadrature. Hence, $f(s,\lambda)$ is approximated by

$$f(s,\lambda) \approx \frac{\pi s^{\frac{2}{\alpha}}}{\alpha \sin\left(\frac{2\pi}{\alpha}\right)} \sum_{m=0}^{N_{GL}} w_m \zeta_m^\epsilon - \frac{s}{4} \sum_{j=0}^{N_{GL}} w_j \zeta_m^{\alpha\epsilon} \sum_{i=0}^{N_G} \frac{c_i}{\eta_i^{\frac{\alpha}{2}} + s\zeta_m^{\frac{\alpha\epsilon}{2}}} \tag{B.3}$$

in which $\zeta_m = \sqrt{\frac{t_m}{\pi\lambda}}$ $(\forall 1 \le m \le N_{GL})$.

Approximate $A_{Str}^{(c)}(T,\epsilon)$ Employing a change of variable $t = \pi\lambda r^2$, then $A_{Str}^{(c)}(T,\epsilon)$ equals

$$A_{Str}^{(c)}(T,\epsilon) \approx \int_0^\infty e^{-t - \frac{T}{SNR}\left(\frac{t}{\pi\lambda}\right)^{\alpha(1-\epsilon)/2}} \mathscr{L}_{I_\theta^{(oc)}}\left(T\left(t/\pi\lambda\right)^{-\alpha\epsilon/2}, \lambda\right) d\zeta \tag{B.4}$$

Using the Gauss - Laguerre Quadrature, $A_{Str}^{(c)}(T,\epsilon)$ is approximately obtained by

$$A_{Str}^{(c)}(T,\epsilon) = \sum_{j=0}^{N_{GL}} w_j e^{-\frac{T}{SNR}\zeta_j^{\alpha(1-\epsilon)}} \mathscr{L}_{I_\theta^{(oc)}}^{(j)}\left(T\zeta_j^{-\alpha\epsilon}, \lambda\right) \tag{B.5}$$

in which $\mathscr{L}_{I_\theta^{(oc)}}^{(j)}(s,\lambda) \approx e^{\pi\lambda\zeta_j\left[\frac{2\pi s^{\frac{2}{\alpha}}}{\alpha\sin\left(\frac{2\pi}{\alpha}\right)} \sum_{m=0}^{N_{GL}} w_j\zeta_m^\epsilon - \frac{s}{2}\sum_{m=0}^{N_{GL}} w_m\zeta_m^{\alpha\epsilon} \sum_{i=0}^{N_G} \frac{c_i}{\eta_i^{\frac{\alpha}{2}} + s\zeta_m^{\frac{\alpha\epsilon}{2}}}\right]}$

Approximate $A_{Sof}^{(c)}(T,\epsilon)$ Similarity, $A_{Sof}^{(c)}(T,\epsilon)$ is approximated by

$$A_{Sof}^{(c)}(T,\epsilon) = \sum_{j=0}^{\infty} w_j e^{-\frac{T}{SNR}\zeta_j^{\alpha(1-\epsilon)}} \mathscr{L}_{I_\theta^{(oc)}}^{(j)}\left(T\zeta_j^{-\alpha\epsilon}, \frac{\Delta-1}{\Delta}\lambda\right) \mathscr{L}_{I_\theta^{(oc)}}^{(j)}\left(\phi T\zeta_j^{-\alpha\epsilon}, \frac{1}{\Delta}\lambda\right) \tag{B.6}$$

The Proposition 3.1.2.3 is proved.

B.2 Theorem 3.2.1.1 - CCU under Strict FR

The coverage probability of a CCU under the Strict FR networks is obtained by

$$\begin{aligned}\mathcal{P}_c^{(c)}(T,\epsilon) =& \frac{\mathbb{P}\left(\frac{P^{(c)}gr^{-\alpha}}{\sigma^2+I_{Str}^{(c)}(\phi)} > \hat{T}, \frac{P^{(c)}g^{(o)}r^{-\alpha}}{\sigma^2+I_{Str}^{(oc)}(\phi)} > T\right)}{\mathbb{P}\left(\frac{Pgr^{\alpha(\epsilon-1)}}{\sigma^2+I_{Str}^{(oc)}(\phi)} > T\right)} \\ &= \frac{\int_0^\infty re^{-\pi\lambda r^2} e^{-\frac{(T+\hat{T})\sigma^2}{P^{(c)}r^{-\alpha}}} \mathbb{E}\left[e^{-\frac{\hat{T}I_{Str}^{(c)}}{P^{(c)}r^{-\alpha}} - \frac{TI_{Str}^{(oc)}}{P^{(c)}r^{-\alpha}}}\right] dr}{\int_0^\infty re^{-\pi\lambda r^2}\left(e^{-\frac{T\sigma^2}{P^{(c)}r^{-\alpha}}}\mathbb{E}\left[-\frac{TI_{Str}^{(oc)}}{P^{(c)}r^{-\alpha}}dr\right]\right)dr}\end{aligned} \tag{B.7}$$

The expectation in the numerator of Equation B.7 is the joint Laplace transform of $I_{Str}^{(oc)}$ and $I_{Str}^{(c)}$ denoted by $\mathscr{L}(s_1', s_2', \lambda)$ and jointly evaluated at $s_1' = Tr^{\alpha(1-\epsilon)}$ and $s_2' = \hat{T}r^{\alpha(1-\epsilon)}$

$$\begin{aligned}\mathscr{L}(s_1', s_2', \lambda) &= \mathbb{E}\left[e^{-s_1'\sum_{j\in\theta} r_j^{\alpha\epsilon} g_{jz} d_{jz}^{-\alpha} - s_2'\sum_{j\in\theta_{Str}^{(c)}} r_j^{\alpha\epsilon} g_{jz}^{(o)} d_{jz}^{-\alpha}}\right] \\ &= \prod_{j\in\theta}\mathbb{E}\left[\frac{1}{1+s_1' r_j^{\alpha\epsilon} d_{jz}^{-\alpha}}\frac{1}{1+s_2' r_j^{\alpha\epsilon} d_{jz}^{-\alpha}}\right]\end{aligned} \tag{B.8}$$

in which Equation B.8 due to the assumption that all channel gains are independent Rayleigh fading.

Since r_j is the distance from user j to its serving BS, the PDF of r_j follows Equation 2.1. Taking the expectation on r_j, we obtain

$$\mathscr{L}(s_1', s_2', \lambda) = \prod_{j\in\theta}\mathbb{E}\left[\int_0^\infty \frac{2\pi\lambda t e^{-\pi\lambda t^2}}{\left(1+s_1' t^{\alpha\epsilon} d_{jz}^{-\alpha}\right)\left(1+s_2' t^{\alpha\epsilon} d_{jz}^{-\alpha}\right)} dt\right] \tag{B.9}$$

Given that d_{jz} is the distance from the interfering user j to the serving BS of user z and the density of the interfering users is as same as the BSs' density, using the

properties of PGF , Equation B.9 becomes

$$= e^{-2\pi\lambda \int_r^\infty \left[1-\int_0^\infty \frac{2\pi\lambda t e^{-\pi\lambda t^2}}{\left(1+s_1' t^{\alpha\epsilon} d_{jz}^{-\alpha}\right)\left(1+s_2' t^{\alpha\epsilon} d_{jz}^{-\alpha}\right)} dt\right] d_{jz} d(d_{jz})} \tag{B.10}$$

By letting $s_1 = Tr^{\alpha\epsilon}$ and $s_2 = \hat{T}r^{\alpha\epsilon}$, and using the change of variable $x = \frac{d_{jz}}{r}$, the joint Laplace transform $\mathscr{L}(s_1, s_2, \lambda) =$

$$e^{-2\pi\lambda r^2 \int_1^\infty \left[1-\int_0^\infty \frac{\pi\lambda t e^{-\pi\lambda t^2}}{(1+s_1 t^{\alpha\epsilon} x^{-\alpha})(1+s_2 t^{\alpha\epsilon} x^{-\alpha})} dt\right] x dx} \tag{B.11}$$

By substituting Equation 3.9 and Equation B.11 into Equation B.7, the Theorem 3.2.1.1 is proved.

Approximate the result in Theorem 3.2.1.1

Approximate $\mathscr{L}(s_1, s_2, \lambda)$ Since $\int_0^\infty \pi\lambda t e^{-\pi\lambda t^2} dt = 1$ and denote $\upsilon(s_1, s_2, \lambda)$ as the integral of the exponent in the joint Laplace transform, we have

$$\upsilon(s_1, s_2, \lambda) = \int_0^\infty \frac{\pi\lambda t e^{-\pi\lambda t^2}}{2} \int_1^\infty \frac{\left(s_1 + s_2 + s_1 s_2 t^{\alpha\epsilon} x^{-\frac{\alpha}{2}}\right) t^{\alpha\epsilon} x^{-\frac{\alpha}{2}}}{\left(1 + s_1 t^{\alpha\epsilon} x^{-\frac{\alpha}{2}}\right)\left(1 + s_2 t^{\alpha\epsilon} x^{-\frac{\alpha}{2}}\right)} dx dt \tag{B.12}$$

The inner integral can be presented as the result of the abstraction between into two integrals $I_0(t)$ and $I_1(t)$ which are defined on intervals $[0, \infty]$ and $[0, 1]$, respectively.

In order to evaluate $I_0(t)$, a change of variable $\gamma = t^{\alpha\epsilon} x^{-\frac{\alpha}{2}}$ is employed, and in case of $\hat{T} \neq T$, we obtained

$$I_0(t) = \frac{2t^\epsilon}{\alpha} \frac{1}{s_1 - s_2} \int_0^\infty \left[\frac{s_1^2 \gamma^{-\frac{2}{\gamma}}}{1 + s_1\gamma} - \frac{s_2^2 \gamma^{-\frac{2}{\gamma}}}{1 + s_2\gamma}\right] d\gamma \tag{B.13}$$

The integral can be separated into two integrals which are evaluated by employing changes of variables $\gamma_1 = s_1\gamma$ and $\gamma_2 = s_2\gamma$, and following the properties of Gamma

function. Consequently, $I_0(t)$ is given by

$$I_0(t) = \frac{2t^{\epsilon}}{\alpha} \frac{s_1^{1+\frac{2}{\alpha}} - s_2^{1+\frac{2}{\alpha}}}{s_1 - s_2} \frac{\pi}{\sin\left(\frac{2\pi}{\alpha}\right)} \tag{B.14}$$

The integral $I_1(t)$ is approximated by using Gauss - Legendre approximation

$$I_1(t) = \sum_{i=1}^{N_G} \frac{ci}{2} \frac{\left(s_1 + s_2\right) t^{\alpha\epsilon} \eta_i^{\frac{\alpha}{2}} + s_1 s_2 t^{\alpha\epsilon}}{\left(\eta_i^{\frac{\alpha}{2}} + s_1 t^{\alpha\epsilon}\right)\left(\eta_i^{\frac{\alpha}{2}} + s_2 t^{\alpha\epsilon}\right)} \tag{B.15}$$

Consequently, using the properties of Gauss - Laguerre Quadrature, $\upsilon(s_1, s_2, \lambda)$ is approximated by

$$\upsilon(s_1, s_1, \lambda) \approx \pi\lambda \sum_{m=1}^{N_{GL}} \frac{w_m}{2} \left(I_0(\zeta_m) + I_1(\zeta_m)\right) \tag{B.16}$$

Approximate Average Coverage Probability of the CCU The average coverage probability expression in Equation 2.18 has a suitable form of Gauss - Laguerre and can be approximated by

$$\frac{\sum_{j=1}^{N_{GL}} w_j e^{-\frac{(T+\hat{T})}{SNR}\zeta_j^{\alpha(1-\epsilon)}} \mathscr{L}\left(\hat{T}\zeta_j^{-\alpha\epsilon}, T\zeta_j^{-\alpha\epsilon}, \lambda\right)}{\sum_{j=1}^{N_{GL}} w_j e^{-\frac{T}{SNR}\zeta_j^{\alpha(1-\epsilon)}} \mathscr{L}_{I_\theta^{(oc)}}(T\zeta_j^{-\alpha\epsilon}, \lambda)} \tag{B.17}$$

The Theorem 3.2.1.1 is proved.

B.3 Theorem 3.2.1.2 - CEU under Strict

The coverage probability of a CEU under the Strict FR networks is obtained based on approach in [39] given that the density of interfering users is λ/Δ. Hence,

$$\mathcal{P}_c^{(e)}(T, \epsilon) = \frac{\int_0^{\infty} 2\pi\lambda r e^{-\pi\lambda r^2} \mathbb{E}\left[e^{-\frac{\hat{T}\left(\sigma^2 + I_\theta^{(e)}\right)}{P^{(e)} r^{-\alpha}}} \left(1 - e^{-\frac{T\left(\sigma^2 + I_\theta^{(oc)}\right)}{P^{(c)} r^{-\alpha}}}\right)\right] dr}{1 - \int_0^{\infty} 2\pi\lambda r e^{-\pi\lambda r^2} e^{-\frac{T\sigma^2}{P^{(c)} r^{-\alpha}}} \mathbb{E}\left[-\frac{T I_\theta^{(oc)}}{P^{(c)} r^{-\alpha}} dr\right] dr}$$

Since the user is defined as the CEU, it will be served on a different RB. Hence, the user experiences new interference from new users. Therefore, the distance from the interfering user to its own serving BS changes from r_j to r_{je} and to the serving BS of user z is d_{ze}. We denote $s_1' = \hat{T} r^{\alpha(1-\epsilon)}$ and $s_2' = T r^{\alpha(1-\epsilon)}$, the numerator can be evaluated as below:

$$\begin{aligned}
&\overset{(a)}{=} \prod_{j\in\theta_e} \mathbb{E}\left[\frac{\upsilon(\frac{\hat{T}}{\phi})}{1+s_2' r_{je}^{\epsilon\alpha} d_{ze}^{-\alpha}}\right]\left(1-\prod_{j\in\theta}\mathbb{E}\left[\frac{e^{-Tr^{\alpha(1-\epsilon)}}}{1+s_1' d_{jz}^{-\alpha}}\right]\right)\\
&\overset{(b)}{=} \upsilon(\frac{\hat{T}}{\phi}) e^{\frac{2\pi\lambda}{\Delta}\int_r^\infty\left[1-\int_0^\infty \frac{\frac{2\pi\lambda t}{\Delta} e^{-\frac{\pi\lambda t^2}{\Delta}}}{1+s_2' t^{\epsilon\alpha} d_{ze}^{-\alpha}} dt\right] d_{ze} d(d_{ze})}\\
&\qquad\qquad \left(1-e^{-Tr^{\alpha(1-\epsilon)}} e^{-2\pi\lambda\int_r^\infty\left[1-\int_0^\infty \frac{2\pi\lambda e^{-\pi\lambda t^2}}{1+s_1' t^{\epsilon\alpha} d_{jz}^{-\alpha}} dt\right] d_{jz} d(d_{jz})}\right)\\
&= \upsilon\left(\frac{\hat{T}}{\phi}\right)\mathscr{L}_{I_\theta^{(oc)}}\left(s_2, \frac{\lambda}{\Delta}\right)\left(1-e^{-Tr^{\alpha(1-\epsilon)}}\mathscr{L}_{I_\theta^{(oc)}}(s_1,\lambda)\right) \qquad \text{(B.18)}
\end{aligned}$$

in which (a) is obtained by assuming that the fading channel has a Rayleigh distribution and by denoting $\upsilon(\frac{\hat{T}}{\phi}) = e^{-\frac{\hat{T}}{\phi SNR} r^{\alpha(1-\epsilon)}}$, $s_1 = Tr^{\alpha\epsilon}$ and $s_2 = \hat{T} r^{\alpha\epsilon}$; (b) is obtained by taking expectation with respects to r_{je} and r_j and follows by the properties of PGF. $\mathscr{L}_{I_\theta^{(oc)}}(s)$ is defined in (3.6)

B.4 Theorem 3.2.1.3 - CCU under Soft FR

The average coverage probability of the CCU in Soft FR is given by

$$\begin{aligned}
\mathcal{P}_c^{(c)}(T,\epsilon) &= \frac{\mathbb{P}\left(\frac{P^{(c)} g r^{-\alpha}}{\sigma^2 + I_{Sof}^{(c)}} > \hat{T}, \frac{P^{(c)} g^{(o)} r^{-\alpha}}{\sigma^2 + I_{Sof}^{(oc)}} > T\right)}{\mathbb{P}\left(\frac{P g r^{\alpha(\epsilon-1)}}{\sigma^2 + I_{Sof}^{(oc)}} > T\right)}\\
&= \frac{\int_0^\infty r e^{-\pi\lambda r^2} e^{-\frac{(T+\hat{T})\sigma^2}{P^{(c)} r^{-\alpha}}} \mathbb{E}\left[e^{-\frac{\hat{T} I_{Sof}^{(c)}}{P^{(c)} r^{-\alpha}} - \frac{T I_{Sof}^{(oc)}}{P^{(c)} r^{-\alpha}}}\right] dr}{\int_0^\infty r e^{-\pi\lambda r^2}\left(e^{-\frac{T\sigma^2}{P^{(c)} r^{-\alpha}}}\mathbb{E}\left[-\frac{T I_{Sof}^{(oc)}}{P^{(c)} r^{-\alpha}} dr\right]\right) dr} \qquad \text{(B.19)}
\end{aligned}$$

The expectation of the numerator in Equation B.19 is the joint Laplace transform $\mathscr{L}_{Sof}(s_1', s_2')$ of interferences during the establishment phase communication phase in

which $s_1' = Tr^{\alpha(1-\epsilon)}$ and $s_2' = \hat{T}r^{\alpha(1-\epsilon)}$. By using the definition of $I_{Sof}^{(z)}$ in Equation 3.3, $\mathscr{L}_{Sof}(s_1', s_2')$

$$= \mathbb{E}\left[e^{-\sum_{j\in\theta_{Sof}^{(c)}}\left(s_2' r_j^{\alpha\epsilon} d_{jz}^{-\alpha} g_{jz} + s_1' r_j^{\alpha\epsilon} d_{jz}^{-\alpha} g_{jz}^{(o)}\right) - \sum_{j\in\theta_{Sof}^{(e)}}\left(\phi s_2' r_j^{\alpha\epsilon} d_{jz}^{-\alpha} g_{jz} + \phi s_1' r_j^{\alpha\epsilon} g_{jz} d_{jz}^{-\alpha} g_{jz}^{(o)}\right)}\right]$$

Since each BS in $\theta_{Sof}^{(c)}$ is distributed independently to any BS in $\theta_{Sof}^{(e)}$ and all channels are independent Rayleigh fading channels, $\mathscr{L}_{Sof}(s_2', s_1') =$

$$= \prod_{j\in\theta_{Sof}^{(c)}} \mathbb{E}\left[e^{-\left(s_2' r_j^{\alpha\epsilon} d_{jz}^{-\alpha} g_{jz} + s_1' r_j^{\alpha\epsilon} d_{jz}^{-\alpha} g_{jz}^{(o)}\right)}\right] \prod_{j\in\theta_{Sof}^{(c)}} \mathbb{E}\left[e^{-\left(\phi s_2' r_j^{\alpha\epsilon} d_{jz}^{-\alpha} g_{jz} + \phi s_1' r_j^{\alpha\epsilon} d_{jz}^{-\alpha} g_{jz}^{(o)}\right)}\right]$$

$$= \prod_{j\in\theta_{Sof}^{(c)}} \mathbb{E}\left[\frac{1}{1+s_2' r_j^{\alpha\epsilon} d_{jz}^{-\alpha}} \frac{1}{1+s_1' r_j^{\alpha\epsilon} d_{jz}^{-\alpha}}\right] \prod_{j\in\theta_{Sof}^{(e)}} \mathbb{E}\left[\frac{1}{1+\phi s_2' r_j^{\alpha\epsilon} d_{jz}^{-\alpha}} \frac{1}{1+\phi s_1' r_j^{\alpha\epsilon} d_{jz}^{-\alpha}}\right]$$

Given that r_j is the distance from user j to its serving BS, whose PDF follows (2.1), and using the properties of PGF with respect to variable d_{jz} over $\theta_{Sof}^{(c)}$ and $\theta_{Sof}^{(e)}$, the joint Laplace transform $\mathscr{L}_{Sof}(s_2', s_1')$ is given by

$$= \prod_{j\in\theta_{Sof}^{(c)}} \mathbb{E}\left[\int_0^\infty \frac{\frac{2\pi(\Delta-1)\lambda}{\Delta} t e^{-\frac{\pi(\Delta-1)\lambda}{\Delta}t^2}}{\left(1+s_2' t^{\alpha\epsilon} d_{jz}^{-\alpha}\right)\left(1+s_1' t^{\alpha\epsilon} d_{jz}^{-\alpha}\right)}\right]$$

$$\prod_{j\in\theta_{Sof}^{(e)}} \mathbb{E}\left[\int_0^\infty \frac{\frac{2\pi\lambda}{\Delta} t e^{-\frac{\pi\lambda}{\Delta}t^2}}{\left(1+\phi s_2' t^{\alpha\epsilon} d_{jz}^{-\alpha}\right)\left(1+\phi s_1' t^{\alpha\epsilon} d_{jz}^{-\alpha}\right)}\right]$$

$$= e^{-\frac{2\pi(\Delta-1)}{\Delta}\lambda \int_r^\infty \left[1-\int_0^\infty \frac{\frac{2\pi(\Delta-1)\lambda}{\Delta} t e^{-\frac{\pi(\Delta-1)\lambda}{\Delta}t^2}}{\left(1+s_2' t^{\alpha\epsilon} d_{jz}^{-\alpha}\right)\left(1+s_1' t^{\alpha\epsilon} d_{jz}^{-\alpha}\right)}\right] d_{jz} d(d_{jz})}$$

$$e^{-\frac{2\pi}{\Delta}\lambda \int_r^\infty \left[1-\int_0^\infty \frac{\frac{2\pi\lambda}{\Delta} t e^{-\frac{\pi\lambda}{\Delta}t^2}}{\left(1+\phi s_2' t^{\alpha\epsilon} d_{jz}^{-\alpha}\right)\left(1+\phi s_1' t^{\alpha\epsilon} d_{jz}^{-\alpha}\right)}\right] d_{jz} d(d_{jz})}$$

By letting $s_2 = \hat{T}r^{-\alpha\epsilon}$ and $s_1 = Tr^{-\alpha\epsilon}$, and using the change of variable $x = \frac{d_{jz}}{r}$, the joint Laplace transform $\mathscr{L}_{Sof}(s_2, s_2)$

$$= e^{-\frac{2\pi(\Delta-1)\lambda r^2}{\Delta} \int_1^\infty \left[1-\int_0^\infty \frac{\frac{2\pi(\Delta-1)\lambda}{\Delta} t e^{-\frac{\pi(\Delta-1)\lambda}{\Delta}t^2}}{\left(1+s_2 t^{\alpha\epsilon} d_{jz}^{-\alpha}\right)\left(1+s_2 t^{\alpha\epsilon} x^{-\alpha}\right)}\right] dx} e^{-\frac{2\pi\lambda r^2}{\Delta} \int_1^\infty \left[1-\int_0^\infty \frac{\frac{2\pi\lambda}{\Delta} t e^{-\frac{\pi\lambda}{\Delta}t^2}}{\left(1+\phi s_2 t^{\alpha\epsilon} d_{jz}^{-\alpha}\right)\left(1+\phi s_2 t^{\alpha\epsilon} x^{-\alpha}\right)}\right] dx}$$

$$= \mathscr{L}(s_1, s_2, \frac{\Delta-1}{\Delta}\lambda)\mathscr{L}(\phi s_1, \phi s_2, \frac{\lambda}{\Delta}) \tag{B.20}$$

By substituting (B.20) into (B.19) and remind that the denominator is given by Appendix A, the Theorem 3.2.1.3 is proved.

The approximated value of the average coverage probability is obtained by using a change of variable $\zeta = \pi\lambda r^2$ and Gauss-Laguerre Quadrature.

B.5 Theorem 3.2.1.4 - CEU under Strict FR

The average coverage probability of the CEU in Soft FR is given by

$$\begin{aligned}\mathcal{P}_c^{(e)}(T,\epsilon) &= \frac{\mathbb{P}\left(\frac{P^{(e)}gr^{-\alpha}}{\sigma^2+I_{Sof}^{(e)}} > \hat{T}, \frac{P^{(c)}g^{(o)}r^{-\alpha}}{\sigma^2+I_{Sof}^{(oc)}} < T\right)}{\mathbb{P}\left(\frac{Pgr^{\alpha(\epsilon-1)}}{\sigma^2+I_{Sof}^{(oc)}} < T\right)} \\ &= \frac{\int_0^\infty 2\pi\lambda r e^{-\pi\lambda r^2}\mathbb{E}\left[e^{-\frac{\hat{T}\left(\sigma^2+I_{Sof}^{(e)}\right)}{P^{(e)}r^{-\alpha}}}\left(1-e^{-\frac{T\left(\sigma^2+I_{Sof}^{(oc)}\right)}{P^{(c)}r^{-\alpha}}}\right)\right]dr}{1-\int_0^\infty 2\pi\lambda r e^{-\pi\lambda r^2}e^{-\frac{T\sigma^2}{P^{(c)}r^{-\alpha}}}\mathbb{E}\left[-\frac{TI_\theta^{(oc)}}{P^{(c)}r^{-\alpha}}dr\right]dr}\end{aligned} \tag{B.21}$$

Since the interfering sources during the communication phase are distributed completely independently to those during the establishment phase, the average coverage probability can be re-written in the following form

$$\mathcal{P}_c^{(e)}(T,\epsilon) = \frac{\int_0^\infty 2\pi\lambda r e^{-\pi\lambda r^2}\mathbb{E}\left[e^{-\frac{\hat{T}\left(\sigma^2+I_{Sof}^{(e)}\right)}{\phi P^{(c)}r^{-\alpha}}}\right]\left(1-\mathbb{E}\left[e^{-\frac{T\left(\sigma^2+I_{Sof}^{(oc)}\right)}{P^{(c)}r^{-\alpha}}}\right]\right)dr}{1-\int_0^\infty 2\pi\lambda r e^{-\pi\lambda r^2}e^{-\frac{T\sigma^2}{P^{(c)}r^{-\alpha}}}\mathbb{E}\left[-\frac{TI_\theta^{(oc)}}{P^{(c)}r^{-\alpha}}dr\right]dr} \tag{B.22}$$

Using the results of Appendix B.1, the Theorem 3.2.1.4 is proved.

Appendix C

Appendices of Chapter 4

C.1 Theorem 4.2.4.2 - CCU classification probability

The average probability where the user in Tier-k is served as a CCU of Soft FR is given by

$$\begin{aligned}\mathbb{P}^{(nc)}_{Soft,k}(T_k) &= \mathbb{P}\left(\frac{P_k g'_k r_k^{\alpha_k}}{\sigma_G^2 + I^{(u)}_{Sof}} > T_k\right) \\ &\overset{(a)}{=} e^{-\frac{T_k r_k^{\alpha_k}}{SNR_k}} \mathbb{E}\left[e^{-\frac{T_k r_k^{\alpha_k} I^{(u)}_{Sof}}{P_k}}\right]\end{aligned} \tag{C.1}$$

where $SNR_k = \frac{P_k}{\sigma^2}$; (a) follows the assumption that the channel fading has Rayleigh distribution.

By substituting Equation 4.8, the expectation can be presented as the product

of $\mathbb{E}(\phi|r_k)$ and $\mathbb{E}(1|r_k)$ where

$$\mathbb{E}(\phi_j|r_k) = \prod_{j=1}^{K} \mathbb{E}\left\{ \prod_{z_e \in \theta_j^{(e)}} \left[1 - E[\tau_k^{(e)} \tau_j^{(z_e)}] \left(1 - e^{-s_{jz_e} g_{jz_e} r_{jz_e}^{-\alpha_j}}\right)\right] \right\} \tag{C.2a}$$

$$\mathbb{E}(1|r_k) = \prod_{j=1}^{K} \mathbb{E}\left\{ \prod_{z_c \in \theta_j^{(c)}} \left[1 - E[\tau_k^{(c)} \tau_j^{(z_c)}] \left(1 - e^{-s_{jz_c} g_{jz_c} r_{jz_c}^{-\alpha_j}}\right)\right] \right\} \tag{C.2b}$$

in which $T_k \frac{\phi_j P_j}{P_k} r_k^{\alpha_k} = s_{jze}$ and $T_k \frac{P_j}{P_k} r_k^{\alpha_k} = s_{jzc}$.

Evaluating $\mathbb{E}(\phi|r_k)$ and since g_{jz_e} is exponential RV, we have

$$\begin{aligned}
\mathbb{E}(\phi_j|r_k) &= \prod_{j=1}^{K} \mathbb{E}\left\{ \prod_{z_e \in \theta_j^{(e)}} \left[1 - \epsilon_k^{(oe)} \epsilon_j^{(oe)} \left(1 - \frac{1}{1 + s_{jz_e} r_{jz_e}^{-\alpha_j}}\right)\right] \right\} \\
&\overset{(b)}{=} \prod_{j=1}^{K} e^{-2\pi \epsilon_k^{(oc)} \epsilon_j^{(oe)} \lambda_j^{(e)} \int_{\sqrt{C_j} r^{\alpha_k/\alpha_j}}^{\infty} \left[1 - \frac{1}{1 + s_{jz_e} r_{jz_e}^{-\alpha_j}}\right] r_{jze} dr_{jze}} \\
&\overset{(c)}{=} e^{-\pi \epsilon_k^{(oc)} \sum_{j=1}^{K} \lambda_j^{(e)} C_j r_k^{2\alpha_k/\alpha_j} \int_0^1 \frac{\epsilon_j^{(oe)}}{\frac{1}{T_k} \frac{B_j}{\phi_j B_k} x^{2-\alpha_j/2} + x^2} dx}
\end{aligned} \tag{C.3}$$

in which (a) is obtained by using the properties of PPP probability generating function and $r_j > \sqrt{C_j} r^{\alpha_k/\alpha_j}$; (c) is obtained by employing a change of variables $x = C_j r_k^{\frac{2\alpha_k}{\alpha_j}} r_{jz_e}^{-2}$.

$$\text{Similarity, } \mathbb{E}(1|r_k) = e^{-\pi \epsilon_k^{(oc)} \sum_{j=1}^{K} \lambda_j^{(c)} C_j r_k^{2\alpha_k/\alpha_j} \int_0^1 \frac{\epsilon_j^{(oc)}}{\frac{1}{T_k} \frac{B_j}{B_k} x^{2-\alpha_j/2} + x^2} dx} \tag{C.4}$$

Substituting $\mathbb{E}(\phi_k|r_k)$ and $\mathbb{E}(1|r_k)$ into Equation C.1, then the results in Theorem 4.3.2 is obtained

C.2 Theorem 4.3.2.1 - CCU under Strict FR

The average coverage probability of a CCU under the Strict FR is given by

$$P_{Str,k}^{(e)}(T_k,\hat{T}_k) \overset{(a)}{=} \frac{\mathbb{P}\left(SINR(1,r_k)>\hat{T}_k, SINR^{(o)}(1,r_k)>T_k\right)}{\mathbb{P}\left(SINR^{(o)}(1,r_k)>T_k\right)} \overset{(b)}{=} \frac{\int_0^\infty 2\pi\lambda_k r_k e^{-\pi\lambda_k r_k^2} e^{-\frac{r_k^{\alpha_k}}{SNR_k}\left(\hat{T}_k+T_k\right)} \mathbb{E}\left[e^{-\left(\frac{T_k I_{Str}^{(oc)}}{P_k}+\frac{\hat{T}_k I_{Str}^{(c)}}{P_k}\right) r_k^{\alpha_k}}\right] dr_k}{\int_0^\infty 2\pi\lambda_k r_k e^{-\pi\lambda_k r_k^2} \mathbb{E}\left[e^{-\frac{T_k}{P_k}\left(I_{Str}^{(oc)}+\sigma^2\right) r_k^{\alpha_k}}\right] dr_k} \tag{C.5}$$

in which (a) follows the Bayes rules and (b) follows the assumption that the fading channel coefficients are independent RV and conditioning on r_k.

The expectation in the numerator can be computed based on the approach in [37]

$$\begin{aligned}\mathbb{E}\left[e^{-\left(\frac{T_k I_{Str}^{(oc)}}{P_k}+\frac{\hat{T}_k I_{Str}^{(c)}}{\phi_k P_k}\right) r_k^{\alpha_k}}\right] &= \mathbb{E}\left[\prod_{z_c\in\theta_j^{(c)}} e^{-\tau_j^{(oc)}\tau_j^{(oz_c)} g_{jz_c}^{(o)} s_{z_c}} e^{-\tau_j^{(c)}\tau_j^{(z_c)} g_{jz_c}\hat{s}_{z_c}}\right] \\ &= \mathbb{E}\left[\prod_{z_c\in\theta_j^{(c)}} \left(1-\epsilon_k^{(oc)}\epsilon_j^{(oc)}\frac{s_{z_c}}{1+s_{z_c}}\right)\left(1-\epsilon_k^{(c)}\epsilon_j^{(c)}\frac{\hat{s}_{z_e}}{1+\hat{s}_{z_e}}\right)\right]\end{aligned} \tag{C.6}$$

where $T_k\frac{P_j}{P_k}\frac{r_{jz_c}^{-\alpha_j}}{r_k^{-\alpha_k}} = s_{z_c}$ and $\hat{T}_k\frac{P_j}{P_k}\frac{r_{jz_c}^{-\alpha_j}}{r_k^{-\alpha_k}} = \hat{s}_{z_c}$; and the second equality follows the properties of the indicator function.

Using the properties of the PPP probability generating function with $r_{jz_c} > \sqrt{C_j} r^{\alpha_k/\alpha_j}$ and employing a change of variable $x = C_j r_k^{\frac{2\alpha_k}{\alpha_j}} r_{jz_c}^{-2}$, then

$$\mathbb{E}\left[e^{-\left(\frac{T_k I_{Str}^{(oc)}}{P_k}+\frac{\hat{T}_k I_{Str}^{(c)}}{\phi_k P_k}\right) r_k^{\alpha_k}}\right] = e^{-2\pi\lambda_j C_j r_k^{2\alpha_k/\alpha_j}\left(\epsilon_k^{(oc)}\upsilon_j^{(c)}(T_k)+\epsilon_k^{(c)}\upsilon_j^{(c)}(\hat{T}_k)-\epsilon_k^{(oc)}\epsilon_k^{(c)}\kappa(T_k,\hat{T}_k)dx\right)} \tag{C.7}$$

in which $\upsilon_j^{(oc)}(T_k) = \int_0^1 \frac{\epsilon_j^{(oc)}}{\frac{1}{T_k}\frac{B_j}{B_k}x^{2-\alpha_j/2}+x^2}dx$; $\upsilon_j^{(c)}(\hat{T}_k) = \int_0^1 \frac{\epsilon_j^{(c)}}{\frac{1}{\hat{T}_k}\frac{B_j}{B_k}x^{2-\alpha_j/2}+x^2}dx$ and

$\kappa^{(c)}(T_k, \hat{T}_k) = \int_0^1 \frac{\epsilon_j^{(oc)}\epsilon_j^{(c)}}{x^2\left(\frac{1}{T_k}\frac{B_j}{B_k}x^{-\alpha_j/2}+1\right)\left(\frac{1}{\hat{T}_k}\frac{B_j}{B_k}x^{-\alpha_j/2}+1\right)}$

C.3 Theorem 4.3.2.2 - CEU under Strict FR

The average coverage probability of a CEU under the Strict FR is evaluated by

$$P_{Str,k}^{(e)}(\hat{T}_k, T_k) = \frac{\mathbb{P}\left(SINR(\phi_k, r_k) > \hat{T}_k, SINR^{(o)}(1, r_k) < T_k\right)}{\mathbb{P}\left(SINR^{(o)}(1, r_k) < T_k\right)}$$
$$= \frac{\int_0^\infty 2\pi\lambda_k r_k e^{-\pi\lambda_k r_k^2}\mathbb{E}\left[e^{-\frac{\hat{T}_k r_k^{\alpha_k}}{\phi_k P}\left(I_{Str}^{(e)}+\sigma^2\right)}\left(1-e^{-\frac{T_k}{P_k}\left(I_{Str}^{(oc)}+\sigma^2\right)r_k^{\alpha_k}}\right)\right]dr_k}{1-\int_0^\infty 2\pi\lambda_k r_k e^{-\pi\lambda_k r_k^2}\mathbb{E}\left[e^{-\frac{T_k}{P_k}\left(I_{Str}^{(oc)}+\sigma^2\right)r_k^{\alpha_k}}\right]dr_k}$$

The expected value of the numerator can be separated into two expectations in which the first one is evaluated using the same approach as in Appendix C.1, i.e, $\mathbb{E}\left[e^{-\frac{\hat{T}_k}{\phi_k P_k}\left(I_{Str}^{(e)}+\sigma^2\right)r_k^{\alpha_k}}\right] = e^{-\frac{\hat{T}_k r_k^{\alpha_k}}{\phi_k SNR_k}-\pi\lambda_k\epsilon_k^{(e)2}r_k^2\upsilon_j^{(e)}(\hat{T}_k)}$, and the second one can be computed in the following steps

$$= \mathbb{E}\left[\prod_{z_c\in\theta_j} e^{-\tau_j^{(oc)}\tau_j^{(oz_c)}g_{jz_c}^{(o)}s_{z_c}}\prod_{z_e\in\theta_j^{(e)}} e^{-\tau_j^{(e)}\tau_j^{(z_e)}g_{jz_e}\hat{s}_{z_e}}\right]$$
$$= \mathbb{E}\left[\prod_{z_c\in\theta_j}\left(1-\epsilon_k^{(oc)}\epsilon_j^{(oc)}\frac{s_{z_c}}{1+s_{z_c}}\right)\prod_{z_e\in\theta_j^{(e)}}\left(1-\epsilon_k^{(e)}\epsilon_j^{(e)}\frac{\hat{s}_{z_e}}{1+\hat{s}_{z_e}}\right)\right]$$

in which $T_k\frac{r_{jz_c}^{-\alpha_j}}{r_k^{-\alpha_k}} = s_{z_c}$ and $\hat{T}_k\frac{\phi_j}{\phi_k}\frac{r_{jz_e}^{-\alpha_j}}{r_k^{-\alpha_k}} = \hat{s}_{z_e}$.

Then, the expectation equals

$$
\begin{aligned}
=&\mathbb{E}_{\theta_j^{(c)}\setminus\theta_j^{(e)}}\left[\prod_{z_c\in\theta_j^{(c)}\setminus\theta_j^{(e)}}\left(1-\epsilon_k^{(oc)}\epsilon_j^{(oc)}\frac{s_{z_c}}{1+s_{z_c}}\right)\right]\\
&\mathbb{E}_{\theta_j^{(e)}}\left[\prod_{z_e\in\theta_j^{(e)}}\left(1-\epsilon_k^{(oc)}\epsilon_j^{(oc)}\frac{s_{z_e}}{1+s_{z_e}}\right)\left(1-\epsilon_k^{(e)}\epsilon_j^{(e)}\frac{\hat{s}_{z_e}}{1+\hat{s}_{z_e}}\right)\right]
\end{aligned}
\tag{C.8}
$$

in which $s_{z_e}=T_k\frac{r_{jz_e}^{-\alpha_j}}{r_k^{-\alpha_k}}$.

Employing the properties of the PPP probability generating function with $r_{jz_c}>\sqrt{C_j}r^{\alpha_k/\alpha_j}$ and the changes of variables $x=C_jr_k^{\frac{2\alpha_k}{\alpha_j}}r_{jz_c}^{-2}$ for the first part and $x=C_jr_k^{\frac{2\alpha_k}{\alpha_j}}r_{jz_e}^{-2}$ for the second part, the expectation equals

$$
=e^{-2\pi\lambda_jC_jr_k^{2\alpha_k/\alpha_j}\left[\epsilon_k^{(oc)}\upsilon_j^{(oc)}(T_k)+\frac{1}{\Delta_j}\epsilon_k^{(e)}\upsilon_j^{(e)}(\hat{T}_k)-\frac{1}{\Delta_j}\epsilon_k^{(oc)}\epsilon_k^{(e)}\kappa(T_k,\hat{T}_k)\right]dx}
\tag{C.9}
$$

in which $\upsilon_j^{(e)}(\hat{T}_k)=\int_0^1\frac{\epsilon_j^{(e)}}{\frac{1}{\hat{T}_k}\frac{\phi_k}{\phi_j}\frac{B_j}{B_k}x^{2-\alpha_j/2}+x^2}dx$

and $\kappa(T_k,\hat{T}_k)=\int_0^1\frac{\epsilon_j^{(oc)}\epsilon_j^{(c)}}{x^2\left(\frac{1}{T_k}\frac{B_j}{B_k}x^{-\alpha_j/2}+1\right)\left(\frac{1}{\hat{T}_k}\frac{\phi_k}{\phi_j}\frac{B_j}{B_k}x^{-\alpha_j/2}+1\right)}$; and $\upsilon_j^{(oc)}(T_k)$ is defined in Equation (C.7).

The expectation of the denominator in Equation C.5 is computed by Appendix A, then

$$
\mathbb{E}\left[e^{-\frac{T_k}{\phi_kP_k}\left(I_{Str}^{(oe)}+\sigma^2\right)r_k^{\alpha_k}}\right]=e^{-\frac{T_kr_k^{\alpha_k}}{SNR_k}}e^{-\pi\sum_{j=1}^{K}\lambda_jC_j\epsilon_k^{(oc)}\upsilon_j^{(oc)}(T_k)r_k^{\frac{2\alpha_k}{\alpha_j}}}
\tag{C.10}
$$

Substituting Equations C.9 and C.10 into Equation C.5, Theorem 4.3.2.2 is proved.

C.4 Theorem 4.3.2.3 - CCU under Soft FR

The coverage probability of a CCU under the Soft FR networks is obtained by

$$P_c^{(c)}(T_k,\hat{T}_k) = \frac{\mathbb{P}\left(\frac{P_k g'_k r_k^{-\alpha_k}}{\sigma_G^2+I_{Soft}^{(c)}} > \hat{T}_k, \frac{P_k g_k r_k^{-\alpha_k}}{\sigma_G^2+I_{Soft}^{(oc)}} > T_k\right)}{\mathbb{P}\left(\frac{P_k g_k r_k^{-\alpha_k}}{\sigma_G^2+I_{Soft}^{(oc)}} > T_k\right)}$$
$$= \frac{\int_0^\infty r_k e^{-\pi\lambda_k r_k^2} e^{-\frac{r_k^{\alpha_k}}{SNR_k}\left(\hat{T}_k+T_k\right)} \mathbb{E}\left[e^{-\frac{r_k^{\alpha_k}}{P_k}\left(\hat{T}_k I_{Soft}^{(c)}+T_k I_{Soft}^{(oc)}\right)}\right] dr_k}{\int_0^\infty r_k e^{-\pi\lambda_k r_k^2}\mathbb{E}\left[e^{-\frac{T_k}{P_k}\left(\sigma_G^2+I_{Soft}^{(oc)}\right)}\right] dr_k} \tag{C.11}$$

Substituting Equation (4.8) into Equation (C.11), the second element of the integrand in the numerator of (C.11) can be evaluated by using the approach in [37]:

$$\overset{(c)}{=} \prod_{j=1}^{K} \mathbb{E}\left[\prod_{z_c\in\theta_j^{(c)}} e^{-\left(\hat{T}_k\tau_k^{(c)}\tau_j^{(z_c)}g'_{jz_c}+T_k\tau_k^{(oc)}\tau_j^{(ozc)}g_{jz_c}\right)\frac{P_j}{P_k}\frac{r_{jz_c}^{-\alpha_j}}{r_k^{-\alpha_k}}}\right]$$
$$\mathbb{E}\left[\prod_{z_e\in\theta_j^{(e)}} e^{-\left(\hat{T}_k\tau_k^{(e)}\tau_j^{(ze)}g'_{jz_e}+T_k\tau_k^{(oe)}\tau_j^{(oze)}g_{jz_e}\right)\frac{\phi_j P_j}{P_k}\frac{r_{jz_e}^{-\alpha_j}}{r_k^{-\alpha_k}}}\right] \tag{C.12}$$

where (c) since each BS is distributed stochastically independent to all the BSs and the fading power gains are independent RVs.

The first element of Equation (C.12) can be evaluated as follows

$$
\begin{aligned}
&\overset{(d)}{=} \mathbb{E}\left[\prod_{z_c\in\theta_j^{(c)}}\left[\begin{array}{l}\left(1-\mathbb{E}\left[\tau_k^{(oc)}\tau_j^{(oz_c)}\right]\left(1-e^{-s_{jz_c}g_{jz_c}r_{jz_c}^{-\alpha_j}}\right)\right)\\ \quad\times\left(1-\mathbb{E}\left[\tau_k^{(c)}\tau_j^{(z_c)}\right]\left(1-e^{-\hat{s}_{jz_c}g_{jz_c}r_{jz_c}^{-\alpha_j}}\right)\right)\end{array}\right]\right]\\
&\overset{(e)}{=} \mathbb{E}\left[\prod_{z_c\in\theta_j^{(c)}}\left[\begin{array}{l}\left(1-\epsilon_k^{(oc)}\epsilon_j^{(oc)}\left(1-\frac{1}{1+s_{jz_c}r_{jz_c}^{-\alpha_j}}\right)\right)\\ \quad\times\left(1-\epsilon_k^{(c)}\epsilon_j^{(c)}\left(1-\frac{1}{1+\hat{s}_{jz_c}r_{jz_c}^{-\alpha_j}}\right)\right)\end{array}\right]\right]\\
&\overset{(f)}{=} e^{-\frac{2\pi\lambda_j C_j(\Delta_j-1)}{\Delta_j}r_k^{\frac{2\alpha_k}{\alpha_j}}\int_0^1\left[\begin{array}{c}\frac{\epsilon_k^{(oc)}\epsilon_j^{(oc)}}{\frac{1}{T_k}\frac{B_j}{B_k}x^{2-\alpha_j/2}+x^2}+\frac{\epsilon_k^{(c)}\epsilon_j^{(c)}}{\frac{1}{\hat{T}_k}\frac{B_j}{B_k}x^{2-\alpha_j/2}+x^2}\\ -\frac{\epsilon_k^{(oc)}\epsilon_k^{(c)}\epsilon_j^{(oc)}\epsilon_j^{(c)}}{x^2\left(1+\frac{1}{T}\frac{B_j}{B_k}x^{-\alpha_j/2}\right)\left(1+\frac{1}{\hat{T}}\frac{B_j}{B_k}x^{-\alpha_j/2}\right)}\end{array}\right]}
\end{aligned}
\tag{C.13}
$$

where (d) follows the properties of the indicator function and by letting $T\frac{P_j}{P_k}r_k^{\alpha_k} = s_{jze}$ and $\hat{T}_k\frac{P_j}{P_k}r_k^{\alpha_k} = \hat{s}_{jze}$; (e) follows the assumption that the channel fading has a Rayleigh distribution; (f) follows the properties of PGF with $r_{jz_c} > \sqrt{C_j}r^{\alpha_k/\alpha_j}$ and by letting $x = C_j r^{\frac{2\alpha_k}{\alpha_j}} r_{jz_e}^{-2}$.

Similarly, the second expectation of Equation (C.12) is obtained by

$$
\begin{aligned}
&= e^{-\frac{2\pi\lambda_j C_j(\Delta_j-1)}{\Delta_j}r_k^{\frac{2\alpha_k}{\alpha_j}}\int_0^1\left[\begin{array}{c}\frac{\epsilon_k^{(oc)}\epsilon_j^{(oe)}}{\frac{1}{T_k}\frac{B_j}{\phi_j B_k}x^{2-\alpha_j/2}+x^2}+\frac{\epsilon_k^{(c)}\epsilon_j^{(e)}}{\frac{1}{\hat{T}_k}\frac{B_j}{\phi_j B_k}x^{2-\alpha_j/2}+x^2}\\ -\frac{\epsilon_k^{(oc)}\epsilon_k^{(c)}\epsilon_j^{(oe)}\epsilon_j^{(e)}}{x^2\left(1+\frac{1}{T}\frac{B_j}{\phi_j B_k}x^{-\alpha_j/2}\right)\left(1+\frac{1}{\hat{T}}\frac{B_j}{\phi_j B_k}x^{-\alpha_j/2}\right)}\end{array}\right]}
\end{aligned}
\tag{C.14}
$$

Substituting Equations C.13 and C.14 into Equation C.11, and note that the denominator of Equation C.11 is evaluated in Appendix A, Theorem 4.3.2.3 is proved.

Bibliography

[1] Cisco, "Cisco visual networking index: Global mobile data traffic forecast update, 2015 ? 2020," 2016.

[2] F. Khan, *LTE for 4G Mobile Broadband: Air Interface Technologies and Performance*. Cambridge University Press, 2009.

[3] S. Sesia, I. Toufik, and M. Baker, *LTE, The UMTS Long Term Evolution: From Theory to Practice*. Wiley Publishing, 2009.

[4] 3GPP TS 36.213 version 8.8.0 Release 8, "LTE; Evolved Universal Terrestrial Radio Access (E-UTRA); Physical layer procedures," November 2009.

[5] 3GPP Release 10 V0.2.1, "LTE-Advanced (3GPP Release 10 and beyond)," June 2014.

[6] A. S. Hamza, S. S. Khalifa, H. S. Hamza, and K. Elsayed, "A Survey on Inter-Cell Interference Coordination Techniques in OFDMA-Based Cellular Networks," *IEEE Commun. Surveys & Tutorials*, vol. 15, no. 4, pp. 1642–1670, 2013.

[7] 3GPP-TSG-RAN-R1-050738. Interference mitigation Considerations and Results on Frequency Reuse. September, 2005, Siemens.

[8] 3GPP TS 36.214 version 9.1.0 Release 9, "LTE; Evolved Universal Terrestrial Radio Access (E-UTRA); Physical layer - Measurements," April 2010.

[9] HUAWEI TECHNOLOGIES CO., LTD, "eLTE2.2 DBS3900 LTE FDD Basic Feature Description," February 2014.

[10] Huawei, "R1-050507 : Soft Frequency Reuse Scheme for UTRAN LTE," in *3GPP TSG RAN WG1 Meeting #41*, May 2005.

[11] S. Sesia, I. Toufik, and M. Baker, *Indoor Wireless Communications: From Theory to Implementation*.

[12] D. Tse and P. Viswanath, Eds., *Fundamentals of wireless communication*. Cambridge, 2005.

[13] O. Somekh and S. Shamai, "Shannon-theoretic approach to a Gaussian cellular multiple-access channel with fading," *IEEE Trans. Inf. Theory*, vol. 46, no. 4, pp. 1401–1425, Jul 2000.

[14] S. Shamai and A. Wyner, "Information-theoretic considerations for symmetric, cellular, multiple-access fading channels. I," *IEEE Trans. Inf. Theory*, vol. 43, no. 6, pp. 1877–1894, Nov 1997.

[15] ——, "Information-theoretic considerations for symmetric, cellular, multiple-access fading channels. II," *IEEE Trans. Inf. Theory*, vol. 43, no. 6, pp. 1895–1911, Nov 1997.

[16] S. Shamai and B. Zaidel, "Enhancing the cellular downlink capacity via co-processing at the transmitting end," in *IEEE VTS 53rd Vehicular Technology Conference, 2001. VTC 2001 Spring.*, vol. 3, 2001, pp. 1745–1749 vol.3.

[17] O. Somekh, B. Zaidel, and S. Shamai, "Sum Rate Characterization of Joint Multiple Cell-Site Processing," *IEEE Trans. Inf. Theory*, vol. 53, no. 12, pp. 4473–4497, Dec 2007.

[18] D. Aktas, M. Bacha, J. Evans, and S. Hanly, "Scaling results on the sum capacity of cellular networks with mimo links," *IEEE Trans. Inf. Theory*, vol. 52, no. 7, pp. 3264–3274, July 2006.

[19] S. Jing, D. Tse, J. Soriaga, J. S. Jilei Hou, and R. Padovani, "Multicell Downlink Capacity with Coordinated Processing," *EURASIP Journal on Wireless Commun. and Networking*, vol. 46, no. 4, pp. 1401–1425, Jul 2000.

[20] J. Xu, J. Zhang, and J. Andrews, "On the Accuracy of the Wyner Model in Cellular Networks," *IEEE Trans. Wireless Commun.*, vol. 10, no. 9, pp. 3098–3109, September 2011.

[21] F. Baccelli, M. Klein, and S. Zouev, "Perturbation Analysis of Functionals of Random Measures," INRIA, Research Report RR-2225, 1994. [Online]. Available: https://hal.inria.fr/inria-00074445

[22] J. G. Andrews, F. Baccelli, and R. K. Ganti, "A new tractable model for cellular coverage," in *2010 48th Annu. Allerton Conference on Communication, Control, and Computing (Allerton)*, pp. 1204–1211.

[23] H. ElSawy, E. Hossain, and M. Haenggi, "Stochastic Geometry for Modeling, Analysis, and Design of Multi-Tier and Cognitive Cellular Wireless Networks: A Survey," *IEEE Commun. Surveys Tutorials*, vol. 15, no. 3, pp. 996–1019, Third 2013.

[24] M. Haenggi, *Stochastic Geometry for Wireless Networks* . Cambridge Univ. Press, November 2012.

[25] D. Daley and D. Vere-Jones, *An Introduction to the Theory of Point Processes: Volume II: General Theory and Structure*, second edition ed. Springer Science & Business Media, 2008.

[26] S. N. Chiu, D. Stoyan, W. S. Kendall, and J. Mecke, *Stochastic Geometry and Its Application* , 3rd ed. Wiley, 2013.

[27] M. A. Pinsky and S. Karlin, *An Introduction to Stochastic Modeling*, fourth edition ed. Elsevier, 2011.

[28] Transformation of Random Variables. [Online]. Available: www.math.uiuc.edu/~r-ash/Stat/StatLec1-5.pdf

[29] F. Baccelli, M. Klein, M. Lebourges, and S. Zuyev, "Stochastic geometry and architecture of communication networks," *Telecommunication Systems*, vol. 7, no. 1, pp. 209–227, 1997. [Online]. Available: http://dx.doi.org/10.1023/A:1019172312328

[30] T. D. Novlan, H. S. Dhillon, and J. G. Andrews, "Analytical modeling of uplink cellular networks," *IEEE Trans. Wireless Commun.*, vol. 12, no. 6, pp. 2669–2679, June 2013.

[31] J. G. Andrews, F. Baccelli, and R. K. Ganti, "A tractable approach to coverage and rate in cellular networks," *IEEE Transactions on Communications*, vol. 59, no. 11, pp. 3122–3134, November 2011.

[32] M. Di Renzo, A. Guidotti, and G. E. Corazza, "Average rate of downlink heterogeneous cellular networks over generalized fading channels: A stochastic geometry approach," *IEEE Trans. Commun.*, vol. 61, no. 7, pp. 3050–3071, 2013.

[33] Y. Xiaobin and A. O. Fapojuwo, "Performance analysis of poisson cellular networks with lognormal shadowed Rayleigh fading," in *2014 IEEE Int. Conf. Commun. (ICC),*, Conference Proceedings, pp. 1042–1047.

[34] S. C. Lam, R. Heidary, and K. Sandrasegaran, "A closed-form expression for coverage probability of random cellular network in composite Rayleigh-Lognormal fading channels," in *2015 Proc. IEEE Int. Telecommun. Networks and Applicat. Conf.(ITNAC)*, 2015, pp. 161–165.

[35] X. Yang and A. O. Fapojuwo, "Coverage probability analysis of heterogeneous cellular networks in rician/rayleigh fading environments," *IEEE Communications Letters*, vol. 19, no. 7, pp. 1197–1200, July 2015.

[36] X. Zhang and J. G. Andrews, "Downlink cellular network analysis with multi-slope path loss models," *IEEE Transactions on Communications*, vol. 63, no. 5, pp. 1881–1894, May 2015.

[37] T. D. Novlan, R. K. Ganti, A. Ghosh, and J. G. Andrews, "Analytical Evaluation of Fractional Frequency Reuse for OFDMA Cellular Networks," *IEEE Trans. Wireless Commun.*, vol. 10, pp. 4294–4305, 2011.

[38] S. C. Lam, K. Sandrasegaran, and P. Ghosal, "Performance analysis of frequency reuse for ppp networks in composite rayleigh–lognormal fading channel," *Wireless Personal Communications*, Apr 2017.

[39] T. D. Novlan and J. G. Andrews, "Analytical Evaluation of Uplink Fractional Frequency Reuse," *IEEE Trans. Commun.*, vol. 61, no. 5, pp. 2098–2108, May 2013.

[40] H. S. Dhillon, R. K. Ganti, F. Baccelli, and J. G. Andrews, "Modeling and Analysis of K-Tier Downlink Heterogeneous Cellular Networks," *IEEE J. Sel. Areas Commun.*, vol. 30, no. 3, pp. 550–560, 2012.

[41] T. D. Novlan, R. K. Ganti, A. Ghosh, and J. G. Andrews, "Analytical Evaluation of Fractional Frequency Reuse for Heterogeneous Cellular Networks," *IEEE Trans. Commun.*, vol. 60, no. 7, pp. 2029–2039, July 2012.

[42] H.-S. Jo, Y. J. Sang, P. Xia, and J. Andrews, "Heterogeneous Cellular Networks with Flexible Cell Association: A Comprehensive Downlink SINR Analysis," *IEEE Trans. Wireless Commun.*, vol. 11, no. 10, pp. 3484–3495, October 2012.

[43] S. Mukherjee, "Distribution of Downlink SINR in Heterogeneous Cellular Networks," *IEEE J. Sel. Areas Commun.*, vol. 30, no. 3, pp. 575–585, 2012.

[44] H. Zhuang and T. Ohtsuki, "A model based on Poisson point process for downlink K tiers fractional frequency reuse heterogeneous networks," *Physical Communication*, vol. Volume 13, Part B, no. Special Issue on Heterogeneous and Small Cell Networks, p. 312, 2014.

[45] Y. Lin, W. Bao, W. Yu, and B. Liang, "Optimizing User Association and Spectrum Allocation in HetNets: A Utility Perspective," *IEEE J. Sel. Areas Commun.*, vol. 33, no. 6, pp. 1025–1039, June 2015.

[46] Y. Lin and W. Yu, "Optimizing user association and frequency reuse for heterogeneous network under stochastic model," in *2013 IEEE Global Commun. Conf.(GLOBECOM)*, Dec 2013, pp. 2045–2050.

[47] S. Singh, H. S. Dhillon, and J. G. Andrews, "Offloading in Heterogeneous Networks: Modeling, Analysis, and Design Insights," *IEEE Trans. Wireless Commun.*, vol. 12, no. 5, pp. 2484–2497, May 2013.

[48] D. Cao, S. Zhou, and Z. Niu, "Improving the Energy Efficiency of Two-Tier Heterogeneous Cellular Networks through Partial Spectrum Reuse," *IEEE Trans. Wireless Commun.*, vol. 12, no. 8, pp. 4129–4141, August 2013.

[49] S. E. Sagkriotis and A. D. Panagopoulos, "Optimal FFR Policies: Maximization of Traffic Capacity and Minimization of Base Station's Power Consumption," *IEEE Wireless Commun. Lett.*, vol. 5, no. 1, pp. 40–43, Feb 2016.

[50] S. Kumar, S. Kalyani, and K. Giridhar, "Optimal design parameters for coverage probability in fractional frequency reuse and soft frequency reuse," *IET Communications*, vol. 9, no. 10, pp. 1324–1331, 2015.

[51] H. Zhuang and T. Ohtsuki, "A Model Based on Poisson Point Process for Analyzing MIMO Heterogeneous Networks Utilizing Fractional Frequency Reuse," *IEEE Trans. Wireless Commun.*, vol. 13, no. 12, pp. 6839–6850, Dec 2014.

[52] L. Su, C. Yang, and C. L. I, "Energy and Spectral Efficient Frequency Reuse of Ultra Dense networks," *IEEE Trans. Wireless Commun.*, vol. 15, no. 8, pp. 5384–5398, Aug 2016.

[53] *E-UTRA Base Station (BS) radio transmission and reception*, 3GPP Std. TS 36.104, 2010.

[54] 3GPP TS 36.211 V14.1.0, "E-UTRA Physical Channels and Modulation," 12 2016.

[55] V. Jones. Radio Propagation Models. [Online]. Available: http://people.seas.harvard.edu/~jones/es151/prop_models/propagation.html#fsl

[56] M. Torlak. [Online]. Available: https://www.utdallas.edu/~torlak/courses/ee4367/lectures/lectureradio.pdf

[57] Kesan Online Calculator. [Online]. Available: http://keisan.casio.com/

[58] 3GPP TR 36.828 V11.0 , "E-UTRA Further enhancements to LTE Time Division Duplex (TDD) for Downlink-Uplink (DL-UL) interference management and traffic adaptation," June 2012.

[59] 3GPP TR 36.819 V11.1.0, "Coordinated multi-point operation for LTE physical layer aspects ," December 2011.

[60] L. Daewon, S. Hanbyul, B. Clerckx, E. Hardouin, D. Mazzarese, S. Nagata, and K. Sayana, "Coordinated multipoint transmission and reception in lte-advanced: deployment scenarios and operational challenges," *IEEE Commun. Mag.*, vol. 50, no. 2, pp. 148–155, 2012.

[61] G. Nigam, P. Minero, and M. Haenggi, "Coordinated Multipoint Joint Transmission in Heterogeneous Networks," *IEEE Transactions on Communications*, vol. 62, no. 11, pp. 4134–4146, Nov 2014.

[62] J. G. Andrews, A. Ghosh, and R. Muhamed, *Fundamentals of WiMAX: Understanding Broadband Wireless Networking*, 1st ed. New York, NY, USA: Prentice Hall, 2007.

[63] G. Y. Li, N. Jinping, L. Daewon, F. Jiancun, and F. Yusun, "Multi-Cell Coordinated Scheduling and MIMO in LTE," *IEEE Commun. Surveys & Tutorials*, vol. 16, no. 2, pp. 761–775, 2014.

[64] P. Marsch and G. Fettweis, "Static clustering for cooperative multi-point (comp) in mobile communications," in *2011 IEEE International Conference on Communications (ICC)*, June 2011, pp. 1–6.

[65] S. Bassoy, H. Farooq, M. A. Imran, and A. Imran, "Coordinated multi-point clustering schemes: A survey," *IEEE Communications Surveys Tutorials*, vol. PP, no. 99, pp. 1–1, 2017.

[66] Y. Abbes, S. Najeh, and H. Besbes, "Tractable framework for modeling and analyzing joint comp transmission and eicic technology in two-tier heterogeneous cellular networks," in *2016 International Symposium on Signal, Image, Video and Communications (ISIVC)*, Nov 2016, pp. 1–6.

[67] S. Y. Jung, H. k. Lee, and S. L. Kim, "Worst-Case User Analysis in Poisson Voronoi Cells," *IEEE Commun. Lett.*, vol. 17, no. 8, pp. 1580–1583, August 2013.

[68] D. Moltchanov, "Survey paper: Distance distributions in random networks," *Ad Hoc Netw.*, vol. 10, no. 6, pp. 1146–1166, Aug. 2012. [Online]. Available: http://dx.doi.org/10.1016/j.adhoc.2012.02.005

[69] P. Marsch and G. P. Fettweis, *Coordinated Multi-Point in Mobile Communications: From Theory to Practice*, 1st ed. New York, NY, USA: Cambridge University Press, 2011.

[70] X. Zhang and M. Haenggi, "A stochastic geometry analysis of inter-cell interference coordination and intra-cell diversity," *IEEE Transactions on Wireless Communications*, vol. 13, no. 12, pp. 6655–6669, Dec 2014.

[71] C. Li, J. Zhang, M. Haenggi, and K. B. Letaief, "User-centric intercell interference nulling for downlink small cell networks," *IEEE Transactions on Communications*, vol. 63, no. 4, pp. 1419–1431, April 2015.

[72] S. Govindasamy and I. Bergel, "Uplink performance of multi-antenna cellular networks with co-operative base stations and user-centric clustering," April 2017.

[73] M. Kamel, W. Hamouda, and A. Youssef, "Ultra-dense networks: A survey," *IEEE Communications Surveys Tutorials*, vol. 18, no. 4, pp. 2522–2545, Fourthquarter 2016.

[74] M. A. Stegun and I. A., *Handbook of Mathematical Functions with Formulas, Graphs, and Mathematical Tables*, 9th ed. Dover Publications, 1972.

[75] A. Neumaier, *Introduction to Numerical Analysis*. New York, NY, USA: Cambridge University Press, 2001.